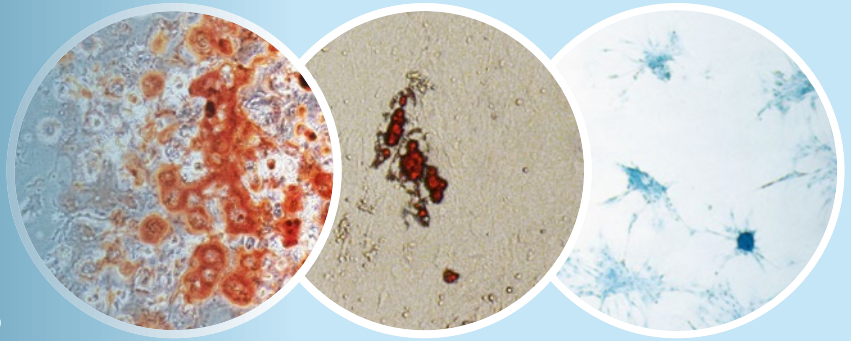


Methods in
Molecular Biology 2567

Springer Protocols



Louis M. Pelus
Jonathan Hoggatt *Editors*

Hematopoietic Stem Cells

Methods and Protocols

 Humana Press

METHODS IN MOLECULAR BIOLOGY

Series Editor

John M. Walker

School of Life and Medical Sciences

University of Hertfordshire

Hatfield, Hertfordshire, UK

For further volumes:

<http://www.springer.com/series/7651>

For over 35 years, biological scientists have come to rely on the research protocols and methodologies in the critically acclaimed *Methods in Molecular Biology* series. The series was the first to introduce the step-by-step protocols approach that has become the standard in all biomedical protocol publishing. Each protocol is provided in readily-reproducible step-by-step fashion, opening with an introductory overview, a list of the materials and reagents needed to complete the experiment, and followed by a detailed procedure that is supported with a helpful notes section offering tips and tricks of the trade as well as troubleshooting advice. These hallmark features were introduced by series editor Dr. John Walker and constitute the key ingredient in each and every volume of the *Methods in Molecular Biology* series. Tested and trusted, comprehensive and reliable, all protocols from the series are indexed in PubMed.

Hematopoietic Stem Cells

Methods and Protocols

Edited by

Louis M. Pelus

*Department of Microbiology & Immunology and Department of Medicine/Hematology
Oncology, Indiana University School of Medicine, Indianapolis, IN, USA*

Jonathan Hoggatt

Moderna Therapeutics, Cambridge, MA, USA

Editors

Louis M. Pelus
Department of Microbiology &
Immunology and Department
of Medicine/Hematology
Oncology, Indiana University
School of Medicine
Indianapolis, IN, USA

Jonathan Hoggatt
Moderna Therapeutics
Cambridge, MA, USA

ISSN 1064-3745

Methods in Molecular Biology

ISBN 978-1-0716-2678-8

<https://doi.org/10.1007/978-1-0716-2679-5>

ISSN 1940-6029 (electronic)

ISBN 978-1-0716-2679-5 (eBook)

© Springer Science+Business Media, LLC, part of Springer Nature 2023

This work is subject to copyright. All rights are reserved by the Publisher, whether the whole or part of the material is concerned, specifically the rights of translation, reprinting, reuse of illustrations, recitation, broadcasting, reproduction on microfilms or in any other physical way, and transmission or information storage and retrieval, electronic adaptation, computer software, or by similar or dissimilar methodology now known or hereafter developed.

The use of general descriptive names, registered names, trademarks, service marks, etc. in this publication does not imply, even in the absence of a specific statement, that such names are exempt from the relevant protective laws and regulations and therefore free for general use.

The publisher, the authors, and the editors are safe to assume that the advice and information in this book are believed to be true and accurate at the date of publication. Neither the publisher nor the authors or the editors give a warranty, expressed or implied, with respect to the material contained herein or for any errors or omissions that may have been made. The publisher remains neutral with regard to jurisdictional claims in published maps and institutional affiliations.

Cover Illustration Caption: The cover photo shows trilineage differentiation of expanded human bone marrow Mesenchymal Stem/Stromal Cells (MSC) to Osteoblasts (left), Adipocytes (Middle) and Chondrocytes (right). MSC are integral components of the hematopoietic niche that nurture and educate Hematopoietic Stem Cells. Osteogenic differentiation was determined by staining for mineralization of extracellular matrix and calcium deposits using Alizarin Red S. Adipocytes were identified by production of lipid droplets using Oil Red O staining. Alcian blue staining of glycosaminoglycans determined chondrocyte differentiation. The cover photo is provided by Dr. Pratibha Singh (Indiana University School of Medicine, Indianapolis, IN, USA).

This Humana imprint is published by the registered company Springer Science+Business Media, LLC, part of Springer Nature.

The registered company address is: 1 New York Plaza, New York, NY 10004, U.S.A.

Preface

The field of experimental hematology, or hematopoiesis or hematopoietic stem cell biology as we mostly refer to it today, has grown tremendously and continues to grow spurred on by ever-increasing technology and sophistication. Having entered the field in the early 1970s (LM Pelus), I was amazed by the ability of techniques to visualize the growth of individual bone marrow cells into colonies of myeloid and erythroid cells when given magical organ-conditioned medium and the utility to evaluate responses to exogenously added entities. Lethally irradiated mice could be salvaged by reintroduction of cells that formed spleen nodules. The poor man's sorting experiments whereby lineage specificity could be observed and altered by separating cloned daughter cells, and the long-term culture systems that allowed for evaluation of hematopoietic differentiation provided some basic understanding of stem and progenitor cell function.

We have come so far from then. The hematopoietic hormones were cloned and made readily available. FACS machines were developed for analysis and selection of single cells. Monoclonal antibodies and unique fluorochromes and mass cytometry were developed that allow us to use these machines to quantify stem and progenitor cell populations and signaling pathways and transcription factors in these cells. Genetic tools to turn on, turn off, or delete genes in living organisms were developed, as were single cell genomics and proteomics. In situ methods let us peer into the living bone marrow. New genetic organisms and more relevant animal models continue to emerge to evaluate true in vivo function of stem and progenitor cells and validate the findings uncovered with all these tools. With these tools, we have a greater understanding of hematopoiesis and cell function, and new technological advances offer the promise to learn more.

Previous editions of this series covering hematopoietic stem cell protocols have provided thorough coverage of many developments in the field, focused on user friendly and detail-oriented format, to allow those inexperienced or new to the areas apply these methods to their research and take advantage of the exceptional guidance offered by expert faculty. In this new edition, our aims were to update technical advances in areas covered in previous editions and incorporate new techniques focused on the molecular/genetic, cellular, and whole organism levels. We were also keen to incorporate methods that apply stress to hematopoiesis, which we believe is a major pathway to understand hematopoietic stem cell biology and drive research in many unexpected and exciting ways in the future. While not exhaustive by any means, this edition now contains chapters focused on better understanding the role of hematopoietic niches and their cellular components. Lastly, we have included chapters dedicated to in vivo models that test and quantitate stem cell function and are key to further development of therapeutic applications.

This book would not be possible without the time and effort of all the contributing authors. Their dedication to the intent of this series is outstanding, and we thank them for their support. We hope that this resource will be a valued addition to all laboratories focused on understanding hematopoietic stem cell biology and the therapeutic advances that can be derived.

*Indianapolis, IN, USA
Cambridge, MA, USA*

*Louis M. Pelus
Jonathan Hoggatt*

Contents

<i>Preface</i>	<i>v</i>
<i>Contributors</i>	<i>ix</i>
PART I OVERVIEW	
1 The Factory of Blood Production: Hematopoietic Stem Cells	3
<i>Jonathan Hoggatt and Louis M. Pelus</i>	
PART II MOLECULAR MODIFICATION AND EVALUATION	
2 Detection of DNA Damage in Hematopoietic Stem Cells	11
<i>Saipriya Ayyar and Isabel Beerman</i>	
3 Evaluating Histone Acetylation in Mouse Hematopoietic Stem and Progenitor Cells Using Chromatin Immunoprecipitation	29
<i>Liqiong Liu</i>	
4 CRISPR Gene Editing of Hematopoietic Stem and Progenitor Cells	39
<i>Reza Shabbazi, Patricia Lipson, Karthikeya S. V. Gottimukkala, Daniel D. Lane, and Jennifer E. Adair</i>	
5 Lentiviral Transduction of Nonhuman Primate Hematopoietic Stem and Progenitor Cells	63
<i>Chuanfeng Wu, So Gun Hong, Aylin Bonifacino, and Cynthia E. Dunbar</i>	
PART III CELLULAR ISOLATION AND CHARACTERIZATION	
6 Identification of Nonhuman Primate Hematopoietic Stem and Progenitor Cells	87
<i>Stefan Radtke and Hans-Peter Kiem</i>	
7 Isolation and Characterization of Fetal Liver Hematopoietic Stem Cells	99
<i>Diego A. López and Anna E. Beaudin</i>	
8 Utilizing CyTOF to Examine Hematopoietic Stem and Progenitor Phenotype	113
<i>Safa F. Mohamad and Maegan L. Capitano</i>	
9 Hematopoietic Stem Cell Identification Postirradiation	127
<i>Andrea M. Patterson, Christie M. Orschell, and Louis M. Pelus</i>	
PART IV THE HEMATOPOIETIC NICHE AND ACCESSORY CELLS	
10 Intravital Microscopy for Hematopoietic Studies	143
<i>Myriam L. R. Haltalli and Cristina Lo Celso</i>	

11 Laser Micromachining of Bone as a Tool for Studying Bone Marrow Biology 163
Christa Haase, Dmitry Richter, and Charles P. Lin

12 MSC and HSPC Coculture: Mimicking Ex Vivo Bone Marrow Niche 181
Pratibha Singh

13 Isolation of Thymus Stromal Cells from Human and Murine Tissue 191
Karin Gustafsson and David T. Scadden

PART V TRANSPLANTATION AND IN VIVO MODELS

14 Experimental Models of Mouse and Human Hematopoietic Stem Cell Transplantation 205
Scott H. Cooper, Maegan L. Capitano, and Hal E. Broxmeyer

15 Hematopoietic Stem and Progenitor Cell Identification and Transplantation in Zebrafish 233
Ellen Frint, Peng Lv, Feng Liu, Teresa V. Bowman, and Owen J. Tamplin

16 Establishing a Murine Model of the Hematopoietic Acute Radiation Syndrome 251
P. Artur Plett, Louis M. Pelus, and Christie M. Orschell

17 Purinergic Signaling and Its Role in Mobilization of Bone Marrow Stem Cells 263
Malwina Suszynska, Mateusz Adamiak, Arjun Thapa, Monika Cymer, Janina Ratajczak, Magdalena Kucia, and Mariusz Z. Ratajczak

Index 281

Contributors

- JENNIFER E. ADAIR • *Fred Hutchinson Cancer Center, Seattle, WA, USA; University of Washington, Seattle, WA, USA*
- MATEUSZ ADAMIAK • *Department of Regenerative Medicine, Warsaw Medical University, Warsaw, Poland*
- SAIPRIYA AYYAR • *Epigenetics and Stem Cell Unit, Translational Gerontology Branch, National Institute on Aging, Baltimore, MD, USA*
- ANNA E. BEAUDIN • *Department of Internal Medicine, Division of Hematology and Hematologic Malignancies, University of Utah School of Medicine, Salt Lake City, UT, USA*
- ISABEL BEERMAN • *Epigenetics and Stem Cell Unit, Translational Gerontology Branch, National Institute on Aging, Baltimore, MD, USA*
- AYLIN BONIFACINO • *Translational Stem Cell Biology Branch, National Heart, Lung, and Blood Institute, National Institutes of Health, Bethesda, MD, USA*
- TERESA V. BOWMAN • *Gottesman Institute for Stem Cell Biology and Regenerative Medicine, Department of Developmental and Molecular Biology, and Department of Medicine (Oncology), Albert Einstein College of Medicine and Montefiore Medical Center, Bronx, NY, USA*
- HAL E. BROXMEYER • *Department of Microbiology & Immunology, Indiana University School of Medicine, Indianapolis, IN, USA*
- MAEGAN L. CAPITANO • *Department of Microbiology and Immunology, Indiana University School of Medicine, Indianapolis, IN, USA*
- CRISTINA LO CELSO • *Imperial College London, London, UK; The Francis Crick Institute, London, UK*
- SCOTT H. COOPER • *Department of Microbiology & Immunology, Indiana University School of Medicine, Indianapolis, IN, USA*
- MONIKA CYMER • *Department of Regenerative Medicine, Warsaw Medical University, Warsaw, Poland*
- CYNTHIA E. DUNBAR • *Translational Stem Cell Biology Branch, National Heart, Lung, and Blood Institute, National Institutes of Health, Bethesda, MD, USA*
- ELLEN FRAINT • *Department of Pediatrics (Pediatric Hematology/Oncology and Cellular Therapy) and Department of Developmental and Molecular Biology, Albert Einstein College of Medicine and Montefiore Medical Center, Bronx, NY, USA*
- KARTHIKEYA S. V. GOTTIMUKKALA • *Fred Hutchinson Cancer Center, Seattle, WA, USA*
- KARIN GUSTAFSSON • *Center for Regenerative Medicine, Massachusetts General Hospital, Boston, MA, USA; Harvard Stem Cell Institute, Cambridge, MA, USA; Department of Stem Cell and Regenerative Biology, Harvard University, Cambridge, MA, USA*
- CHRISTA HAASE • *Wellman Center for Photomedicine, Massachusetts General Hospital and Harvard Medical School, Boston, MA, USA; Center for Systems Biology, Massachusetts General Hospital and Harvard Medical School, Boston, MA, USA*
- MYRIAM L. R. HALTALLI • *Imperial College London, London, UK; The Francis Crick Institute, London, UK; Wellcome – Medical Research Council Cambridge Stem Cell Institute, University of Cambridge, Cambridge, UK*
- JONATHAN HOGGATT • *Moderna Therapeutics, Cambridge, MA, USA*

- SO GUN HONG • *Translational Stem Cell Biology Branch, National Heart, Lung, and Blood Institute, National Institutes of Health, Bethesda, MD, USA*
- HANS-PETER KIEM • *Stem Cell and Gene Therapy Program, Fred Hutchinson Cancer Research Center, Seattle, WA, USA; Department of Medicine, University of Washington School of Medicine, Seattle, WA, USA; Department of Pathology, University of Washington School of Medicine, Seattle, WA, USA*
- MAGDALENA KUCIA • *Stem Cell Institute, James Graham Brown Cancer Center, University of Louisville, Louisville, KY, USA; Department of Regenerative Medicine, Warsaw Medical University, Warsaw, Poland*
- DANIEL D. LANE • *Fred Hutchinson Cancer Center, Seattle, WA, USA*
- CHARLES P. LIN • *Wellman Center for Photomedicine, Massachusetts General Hospital and Harvard Medical School, Boston, MA, USA; Center for Systems Biology, Massachusetts General Hospital and Harvard Medical School, Boston, MA, USA; Harvard Stem Cell Institute, Cambridge, MA, USA*
- PATRICIA LIPSON • *Fred Hutchinson Cancer Center, Seattle, WA, USA*
- FENG LIU • *State Key Laboratory of Membrane Biology, Institute of Zoology, Chinese Academy of Sciences, Beijing, China; Institute for Stem Cell and Regeneration, Chinese Academy of Sciences, Beijing, China; University of Chinese Academy of Science, Beijing, China*
- LIQIONG LIU • *Department of Microbiology and Immunology, Indiana University School of Medicine, Indianapolis, IN, USA; TriArm Therapeutics, Shanghai, PR China*
- DIEGO A. LÓPEZ • *Department of Pathology, University of Utah School of Medicine, Salt Lake City, UT, USA*
- PENG LV • *State Key Laboratory of Membrane Biology, Institute of Zoology, Chinese Academy of Sciences, Beijing, China; Institute for Stem Cell and Regeneration, Chinese Academy of Sciences, Beijing, China; University of Chinese Academy of Science, Beijing, China*
- SAFA F. MOHAMAD • *Department of Hematology and Oncology, Boston Children's Hospital/Harvard School of Medicine, Boston, MA, USA*
- CHRISTIE M. ORSCHELL • *Department of Medicine/Hematology Oncology, Indiana University School of Medicine, Indianapolis, IN, USA*
- ANDREA M. PATTERSON • *Department of Medicine/Hematology Oncology, Indiana University School of Medicine, Indianapolis, IN, USA*
- LOUIS M. PELUS • *Department of Microbiology & Immunology and Department of Medicine/Hematology Oncology, Indiana University School of Medicine, Indianapolis, IN, USA*
- P. ARTUR PLETT • *Department of Medicine/Hematology Oncology, Indiana University School of Medicine, Indianapolis, IN, USA*
- STEFAN RADTKE • *Stem Cell and Gene Therapy Program, Fred Hutchinson Cancer Research Center, Seattle, WA, USA*
- JANINA RATAJCZAK • *Stem Cell Institute, James Graham Brown Cancer Center, University of Louisville, Louisville, KY, USA*
- MARIUSZ Z. RATAJCZAK • *Stem Cell Institute, James Graham Brown Cancer Center, University of Louisville, Louisville, KY, USA; Department of Regenerative Medicine, Warsaw Medical University, Warsaw, Poland*

- DMITRY RICHTER • *Wellman Center for Photomedicine, Massachusetts General Hospital and Harvard Medical School, Boston, MA, USA; Center for Systems Biology, Massachusetts General Hospital and Harvard Medical School, Boston, MA, USA*
- DAVID T. SCADDEN • *Center for Regenerative Medicine, Massachusetts General Hospital, Boston, MA, USA; Harvard Stem Cell Institute, Cambridge, MA, USA; Department of Stem Cell and Regenerative Biology, Harvard University, Cambridge, MA, USA*
- REZA SHAHBAZI • *Fred Hutchinson Cancer Center, Seattle, WA, USA*
- PRATIBHA SINGH • *Department of Medicine/Hematology Oncology, Indiana University School of Medicine, Indianapolis, IN, USA*
- MALWINA SUSZYNSKA • *Stem Cell Institute, James Graham Brown Cancer Center, University of Louisville, Louisville, KY, USA; Department of Molecular Genetics, Institute of Bioorganic Chemistry, Polish Academy of Sciences, Poznan, Poland*
- OWEN J. TAMPLIN • *Department of Cell and Regenerative Biology, University of Wisconsin-Madison, Madison, WI, USA*
- ARJUN THAPA • *Stem Cell Institute, James Graham Brown Cancer Center, University of Louisville, Louisville, KY, USA*
- CHUANFENG WU • *Translational Stem Cell Biology Branch, National Heart, Lung, and Blood Institute, National Institutes of Health, Bethesda, MD, USA*

Part I

Overview



Chapter 1

The Factory of Blood Production: Hematopoietic Stem Cells

Jonathan Hoggatt and Louis M. Pelus

Abstract

Hematopoietic stem cells (HSCs) support the lifelong production of hundreds of billions of blood cells per day. This unique, incredible ability of HSCs also creates an incredible therapeutic potential for patients. To advance this potential, effective methods to study HSCs are continually evolving. This chapter summarizes the variety of protocols and techniques covered in this book used to evaluate HSCs – modification, characterization, interaction with their niche, and in vivo function.

Key words Hematopoietic stem cell, Hematopoietic methods, Hematopoietic protocols, Gene therapy, Radiation, In vivo models, In vivo imaging

1 Introduction

A massive, state-of-the-art factory sitting on 370 acres of land, growing to 10 million square feet and employing >10,000 workers, builds Tesla cars. Contained within the factory are advanced robotics for automation, solar cells for energy, and even a tunnel system to transport workers. All this massive effort to try and build 500,000 cars a year.

The human body, in contrast, produces ~300,000,000,000 blood cells per day. Remarkably, this blood production output comes from a similar number of workers, the hematopoietic stem cells (HSCs), of which there are estimated to be about 11,000–50,000. This lifelong production of billions of cells a day from such a small number of precursor cells is part of what makes bone marrow transplant clinically feasible and what allows humans to rebound from injuries to the hematopoietic system like massive blood loss or radiation exposure. Similarly, the ability to insert a gene or edit the genome of a small number of HSCs, which then give rise to billions of altered cells a day, allows for emerging gene therapy and editing strategies. These HSCs cannot do this alone, however, and require their own factory, the bone marrow, that is

often referred to as the hematopoietic stem cell niche, and accessory factories, like the thymus, to further refine the output.

For therapeutic development for blood diseases to be effective, scientific understanding of HSC modification, characterization, interaction with their niche, and *in vivo* function is required. As our understanding of the complexity of this blood-producing factory is further advanced, so too must the techniques and tools used to study this factory advance. This chapter briefly summarizes the advancements in HSC scientific protocols covered in this book.

2 Molecular Modification and Evaluation

To maintain lifelong blood production, it is vital for HSCs to maintain their genomic integrity. Techniques to evaluate DNA damage have existed for decades, but due to the rarity of HSCs, methods capable of evaluating DNA damage in a small number of cells, or even single cells, are required. However, many of these techniques are notoriously variable. Ayyar and Beermen (Chap. 2) describe their techniques for measuring DNA damage in HSCs, with suggestions on how to minimize variability to maximize the data quality. Liu in the following chapter (Chap. 3) also outlines techniques to assess histone acetylation and gene transcription in rare hematopoietic stem and progenitor cells.

HSCs have numerous methods to maintain their genome and stemness, but this intrinsic ability of HSCs also presents challenges when trying to modify them to treat genetic defects that cause blood diseases, such as hemoglobinopathies like sickle cell and thalassemia. The number of tools available to create genetic edits is constantly expanding, and likely has increased even after the publishing of this book. Shahbazi et al. (Chap. 4) highlight many of the available editing tools, with specific strategies for utilizing them for HSC therapeutic evaluation. Correction of genetic blood diseases can also be accomplished by inserting a new, functional copy of the defective gene. A few lentiviral-delivered gene therapies are currently approved, with several more in development. The nonhuman primate (NHP) animal model is a key asset for the clinical development of these emerging gene therapies. Wu et al. (Chap. 5) provide a detailed protocol for the isolation and transduction of NHP HSCs and subsequent evaluation of their efficacy.

3 Cellular Isolation and Characterization

Studying HSCs first requires appropriately identifying them among the vast number of other cells within the body. Identification is routinely performed by using advanced, multicolor flow cytometry techniques. While standard identification of mouse and human

bone marrow HSCs is now well known in most labs, and well covered in the literature, methods in other species or other tissues often have several nuances that dictate successful identification. Building on the protocols in Chap. 5, Radtke and Kiem (Chap. 6) describe their flow cytometry protocol to identify hematopoietic stem and progenitor cell (HSPC) subsets in multiple NHP species. López and Beaudin (Chap. 7) outline their protocol for isolating and characterizing fetal liver HSCs, the early precursors during development that then seed the fetal bone marrow shortly before birth. Fetal HSCs are highly potent in transplant models, and methods to isolate and study them may lead to better understanding of how to improve HSC therapeutic efficacy. While an ever-increasing number of fluorescent colors is available for flow cytometric characterization of HSCs, often there are practical limitations to the number of colors that can be used due to either machine capability and/or spectral overlaps. CyTOF, which is a method that uses heavy metal labeling instead of fluorescent labels, allows for a mass-spectrometry-based method to study dozens of proteins on a cell simultaneously. Mohamad and Capitano (Chap. 8) outline protocols to utilize this new technology to examine HSPC phenotypes and subpopulations. These chapters help expand the diversity of HSC populations that can be assessed, but generally, the methods have been developed using animals at steady-state conditions. Injury to the hematopoietic system, such as radiation, can cause changes in the surface expressed proteins on HSCs, making traditional characterization difficult. As radiation is commonly used in HSC animal experiments, particularly for bone marrow transplant or recovery models, Patterson et al. (Chap. 9) describe their experience and protocols of appropriately identifying HSCs post irradiation.

4 The Hematopoietic Niche and Accessory Cells

Hematopoiesis is largely contained within the bone marrow in mammals. Early on this was supported by irradiation and lead shielding studies that demonstrated blood production was within bones and was closely followed by studies in which the bone marrow was progressively bored out from the central cavity to the outer bone surface and found that there was greater hematopoietic potential found near the bone surface. The bone marrow is complex, and while it is clear that there is something unique about the bone marrow that supports hematopoiesis, that uniqueness perhaps is not due to proximity to osteolineage cells. There are many efforts to explore HSCs within this dynamic bone marrow environment, particularly in real time, to allow for greater understanding of the “factory floor” of blood production. Haltalli and Lo Celso (Chap. 10) describe methods of intravital microscopy, allowing

for visualization of HSCs within the bone marrow of live mice. Haase et al. (Chap. 11) then describe their variation of imaging utilizing laser micromachining of the bone that not only improves optical clarity but also provides physical access into the bone marrow to insert or acquire cells from precise locations. In vivo imaging is a powerful tool to evaluate spatial organization, but many times studying function of specific stromal cells in vivo is difficult without specific genetically altered mice, or molecules with bioavailability. Mimicking bone marrow stromal interactions in an ex vivo system is an alternative method when direct in vivo comparison is impractical or not currently possible with available tools. Singh (Chap. 12) provides an ex vivo coculture protocol, which can be adapted to study stromal and HSC interactions. Expanding upon the bone marrow analysis into other stromal tissues involved in hematopoietic function, Gustafsson and Scadden (Chap. 13) detail a thymus stromal cell isolation technique for downstream assays such as flow cytometry and RNA-sequencing, facilitating study of the microenvironmental niche for T cell progenitor maturation.

5 Transplantation and In Vivo Models

Many studies evaluating HSCs use phenotypic characterization to identify the cells, and many of the chapters in this book outline key advances in this phenotypic characterization. However, even the most advanced methods of phenotypic characterization are not 100% efficient, and cell surface phenotype is not always faithful to cell type, as discussed in Chap. 9. The gold standard for HSC analysis is transplantation. Cooper et al. (Chap. 14) outline the methods for mouse and human models of HSC transplantation and discuss their protocols for the collection and processing of HSCs in hypoxic environments. Fraint et al. (Chap. 15) describe the protocols for both phenotypic characterization and transplantation of HSCs using the zebrafish model.

Bone marrow transplantation was originally born out of a fear of nuclear disasters, either from nuclear power plants or weapons. The constant factory output of billions of blood cells makes the hematopoietic system uniquely sensitive to the DNA-damaging consequences of radiation exposure. While bone marrow transplant can potentially treat individuals exposed to radiation, in a mass casualty event, transplants are not practical. Therefore, accurate animal models are needed to explore the effects of radiation on HSCs and their niche, to develop alternative therapies. Plett et al. (Chap. 16) describe a robust and highly relevant mouse model of acute radiation syndrome that can be used to explore therapeutic interventions. Finally, Susynska et al. (Chap. 17) describe evidence of purinergic signaling in regulating HSC trafficking, and methods to explore this role of purines in animal models.

6 Conclusions

There is a long track record of success in the field of hematology of advancing basic science explorations of HSCs into therapies for patients. As the tools and techniques to study HSCs evolve, the horizon of new therapeutic development is promising. A factory producing 300 billion cells a day has a lot of moving parts, and the methods and protocols in this book add to the ability to inspect the factory to explore how it works.

Part II

Molecular Modification and Evaluation



Detection of DNA Damage in Hematopoietic Stem Cells

Saipriya Ayyar and Isabel Beerman

Abstract

Single-cell gel electrophoresis (SCGE or Comet assay) and the Fast Halo assay, also known as the Halo assay, are powerful tools to generate DNA damage measurements with single-cell resolution. Though these techniques are prone to have variability, they can be robust tools for quantifying DNA damage when planned and executed carefully. Here, we present both assays and highlight each technique's advantages and challenges in measuring DNA damage in cells with limiting cell number, such as hematopoietic stem cells (HSCs). The Comet assay is highly sensitive at the cost of increased variability. The Halo assay attenuates some of the effects of variability present in the Comet assay but does not eliminate them entirely and is less sensitive. Overall, the Comet and Halo assays are powerful means of directly measuring DNA damage. We recommend the below methods for detecting damage in hematopoietic stem cells, but the methods can easily be adjusted for measuring damage in any type of single cells in suspension.

Key words Hematopoietic stem cell, DNA damage, Comet assay, Fast Halo Assay, Electrophoresis

1 Introduction

Hematopoietic stem cells (HSCs) are responsible for maintaining and replenishing the blood system. Thus, the genomic stability of HSCs is critical to maintaining their functional potential [1]. While genomic insults occur naturally during the normal cell cycle, accumulation of DNA damage, especially by increased levels of reactive oxygen species, contributes to a loss of stem cell function [2]. Furthermore, DNA damage, as measured by strand breaks, accumulates in aged HSCs as well as in other stem cells [3–5], and terminally differentiated cells [6].

Several techniques for assaying DNA damage have been developed to examine, both directly and indirectly, levels of strand breaks. One of these techniques is the Single-Cell Gel Electrophoresis (SCGE) assay [7–9], which provided the foundation for direct measures of DNA lesions with single-cell resolution. Following this assay, Sestili et al. developed two quicker and simpler methods for analyzing DNA damage, called the alkaline Halo assay (AHA) and the fast Halo assay (FHA) [10, 11]. In these assays, neutral

conditions are believed to reveal only double-stranded breaks, while alkaline conditions show double- and single-stranded breaks. However, unwinding of the supercoils in DNA can occur under both alkaline and neutral conditions [12]. Therefore, we will focus on the use of the alkaline SCGE and FHA, with slight modifications, for quantifying DNA damage in HSCs.

Briefly, the SCGE assay directly measures endogenous or exogenous DNA damage in single cells. Single cells are embedded in agarose, plated onto microscope slides, lysed, and finally undergo low-voltage electrophoresis. As a result, damaged DNA is pulled away from intact DNA in the cell's nucleus, thus forming the tail of the "Comet" (*see* Fig. 1a), which is why this technique is often referred to as the Comet assay. After a series of wash steps, the slides are stained with a nucleic acid stain such as ethidium bromide, imaged, and analyzed using computer software. Similarly, the FHA protocol examines single-cell strand breaks by the migration of nonintact DNA away from the "nucleus" without using electrophoresis. This leads to their identifiable rings, or halos, around the intact DNA, thus aptly referred to as the Halo assay.

The Comet and Halo assays (and their derivations) provide powerful tools to directly measure DNA damage. Additional DNA damage assays such as γ H2AX and 53BP1 immunostaining are well established and widely used, but are indirect measures of DNA damage, and we suggest that they be used in conjunction with either the Comet or Halo assay. The Comet and Halo assays can also be modified to measure oxidative damage and repair through inclusion of DNA digestion of oxidized bases with a redoxo-endonuclease. These enzyme digestions cause nicks in the DNA at unrepaired oxidative bases leading to strand breaks [13].

These single-cell assays are simple and straightforward in concept, but the Comet assay is notorious for being highly variable and challenging to objectively score [14]. For example, in their meta-analysis, Forchhammer et al. found that variation in interlaboratory iterations of the Comet assay on the same samples can be attributed to the dose of damage-inducing agent used (ionizing radiation), variations in agarose concentration, incubation times, electrophoresis conditions, different analysis software, and sources of unexplained variation. The greatest factor leading to variation was found to be related to the dose of ionizing radiation, but among the other factors, residual variation contributed the most to the discrepancies in the results. The variability in the Comet assay is predominantly influenced by agarose concentration, electrophoresis time, and voltage gradient [15]. In addition, lysis time, alkaline incubation period, and electrophoresis temperature have important but less dominant influences on the variability seen in the Comet assay.

Though some of these variables can be mitigated with use of commercial products, Comet assays can remain variable in their results. With the removal of the electrophoresis step, Halo assays

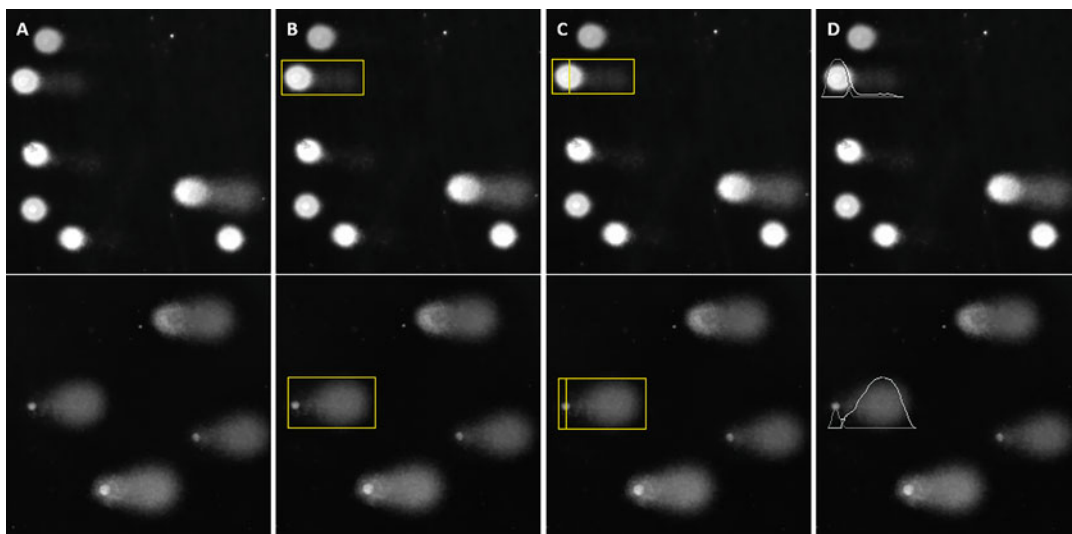


Fig. 1 Sample Comet assay images generated by DeltaVision microscope and scoring process carried out in CometScore with low (top row) and high (bottom row) levels of damage. (a) Example of images obtained from microscope. (b–d) “Single hue” view in the CometScore program. (b) Result of the first step of scoring in CometScore where a box is drawn around the comet. (c) The second step of scoring in CometScore in which the user marks the center of the head of the comet, depicted by a yellow vertical line. (d) CometScore output after carrying out steps shown in b and c

reduce the potential for variation introduced by electrophoresis time, voltage gradient, electrophoresis temperature, and buffer concentration. However, the reduction in potential variability comes at the cost of sensitivity. Residual variability in these assays is inevitable but can be ameliorated through careful optimization and adherence to the recommended concentrations and incubation times.

One important step for generating reliable data is carefully considering the slide layout and necessary controls. While planning experiments, all cells and appropriate controls should be run on the same slide to ensure the experimental conditions for each population of cells are as identical as possible. If the number of conditions or replicates exceeds the number of wells or amount of space on a single slide, the number of slides may be increased to accommodate these samples. However, to ensure that comparisons can be made across all samples and conditions, it is imperative that the same set of controls is included on every slide.

Ideally, all experimental conditions and controls will be assayed on the same day. For some experiments such as large-scale and longitudinal studies, however, this may not be possible. In such situations, we recommend including control populations of cells with varying levels of damage such as the control cells included in the Trevigen[®] CometAssay[™] kit. Alternatively, controls may be generated in-house using any standard cell line and stepwise

increases in exposure to DNA-damaging agents (UV, IR, chemical induction, etc.). By plotting the standard curve formed by these control cell populations, the damage levels of the experimental cell populations can be determined relative to the control cells. While the raw damage measurements may vary, the damaged cell populations can be used as a consistent control across all slides. Thus, relative levels of DNA damage can be determined despite variable experimental circumstances.

Another obstacle of these single-cell assays is the standardized scoring. A bottleneck is created by the amount of time required to manually score these data, impeding high-throughput analyses. In addition to this bottleneck, scoring is subjective and susceptible to bias. There are several tools available for the manual analysis of each cell, and there are automated platforms available as well. We prefer to score the Comet assays manually through a program called CometScore on blinded samples to minimize scorer bias (*see* Fig. 1). This software allows for manual scoring of each Comet and automatically calculates measurements of interest such as the olive tail moment (OTM) and percent DNA in tail (%Tail).

Similarly, Halo data can be manually scored using ImageJ by identifying the area of damaged and undamaged DNAs (*see* Fig. 2a). Common metrics used to describe DNA damage in this assay are Nuclear Diffusion Factor (NDF) and Percent DNA in Halo (%Halo). These are comparable to the OTM and %Tail values of the Comet assay. While scoring of Halos is simpler and less time-consuming than scoring of Comets, scoring of individual Halos still requires substantial amount of time, sometimes longer than it takes to run the assay itself, depending on the number of conditions. To address this issue, Maurya developed an Image-J plug-in called HaloJ, a semiautomatic pipeline that allows for quicker analysis of Halos [16]. Currently, there is no fully automated platform for Halo data analysis; however, we have created a pipeline made with CellProfiler, which is fully automated and can be provided upon request. Perhaps, with the growing popularity of machine learning algorithms, Comet and Halo analysis can be fully automated with increasing accuracy, thus removing limitations on the number of cells scored, the need for blinding images, and other sources of variation stemming from the subjective scoring process.

Given the many sources of variability in running these single-cell DNA damage assays, we propose the methods and procedures outlined below to maximally benefit from the strengths of the Comet and Halo assays while minimizing the effects of variability in a consistent and reliable manner.

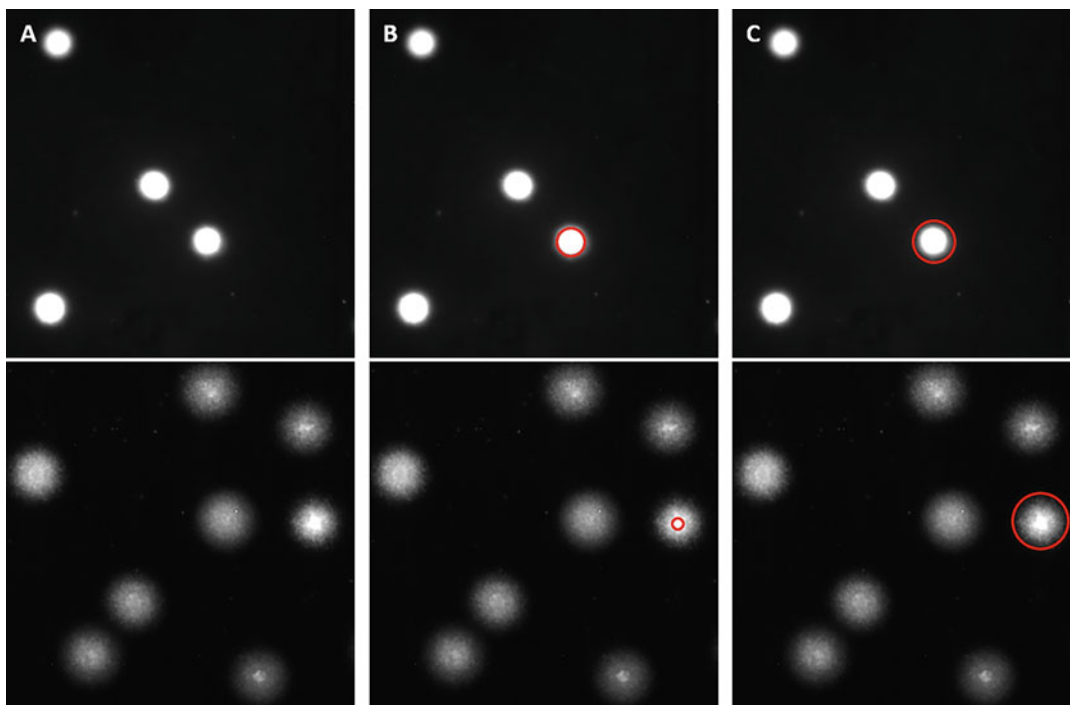


Fig. 2 Sample Halo assay images generated by DeltaVision microscope and scoring process carried out through ImageJ with low (top row) and high (bottom row) levels of damage. **(a)** Example of images obtained from microscope. **(b and c)** Image view and scoring in ImageJ program. **(b)** Result of the first step of scoring Halos in ImageJ. The red circle marks the intact DNA or “nucleus” of the Halo. **(c)** In the second step of scoring Halos in ImageJ, the entire object or “halo” is identified (red circle)

2 Materials

2.1 Obtaining Hematopoietic Stem Cells

1. Adult murine bone marrow
2. Sterile PBS
3. Flow Cytometer
4. Sample Media: PBS (sterile) supplemented with 2% heat-inactivated FBS, and 2mM EDTA. Vacuum filter solution after combining.
5. C57BL/6 mouse (*see Note 1*)
6. Mortar and Pestle
7. 70 um cell strainer/filter
8. Magnetic beads
9. Ckit enrichment beads or Streptavidin beads (lineage depletion)
10. PE-conjugated anti-ckit
11. Round-bottom Polystyrene tubes (14 ml)

12. Magnets for enrichment or depletion
13. Staining cocktail of antibodies diluted in Sample Media consisting of
 - (a) Antilineage cocktail consisting of the following biotin-conjugated antibodies in 1:100 dilution:
 - (i) Anti-B220 (RA3-6B2)
 - (ii) Anti-Mac1 (M1/70)
 - (iii) Anti-Gr1 (RB6-8C5)
 - (iv) Anti-Ter119 (TER-119)
 - (v) Anti-CD3 (17A2)
 - (vi) Anti-IL7R α (A7R34)
 - (b) APC-conjugated anti-Flk2 (A2F10; 1:50 dilution)
 - (c) FITC-conjugated anti-CD34 (RAM34; 1:50 dilution)
 - (d) PE-conjugated anti-c-kit (2B8; 1:200 dilution)
 - (e) APC.Cy7-conjugated anti-Sca1 (D7; 1:200 dilution)
 - (f) PE.Cy7-conjugated anti-CD150 (TC15-12F12.2; 1:200 dilution)
14. Pacific Orange-conjugated Streptavidin (S32365; 1:200 dilution in Sample Media)
15. Flow cytometer

2.2 Generating Control Cells

1. Sterile PBS
2. UV Crosslinker (or any other method of creating strand breaks such as IR, chemical induction, etc.)
3. Cell line, sorted cell population, or any single-cell suspension (*see Note 2*)

2.3 Sample and Agarose Preparation

1. HSCs sorted into PBS.
2. Control cells in PBS (cell line or sorted).
3. Hot water bath, 55–65 °C.
4. Sterile PBS.
5. CometAssay™ LMAgarose.
6. Heat block set to 37 °C.
7. 20-well Trevigen CometSlide™ (*see Note 3*).
8. Graphite pencil.
9. 1.7 mL microfuge tubes.
10. Centrifuge at 4 °C (all centrifugations are carried out at 4 °C unless otherwise noted).
11. Slide map (*see Fig. 3*).

White Strip	A04	B04	C04	D04	E04
	A03	B03	C03	D03	E03
	A02	B02	C02	D02	E02
	A01	B01	C01	D01	E01

Fig. 3 Sample slide layout where each well has a unique location ID. Each sample can be written into a box on the slide map and can be referenced after scoring the slide to determine which wells contained which samples

2.4 Sample Lysis and Agarose Preparation

While the Comet and Halo assays operate using similar principles, the specific materials required are slightly different due to the electrophoresis step of the Comet assay. We suggest using the electrophoresis chamber and lysis solution commercially available through Trevigen®; however, any electrophoresis chamber and lysis solution (such as the one described by Sestili et al. [10]) can be used. Additionally, there are slight differences in the materials required for the Comet and Halo assays due to the extra electrophoresis step in the Comet assay.

2.4.1 Comet Assay

1. Trevigen’s CometAssay™ Lysis Solution
2. Slide Tray
3. Deionized water
4. Sodium hydroxide (NaOH) pellets
5. 0.5 M EDTA
6. 100 mL graduated cylinders
7. 1 L Corning Glass Bottle
8. Aluminum foil
9. Trevigen’s CometAssay™ Electrophoresis System including Rack System
10. Trevigen’s CometAssay™ Power Supply with Power Cord

2.4.2 Halo Assay

1. Trevigen’s CometAssay™ Lysis Solution
2. Slide Tray
3. Deionized water
4. Sodium hydroxide (NaOH) pellets
5. 100 mL graduated cylinders
6. Aluminum foil

2.5 Sample Staining and Imaging

1. SYBR™ Gold Nucleic Acid Gel Stain (10,000× Concentrate in DMSO)
2. 1× Tris EDTA Buffer
3. Fluorescence microscope with FITC or equivalent channel connected to computer

2.6 DNA Damage Quantification

1. CometScore
2. ImageJ
3. Excel
4. GraphPad Prism or other data visualization software

3 Methods

3.1 Obtaining Hematopoietic Stem Cells

Human HSCs can be found in the bone marrow, cord blood, and in small numbers in the peripheral blood during homeostasis, whereas murine HSCs are found in the fetal liver of adult bone marrow. Regardless of the initial sample that is collected, the resulting cells should be filtered into single-cell suspensions for progenitor cell enrichment and cell surface marker staining. Finally, the cells are suspended in a live/dead stain and a flow cytometer is used to sort the HSC population defined as Lineage⁻/Sca1⁺/CD34⁻/Flk2⁻/CD150⁺ cells. The purified cells should be sorted into PBS (with no FBS or BSA present).

1. Isolate right and left tibia, femur, and pelvis from C57BL/6 mouse. Clean muscle off bones and place clean bones into a 15 mL conical tube prefilled with 3 mL sample media.
2. Once all bones have been collected, pour contents of 15 mL conical (solution and bones) into a clean mortar.
3. Using a pestle, gently crush bones to release bone marrow. Use a pipet to homogenize any red clumps and 70 μm filters to filter bone marrow back into a 15 mL conical. Add more sample media and gently crush bones to release more bone marrow. Continue adding media and removing and filtering bone marrow until the bones are white and there is little to no pink/red in the bones.
4. Spin down cells at 500 g for 5 min at 4 °C. (All centrifugations are carried out with these settings unless otherwise noted.) Pour off supernatant and resuspend in 1 mL of sample media
5. Use magnets and magnetic beads to obtain ckit-enriched or lineage-depleted samples.
6. Add a staining cocktail composed of antibodies and dilutions detailed in Subheading 2.1 to enriched samples.

7. Transfer cells to a new 1.5 mL tube and incubate cells in this cocktail for 1.5 h on ice in dark (*see Note 4*).
8. Add 1 mL sample media to the cells and spin down. Pour off the supernatant and resuspend cells in 100 μ L of PO-conjugated Streptavidin in 1:200 dilution in sample media. Incubate on ice for 15–30 min on ice in dark.
9. Add 1 mL sample media to dilute/wash antibody and spin down. Discard supernatant and resuspend in propidium iodide to distinguish live cells from dead cells during the sorting process.
10. Sort Lineage⁻/Scal⁺/CD34⁻/Flk2⁻/CD150⁺ cells into PBS using flow cytometer (*see Note 5*).

3.2 Generating Control Cells

Positive control cells can be generated by inducing strand breaks to any cell population. These cells may come from a standard cell line or from a single-cell suspension. Often, while sorting HSCs, we will also sort myeloid progenitors to use as control cells. We generate strand breaks in these cells by exposing them to UV-C radiation (254 nm) at 4.8 kJ or by 2 min of cesium irradiation. The positive control is to ensure the assay ran correctly (Comet tails or Halos present), and can also be used as an internal validation that slides run at the same time in the same conditions are comparable (i.e., control cells run on different slides have similar levels of damage) (*see Notes 6–8*).

1. Sort a side population of cells, for example, myeloid progenitors, or obtain cells from a common cell line. These cells should be suspended in PBS and in a clear centrifuge tube.
2. Place the tube of cells inside the UV crosslinker and apply 4.8 kJ of UV-C radiation (254 nm).
3. Remove cells from UV crosslinker and place on ice until use in the Comet or Halo assay.

3.3 Sample and Agarose Preparation

To mitigate some of the variables inherent to the Comet and Halo assays, commercially available kits with premade slides, agarose, and lysis buffer are available. We use these kit materials due to the industry-grade consistency and reliability they provide. While the costs of these commercial kits may be prohibitive, all materials required for running the assay can easily be prepared from common lab reagents or obtained at low cost [10]. The protocol below is written for use of Trevigen's 20-well Comet slides in addition to other Trevigen products as described in the Materials section. Additionally, some details such as volumes and concentrations differ slightly from the manufacturer's recommendations.

1. Determine the number of samples, including controls and replicates, that will be assessed for DNA damage. We recommend running each condition in triplicate or quadruplicate to account for variation across each slide. Remember to include at least one positive control and any other controls of interest.
2. Create a slide map detailing the location of each sample on the slide. (*see* Fig. 3)
3. 1–5 h before running the Comet or Halo assay, melt Trevigen CometAssay™ LM Agarose in the hot water bath (55–65 °C) for 5 min or until agarose is completely melted (*see* Note 9).
4. After ensuring that the agarose is melted and homogenized, pipette 50 uL of agarose into a 1.7 mL centrifuge tube for each well you will be plating (*see* Note 10).
5. Place 1.7 mL tubes containing agarose in a heat block set to 37 °C for the agarose to cool to physiological temperature before adding cells (*see* Note 11).
6. Spin down HSCs sorted into PBS and any control cells for 10 min at 500 g and 4 °C.
7. Based on the number of cells sorted into each tube, calculate the resuspension volume needed to reach a cell concentration of approximately 500 cells/uL (*see* Note 12).
8. Remove excess solution from sample until the volume left in the tube is the volume calculated in the above step. Do this carefully so as to not disrupt the likely nonvisible pellet and resuspend the pellet with the remaining volume of PBS in the tube.
9. Take 5 uL of this resuspension per well for a total of approximately 2500 cells per well and add to the appropriate tube of agarose (*see* Note 13). Pipette gently to homogenize.
10. Pipet ~50 uL of agarose containing cells onto each well of the Comet slide according to the slide map. Take care not to let agarose spread into other wells (*see* Note 14).
11. After the slide has been plated with cells suspended in agarose, place slide at 4 °C for 20–30 min until wells have solidified. Place the Trevigen CometAssay® Lysis Solution at 4 °C as well.
12. After wells have solidified, lay the slide flat onto a slide tray and pour cooled lysis solution into tray until all wells on all slides are entirely covered with solution taking care to not pour directly onto the slide. Incubate at 4 °C overnight.

3.4 *Sample Lysis and DNA Separation*

The following steps occur on day 2 of the assay.

3.4.1 *Comet Assay*

1. Make an alkaline unwinding solution by dissolving 0.8 g of NaOH pellets in 100 mL of deionized water + 200 μ L of 0.5 M EDTA to this solution. A magnetic stir bar and stir plate may help homogenize solution. Typically, 50 mL of solution is enough to completely cover 1 or 2 20-well Trevigen CometAssay™ slides but may need be scaled up based on the size and number of slides/slide trays. Ensure that all wells are completely covered in the alkaline solution.
2. At the same time, make an alkaline solution for the electrophoresis chamber by combining 8 g of NaOH pellets in 1 L of deionized water + 2 mL of 0.5 M EDTA. Once homogenized, place solution in a cold room or at 4 °C. Be sure to wear proper lab safety equipment such as gloves and a lab coat as NaOH is an irritant and may cause skin burns.
3. Once NaOH has fully dissolved and solution has come to room temperature (typically 30–45 min), carefully remove slide from cold lysis solution. Dab one corner onto paper towels to remove any excess lysis solution.
4. Place the slide in a clean tray and cover with alkaline unwinding solution for 30 min in the dark at room temperature – again do not pour directly onto the slide.
5. During this incubation, place the ice pack that comes with the Trevigen CometAssay™ kit at –20 °C. Additionally, set up and assemble the electrophoresis chamber as described in the Trevigen CometAssay® manual. Alternatively, place a large electrophoresis unit at 4 °C.
6. After 30 min have passed, remove the slide carefully from the alkaline solution and dab excess liquid onto paper towels carefully without disrupting the wells.
7. Then, place slide into the slide rack included in the Trevigen CometAssay™ kit making sure that it is flush at the bottom and has minimal room for movement. Additionally, note the orientation of the slide. Cover the slide gently with the dark cover piece also included in the kit. (The Slide rack is optional, but if not using, take care to ensure the slide is level, as the “Comets” will not be horizontal if the slide is not straight.)
8. Pour the electrophoresis solution from the cold room into the electrophoresis chamber until wells are covered. Replace chamber lid and run the apparatus for 30 min at 21 V. This should be run in the dark or in a covered unit.
9. After the run is complete, remove the slide carefully and dab off excess liquid on to paper towels.

10. Place slide in a clean tray and cover wells with dH₂O for 5 min. Dab on paper towels to dry and repeat this step once more with dH₂O.
11. Dab to dry slides and cover wells with 70% ethanol for 5 min.
12. After the ethanol wash, dab the slides on paper towels to dry them, and place in a cool, dry place with desiccant. Once wells have fully dried, proceed to staining and imaging as described below. For long-term storage, keep slides in the dark at room temperature.

3.4.2 Halo Assay

1. Make an alkaline unwinding solution by dissolving 1.2 g of NaOH pellets in 100 mL of deionized water. Typically, 50 mL of solution is enough to completely cover 1 or 2 20-well Trevigen CometAssay™ slides and can be scaled up based on the size and number of slides/slide trays.
2. Carefully remove slide(s) from lysis solution. Dab on paper towels to remove any excess solution and place in a clean slide tray.
3. Once NaOH has fully dissolved and the solution has come to room temperature, cover the slide with the freshly prepared alkaline unwinding solution for 30 min in the dark at room temperature.
4. After 30 min have passed, remove the slide carefully from the alkaline solution and dab excess liquid onto paper towels carefully without disrupting the wells.
5. Place slide in a clean tray and cover wells with dH₂O for 5 min. Dab to dry and repeat this step once more with dH₂O and once with ethanol.
6. After the ethanol wash step, place the slide in a cool, dry place with desiccant. Once wells have fully dried, proceed to staining and imaging as described below. For long-term storage, keep in dark at room temperature.

3.5 Sample Staining and Imaging

1. Make a 1:30,000 dilution of SYBR™ Gold by adding 1 uL of 10,000× SYBR™ Gold to 30 mL of 1× Tris EDTA Buffer.
2. Once wells are dry, carefully pipette ~65 uL of stain onto each well or enough to cover the entire well.
3. Place the slide(s) in the dark at room temperature for 30 min.
4. After incubation, rinse the stain off by carefully dipping each slide into a tray of deionized water.
5. Place slide in a cool, dark, dry place with desiccant until wells have dried.
6. Once wells are completely dry, image each well at 10× magnification, using an FITC or equivalent filter. Set the exposure to 0.2 s (*see Note 15*).

3.6 DNA Damage Quantification

Each experiment should be scored by the same person and using the same settings. While scoring is subjective, it is more important for the same individual to score all cells in each experiment as well as for the scoring to be consistent.

3.6.1 Evaluation of Comet Data

1. Download CometScore 2.0 (<http://rexhoover.com/index.php?id=Cometscore>).
2. Convert any images to .bmp format.
3. To reduce the effects of bias, it is recommended that the images are blinded before scoring.
4. Open CometScore. Go to File->Open and select an image to begin scoring.
5. To score, first use the “Cutoff” scroll bar to reduce the background noise until background noise is not interfering with the Comet (*see Note 16*).
6. Draw a box around the entire Comet including the tail (*see Fig. 1b*).
7. Click at the center of the head of the Comet (*see Fig. 1c*). CometScore will automatically notate the Comet as shown in *Fig. 1d*.
8. If this is the first Comet being scored, a dialog box will pop up with a prompt to save the data as a .txt file. Enter a filename and save the file in the desired location. This first Comet will not be saved and will need to be rescored after creating the .txt file.
9. To score the rest of the Comets, repeat steps 5 and 6 until the desired number of Comets has been scored (*see Note 17*).
10. To quantify DNA damage, obtain Olive Tail Moment (OTM) and Percent DNA in Tail (%Tail) metrics. These can be obtained directly from the .txt file that is created. OTM is calculated by: Tail length x Total DNA in Tail. %Tail is calculated by dividing the fluorescence intensities in the tail by the fluorescence intensities in the entire Comet.
11. Copy and paste the metrics of interest (OTM and %Tail) into an Excel file with the experimental conditions as the column headers and the DNA damage measurement (ex. OTM) for each scored Comet under the appropriate column header.

3.6.2 Evaluation of Halo Data

1. Download ImageJ from <https://imagej.nih.gov/ij/download.html> (*see Note 18*).
2. Double-click on the “magic wand” tool.
3. Set the “Tolerance” to 0.05. Keep all other settings as they are and click “OK.”
4. Open the “Analyze” toolbar and select “Set Measurements.”

5. Check the boxes for “Area,” “Mean gray value,” “Min & max gray value,” and “Integrated density.” Click “Ok”.
6. Select an image to score using “File” -> “Open...”. You can maximize the window to make the Halo easier to see. Sample image is shown in Fig. 2a.
7. For each Halo:
 - (a) Click at the center of the Halo until the yellow outline marks what you deem to be the nucleus. It may take a few clicks to obtain the shape you would like (*see* Fig. 2b) (*see Note 19*).
 - (b) Press “M” key on keyboard to “measure” the shape. The measurements will show up in another window.
 - (c) Click around the margins of the Halo until the yellow outline marks where the Halo ends and where background begins (*see* Fig. 2c). (*see Note 20*).
 - (d) Press “M” key again to record the measurement.
8. Press “Ctrl” + “Shift + O” or go to “File” -> “Open Next” to open the next image in the sequence.
9. “Score” each Halo in this manner until you have recorded 2 measurements (nucleus and Halo) for each Halo. For example, if scoring 250 Halos, there should be a total of 500 measurements in the “Results” window.
10. Press “File” -> “Save As” in the “Results” window and Save the results in the desired location. The results will save as an Excel file.
11. To quantify DNA damage, obtain the NDF and %Halo metrics. NDF can be calculated by the following formula: $(\text{Halo area} - \text{Nucleus area}) / \text{Halo area}$. %Halo is calculated by dividing the pixel intensities (saved as Integrated Density by ImageJ) of the damaged DNA outside the nucleus of the Halo by the pixel intensities of intact DNA within the nucleus (*see Note 21*).
12. When compiling data, ensure that damage values are in a column under the appropriate experimental condition heading.

3.7 Visualization of Data

1. Data can be visualized using GraphPad prism software (or any other visualization software) in column format by simply copying and pasting the excel table into GraphPad.
2. Plot OTM and NDF values as individual points in the vertical direction and mark the mean and SEM (*see* Fig. 4a, c).
3. Plot %Tail and %Halo values as frequency distributions with 10 bins, each bin spanning a range of 10 percentage points (*see* Fig. 4b, d).

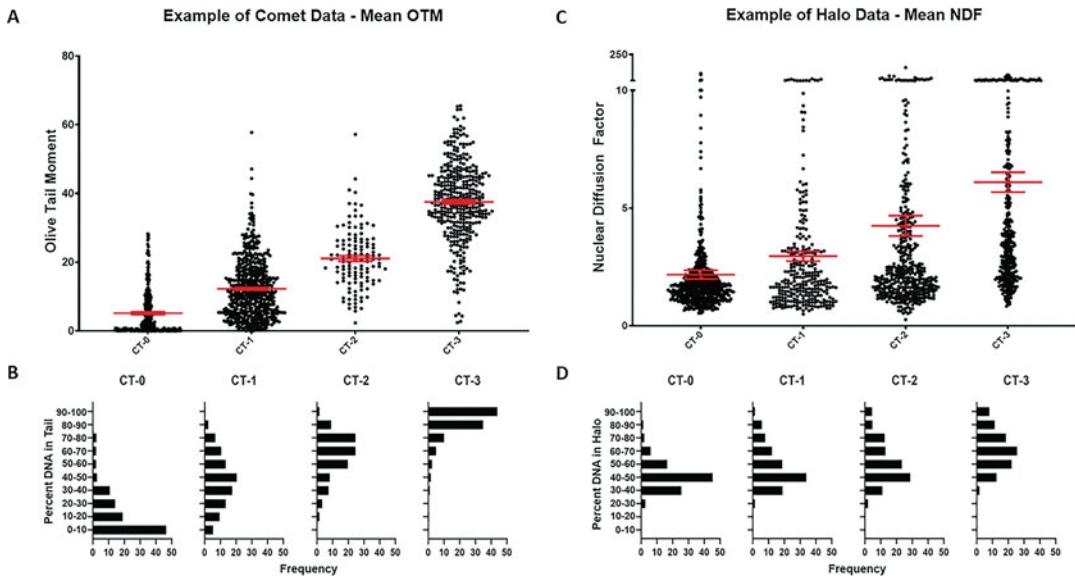


Fig. 4 Example plots of Comet and Halo assay results. The cells used are the four different control cell populations (referred to here as CT-0, CT-1, CT-2, and CT-3) provided in the Trevigen CometAssay™ kit. (a and c) Olive Tail Moment (OTM) from the Comet assay and Nuclear Diffusion Factor (NDF) from the Halo assay for the control cell populations. Each dot represents the damage score of an individual cell (Comet or Halo) and red lines mark the mean and SEM. (b and d) Percent DNA in Tail (%Tail) from the Comet assay and Percent DNA in Halo (%Halo) from the Halo assay represented as a frequency distribution. Each bar represents the percentage of cells from the entire scored population that have a damage level as determined by %Tail or %Halo within a bin of 10 percentage points

4 Notes

1. This staining and isolation protocol is specific to C57BL/6 mice. If using a different strain, it may be advisable to use a different panel of markers for HSC identification (typically the CD150/CD48 combination) [17].
2. We typically use myeloid progenitors as a control cell population, since they can be sorted alongside the HSCs; however, any cell type or cell line will serve the same purpose.
3. 1-, 3-, or 20-well Trevigen slides, or slides generated using the methods described by Sestili et al. [10], may also be used with slight modifications to the protocol presented here.
4. 1.5-h incubation is key for a good CD34 stain.
5. Solutions containing FBS such as the sample media used while isolating HSCs can decrease the affinity of the wells to the slide, thus increasing the risk of losing wells. For this reason, we recommend sorting cells directly into PBS or resuspending them in PBS.
6. Be sure to include control cells on every slide.

7. When making comparisons between samples run on different slides on different days (e.g., human samples that are not collected at the same time), we would suggest a slightly more complex control cell population. Ideally, these cells would be derived from a single population of cells with specific levels of incremental damage. We have found the control cells included in the Trevigen CometAssay™ kit to be suitable for this purpose. Additionally, control cells can be generated in-house by exposing large quantities of cells to various levels of DNA damage. The control cells should be made up of enough conditions to generate a “standard damage curve” consisting of at least 3 distinct levels of damage, spanning a range of no damage to heavy damage. We recommend making 5–10 uL aliquots of the damaged cell populations to ensure that the control cells are a reliable and consistent standard. By using aliquots of the same cells as controls, the damage curve of each slide can be used as a standard across multiple slides.
8. If planning longitudinal or long-term experiments, enough control cells should be generated such that the same control population is used throughout the experiment.
9. The agarose stock can be melted once and aliquoted. Once agarose is melted and homogenized, make 1–2 mL aliquots in centrifuge tubes and store at 4 °C. Agarose can be used fresh as well, but it is recommended to avoid solid-liquid cycles by making aliquots.
10. Alternatively, you may pool agarose for each condition into one centrifuge tube and then pipette 50 uL of agarose-containing cells onto each well from the same tube. For example, if running samples in quadruplicate, pipette 200 uL of agarose into a labelled tube, 50 uL per well.
11. If the agarose is too hot, it may kill the cells after they are added. This temperature is selected to keep agarose cool enough that it will not harm the cells but warm enough that it will not solidify and can be easily spread across the slide wells.
12. A concentration of 500 cells/uL is a recommendation. Usually, there is cell loss during plating of the cells onto the slide; so, this concentration ensures that there will be enough cells to score. If the concentration of cells is greater than this, cells may begin to overlap and cannot be scored.
13. If plating one well per condition, add 5 uL of cell suspension to 50 uL of LM Agarose. Otherwise, add 5 uL per replicate to the appropriate tube of agarose. For example, if each tube of agarose contains 50 uL of agarose (enough for one well), then add 5 uL of the cell suspension to this volume for a total of 55 uL of solution in the agarose tube. If the tube of agarose contains 200 uL of agarose for four replicates, add 5 uL of cell

suspension per replicate. In this case, 20 uL of cell suspension would be added to 200 uL of agarose for a total volume of 220 uL in the agarose tube. Scale up according to the number of replicates.

14. It may help to plate wells from the center toward the periphery or the opposite way. The center of the wells may be higher than the periphery forming a “dome”-like shape.
15. These settings are specific to the DeltaVision microscope and may need to be altered based on each microscope’s features.
16. There are two options under the “View” tab: “Single Hue” and “Full Spectrum.” Either of these views can be used as long as the background noise is reduced accordingly, and the same view is used to score all Comets from the experiment.
17. Typically, 50–100 Comets are scored per condition. We suggest scoring at least 250 Comets per well. If conditions are run in replicate, this ensures that across-slide variation is factored into the calculated average.
18. These directions are for 8-bit .tif or .bmp images. Some settings such as the magic wand “Tolerance” setting may need to be adjusted until the Halo and nucleus can be identified accurately.
19. Figure 2b, c show the outlines in red to increase visibility on the image. Outlines drawn in ImageJ will be yellow.
20. The yellow outlines may not perfectly mark the nucleus and Halo. Adjusting the “Tolerance” settings may help with this, but the Tolerance settings should remain consistent across all Halos scored in an experiment.
21. Each line of the output file will alternate between a Nucleus measurement and a Halo measurement. An easy way to determine if data was collected properly is to make sure that the “area” measurement on odd-numbered lines is smaller than the “area” measurement on the following line. The first line in the file should correspond to the measurements obtained for the “nucleus,” while the second line should correspond to the measurements obtained for the “halo” of the same cell.

Acknowledgments

This research was supported by the Intramural Research Program of the National Institutes of Health, National Institute on Aging.

References

1. Wang J, Sun Q, Morita Y, Jiang H, Gross A, Lechel A, Hildner K, Guachalla LM, Gompf A, Hartmann D, Schambach A, Wuestefeld T, Dauch D, Schrezenmeier H, Hofmann WK, Nakauchi H, Ju Z, Kestler HA, Zender L, Rudolph KL (2012) A differentiation checkpoint limits hematopoietic stem cell self-renewal in response to DNA damage. *Cell* 148(5):1001–1014. <https://doi.org/10.1016/j.cell.2012.01.040>
2. Yahata T, Takanashi T, Muguruma Y, Ibrahim AA, Matsuzawa H, Uno T, Sheng Y, Onizuka M, Ito M, Kato S, Ando K (2011) Accumulation of oxidative DNA damage restricts the self-renewal capacity of human hematopoietic stem cells. *Blood* 118(11):2941–2950. <https://doi.org/10.1182/blood-2011-01-330050>
3. Rossi DJ, Bryder D, Zahn JM, Ahlenius H, Sonu R, Wagers AJ, Weissman IL (2005) Cell intrinsic alterations underlie hematopoietic stem cell aging. *Proc Natl Acad Sci U S A* 102(26):9194–9199. <https://doi.org/10.1073/pnas.0503280102>
4. Beerman I, Seita J, Inlay MA, Weissman IL, Rossi DJ (2014) Quiescent hematopoietic stem cells accumulate DNA damage during aging that is repaired upon entry into cell cycle. *Cell Stem Cell* 15(1):37–50. <https://doi.org/10.1016/j.stem.2014.04.016>
5. McNeely T, Leone M, Yanai H, Beerman I (2019) DNA damage in aging, the stem cell perspective. *Hum Genet.* <https://doi.org/10.1007/s00439-019-02047-z>
6. Vijg J (2000) Somatic mutations and aging: a re-evaluation. *Mutat Res* 447(1):117–135. [https://doi.org/10.1016/s0027-5107\(99\)00202-x](https://doi.org/10.1016/s0027-5107(99)00202-x)
7. Kohn KW, Erickson LC, Ewig RA, Friedman CA (1976) Fractionation of DNA from mammalian cells by alkaline elution. *Biochemistry* 15(21):4629–4637. <https://doi.org/10.1021/bi00666a013>
8. Ostling O, Johanson KJ (1984) Microelectrophoretic study of radiation-induced DNA damages in individual mammalian cells. *Biochem Biophys Res Commun* 123(1):291–298. [https://doi.org/10.1016/0006-291x\(84\)90411-x](https://doi.org/10.1016/0006-291x(84)90411-x)
9. Singh NP, McCoy MT, Tice RR, Schneider EL (1988) A simple technique for quantitation of low levels of DNA damage in individual cells. *Exp Cell Res* 175(1):184–191. [https://doi.org/10.1016/0014-4827\(88\)90265-0](https://doi.org/10.1016/0014-4827(88)90265-0)
10. Sestili P, Calcabrini C, Diaz AR, Fimognari C, Stocchi V (2017) The Fast-Halo assay for the detection of DNA damage. *Methods Mol Biol* 1644:75–93. https://doi.org/10.1007/978-1-4939-7187-9_6
11. Sestili P, Martinelli C, Stocchi V (2006) The fast halo assay: an improved method to quantify genomic DNA strand breakage at the single-cell level. *Mutat Res* 607(2):205–214. <https://doi.org/10.1016/j.mrgentox.2006.04.018>
12. Collins AR, Oscoz AA, Brunborg G, Gaivao I, Giovannelli L, Kruszewski M, Smith CC, Stettina R (2008) The comet assay: topical issues. *Mutagenesis* 23(3):143–151. <https://doi.org/10.1093/mutage/gem051>
13. Collins AR, Ma AG, Duthie SJ (1995) The kinetics of repair of oxidative DNA damage (strand breaks and oxidised pyrimidines) in human cells. *Mutat Res* 336(1):69–77. [https://doi.org/10.1016/0921-8777\(94\)00043-6](https://doi.org/10.1016/0921-8777(94)00043-6)
14. Forchhammer L, Johansson C, Loft S, Moller L, Godschalk RW, Langie SA, Jones GD, Kwok RW, Collins AR, Azqueta A, Phillips DH, Sozeri O, Stepnik M, Palus J, Vogel U, Wallin H, Routledge MN, Handforth C, Allione A, Matullo G, Teixeira JP, Costa S, Riso P, Porrini M, Moller P (2010) Variation in the measurement of DNA damage by comet assay measured by the ECVAG interlaboratory validation trial. *Mutagenesis* 25(2):113–123. <https://doi.org/10.1093/mutage/gep048>
15. Collins AR, El Yamani N, Lorenzo Y, Shaposhnikov S, Brunborg G, Azqueta A (2014) Controlling variation in the comet assay. *Front Genet* 5:359. <https://doi.org/10.3389/fgene.2014.00359>
16. Maurya DK (2014) HaloJ: an ImageJ program for semiautomatic quantification of DNA damage at single-cell level. *Int J Toxicol* 33(5):362–366. <https://doi.org/10.1177/1091581814549961>
17. Kiel MJ, Yilmaz OH, Iwashita T, Yilmaz OH, Terhorst C, Morrison SJ (2005) SLAM family receptors distinguish hematopoietic stem and progenitor cells and reveal endothelial niches for stem cells. *Cell* 121(7):1109–1121. <https://doi.org/10.1016/j.cell.2005.05.026>



Evaluating Histone Acetylation in Mouse Hematopoietic Stem and Progenitor Cells Using Chromatin Immunoprecipitation

Liqiong Liu

Abstract

Epigenetics is the study of how cells control gene activity without changing the DNA sequence. Various epigenetic processes have been identified, including methylation, acetylation, phosphorylation, and ubiquitylation. Epigenetic processes are natural and essential to cell functions; however, when they occur improperly or at the wrong time, adverse effects can occur. A significant epigenetic process is chromatin modification. Chromatin–DNA complexes can be modified by acetylation, altering chromatin structure to influence gene expression. Stresses to hematopoietic stem and progenitor cells, such as ionizing radiation and aging, have significant effects on genomic function. Understanding epigenetic regulation in hematopoietic cells, particularly under stress, offers the potential for therapeutic intervention. We have utilized Chromatin immunoprecipitation (ChIP) in HSPCs to understand epigenetic regulation in response to ionizing radiation. This technique can be applied reliably to rare hematopoietic cells and offers a powerful tool to explore epigenetic regulation in HSPCs.

Key words Histone acetylation, Epigenetics, Histones, ChIP, Hematopoietic stem and progenitor cells (HSPCs)

1 Introduction

Histone deacetylases (HDACs) are enzymes that play an important role as epigenetic regulators of gene expression via histone modification and chromatin remodeling [1]. Acetylation, which targets the amino terminal regions of core histones and results in chromatin decondensation, allows access to transcription factors or regulators. Histone acetylation and chromatin remodeling play an important role in DNA replication, transcription, and DNA repair. The dramatic changes in promoter structure that accompany transcriptional activation are the direct result of acetylation. Site-specific acetylation or deacetylation could lead to locally restricted activation or repression of transcription, respectively [2, 3]. Chromatin immunoprecipitation (ChIP) is a well-established tool to identify

specific proteins associated with a region of the genome and investigate the interactions between regulatory proteins and DNA at distinct stages of gene activation. ChIP can be used to “measure” the amount of the histone modification. An example of this would include measurement of the amount of histone H3 acetylation associated with a specific gene promoter region under various conditions that might alter expression of the gene. Successful ChIP requires $\sim 1 \times 10^6$ cells per reaction. Due to limited number of hematopoietic stem cell (HSC) in bone marrow, the procedure requires isolation of sufficient bone marrow cells and cellular enrichment to be able to identify effects in rare HSCs.

The chapter provides details for exploring interactions between protein and DNA at gene promoters in HSC by ChIP and to provide a few “tips” that may be useful for investigators exploring and discovering new mechanistic insights into the HSC fate regulation through histone acetylation.

2 Materials

1. EasySep™ Mouse Hematopoietic Progenitor Cell Isolation Kit (STEMCELL Technologies #19856).
2. Optional: EasySep™ Mouse CD117(c-kit) Positive Selection Kit (STEMCELL Technologies # 18757).
3. EasySep Magnet (STEMCELL Technologies #18000).
4. EZ-ChIP™ kit (EMD Millipore # 17-371) has all the necessary buffers and reagents to perform successful ChIP.
5. Recommended medium: PBS containing 2% fetal bovine serum (FBS) and 1 mM EDTA.
6. PCR reagent: Fast SYBR®-Green Master Mix (ThermoFisher # 4385612).
7. Probe Sonicator.
8. Test tube rotating platform.

3 Methods

3.1 Bone Marrow Isolation

1. Harvest bones from a freshly sacrificed mouse. Since HSPC are rare, we usually harvest 2 femurs, 2 tibias, 2 hips, and tail vertebrae from each mouse.
2. Clean bones with sterile gauze and crush bones in cold PBS, 2% FBS, 1 mM EDTA using a sterile mortar and pestle.
3. Remove aggregates and debris by passing cell suspension through a 40 μm mesh nylon strainer.

4. Centrifuge at $300 \times g$ for 10 min and resuspend cells at 1×10^8 cells/mL in PBS, 2% FBS, 1 mM EDTA.

3.2 Mouse Hematopoietic Progenitor Cell Isolation

1. Add 50 μ L rat serum to 1 mL of bone marrow cells in 12×75 mm (5 mL) polystyrene round-bottom tubes.
2. Add 50 μ L isolation cocktail to samples (*see Note 1*). Mix and incubate at 2–8 °C for 15 min.
3. Vortex RapidSpheres for 30 s (*see Note 2*) and add 75 μ L RapidSpheres to samples. Mix and incubate at 2–8 °C for 10 min.
4. Add recommended medium to top up the samples to 2.5 mL. Mix by gently pipetting up and down 2–3 times.
5. Place the tube (without lid) into the separation magnet and incubate at room temperature for 3 min.
6. Pick up the magnet, and in one continuous motion invert the magnet and tube, pouring off the enriched cell suspension into a new 14 mL tube.
7. Remove the tube from the magnet and add recommended medium to the indicated volume (2.5 mL). Mix by gently pipetting up and down 5–6 times.

Repeat **steps 5–6** and combine with first poured-off fraction from **step 6**, isolated cells are ready for use.

3.3 In Vivo Crosslink and Lysis

Prior to starting this section, finish the HSPC isolation so that you are sure you have sufficient cells.

1. Add 137.5 μ L of 37% formaldehyde (or 1.15 mL of fresh 18.5% formaldehyde) to 5 mL of cells (1×10^7 cells/each tube) to cross-link and gently mix. Final concentration is 1% (*see Note 3*).
2. Incubate at room temperature for 10 min.
3. Meanwhile, aliquot 0.5 mL of ice cold 1X PBS into a separate tube. Add 1.25 μ L of Protease Inhibitor Cocktail II to each 1 mL of 1X PBS and put tubes on ice.
4. Add 0.5 mL of 10X glycine to each tube to quench unreacted formaldehyde.
5. Swirl to mix and incubate at room temperature for 5 min.
6. Place tubes on ice.
7. Aspirate medium, removing as much medium as possible, and being careful not to disturb the cells.
8. Add 5 mL of cold 1X PBS to wash cells.
9. Remove PBS and repeat PBS wash, **steps 8 and 9**.

10. Add 0.5 mL cold PBS containing 1X Protease Inhibitor Cocktail II to tube (made in **Step 3**).
11. Spin at $700 \times g$ at 4°C for 2–5 min to pellet cells.
12. During spin, prepare lysis buffer by adding 5 μL of Protease Inhibitor Cocktail II to each 1 mL of SDS Lysis Buffer required.
13. After spinning down, remove supernatant.
14. Resuspend each cell pellet in 1 mL of SDS Lysis Buffer containing 1X Protease Inhibitor Cocktail II for every 1×10^7 Lin-cells (*see Note 4*).
15. Aliquot 300–400 μL per microfuge tube (*see Note 5*).

3.4 Sonication to Shear DNA

1. If cell lysate was previously frozen, thaw on ice.
2. Sonicate cell lysate on wet ice (*see Fig. 1*) (*see Note 6*).
3. Spin at a minimum of 10,000 but not exceeding $15,000 \times g$ at 4°C for 10 min to remove insoluble material.
4. Remove supernatant to fresh microfuge tubes in 100 μL aliquots. Each 100 μL aliquot contains 1×10^6 cell equivalents of lysate, which is enough for one immunoprecipitation (*see Note 7*).
5. Prepare enough Dilution Buffer containing protease inhibitors for the number of desired samples. Each IP requires the addition of 900 μL of Dilution Buffer and 4.5 μL of Protease Inhibitor Cocktail II.



Fig. 1 Perform sonicating cell lysate. Sheared with 4–5 sets of 10-second pulses on wet ice



Fig. 2 Samples are rotated at low speed at 4 °C

6. Prepare one microfuge tube containing 100 μL of sheared cross-linked chromatin for the number of desired immunoprecipitations and put on ice. If chromatin has been previously frozen, thaw on ice (*see Note 8*). Each 100 μL will contain $\sim 1 \times 10^6$ cell equivalents of chromatin.
7. Add 900 μL of Dilution Buffer containing Protease Inhibitor Cocktail II into each tube containing 100 μL of chromatin.
8. Add 60 μL of Protein G Agarose for each IP. Incubate for 1 h at 4 °C with rotation (*see Note 9*). Rotate samples at low speed at 4 °C (*see Fig. 2*).
9. Pellet agarose by brief centrifugation $3000\text{--}5000 \times g$ for 1 min (*see Note 10*).
10. Remove 10 μL (1%) of the supernatant as Input and save at 4 °C (*see Note 11*).
11. Collect the remaining supernatant and dispense 1 mL aliquots into fresh microfuge tubes. Discard agarose pellet.
12. Add 2 μg the immunoprecipitating antibody (H3K9 or H4K16) to the supernatant fraction (*see Note 12*).
13. Incubate overnight at 4 °C with rotation (*see Note 13*).
14. Add 60 μL of Protein G Agarose to each IP and incubate for 1 h at 4 °C with rotation. This serves to collect the antibody/antigen/DNA complex.

15. Pellet Protein G Agarose by brief centrifugation ($3000\text{--}5000 \times g$ for 1 min) and remove the supernatant fraction.
16. Wash the Protein G Agarose-antibody/chromatin complex by resuspending the beads in 1 mL each of the cold buffers in the order listed below and incubating for 3–5 min on a rotating platform followed by brief centrifugation ($3000\text{--}5000 \times g$ for 1 min) and careful removal of the supernatant fraction:
 - (a) Low Salt Immune Complex Wash Buffer, one wash
 - (b) High Salt Immune Complex Wash Buffer, one wash
 - (c) LiCl Immune Complex Wash Buffer, one wash
 - (d) TE Buffer, two washes

3.5 Elution of Protein/DNA Complexes

Prior to starting this section: Bring 1 M NaHCO_3 to room temperature. A precipitate may be observed but will go into solution once room temperature is achieved, vortex if necessary

1. Make Elution Buffer for all IP tubes as well as all Input tubes. For each tube, prepare 200 μL of elution buffer as follows: 10 μL 20% SDS, 20 μL 1 M NaHCO_3 and 170 μL sterile, distilled water.
2. Alternatively, make a large volume to accommodate all tubes. For example, if there are 10 tubes, mix together 105 μL 20% SDS, 210 μL 1M NaHCO_3 and 1.785 mL sterile, distilled water.
3. For Input tubes, add 200 μL of Elution Buffer and set aside at room temperature until Subheading 3.5, step 5
4. Add 100 μL of Elution Buffer to each tube containing the antibody/agarose complex. Mix by flicking tube gently.
5. Incubate at room temperature for 15 min.
6. Pellet agarose by brief centrifugation ($3000\text{--}5000 \times g$ for 1 min) and collect supernatant into new microfuge tubes.
7. Repeat steps 4–6 and combine eluates (total volume = 200 μL).

3.6 Reverse Cross-Links of Protein/DNA Complexes to Free DNA and DNA Purification

1. To all tubes (IPs and Inputs), add 8 μL 5 M NaCl and incubate at 65 °C for 4–5 h or overnight to reverse the DNA–Protein cross-links. After this step, the sample can be stored at –20 °C and the protocol continued the next day.
2. To all tubes, add 1 μL of RNase A and incubate for 30 min at 37 °C.
3. Add 4 μL 0.5 M EDTA, 8 μL 1M Tris-HCl and 1 μL Proteinase K to each tube and incubate at 45 °C for 1–2 h.

4. Remove one Spin Filter in Collection Tube and one separate Collection Tube for each sample tube
5. Add 1 mL of Bind Reagent “A” to each 200 μ L DNA sample tube (IPs and Inputs) and mix well (*see Note 14*).
6. Transfer 600 μ L of sample/Bind Reagent “A” mixture to the Spin Filter in Collection Tube.
7. Centrifuge for 30 s at a minimum of 10,000 but not exceeding 15,000 $\times g$.
8. Remove the Spin Filter from the Collection Tube, save the Collection Tube and discard the liquid (*see Note 15*).
9. Put the Spin Filter back into the *same* Collection Tube. Transfer the remaining 600 μ L of sample/Bind Reagent “A” mixture from **Step 2** into the Spin Filter and repeat **steps 4–6**.
10. Add 500 μ L of the Wash Reagent “B” to the Spin Filter in Collection Tube. Centrifuge for 30 s at a minimum of 10,000 but not exceeding 15,000 $\times g$.
11. Remove the Spin Filter from the Collection Tube, save the Collection Tube, and discard the liquid. Put the empty Spin Filter back into the *same* Collection Tube.
12. Centrifuge for 30 s at a minimum of 10,000 but not exceeding 15,000 $\times g$. Discard the Collection Tube and liquid. Put the Spin Filter into a clean Collection Tube. Add 50 μ L of Elution Buffer “C” directly onto the center of the white Spin Filter membrane.
13. Centrifuge for 30 s at a minimum of 10,000 but not exceeding 15,000 $\times g$. Remove and discard Spin Filter. The eluate in the collection tube is now purified DNA. It can be analyzed immediately or stored frozen at $-20\text{ }^{\circ}\text{C}$.

3.7 Design Primers for the Genes and Perform Real-Time Quantitative PCR

1. Obtain the promoter sequence of each gene of interest from PubMed, and design primers using a software package of choice; we typically used Primer express v3.0. Order primers commercially – we use Integrated DNA Technologies (IDT).
2. Add 2 μ L of the sample to the PCR plate suitable for ABI Q6 instrument, performing triplicate of qPCR reactions per ChIP sample.
3. Prepare a master reaction mix as shown in Table 1 (*see Note 16*).
4. Add 23 μ L of qPCR mix to the 2 μ L of the sample and run qPCR. PCR conditions that work well in our hands are shown in Table 2.

Data can be presented as fold change in DNA relative to control. An example of data is presented in Fig. 3. In this experiment, animals received 16,16 dimethyl Prostaglandin E₂

Table 1
Components for quantitative PCR setup

Reagent	Volume per reaction (μL)
DNA	2
ddH ₂ O	7
2X SYBR-Green Mastr Mix	10
Primer	1 (at 10 μM)
Total	20 μL

Table 2
Quantitative PCR cycle conditions

Step	Initial denaturation	Denature	Anneal & extension	Melt curve stage	
Temperature	95 °C	94 °C	60 °C	95 °C	60 °C
Time	10 min	30 s	1 min	30 s	1 min
Cycles = 40 from 94 °C to 60 °C					

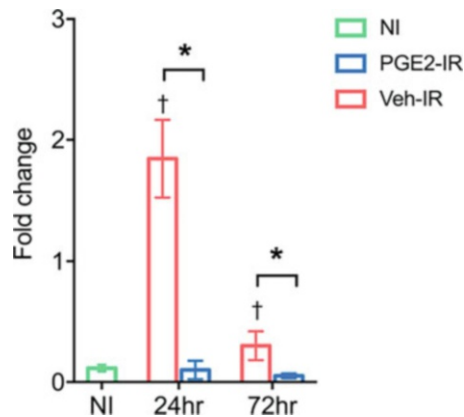


Fig. 3 Example of H4K16 binds DNA at p53 promoter from 1×10^6 HSPCs. H4K16ac are identified to be enriched in the promoters and the coding regions of the highly transcribed genes, such as p53 [4]. Global level of ac-H4K16 was increased by high level irradiation, p53 is regulated by H4K16 directly in HSPCs postirradiation

(dmPGE₂) or vehicle 30 min before lethal total body irradiation (8.73 Gy). Nonirradiated animals were also included. Bone marrow was harvested, and hematopoietic stem and progenitor cells analyzed by ChIP, using antibody to pull down acetylated histone H4K16 associated with the p53 promoter. Irradiation resulted in significant transcriptional upregulation of p53 as a consequence of acetylation of H4K16. Treatment with dmPGE₂ significantly prevented p53 upregulation by decreasing acetylation of H4K16.

4 Notes

1. Do not vortex cocktail.
2. Particles should appear evenly dispersed.
3. Use high-quality formaldehyde; make fresh before each experiment.
4. One mL of SDS Lysis Buffer is recommended. Adjust accordingly if using different cell concentrations, as the ratio of lysis buffer to cell density is important for reliable cell lysis.
5. Lysate can be frozen at -80°C for no more than 2 months at this step.
6. Cells in SDS Lysis Buffer at a cell concentration of 1×10^7 per mL sheared with 4–5 sets of 10-second pulses on wet ice using a Cole Parmer, High Intensity Ultrasonic Processor/Sonicator, 50-watt model equipped with a 2 mm tip and set to 30% of maximum power gave the appropriate length DNA fragments. Keep cell lysate ice-cold. Sonication produces heat, which can denature the chromatin.
7. Sheared cross-linked chromatin can be stored at -80°C for up to 2 months.
8. Alternatively, if multiple immunoprecipitations will be performed from the same chromatin preparation, place the entire volume for the number of desired immunoprecipitations in one large tube that will be able to accommodate a volume of 1.1 mL for each IP. The Protein G Agarose is a 50% slurry. Gently mix by inversion before pipetting. Do not spin Protein G Agarose beads at high speeds. Applying excessive g-force may crush or deform the beads and cause them to pellet inconsistently. If different chromatin preparations are being carried together through this protocol, remove 1% of the chromatin as Input from each.
9. For the positive control, anti-RNA Polymerase, add 1.0 μg of antibody per tube.
10. For the negative control, Normal Mouse IgG, add 1.0 μg of antibody per tube.
11. For user-provided antibody and controls, add 1–10 μg of antibody per tube. The appropriate amount of antibody needs to be determined empirically.
12. It may be possible to reduce the incubation time of the IP. This depends on many factors (antibody, gene target, cell type, etc.) and will have to be tested empirically.
13. Five volumes of Bind Reagent “A” should be used for every 1 volume of sample.

14. A precipitate may be observed. This will not interfere with this procedure.
15. If a precipitate formed in **Step 2**, it may be observed in the bottom of the Collection Tube; it will not interfere with this procedure.
16. Dispense enough reagents for at least one extra tube to account for loss of volume.

Acknowledgments

This work was supported by partnering grant W1XWH-15-1-0254/0255 from the US Dept. of Defense.

References

1. Bolden JE, Peart MJ, Johnstone RW (2006) Anticancer activities of histone deacetylase inhibitors. *Nat Rev Drug Discov* 5:769–784
2. Guo B, Huang X, Cooper S et al (2017) Glucocorticoid hormone-induced chromatin remodeling enhances human hematopoietic stem cell homing and engraftment. *Nat Med* 23:424–428
3. Eberharter A, Becker PB (2002) Histone acetylation: a switch between repressive and permissive chromatin. *EMBO Rep* 3:224–229
4. Guillemette B, Drogaris P, Lin HS et al (2011) H3 lysine 4 is acetylated at active gene promoters and is regulated by H3 lysine 4 methylation. *PLOS Genetics* 7:e1001354



CRISPR Gene Editing of Hematopoietic Stem and Progenitor Cells

Reza Shahbazi, Patricia Lipson, Karthikeya S. V. Gottimukkala, Daniel D. Lane, and Jennifer E. Adair

Abstract

Genetic editing of hematopoietic stem and progenitor cells can be employed to understand gene-function relationships underlying hematopoietic cell biology, leading to new therapeutic approaches to treat disease. The ability to collect, purify, and manipulate primary cells outside the body permits testing of many different gene editing approaches. RNA-guided nucleases, such as CRISPR, have revolutionized gene editing based simply on Watson-Crick base-pairing, employed to direct activity to specific genomic loci. Given the ease and affordability of synthetic, custom RNA guides, testing of precision edits or large random pools in high-throughput screening studies is now widely available. With the ever-growing number of CRISPR nucleases being discovered or engineered, researchers now have a plethora of options for directed genomic change, including single base edits, nicks or double-stranded DNA cuts with blunt or staggered ends, as well as the ability to target CRISPR to other cellular oligonucleotides such as RNA or mitochondrial DNA. Except for single base editing strategies, precise rewriting of larger segments of the genetic code requires delivery of an additional component, templated DNA oligonucleotide(s) encoding the desired changes flanked by homologous sequences that permit recombination at or near the site of CRISPR activity. Altogether, the ever-growing CRISPR gene editing toolkit is an invaluable resource. This chapter outlines available technologies and the strategies for applying CRISPR-based editing in hematopoietic stem and progenitor cells.

Key words CRISPR, Hematopoietic stem cells (HSCs), Gene editing, CD34+ cells, Ex vivo

1 Introduction

1.1 Overview

The ability to engineer genomes provides tremendous research and clinical potential. Understanding the fundamental relationships between genetic code, cellular function, and behavior is paramount to developing new treatments for disease. In disease settings where manipulation of genetic code can serve as a treatment strategy itself, rigorous preclinical evaluations in primary cells and appropriate model systems to adequately assess risk-to-benefit ratio are paramount.

Programmable nuclease proteins have been at the forefront of genome engineering, beginning with zinc-finger nuclease (ZFN) and meganuclease proteins, transcription-activator-like effector nucleases (TALENs) and later meganuclease-TALEN fusions known as mega-TALEs [1]. However, the greatest explosion of genome editing capability began with the discovery of clustered, regularly interspaced short palindromic repeats (CRISPR) sites in the genomes of bacteria, reported in 1987 [2]. It took 18 years for researchers to elucidate these repeats as part of bacterial acquired immunity and to coin the term “CRISPR” [3]. However, it was not long after that the mechanism of this system, an RNA-guided nuclease complex we now know as CRISPR-Cas, was elucidated and its potential ease and versatility in genomic engineering began to unfold.

The ease of collection, *ex vivo* manipulation, and reinfusion of hematopoietic blood stem and progenitor cells (HSPCs) into a conditioned recipient made these cells an early primary cell target for evaluating CRISPR gene editing [4]. Figure 1 outlines the basic steps involved in *ex vivo* CRISPR gene editing of HSPC, regardless of species origin or type of CRISPR nuclease. The purpose of this

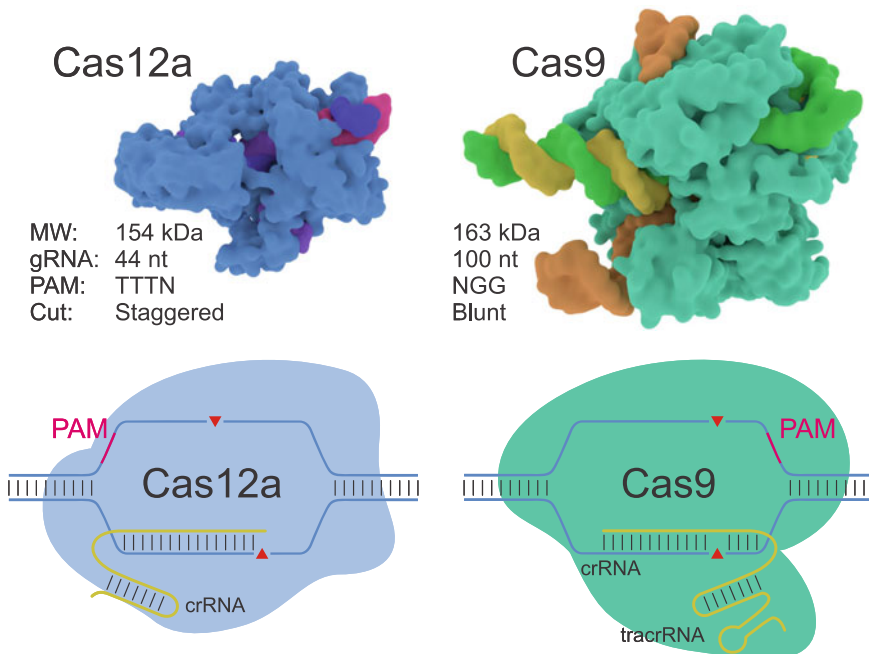


Fig. 1 CRISPR-Cas nucleases. (Top) Three-dimensional structures of the two most common CRISPR-Cas nuclease systems applied in HSPC to date, Cas12a (Cpf1) and Cas9. Each CRISPR system includes a protein component and a 1-part or 2-part guide RNA (gRNA). The cognate PAM sequence for each nuclease is listed as well as the type of DSB made. (Bottom) schematic of both nuclease bound to heteroduplex DNA via PAM sequence with gRNA (yellow) base-pairing and cut sites indicated by red triangles. *MW* molecular weight

chapter is to provide general methods for applying CRISPR gene editing in HSPC, as well as tips, tricks, and considerations for investigators exploring hematopoietic cell biology or developing new therapeutic strategies.

1.2 HSPCs

For any given application, parameters of the HSPCs are the first consideration. It has been widely established that CRISPR-Cas systems display species-dependent characteristics, which must be considered in experimental design for CRISPR-mediated genetic editing [5]. In addition, the method used to collect HSPC may influence CRISPR-Cas activity. Mobilized HSPCs, which have been stimulated to divide and have contacted peripheral blood serum components, may respond differently to CRISPR gene editing than the relatively quiescent HSPCs in bone marrow. Once the source tissue has been obtained, purification of HSPC typically includes immunomagnetic-bead-based separation or fluorescence-activated cell sorting (FACS) [6]. Purified HSPC can be cryopreserved for future use with several commercial sources offering prepurified, species-specific HSPC. Consideration of the HSPC sources available for each model and the goal of the gene editing experiment should dictate the method of HSPC collection and purification.

1.3 CRISPR Nucleases

Basic features of nearly all CRISPR-Cas systems include an RNA and protein component (*see* Fig. 2). Since 2005, multiple CRISPR nuclease variants covering two distinct classes have been described

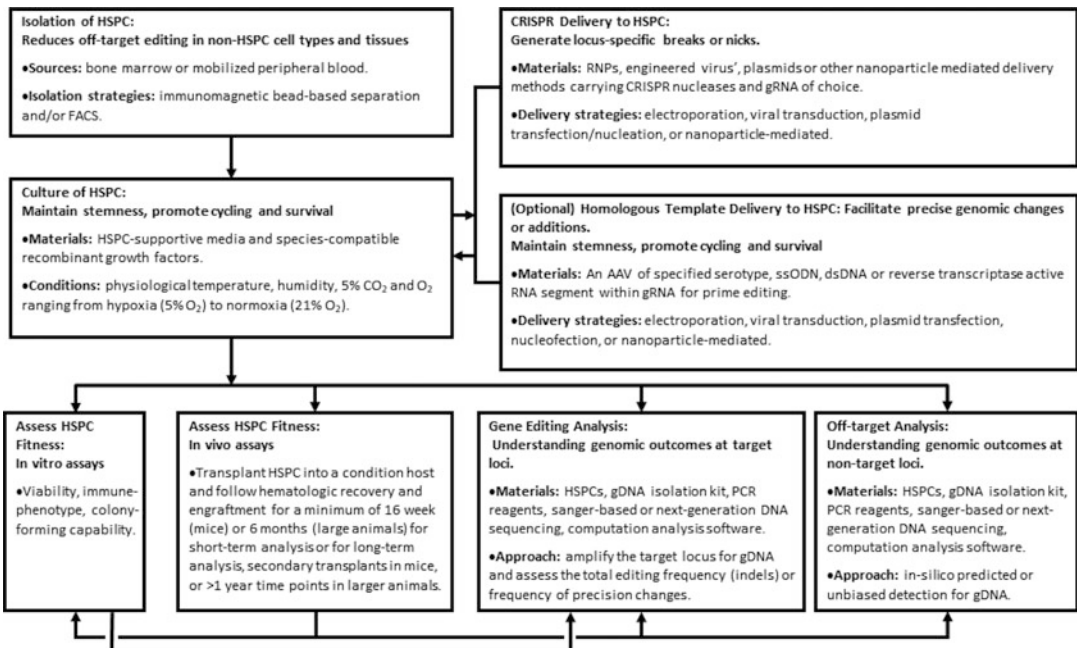


Fig. 2 Schematic of general process for CRISPR gene editing of HSPC

(reviewed in [7]). The protein component of this system, Cas, contains both helicase and twin nuclease domains, forming a stable complex with the RNA component(s). The RNA component is commonly referred to as the guide RNA (gRNA). The Cas protein searches DNA, binding to oligonucleotides, which contain the specified protospacer adjacent motif (PAM) sequence, specified by a domain within the Cas protein's structure. The helicase activity then unwinds the double-stranded genomic DNA (gDNA) and Cas presents the gRNA to the sequence of single-stranded oligonucleotide adjacent to the PAM. If base pairing occurs, the nuclease domains activate and each cut one strand of the target oligonucleotide to render a double-strand break (DSB). Cas protein variants can make blunt or staggered DSB; Table 1 lists currently known CRISPR-Cas variants and their relevant characteristics. At present, CRISPR-Cas9 is the most widely used variant in HSPC, although studies applying CRISPR-Cas12a (Cpf1) have emerged [8–10].

Other approaches to facilitate increased precision in editing HSPC include engineered Cas proteins designed for nickase (causing only a single strand break) activity through functional deactivation of one nuclease domain. This selective nicking allows selective editing of single nucleotide bases [11]. A major limitation of these “base editors” is the small amount of flexibility in the types of base changes that can be made and the scarcity of the required PAM site proximal to the desired genomic locus of the target base. More recently, search-and-replace “prime editing” has been described, wherein fusion of a Cas nickase mutant with a reverse transcriptase permits direct polymerization of DNA onto the nicked strand by encoding a desired genetic edit onto an extended gRNA [12]. This approach has greater potential for introducing small changes; however, it is limited by the length of RNA, which can be readily synthesized or produced from a DNA template, as well as the amount of RNA, which can be reasonably accommodated by the Cas protein, which is yet to be determined. The activity of base editors in HSPC has been demonstrated [13–15], while the activity of prime editors is in progress at the time of this writing. Additionally, recent discoveries suggest CRISPR-Cas complexes are co-opted in bacteria for directed transfer of mobile genetic elements. This presents the opportunity for inserting new DNA in a site-specific manner without the need for homologous recombination [16]. Further research is needed to explore the size of new DNA inserts and whether these programmable integrases show activity in HSPC.

CRISPR nucleases can be delivered as proteins, mRNA, or encoded within nonintegrating viral vectors such as integration-deficient lentiviruses (IDLVs). In HSPC, direct delivery of the nuclease protein in complex with gRNA as a ribonucleoprotein (RNP) complex has been shown to be highly effective [17–21]. mRNA, meanwhile, can produce multiple nuclease proteins

Table 1
Available CRISPR nuclease platforms

Name	Origin	PAM ^e or PFS sequence	Guide details	Type of nuclease activity	Specificity	References
CRISPR-Cas system: Class 2						
Cas9	<i>Streptococcus pyogenes</i> (most common)	5'-NGG-3'	2-part 42 nt crRNA ^c and 75 nt tracrRNA ^d or a chimeric single guide RNA (sgRNA) ^a	Blunt-ended DSB	Limited in sequences with low GC content, loose complementarity	[55–60]
Cas12a (Cpf1)	<i>Acidaminococcus</i> and <i>Lachnospiraceae</i>	5'-TTTN-3' Engineered Cas12a (cnAsCas12a) shows increased promiscuity in PAM recognition	A 42 nt crRNA with a 23 nt recognition sequence at the 3' end	Staggered DSB with 5'overhangs of 5 bp each	Highly sensitive to mismatches at most positions between 1 and 18 bp of the recognition sequence	[28, 61–64]
Cas13	Cas13a – <i>Leptotrichia shahii</i> Cas13b – <i>Prevotella sp.</i> Cas13d – <i>Ruminococcus flavefaciens</i>	Protospacer flanking sequence (PFS): 3'-AUC-5'	Single ~64 nt crRNA	Cleaves ssRNA	Difficulty discriminating between targets off by 1 bp	[65–69]
Cas14	Superphylum of extremophile archaea known as DPANN	No PAM required for ssDNA cleavage; T-rich PAM (TTTR/TTAT) for dsDNA cleavage	2-part ~140 nt sgRNA made up of crRNA and tracrRNA	Detection and cleavage of ssDNA, staggered cutting of dsDNA	Sensitive to even 1 bp mismatches	[70–72]

(continued)

Table 1
(continued)

Name	Origin	PAM ^e or PFS sequence	Guide details	Type of nuclease activity	Specificity	References
CRISPR-CasΦ	Huge Bacteriophages isolated by Al-Shayeb et al. [73]	CasΦ1-5'-BTTA-3' CasΦ2-5'-TT-3' CasΦ3-5'-BTT-3' "B" is A, C, or G	Single 14–20 nt crRNA	Staggered DSB with 5' overhangs of 8–12 nt each	Unknown	[74]
CRISPR-Cas system: Class I						
Cas3	<i>Escherichia coli</i>	5'-ARG-3'	A gRNA ^b composed of a 32 nt crRNA	Unidirectional deletion by "shredding."	Useful in repetitive sequences, sites far from PAM, or in transposable elements	[75, 76]
Cas9 Nickase (Cas9n)	Engineered	5'-NGG-3' (PAM-in or PAM-out but PAM-out is advised)	Two proximal sgRNAs targeting opposite strands; a native 2-part ~36 nt crRNA and a ~67 nt tracrRNA or a 100 nt sgRNA	Nicking, which leads to DSB with 5' overhangs or 3' overhangs	Relies on two guide RNAs, which reduce the number of potential target sites in the genome	[57, 77–79]
dCas9-FokI	Engineered	5'-NGG-3'	Two sgRNAs that bind 15–25 bp apart	Dimerization of FokI leads to DSB.	Better than wtCas9; possible promiscuity at sites with NGG PAM and a "seed" sequence ~5 bp located 5' of PAM	[79]
Base editors (Cytosine and Adenine Base editor)	Engineered	5'-NGG-3'	sgRNA consisting of crRNA with 20 nt target protospacer at 5' end	Alters 1 bp of gDNA without DSB	CBEs convert C→T and G→A; ABEs convert A→G and T→C	[11, 80, 81]

Prime editors	Engineered	5'-NGG-3' (not substantially constrained by proximal PAM availability)	Prime editing guide RNA (pegRNA) includes gRNA target sequence, primer binding sequence (PBS), and template with edited RNA sequence	Directly reverse transcribes template RNA into gDNA	Permits indels and point mutations ranging from 3 bp upstream to 29 bp downstream of PAM without DSBs	[12]
INTEGRATE (INsert Transposable Elements by Guide RNA-Assisted TargeTing)	<i>Vibrio cholera</i>	5'-CC-3'	Cascade complex includes 32 nt crRNA complementary to target sequence	DNA is integrated in a replicative transposition manner	Cannot tolerate mismatches within the 8 nt seed sequence nor at positions 25–28	[16]
shCAST (CRISPR-associated transposases)	<i>Scytonema hofmanni</i>	Preference for 5'-NGTN-3'	2-part 28–34 nt long crRNA with 11–14 nt of direct repeat (DR) sequence, 17–20 nt spacer and long, putative tracrRNA	Inserts segments of DNA 60–66 bp downstream of the protospacer	Unknown	[82]
CRISPR-X	Engineered	5'-NGG-3'	~20 nt sgRNA with two MS2 binding stem loops to recruit activation-induced cytidine deaminase (AID) enzyme	Associated AID causes hypermutation in the region ±100 bp of the PAM	Unknown	[83]

^asgRNA: single-guide RNA, which includes both a crRNA sequence fused to the scaffold tracrRNA sequence

^bgRNA: guide RNA that includes just a crRNA sequence

^ccrRNA: CRISPR RNA, a variable sequence complementary to the target DNA

^dtracrRNA: transactivating crRNAs are constant and provide the “stem loop” structure bound by the nuclease

^ePAM: protospacer adjacent motif; is generally around 3–4 nt downstream from the cut site

in the cell, though stability is a concern. In this regard, chemical modification of the mRNA has been shown to improve activity, reduce immunogenicity, and increase transcriptional lifetime (reviewed in [22]). IDLV-mediated delivery can also ensure a long-lasting supply of nuclease protein within cells, but persistent Cas expression has also been associated with increased off-target cutting and potential genotoxicity [23]. The addition of peptide nuclear localization signals (NLSs) on CRISPR nucleases is associated with increased activity in HSPC, with two or three NLS repeats showing the highest efficiencies [24].

1.4 Guide RNA

The gRNA can be made up of one or two parts; all CRISPR systems have a CRISPR RNA (crRNA), which is the effector RNA responsible for pairing with oligonucleotides unwound by Cas, and some contain trans-activating CRISPR RNA (tracrRNA), which partially base pair with the crRNA to form the gRNA complex. In two-part CRISPR systems, the crRNA and tracrRNA can be engineered as a chimeric single guide RNA (sgRNA) [25]. The ideal gRNA should base pair specifically with the target oligonucleotide sequence for editing and not any alternative loci in the genome, but PAM availability and sequence complementarity can influence gRNA design. In cases where the ideal is not possible, the goal of CRISPR gene editing experiments should dictate whether to compromise on complementarity or proximity to the genomic locus. Some studies have demonstrated that multiple gRNAs targeting the same genetic locus can increase specificity and decrease off-target effects (reviewed in [26]).

1.5 Targeted Genomic Loci for Gene Editing

Central to any CRISPR experiment is an in-depth understanding of the targeted genomic sequence. If the goal of gene editing is knock-out, then the target locus should be in a coding or critical control region for protein expression or regulation. If the goal is knock-in, then the nuclease cut site must be close to the desired locus or a genomic safe harbor site (an open but not biologically vital site) for DNA addition. Regions with high frequency of single-nucleotide polymorphisms (SNP) can be extremely difficult to engineer due to the need for base pairing of the gRNA to initiate Cas nuclease activity. Likewise, regions with repetitive elements can diminish specificity.

Once the optimal target locus for gene editing is determined, the presence of the cognate PAM sequence for the nuclease variant of interest must be verified. The need for a specific PAM sequence within the target oligonucleotide sequence to be edited is a limitation of CRISPR-nuclease systems. As more CRISPR-nuclease systems with variable PAM recognition sequences are discovered (*see* Table 1), the probability of a cognate PAM being present within a given genomic sequence increases. In addition, the ability to engineer more

permissive PAM recognition domains of these proteins has reduced this limitation [27, 28].

1.6 DNA Repair

1.6.1 Nonhomologous DNA Repair

Critical to the aim of gene editing is what happens *after* the CRISPR-Cas complex generates a break in the DNA or target oligonucleotide of interest. DSBs are repaired by one of several possible DNA repair pathways, the most common being nonhomologous end joining (NHEJ) [7]. The NHEJ pathway is active in all phases of the cell cycle and, as the name implies, involves direct ligation of the free DNA ends at the site of the break. When these ends are staggered, NHEJ can use the exposed microhomology present in the single-stranded overhangs to repair the break accurately. However, when the free DNA ends at the break site are blunt, as is the case after Cas9-mediated cutting, NHEJ-mediated DNA repair becomes imprecise, causing indels, which are gains (insertions) or losses (deletions) of nucleotides. This system is therefore useful in gene editing strategies designed to introduce mutations. In some genomic contexts, specific mutations are favored following a blunt-end DSB due to microhomologies that can facilitate a more error-prone DNA repair mechanism called microhomology-mediated end joining (MMEJ) or alternative (alt)-NHEJ [29].

1.6.2 Homologous DNA Repair

When DSBs occur with incompatible ends, another DNA repair mechanism called homology-directed repair (HDR) can be employed to introduce precise changes into the genome at or near the site of the break. This DNA repair pathway uses a template oligonucleotide with homology to the genome at the site of the break flanking the desired changes to be introduced [7]. Thus, HDR requires delivery of a homologous DNA template (HDT) in addition to the CRISPR-Cas complex. While this approach is attractive, it has been shown to be particularly difficult to accomplish in human cells such as HSPC [30]. This is partly due to the naturally quiescent state of repopulating HSPC, which is not conducive for the HDR pathway, which is typically only active during G2 and S phases of the cell cycle. While several strategies to improve HDR efficiency in other cell types have been described, it is important to note that uncontrolled HDR leads to hyper-recombination and genomic instability, and that demonstrated safety and feasibility of these approaches in HSPC is mostly nonexistent [31].

There are various types of HDTs including dsDNA in the form of plasmids or double-stranded oligonucleotides, single-stranded donor oligonucleotides (ssODN), and engineered nonintegrating DNA viruses such as adeno-associated viruses (AAVs). The two most used in HSPC are ssODN for smaller genetic changes (total capacity of ~2000 nucleotides) and AAV for larger genetic changes (total capacity of 4.7 kb). dsDNA or plasmids have been shown to be more readily incorporated into genomes by the error-prone

NHEJ repair method, both at target DSBs but also at off-target DSBs in gDNA [32, 33]. ssODN allow shorter homology arms with higher demonstrated insertion frequencies compared to dsDNA [34, 35] and can be delivered at the same time as CRISPR-Cas. Engineered, recombinant AAVs have been shown to naturally mediate HDR in mammalian cells with serotype 6 showing the highest efficiency in HSPC [36]. While ssODN can be easily synthesized, AAV must be produced through a more laborious process. Fortunately, excellent resources exist to describe this process and reagents are commercially available [37, 38].

1.7 Analysis of Gene Editing

While some cases of successful gene editing results in expression of a reporter, which can be empirically measured in cells, this option often does not adequately inform all gene editing outcomes at the target genomic locus of interest. Additionally, off-target mutagenesis can be induced by CRISPR-Cas nucleases in human cells via unintended point mutations, indels, or even inversions and/or translocations [39]. The level of tolerance to base pair mismatches between the gRNA and the target oligonucleotide sequence can influence likelihood of off-target effects and is variable across CRISPR nucleases (*see* Table 1). Even with engineered nucleases, modified PAM sequences and/or truncated gRNA strategies to improve specificity, at least a confirmatory screen for unintended genomic events should be performed to adequately interpret biological consequences of CRISPR-mediated gene editing in HSPC studies.

1.7.1 Analysis of On-Target Gene Editing

Analysis of gene editing outcomes at the target genomic locus generally begins with isolation of gDNA followed by polymerase chain reaction (PCR) amplification of the target locus. Once PCR products are obtained, an *in vitro* cleavage assay to measure gene editing levels can be performed or direct DNA sequencing and computational analysis to interpret gene editing levels may be attempted.

There are several options for analysis of gene editing results with the quickest and dirtiest being the T7 endonuclease I (T7E1) *in vitro* assay (reviewed in [40]). This assay relies on the T7E1 structure-selective enzyme, which recognizes and cuts structural deformities characteristic of mismatches in heteroduplex DNA. This enzyme can be used to identify the proportion of PCR products containing indels but is considered much less sensitive than direct sequencing-based methods. It also cannot reliably detect successful HDT integration [40]. Next-generation sequencing (NGS) and bioinformatic analysis is considered the most sensitive method for detecting gene editing outcomes, and there are several NGS platforms available. However, sequencing costs and analysis algorithms are not trivial. In between these two options in terms of ease and sensitivity is Sanger sequencing and publicly available computational programs to assess both indels and HDT

integrations such as Tracking of Indels by DEcomposition (TIDE; www.tide.deskgen.com) [41] or Inference of CRISPR Edits (ICE; www.ice.synthego.com/#/).

1.7.2 Analysis of Off-Target CRISPR-Cas Activity

Methods to analyze off-target effects are divided into three categories: [1] *in silico*, [2] unbiased gDNA-based, and [3] unbiased cell-based assays (*see* Table 2). *In silico* methods narrowly presume genomic sequence homology to the gRNA as the only source of unintended CRISPR-Cas activity, and thus are considered least thorough [42]. They begin with identifying similar sequences in the genome of interest, which are most likely to be off-target loci, followed by individual PCR amplification and analysis of gene editing at those loci. Several tools to identify *in silico* predicted sites are available and reference sequences should be checked by multiple tools to determine the best-predicted sequences to test (*see* Table 2).

Whole genome sequencing is the most robust method. However, it is also the most expensive and time-consuming and requires a reference genome to make inferences. Whole exome sequencing is also unbiased, but also requires a reference exome and will not indicate off-target events in noncoding regions of the genome. Thus, most studies utilize one of the other unbiased methods outlined in Table 2. For preclinical studies supporting clinical trials of CRISPR gene editing in HSPC, measurement of off-target effects by at least two different methods is recommended.

2 Materials

2.1 HSPC Culture

Institutional guidelines for collection of HSPC should be followed. Any use of cells or tissue procured from human subjects requires Institutional Review Board approval. This protocol follows after CD34⁺ cell purification of HSPCs from human bone marrow aspirate.

Priming of HSPC in serum-free media conditions that support cycling while maintaining stemness is a typical first step in every CRISPR gene editing experiment [43]. Culture media for bone marrow-derived CD34⁺ cells is StemSpan SFEM II Media (Stem Cell Technologies) with 100 ng/mL each of stem cell factor (SCF), thrombopoietin (TPO), and *fms*-like tyrosine kinase 3 (*flt3*) ligand. Dulbecco's phosphate-buffered saline (D-PBS) was purchased from Thermo Fisher.

2.2 Gene Editing Reagents and Equipment

The most well-described method for CRISPR-mediated gene editing in HSPC includes CRISPR-Cas9 delivered to HSPC as an RNP complex through electroporation [20, 36, 44–46]. Purified Cas9 protein (Aldevron, Thermo Fisher, Abcam) is paired with off-the-shelf gRNA (Integrated DNA Technologies, Synthego) for the

Table 2
Available CRISPR off-target analysis tools

In silico prediction assays	
Tool	Resources
Cas-OFFinder	http://www.rgenome.net/cas-offinder/ Offline version available [84]
CasFinder	http://arep.med.harvard.edu/CasFinder/ Doi: https://doi.org/10.1101/005074 [85]
E-CRISP	http://www.e-crisp.org/E-CRISP/index.html [86]
Breaking-cas	https://bioinfo.gp.cnb.csic.es/tools/breakingcas/ [87]
CRISPOR	http://crispor.tefor.net [88]
CHOPCHOP	https://chopchop.cbu.uib.no [89]
sgRNA designer	https://portals.broadinstitute.org/gpp/public/analysis-tools/sgrna-design [90]
CCTop	https://crispr.cos.uni-heidelberg.de [91]
GT-Scan	https://gt-scan.csiro.au [92]
CRISPR direct	https://crispr.dbcls.jp [93]
sgRNAcas9	Software package [94]
In vitro genome wide assays	
Assay	Resources
CIRCLE-Seq (Circularization for in vitro reporting of cleavage effects by sequencing)	[95] Github: https://github.com/tsailabSJ/circleseq
Digenome-Seq (Cas9-digested whole genome sequencing to profile genome-wide Cas9 off-target effects)	[96] Github: https://github.com/chizksh/digenome-toolkit2 http://www.rgenome.net/digenome-js/#!

(continued)

Table 2
(continued)

SITE-Seq (selective enrichment and identification of adapter-tagged DNA ends by sequencing)	[97] Protocol-DOI: 10.1038/protex.2017.043
Cell-based genome wide assay	
Assay	Resources
BLISS (Breaks Label In Situ and Sequencing)	[98]
GUIDE-Seq (Genome-wide, unbiased identification of double-strand breaks enabled by sequencing)	[99] Github: https://github.com/aryeelab/guideseq
LAM-HTGTS (linear-amplification-mediated high-throughput genome-wide sequencing)	[100] Github: http://robinmeyers.github.io/transloc_pipeline/index.html
DISCOVER-Seq (Discovery of In situ Cas off-targets and verification by sequencing)	[101] Github: https://github.com/staciawyman/blender

targeted loci. To generate custom gRNA, there are multiple online tools available such as the Benchling CRISPR Guide RNA Design Tool (www.benchling.com/crispr/), and most commercial sources of synthetic gRNAs host their own online tool. Similar tools exist for ssODN (Integrated DNA Technologies) design if attempting HDR.

Electroporation is carried out using the Lonza P3 Primary Nucleofection Kit with the Lonza Nucleofector™ System and supplied electroporation buffer.

Additional delivery methods include encoded CRISPR nuclease transgenes and gRNA cassettes packaged into virus-like vector agents like retroviral, lentiviral, or adenoviral vectors, along with nonviral transfection agents such as poly(ethylenimine) (PEI), poly(L-lysine) (PLL), and lipofectamine. Viral vectors require specific packing methods and development, while most nonviral vectors are produced commercially and should be used according to manufacturer's requirements. Generally viral vectors have higher transfection efficiencies but can be immunogenic. For some retroviral vectors, semirandom genomic integration of the proviral cassette has led to genomic instability in HSPCs. Also under investigation are nanoparticle constructs such as colloidal gold cores, which carry CRISPR-Cas and ssODN into HSPC with the combined advantages of viral and nonviral methods [10].

2.3 Analysis Reagents

Analysis of in vitro and in vivo HSPC fitness in response to treatments, gene editing efficiency at the genomic locus of interest, and in silico and unbiased evaluations of off-target CRISPR-Cas activity

are recommended. All primers, oligonucleotides, and gRNA were purchased from Integrated DNA Technologies, gDNA extraction was performed with a Purelink Genomic DNA Mini Kit (Invitrogen) preanalysis. Primers were designed through PrimerBLAST software (NCBI).

Viability was determined via the trypan blue dye exclusion assay [47]. A 10 μL volume of 0.4% trypan blue dye (Gibco) is mixed with an equal volume of HSPC cell suspension, then 10 μL of this mixture is transferred to a Countess II automated hemocytometer (Thermo Fisher).

3 Methods

3.1 HSPC Priming in Culture

1. Thawed or freshly purified HSPC should be seeded in cytokine-rich supportive media, typically at a density of $0.25\text{--}1.0 \times 10^6$ cells/mL and incubated at 37 °C, 5% CO₂, and 5–21% O₂ with 85% relative humidity.
2. HSPC should be maintained in culture for 3–48 h (<1–2 days). If cultures exceed 2×10^6 cells/mL, additional media or sub-culturing should be performed to maintain optimal viability and cycling.

3.2 Electroporation and Transduction

1. After priming, harvest HSPC and determine the number and viability of HSPC using the trypan blue dye exclusion assay.
2. Prewarm an aliquot of cytokine-rich supportive media to 37 °C.
3. Prepare electroporation solution or commercial reagents per manufacturer's recommendations. Electroporation reagents are optimized for each cell type and electroporation device. Most commercial device manufacturers have specific recommendations for optimized HSPC reagents available for purchase.
4. Prepare RNP complexes by slowly adding a molar excess of gRNA to Cas9 and incubating at room temperature for 5 min. The optimal molar ratio of nuclease protein to gRNA will be different for each CRISPR-Cas system. Ratios from 1:2 to 1:5 have been reported to be effective.
5. Harvest and pellet HSPC by centrifugation using conditions appropriate for the species being tested. Generally, 300–800 rcf for 5–10 min at room temperature with the brake on is considered sufficient.
6. Remove as much supernatant as possible without disturbing the cell pellet and resuspend the pellet in electroporation solution to form a single-cell suspension.

7. Mix the required volume of cell suspension (determined by the electroporator cuvette size) with the prepared RNP solution and mix via pipetting to maintain a single-cell suspension.
8. (Optional) Addition of ssODN (0.1 μmol) for simultaneous electroporation with RNP. ssODN should be added to the cell suspension at the same time as RNP.
9. Immediately transfer HSPC to cuvette and perform electroporation as recommended by the program or determined experimentally for optimal performance.
10. Immediately following electroporation, add prewarmed cytokine-rich HSPC supportive media to cuvette and transfer HSPC to a sterile, culture vessel. The final cell density should be the same as that used for priming culture. For human HSPC, a density of $0.25\text{--}1 \times 10^6$ cells/mL is recommended.
11. (Optional) AAV donor vector can be added immediately to electroporated cells, or after cells have rested in culture for up to 48 h.
12. Add cytokine-rich HSPC supportive media to maintain cells at optimal cell density and culture for an additional 2–3 days after electroporation and/or transduction before analysis.

3.3 Analysis of CRISPR Gene Edited HSPC

1. Harvest HSPC from each sample and pellet cells by centrifugation at 300–800 rcf at room temperature with the brake on.
2. Carefully remove as much supernatant as possible without disturbing the cell pellets.
3. Resuspend cell pellet in sterile D-PBS and determine cell count and viability by trypan blue dye exclusion assay.
4. Aliquot HSPC from each sample for appropriate analyses for fitness, on-target gene editing and off-target activity. At the very minimum, on-target gene editing analysis should be performed. At maximum, cells should be distributed for colony-forming assay, flow cytometry for phenotype and viability, gDNA extraction for on- and off-target gene editing analysis with sufficient gDNA for two different methods of detecting off-target activity, and finally retransplantation into conditioned recipients for in vivo analysis.

3.4 Extraction of gDNA from Bulk HSPC and Peripheral Blood Following Transplantation

1. Commercially available kits such as the Qiagen DNeasy Blood and Tissue Kit are the recommended method for extracting gDNA from HSPC and should be applied according to the manufacturer's instructions.

3.5 Extraction of gDNA from Colony-Forming Cells

1. Individual colonies should be transferred from methylcellulose to a single well of a U-bottom, 96-well plate and diluted with sterile D-PBS and pipetting to create a single-cell suspension.
2. The 96-well plate should be centrifuged at 300–500 rcf for 5 min at room temperature with the brake on to pellet cells.
3. Invert the plate onto an absorbent paper towel to remove supernatant.
4. Resuspend cell pellets in an additional volume of sterile D-PBS to wash and repeat steps 2 and 3.
5. Add 25 μ L of DNA Extraction Solution to each cell pellet and mix by pipetting.
6. Transfer cells to a 96-well PCR-compatible plate and incubate at 60 °C for 10 min, then at 100 °C for an additional 10 min to complete gDNA extraction.
7. Store extracted gDNA at –20 °C for up to 1 year.

3.6 PCR Amplification and Sequencing of Target Genomic Loci of Interest

1. Prepare a PCR master mix sufficient for the number of samples to be tested plus one. PCR master mix should contain DNA polymerase, primers, nucleotides, and buffer. (Optional) if NGS will be used, primers should be designed to contain appropriate adaptors for the NGS platform of choice.
2. Distribute PCR master mix evenly across the appropriate number of thermocycler-compatible tubes.
3. Add extracted gDNA to each tube.
4. Run PCR on a thermocycler programmed with an initial denaturation step, then repeating cycles of denaturing, annealing, and extension, with a final hold at 4 °C. Sample PCR conditions include an initial denaturing step of 98 °C held for 30 s, followed by 35 cycles of 98 °C for 30 s, then 60 °C for 30 s and then 72 °C for 30 s for each kb of desired amplicon length, then a final extension step of 72 °C for 5 min followed by an infinite hold at 4 °C.
5. PCR products should be resolved alongside an appropriate DNA ladder in the presence of a dye on a 1–2% (wt/vol) agarose gel under electrophoresis at 100 V to confirm amplicon size. Monitoring the dye front facilitates visualization of DNA progress through the gel to prevent overrunning.
6. Resolved PCR products can be excised and purified from the agarose gel using any number of commercially available gel purification kits (NucleoSpin Gel and PCR Cleanup Kit, Macherey-Nagel) according to the manufacturer's instructions. Alternatively, PCR products can be subjected to a PCR clean-up using commercially available kits according to the manufacturer's instructions.

7. Sanger sequencing (Applied Biosystems 3730xl DNA Analyzer system) can be performed using appropriate primers from the PCR amplification. For NGS, resulting PCR products should be subjected to NGS library preparation and sequencing.
8. Resulting sequence reads should be aligned to the reference genome to determine resulting gene editing outcomes (TIDER software). Some HDR events can be noticeable by changes in band sizes across samples resolved by agarose gel electrophoresis but should still be sequenced for validation and quantitation.

3.7 Analysis of Off-Target Effects

For analysis of off-target activity at in silico predicted genomic loci, the same steps described above for gDNA extraction, PCR amplification, and sequencing in subheadings 3.5 and 3.6 can be performed with primers unique for each predicted locus. For all other methods, refer to the protocols referenced in Table 2.

4 Notes

Notes which refer to a specific step in the methods section are prefaced with **Subheading (Section Number), Step (Number)**.

4.1 Controls

Controls should be included to permit interpretation of on-target gene editing results, off-target activity, and implications for HSPC performance or “fitness.” Recommended controls include a targeting control or “mock” sample, which receives the same treatments as other HSPC, but no CRISPR-Cas system. For example, an HSPC sample, which is primed and electroporated without CRISPR-Cas. If an HDT is included, the targeting control should be split into two samples, one that receives HDT and one that does not.

4.2 HSPC Media Selection

Basic media components depend upon the HSPC type and can use commercially available stem cell media formulation such as the StemSpan Serum Free Expansion Media (Stem Cell Technologies) used here or X-Vivo (Lonza), StemPro-34 Serum Free Media (Thermo Fisher), etc. Generally, a cocktail of recombinant species-specific cytokines (i.e., growth factors; GFs) is added to this base media. The minimum GF cocktail used in human HSPC culture is stem cell factor (SCF), thrombopoietin (TPO), and fms-like tyrosine kinase 3 (flt3) ligand at 100 ng/mL each. Some groups also add interleukin-6 (IL-6) at the same concentration, as well as commercially available molecules, which have been reported to maintain stemness such as UM171 (Stem Cell Technologies; 35 nM) and Stem Regenin I (SRI: Cellagen Technologies; 0.75 μ M) [36].

Similar cocktails have been described for nonhuman primate HSPC [44]. Murine HSPC culture typically consists of the same base media options mentioned above, but growth factor cocktails and additional supplements vary more widely across experiments. Gundry et al. reported high efficiency CRISPR-Cas9 gene editing for both knock-out and knock-in in murine HSPC when media conditions included X-Vivo 15 or StemPro-34 media supplemented with 2% fetal bovine serum, murine SCF and TPO and at 50 ng/mL, and human IL-3 and IL-6 at 10 ng/mL each [20, 45]. In contrast, Tran et al. described highly efficient CRISPR-Cas9-mediated gene knock-in in murine HPSC cultured in StemSpan Serum Free Expansion Media II supplemented with 50 ng/mL of murine SCF, TPO and flt3, and human IL-11 [46]. The addition of antibiotics such as penicillin and streptomycin is variably reported. Again, the goal of the experiment should dictate the choice of HSPC media and supplements.

4.3 gRNA Search

Multiple studies have highlighted the need to test several (typically four to eight) gRNAs, depending on the number of available PAM sites in the targeted genomic locus of interest. In addition, both the target and nontarget DNA strand should be evaluated for cutting efficiency at least in vitro with a synthetic oligonucleotide or PCR product of the target genomic locus [25]. Testing in an HSPC-like cell line such as human-derived K562 cells (American Type Culture Collection (ATCC) cat. no. CCL-243) is highly recommended. The most potent gRNA(s) is typically synthesized by a commercial source with chemical modifications to promote stability once inside the cell. Chemical modifications typically include 2'-O-methylphosphorothioate or 2'-O-methyl 3' thiophonoacetate (thioPACE) on the three terminal nucleotides of both the 5' and 3' ends [17].

4.4 Analysis of HSPC Fitness

4.4.1 Flow Cytometry

Flow cytometry with species-specific antibodies to known HSPC markers can be combined with a viability stain to simultaneously measure both parameters. Typically, cell surface proteins are used as HSPC markers, which can permit FACS-based sorting of samples for more in-depth analyses. Example markers include CD34, CD133, CD38, CD45RA, CD90 (Thy1), and CD49f for human cells, purchasable from Biolegend, BD Biosciences, etc. Cells are suspended in BD FACS Presort Buffer (BD Biosciences) for analysis on a FACSymphony Flow Cytometer (BD Biosciences). Markers for murine HSPCs include CD150, CD48, Sca-1, B220, CD2, Cd3, CD8, Gr-1, and Ter119.

When wanting to fully track HSPC modification, it is important to consider the number of HSPCs on hand and the type of selection antibodies you are using. Importantly, viability dyes for use in flow cytometry come in two varieties: [1] “fixable” (i.e., those requiring cell fixation for staining), and [2] “nonfixable” (i.e., no cell fixation required). If FACS and further cell analysis is

to be performed, nonfixable dyes are recommended. One example of a fixable viability dye is the LIVE/DEAD kit from Thermo Fisher. Nonfixable viability dyes include DNA binding dyes, calcein AM, or SYTOX dyes (Thermo Fisher).

4.4.2 Colony-Forming Assay

The colony-forming assay in methylcellulose is used to determine the proportion of HSPC, which can form blood cell colonies and can be used to assess clonal gene editing efficiencies. Colony-forming assays are well described elsewhere and commercial reagents to perform these assays are available for most species [48, 49].

4.4.3 In Vivo Transplantation

The most robust analysis of HSPC fitness is repopulation potential in a myeloablated or myelosuppressed recipient. For mice, syngeneic transplantation is typical. In larger animal models such as canines and nonhuman primates, autologous transplantation is possible, but for human HSPC studies, primary and secondary xenotransplantation into immunocompromised mouse strains such as NSG™ (The Jackson Laboratory) is the recommended surrogate to autologous testing. Transplantation studies also permit longitudinal follow-up of gene editing levels and off-target effects in vivo.

4.5 Electroporation

Most commercial manufacturers of electroporation devices offer electroporation solutions and protocols preoptimized for HSPC. Other systems include Harvard Apparatus' BTX Square Wave Electroporator used with BTXpress Buffer, or the Thermo Fisher Neon Transfection System [50]. Alternatively, a standard electroporation solution consisting of 5 mM potassium chloride (KCl), 15 mM magnesium chloride (MgCl_2), 120 mM sodium phosphate $\text{Na}_2\text{HPO}_4/\text{NaH}_2\text{PO}_4$ (pH 7.2), and 50 mM mannitol can be made and stored at -20°C for up to 1 year. Each electroporation system has its own specifications and limitations, which should be carefully considered.

Subheading 3.2, Step 4

The total amount of CRISPR-Cas9 to be prepared depends on the number of cells to be electroporated and should not exceed a total volume equivalent to 20% of the electroporation volume.

After the centrifugation and isolation of HSPC, the cells should be divided into individual samples and controls. The ideal number of HSPC per μg of nuclease protein should be empirically determined, but for human HSPC, it has been shown to be as high as 200×10^6 HSPC/mL.

Subheading 3.2, Step 8

The standard HDT design includes the desired genetic change flanked by two homology arms. Typical homology arms range from 40 to >500 bases in length [51–53]. However, the optimal length and symmetry should be evaluated for each target genomic locus of interest. The optimal ssODN concentration to be added should be empirically determined, but 0.1 μ moles (1 μ L of a 100 μ M solution, \sim 1 μ g) is a standard amount.

Electroporation solutions for cells recommended here are different than those used for primary cells and are described in detailed protocols elsewhere [54].

Subheading 3.2, Step 9

The ideal time in culture to achieve optimal priming for gene editing is variable across species and should be empirically determined if not established in reported studies using the same culture conditions. Standard incubation time variance should be on the scale of 30 min–2 days, depending upon the exact system.

Extended periods of time in electroporation solution have been shown to reduce HSPC viability and efficiency of electroporation. Cells should be immediately electroporated after addition to media, then purified, and readded to growth media immediately.

Subheading 3.2 Step 11

One study suggests that transduction immediately after electroporation facilitates higher AAV uptake in human HSPC [43]. AAV transduction should proceed overnight or for a maximum of 24 h. The volume of AAV donor vector added should be \leq 20% of the total culture volume.

**4.6 PCR
Amplification and
Sequencing of
Genomic Target**

When starting PCR experiments, the standard rules for PCR primer design apply. Multiple primers should be tested for functionality and optimal annealing temperature using a gradient thermocycler and relevant DNA template.

Primers should be tested for specificity and activity prior to analysis. The target amplicon should be sufficient in size to permit analysis of large deletions, where applicable. Where knock-in of large templates is the goal, an “in-and-out” PCR strategy can be employed, which employs one primer in the homologous region outside of the insert and the other primer binds within the integrated DNA, preferably with two primer sets and PCR samples to identify both the 5' and 3' junctions of the edited locus.

4.7 CFU Analysis

Subheading 3.5, Step 1

Before beginning extraction of gDNA from a CFU, microscopy analysis of the colonies should be undertaken. This can reveal possible gene editing effects on the stemness of the modified cells.

References

1. Broeders M et al (2020) Sharpening the molecular scissors: advances in gene-editing technology. *iScience* 23:100789
2. Ishino Y et al (1987) Nucleotide sequence of the *iap* gene, responsible for alkaline phosphatase isozyme conversion in *Escherichia coli*, and identification of the gene product. *J Bacteriol* 169:5429–5433
3. Mojica FJ et al (2005) Intervening sequences of regularly spaced prokaryotic repeats derive from foreign genetic elements. *J Mol Evol* 60: 174–182
4. Anderson WF, Blaese RM, Culver K (1990) The ADA human gene therapy clinical protocol: points to consider response with clinical protocol. *Hum Gene Ther* 1:331–362
5. Bortesi L et al (2016) Patterns of CRISPR/Cas9 activity in plants, animals and microbes. *Plant Biotechnol J* 14:2203–2216
6. Avecilla ST et al (2016) How do I perform hematopoietic progenitor cell selection? *Transfusion* 56:1008–1012
7. Pickar-Oliver A, Gersbach CA (2019) The next generation of CRISPR-Cas technologies and applications. *Nat Rev Mol Cell Biol* 20: 490–507
8. Xu S, Luk K, Yao Q et al (2019) Editing aberrant splice sites efficiently restores beta-globin expression in beta-thalassemia. *Blood* 133:2255–2262
9. Agudelo D, Durringer A, Bozoyan L et al (2017) Marker-free coselection for CRISPR-driven genome editing in human cells. *Nat Methods* 14:615–620
10. Shahbazi R, Sghia-Highes G, Reid JL et al (2019) Targeted homology-directed repair in blood stem and progenitor cells with CRISPR nanoformulations. *Nat Mater* 18: 1124–1132
11. Thuronyi BW, Koblan LW, Levy JM et al (2019) Continuous evolution of base editors with expanded target compatibility and improved activity. *Nat Biotechnol* 37: 1070–1079
12. Anzalone AV, Randolph PB, Davis JR et al (2019) Search-and-replace genome editing without double-strand breaks or donor DNA. *Nature* 576:149–157
13. Zeng J, Wu Y, Ren C et al (2020) Therapeutic base editing of human hematopoietic stem cells. *Nat Med* 26:535–541
14. Newby GA, Yen JS, Woodard KJ et al (2021) Base editing of haematopoietic stem cells rescues sickle cell disease in mice. *Nature* 595: 295–302
15. Wu Y, Zeng J, Roscoe BP et al (2019) Highly efficient therapeutic gene editing of human hematopoietic stem cells. *Nat Med* 25: 776–783
16. Klompe SE, Vo PLC, Halpin-Healy TS et al (2019) Transposon-encoded CRISPR-Cas systems direct RNA-guided DNA integration. *Nature* 571:219–225
17. Hendel A, Bak RO, Clark JT et al (2015) Chemically modified guide RNAs enhance CRISPR-Cas genome editing in human primary cells. *Nat Biotechnol* 33:985–989
18. Osborn MJ, Webber BR, Knipping F et al (2016) Evaluation of TCR gene editing achieved by TALENs, CRISPR/Cas9, and megaTAL nucleases. *Mol Ther* 24:570–581
19. Schumann K, Lin S, Boyer E et al (2015) Generation of knock-in primary human T cells using Cas9 ribonucleoproteins. *Proc Natl Acad Sci U S A* 112:10437–10442
20. Gundry MC, Brunetti L, Lin A et al (2016) Highly efficient genome editing of murine and human hematopoietic progenitor cells by CRISPR/Cas9. *Cell Rep* 17:1453–1461
21. DeWitt MA, Magis W, Bray NL et al (2016) Selection-free genome editing of the sickle mutation in human adult hematopoietic stem/progenitor cells. *Sci Transl Med* 8: 360ra134
22. Lau CH, Tin C (2019) The synergy between CRISPR and chemical engineering. *Curr Gene Ther* 19:147–171
23. Ortinski PI, O'Donovan BO, Dong X et al (2017) Integrase-deficient lentiviral vector as an all-in-one platform for highly efficient CRISPR/Cas9-mediated gene editing. *Mol Ther Methods Clin Dev* 5:153–164

24. Maggio I, Zittersteijn HA, Wang Q et al (2020) Integrating gene delivery and gene-editing technologies by adenoviral vector transfer of optimized CRISPR-Cas9 components. *Gene Ther* 27:209–225
25. Ran FA, Hsu PD, Wright J et al (2013) Genome engineering using the CRISPR-Cas9 system. *Nat Protoc* 8:2281–2308
26. Tycko J, Myer VE, Hsu PD (2016) Methods for optimizing CRISPR-Cas9 genome editing specificity. *Mol Cell* 6:355–370
27. Nishimasu H, Shi X, Ishiguro S et al (2018) Engineered CRISPR-Cas9 nuclease with expanded targeting space. *Science* 361:1259–1262
28. Kleinstiver BP, Sousa AA, Walton RT et al (2019) Engineered CRISPR-Cas12a variants with increased activities and improved targeting ranges for gene, epigenetic and base editing. *Nat Biotechnol* 37:276–282
29. Cortizas EM, Zahn A, Hajjar MR et al (2013) Alternative end-joining and classical nonhomologous end-joining pathways repair different types of double-strand breaks during class-switch recombination. *J Immunol* 191:5751–5763
30. Yu KR, Natanson H, Dunbar CE (2016) Gene editing of human hematopoietic stem and progenitor cells: promise and potential hurdles. *Hum Gene Ther* 27:729–740
31. Yeh CD, Richardson CD, Corn JE (2019) Advances in genome editing through control of DNA repair pathways. *Nat Cell Biol* 21:1468–1478
32. Roth TL, Puig-Saus C, Yu R et al (2018) Reprogramming human T cell function and specificity with non-viral genome targeting. *Nature* 559:405–409
33. Hornung V, Latz E (2010) Intracellular DNA recognition. *Nat Rev Immunol* 10:123–130
34. Yoshimi K, Kunihiro Y, Kaneko T et al (2016) ssODN-mediated knock-in with CRISPR-Cas for large genomic regions in zygotes. *Nat Commun* 7:10431–10431
35. Miura H, Quadros RM, Gurumurthy CB et al (2018) Easi-CRISPR for creating knock-in and conditional knockout mouse models using long ssDNA donors. *Nat Protoc* 13:195–215
36. Bak RO, Dever DP, Porteus MH (2018) CRISPR/Cas9 genome editing in human hematopoietic stem cells. *Nat Protoc* 13:358–376
37. Khan IE, Hirata RK, Russell DW (2011) AAV-mediated gene targeting methods for human cells. *Nat Protoc* 6:482–501
38. Grieger JC, Choi VW, Samulski RJ (2006) Production and characterization of adeno-associated viral vectors. *Nat Protoc* 1:1412–1428
39. Fu Y, Folden JA, Khayter C et al (2013) High-frequency off-target mutagenesis induced by CRISPR-Cas nucleases in human cells. *Nat Biotechnol* 31:822–826
40. Sentmanat MF, Peters ST, Florian CP et al (2018) A survey of validation strategies for CRISPR-Cas9 editing. *Sci Rep* 8:888
41. Brinkman EK, Chen T, Amendola M et al (2014) Easy quantitative assessment of genome editing by sequence trace decomposition. *Nucleic Acids Res* 42:e168
42. Martin F, Sanchez-Hernandez S, Gutierrez-Guerrero A et al (2016) Biased and unbiased methods for the detection of off-target cleavage by CRISPR/Cas9: an overview. *Int J Mol Sci* 17(9):1507
43. Charlesworth CT, Camarena J, Cromer MK et al (2018) Priming human repopulating hematopoietic stem and progenitor cells for Cas9/sgRNA gene targeting. *Mol Ther Nucleic Acids* 12:89–104
44. Humbert O, Radtke S, Samuelson C et al (2019) Therapeutically relevant engraftment of a CRISPR-Cas9-edited HSC-enriched population with HbF reactivation in nonhuman primates. *Sci Transl Med* 11:eaaw3768
45. Brunetti L, Gundry MC, Kitano A et al (2018) Highly efficient gene disruption of murine and human hematopoietic progenitor cells by CRISPR/Cas9. *J Vis Exp* 10:57278
46. Tran NT, Sommermann T, Graf R et al (2019) Efficient CRISPR/Cas9-mediated gene knockin in mouse hematopoietic stem and progenitor cells. *Cell Rep* 28:3510–3522 e5
47. Kaltenbach JP, Kaltenbach MH, Lyons WB (1958) Nigrosin as a dye for differentiating live and dead ascites cells. *Exp Cell Res* 15:112–117
48. Kerenyi MA (2014) LT-HSC methylcellulose assay. *Bio Protoc* 4(5). <https://doi.org/10.21769/BioProtoc.1067>
49. Wognum B, Yuan N, Lai B et al (2013) Colony forming cell assays for human hematopoietic progenitor cells. *Methods Mol Biol* 946:267–283
50. Kuo CY, Long JD, Campo-Fernandez B et al (2018) Site-specific gene editing of human hematopoietic stem cells for X-linked Hyper-IgM syndrome. *Cell Rep* 23:2606–2616
51. Thomas KR, Folger KR, Capecchi MR (1986) High frequency targeting of genes to specific

- sites in the mammalian genome. *Cell* 44: 419–428
52. Chen F, Pruett-Miller HY et al (2011) High-frequency genome editing using ssDNA oligonucleotides with zinc-finger nucleases. *Nat Methods* 8:753–755
 53. Davis L, Maizels N (2014) Homology-directed repair of DNA nicks via pathways distinct from canonical double-strand break repair. *Proc Natl Acad Sci U S A* 111: E924–E932
 54. Laustsen A, Bak RO (2019) Electroporation-based CRISPR/Cas9 gene editing using Cas9 protein and chemically modified sgRNAs. *Methods Mol Biol* 1961:127–134
 55. Jinek M, Chylinski K, Fonfara I et al (2012) A programmable dual-RNA-guided DNA endonuclease in adaptive bacterial immunity. *Science* 337:816–821
 56. Mali P, Yang L, Esvelt KM et al (2013) RNA-guided human genome engineering via Cas9. *Science* 339:823–826
 57. Cong L, Ran FA, Cox D et al (2013) Multiplex genome engineering using CRISPR/Cas systems. *Science* 339:819–823
 58. Slaymaker IM, Gao L, Zetsche B et al (2016) Rationally engineered Cas9 nucleases with improved specificity. *Science* 351:84–88
 59. Kleinstiver BP, Pattanayak V, Prew MS et al (2016) High-fidelity CRISPR-Cas9 nucleases with no detectable genome-wide off-target effects. *Nature* 529:490–495
 60. Chen JS, Dagdas YS, Kleinstiver BP et al (2017) Enhanced proofreading governs CRISPR-Cas9 targeting accuracy. *Nature* 550:407–410
 61. Fonfara I, Richter H, Bratovic M et al (2016) The CRISPR-associated DNA-cleaving enzyme Cpf1 also processes precursor CRISPR RNA. *Nature* 532:517–521
 62. Kleinstiver BP, Tsai SQ, Prew MS et al (2016) Genome-wide specificities of CRISPR-Cas Cpf1 nucleases in human cells. *Nat Biotechnol* 34:869–874
 63. Kim D, Kim J, Hur JK et al (2016) Genome-wide analysis reveals specificities of Cpf1 endonucleases in human cells. *Nat Biotechnol* 34:863–868
 64. Safari F, Zare K, Negahdaripour M et al (2019) CRISPR Cpf1 proteins: structure, function and implications for genome editing. *Cell Biosci* 9:36
 65. Abudayyeh OO, Gootenberg JS, Konermann S et al (2016) C2c2 is a single-component programmable RNA-guided RNA-targeting CRISPR effector. *Science* 353:aaf5573
 66. Cox DBT, Gootenberg JS, Abudayyeh OO et al (2017) RNA editing with CRISPR-Cas13. *Science* 358:1019–1027
 67. Abudayyeh OO, Gootenberg JS, Essletzbichler et al (2017) RNA targeting with CRISPR-Cas13. *Nature* 550:280–284
 68. Konermann S, Lotfy P, Brideau NJ et al (2018) Transcriptome engineering with RNA-targeting type VI-D CRISPR effectors. *Cell* 173:665–676
 69. Granados-Riveron JT, Aquino-Jarquín G (2018) CRISPR-Cas13 precision transcriptome engineering in cancer. *Cancer Res* 78: 4107–4113
 70. Makarova KS, Wolf YI, Alkhnbashi OS et al (2015) An updated evolutionary classification of CRISPR-Cas systems. *Nat Rev Microbiol* 13:722–736
 71. Harrington LB, Burstein D, Chen JS et al (2018) Programmed DNA destruction by miniature CRISPR-Cas14 enzymes. *Science* 362:839–842
 72. Moon SB, Kim DY, Ko J-H et al (2019) Recent advances in the CRISPR genome editing tool set. *Exp Mol Med* 51:130
 73. Al-Shayeb B, Sachdeva R, Chen L-X et al (2020) Clades of huge phages from across Earth's ecosystems. *Nature* 578:425–431
 74. Pausch P, Al-Shayeb B, Bisom-Rapp E et al (2020) CRISPR-CasPhi from huge phages is a hypercompact genome editor. *Science* 369: 333–337
 75. Dolan AE, Hou Z, Xiao Y et al (2019) Introducing a spectrum of long-range genomic deletions in human embryonic stem cells using Type I CRISPR-Cas. *Mol Cell* 74: 936–950 e5
 76. Morisaka H, Yoshimi K, Okuzaki Y et al (2019) CRISPR-Cas3 induces broad and unidirectional genome editing in human cells. *Nat Commun* 10:5302
 77. Ran FA, Hsu PD, Lin C-Y et al (2013) Double nicking by RNA-guided CRISPR Cas9 for enhanced genome editing specificity. *Cell* 154:1380–1389
 78. Mal P, Aach J, Stranges PB et al (2013) CAS9 transcriptional activators for target specificity screening and paired nickases for cooperative genome engineering. *Nat Biotechnol* 31: 833–838
 79. Guilinger JP, Thompson DB, Liu DR (2014) Fusion of catalytically inactive Cas9 to FokI nuclease improves the specificity of genome modification. *Nat Biotechnol* 32:577–582
 80. Rees HA, Liu DR (2018) Base editing: precision chemistry on the genome and

- transcriptome of living cells. *Nat Rev Genet* 19:770–788
81. Gaudelli NM, Komar AC, Rees HA (2017) Programmable base editing of A*T to G*C in genomic DNA without DNA cleavage. *Nature* 551:464–471
 82. Strecker J, Ladha A, Gardner Z et al (2019) RNA-guided DNA insertion with CRISPR-associated transposases. *Science* 365:48–53
 83. Hess GT, Fresard L, Han K et al (2016) Directed evolution using dCas9-targeted somatic hypermutation in mammalian cells. *Nat Methods* 13:1036–1042
 84. Bae S, Park J, Kim JS (2014) Cas-OFFinder: a fast and versatile algorithm that searches for potential off-target sites of Cas9 RNA-guided endonucleases. *Bioinformatics* 30:1473–1475
 85. Aach J, Mali P, Church GM (2014) CasFinder: flexible algorithm for identifying specific Cas9 targets in genomes (unpublished). *bioRxiv*. <https://doi.org/10.1101/005074>
 86. Heigwer F, Kerr FG, Boutros M (2014) E-CRISP: fast CRISPR target site identification. *Nat Methods* 11:122–123
 87. Oliveros JC, Franch M, Tabas-Madrid D et al (2016) Breaking-Cas-interactive design of guide RNAs for CRISPR-Cas experiments for ENSEMBL genomes. *Nucleic Acids Res* 44:W267–W271
 88. Haeussler M, Schonig K, Eckert H et al (2016) Evaluation of off-target and on-target scoring algorithms and integration into the guide RNA selection tool CRISPOR. *Genome Biol* 17:148
 89. Labun K, Montague TG, Krause M et al (2019) CHOPCHOP v3: expanding the CRISPR web toolbox beyond genome editing. *Nucleic Acids Res* 47:W171–W174
 90. Sanson KR, Hanna RE, Hegde M et al (2018) Optimized libraries for CRISPR-Cas9 genetic screens with multiple modalities. *Nat Commun* 9:416
 91. Stemmer M, Thumberger T, Keyer M et al (2017) Correction: CCTop: an intuitive, flexible and reliable CRISPR/Cas9 target prediction tool. *PLoS One* 12:e0176619
 92. O'Brien A, Bailey TL (2014) GT-scan: identifying unique genomic targets. *Bioinformatics* 30:2673–2675
 93. Naito Y, Hino K, Bono H et al (2015) CRISPRdirect: software for designing CRISPR/Cas guide RNA with reduced off-target sites. *Bioinformatics* 31:1120–1123
 94. Xie S, Shen B, Zhang C et al (2014) sgRNA-cas9: a software package for designing CRISPR sgRNA and evaluating potential off-target cleavage sites. *PLoS One* 9:e100448
 95. Tsai SQ, Nguyen NT, Malagon-Lopez J et al (2017) CIRCLE-seq: a highly sensitive in vitro screen for genome-wide CRISPR-Cas9 nuclease off-targets. *Nat Methods* 14:607–614
 96. Kim D, Bae S, Park J et al (2015) Digenome-seq: genome-wide profiling of CRISPR-Cas9 off-target effects in human cells. *Nat Methods* 12:37–43
 97. Cameron P, Fuller CK, Donohoue PD et al (2017) Mapping the genomic landscape of CRISPR-Cas9 cleavage. *Nat Methods* 14:600–606
 98. Yan WX, Mirzazadeh R, Garnerone S et al (2017) BLISS is a versatile and quantitative method for genome-wide profiling of DNA double-strand breaks. *Nat Commun* 8:15058
 99. Tsai SQ, Zheng Z, Ngguyen NT et al (2015) GUIDE-seq enables genome-wide profiling of off-target cleavage by CRISPR-Cas nucleases. *Nat Biotechnol* 33:187–189
 100. Hu J, Meyers RM, Dong J et al (2016) Detecting DNA double-stranded breaks in mammalian genomes by linear amplification-mediated high-throughput genome-wide translocation sequencing. *Nat Protoc* 11:53–871
 101. Wienert B, Wyman SK, Richardson CD et al (2019) Unbiased detection of CRISPR off-targets in vivo using DISCOVER-Seq. *Science* 364:286–289



Lentiviral Transduction of Nonhuman Primate Hematopoietic Stem and Progenitor Cells

Chuanfeng Wu, So Gun Hong, Aylin Bonifacino, and Cynthia E. Dunbar

Abstract

The nonhuman primate (NHP) animal model is an important predictive preclinical model for developing gene and cell therapies. It is also an experimental animal model used to study hematopoietic stem and progenitor cell (HSPC) biology, with the capability of serving as a step for the translation of the basic research concepts from small animals to humans. Lentiviral vectors are currently the standard gene delivery vehicles for transduction of HSPCs in the clinical setting. They have proven to be less genotoxic and more efficient than the previously used murine γ -retroviruses. Transplantation of lentiviral vector–transduced HSPCs into autologous macaques has been well developed over the past two decades. In this chapter, we provide detailed methodologies for lentiviral vector transduction of rhesus macaque HSPCs, including production and titration of lentiviral vector, purification of CD34⁺ HSPCs, and lentiviral vector transduction and assessment.

Key words Hematopoietic stem cell, Nonhuman primate, Lentiviral vector, Transduction, Gene therapy

1 Introduction

Hematopoietic stem cells (HSCs) are self-renewing and multipotent stem cells that can continuously differentiate into multiple hematopoietic lineages to maintain the blood and immune system. Allogeneic or autologous hematopoietic stem and progenitor cells (HSPCs) can be delivered to patients to regenerate hematopoiesis in clinical hematopoietic stem cell transplantation (HSCT) and have become standard therapies for a number of diseases, including hematological malignancies, bone marrow failure disorders, and immunological diseases. Over the past 30 years, gene therapies have been devised using gene therapy vectors that are able to integrate into the genome to deliver corrective genes via autologous transplantation of transduced HSPCs, thereby providing therapeutic gene products for the life of the individual [1]. The path to clinical application of these technologies has been challenging, due

to the complexity of gene transfer methodologies, the resistance of long-term repopulating HSPCs to genetic modification, and the genotoxic risks associated with the use of integrating viruses as gene transfer vectors. Lack of predictive *in vitro* or small animal models hampered progress, evidenced by disappointing results in early clinical HSPC clinical trials [2].

The nonhuman primate (NHP) animal model has great relevance to human biology and preclinical development, with comparable body size, life span, genomic parameters, and blood and immune system characteristics. NHP HSPCs have similar telomere lengths, phenotypes, and frequency to human HSPCs; respond to human hematopoietic cytokines; and generally react with antibodies developed against human cell surface antigens [3–5]. NHP HSPC transplantation has served as an important predictive preclinical model for the development of human HSPC transplantation and genetic modification therapies [2, 6–8]. In addition, NHPs can serve as an experimental animal model to study basic HSPC biology via genetic tagging of transplanted HSPCs, with the capability of bridging basic research findings between small animals and humans [4, 9–12]. The use of NHP and other improved preclinical models to optimize and test HSPC gene therapies has resulted in safer and more efficient viral vectors systems, more supportive *ex vivo* transduction methodologies, and improved pretransplantation conditioning, culminating in HSPC gene therapy trials demonstrating clinical efficacy for a number of serious human diseases, including severe immunodeficiencies, hemoglobinopathies, and central nervous system metabolic disorders, as summarized in recent reviews [1, 13].

HSPC-targeted gene therapies or tagging require the integration of transferred genes into the HSPC genome, ensuring passage of the new genetic material to all daughter cells. Lentiviral gene therapy vectors have proven to be safer gene delivery vehicles with a lower risk of genotoxicity compared to murine γ -retroviral vectors, and are capable of transducing quiescent cells, such as self-renewing long-term HSCs [14–16]. Researchers have optimized transduction conditions to both enhance lentiviral vector HSPC transduction efficiency and maintain HSPC function and engraftment ability during *ex vivo* culture via inclusion of specific supportive cytokines, use of culture dishes coated with a fibronectin fragment binding to VLA4 expressed on HSPCs [17], and addition of protamine sulfate to counteract repulsive electrostatic effects between target cells and vector particles [18]. A number of other adjuvants such as poloxamer 407 (P407) and prostaglandin E2 (PEG2) have also been demonstrated to increase the transduction efficiency of human HSPCs [19, 20].

Over the past three decades, the NHLBI NHP program has developed the rhesus macaque (RM) autologous transplantation model for the preclinical development of cell and gene therapies

and the investigation of primate hematopoiesis and immunology. In this chapter, we will provide detailed protocols for lentiviral transduction of transplantable RM HSPCs. Several other groups have also developed similar approaches for lentiviral transduction of HSPC from closely related NHP species, including cynomolgus or pigtail macaques [21, 22]. In general, macaque HSPCs are more resistant to transduction via lentiviruses than human HSPCs. Intracellular intrinsic “restriction factors” such as TRIM5 α prevent natural HIV infection of most macaque species and decrease the efficiency of transduction of macaque HSPCs with standard HIV-derived lentiviral vectors [23]. TRIM5 α binds to the HIV-1 viral capsid and facilitates degradation prior to integration. This block can be at least partially overcome by packaging of lentiviral vectors with a chimeric SIV/HIV capsid, given that SIV can evade TRIM5 α restriction, as shown by Uchida, Tisdale, and coworkers, and the protocols presented in this chapter utilize these chimeric vectors [24, 25]. In addition, we screen RMs to be used for lentiviral vector (LV) transduction studies for the presence of TRIM5 α polymorphisms, selecting those with alleles favoring more efficient transduction [26].

We currently utilize granulocyte-colony-stimulating factor (G-CSF)/plerixafor (AMD3100)-mobilized peripheral blood as a preferred source of HSPCs, given higher HSPC yields in mobilized blood compared to bone marrow and the extensive clinical use of mobilized peripheral blood stem cells (PBSCs); however, bone marrow HSPCs can be substituted without modification in our protocols if apheresis is not available or if the bone marrow is a more relevant source for preclinical investigations [27]. Details of our protocol for apheresis collection of macaque HSPCs have been previously published and are beyond the scope of this chapter [28, 29]. The mobilization regimen used in our facility currently is human recombinant G-CSF at a dose of 10–20 $\mu\text{g}/\text{kg}$ SQ daily for 5 days and a single dose of the CXCR4 antagonist AMD3100 (plerixafor) 1 mg/kg SQ 2–6 h prior to leukapheresis. Mobilized peripheral blood cells are collected via leukapheresis using the Fenwal CS-3000 cell separator blood cell separator. Readers are referred to protocols from other investigators describing use of currently available apheresis machines for collection from macaques, since the CS-3000 is no longer available [30].

The majority of our studies have utilized two doses of 500 rads total body irradiation (TBI) as conditioning prior to HSPC infusion. Details of this conditioning regimen and posttransplantation supportive care have been previously published [29]. This TBI dosing is close to the tolerable limit for macaques in terms of lung toxicity [31], but doses below 900 rads can result in rejection of HSPCs transduced with foreign transgenes such as GFP [32]. We have more recently explored busulfan as an alternative and more clinically applicable conditioning regimen, with

reasonable engraftment of transduced HSPCs, but rejection of foreign transgenes is an issue unless potent T cell immunosuppression is added to the regimen [33]. Finally, antibody-mediated depletion of endogenous HSPCs has been shown to be a nontoxic approach to pretransplantation conditioning in mice and is currently being explored in our NHP model [34, 35].

The optimal level of engrafted transduced HSPC depends on the experimental questions being asked. Many of our recent studies have focused on genetic barcoding of HSPC to investigate the frequency, engraftment dynamics, and lineage output of macaque HSPC [9–12]. For these studies, we target integration of the barcoded LV into no more than 10–30% of engrafting HSPCs to ensure that the vast majority of individual cells contain only a single barcode [36]. The methods detailed in this chapter result in long-term engraftment with transduced cells in this range following TBI conditioning, with greater than 80–90% of cells containing a single integrant per cell [9]. However, a much higher fraction of transduced HSPC or a higher number of vector copies per cell may be desirable for preclinical modeling of gene therapy efficacy and safety. We have added notations indicating where modifications may be used in an attempt to increase transduction efficiency. However, in our experience, the very high copy numbers achieved in hematopoietic cells long term in some human clinical trials cannot be reached in macaques with LVs, even using chimeric SIV/HIV packaging systems.

2 Materials

2.1 Animals

All RMs to be used for transplantation of HSPCs should be seronegative and/or viral genome-free for a number of potential pathogens (“specific pathogen free”), including simian type D retrovirus (SRV), simian immunodeficiency virus (SIV), simian T-lymphotropic virus (STLV), and Herpes B virus [37]. However, all RM cells and tissues should be handled as if they are infectious using Biosafety Level 2 or equivalent practices, due to the potential severity of zoonotic Herpes B virus transmission to humans. Before working with RM cells, institutional biosafety registrations and approvals should be obtained. Animals should be housed and handled conforming to all regulatory standards and enrolled in a protocol approved by an institutional animal care and use committee.

2.2 Lentivirus Production and Titration Reagents and Supplies

1. 293 T packaging cells (ATCC, USA).
2. HeLa cells (ATCC, USA).
3. Nunc TripleFlask cell culture flasks (Thermo Fisher Scientific, USA): This is a triple layer flask, providing a total of 500 cm²

surface area for cell attachment, but with the footprint of a single T175 flask. Use of these flasks saves incubator space and improves productivity when producing the large-scale lentivirus vector preparations required for RM experiments.

4. T175 flasks (Corning Costar, USA).
5. 12-well plates (Corning Costar, USA).
6. 50 mL conical polypropylene centrifuge tubes (Sarstedt, USA).
7. 15 mL conical polypropylene centrifuge tubes (Greiner bio-one, USA).
8. 1.5 mL conical polypropylene centrifuge tubes (Sarstedt, USA).
9. Electric pipette aids (Drummond Scientific, USA).
10. Phosphate-buffered saline (PBS) (Quality Biological, USA).
11. Trypsin-EDTA stock solution-0.05% (Thermo Fisher Scientific, USA).
12. Penicillin/streptomycin/glutamine (PSG) (Thermo Fisher Scientific, USA).
13. Iscove's modified Dulbecco's medium (IMDM) (Thermo Fisher Scientific, USA).
14. Dulbecco's modified Eagle medium (DMEM) (Thermo Fisher Scientific, USA).
15. Fetal bovine serum (FBS) (Sigma, USA).
16. I10 media: IMDM+10% FBS + 1% PSG.
17. I10 without antibiotics: IMDM+10% FBS.
18. D10 media: DMEM+10%FBS+ 1% PSG.
19. Sterile and endotoxin-free plasmid DNAs for transfection at concentrations of 1 μ g/mL:
 - (a) χ HIV (HIV-1 Gag/Pol-plus-sCA) plasmid: This plasmid expresses a chimeric HIV-1/SIV gag/pol capsid with improved ability to evade TRIM5 α restriction in macaque cells (can be obtained from John Tisdale at the NHLBI, Bethesda, MD, johntis@nih.gov).
 - (b) HIV-1/rev-tat plasmid.
 - (c) pCAGGS-VSV-G envelope plasmid.
 - (d) LV plasmid of choice.
20. 2 M CaCl₂ (Quality Biological, USA).
21. 2X HBS (see preparation instructions in Table 1).
22. Protamine sulfate (Sigma, USA).
23. Ultracentrifuge (Beckman Coulter, USA).
24. 0.45 micron vacuum filter bottle with a PES (Polyethersulfone) membrane (Thermo Fisher Scientific, USA).

Table 1
2X HBS buffer preparation

Component	Volume or mass
5 M NaCl	56 mL
KCl (FW: 75.55 g/mole)	0.74 g
Na ₂ HPO ₄ × 7 H ₂ O (FW: 268.07 g/mole)	0.40 g
Dextrose	2.00 g
1 M HEPES	50 mL
Adjust the final volume to	1 L
Adjust the pH to	7.05

2.3 CD34
Immunoabsorption
Reagents and Supplies

1. Ficoll density separation media (GE Healthcare, USA).
2. 1 × Red Cell Lysis solution (BD Pharmingen, USA).
3. Phosphate-buffered saline (PBS) without Ca⁺⁺ and Mg⁺⁺ (Thermo Fisher Scientific, USA).
4. CD34 immunoselection antibody: anti-CD34 IgM hybridoma clone 12.8 was provided by Dr. Irwin Bernstein (Fred Hutchinson Cancer Center, Seattle, WA, USA).
5. IgM microbeads (Miltenyi Biotec, USA).
6. LS MACS separation columns (Miltenyi Biotec, USA).
7. VarioMACS Separator (Miltenyi Biotec, USA).
8. Recovery™ Cell Culture Freezing Medium for freezing CD34-negative MNCs (Thermo Fisher Scientific, USA).
9. CryoStor™ CS10 Freezing Medium for freezing CD34-positive cells (STEMCELL Technologies, USA).
10. 100 µm cell strainer (Falcon Corning, USA).
11. 40 µm cell strainer (Falcon Corning, USA).
12. PE-conjugated mouse Anti-human CD34 antibody (clone 563) (BD Pharmingen, USA).
13. 0.5 M EDTA, pH 8.0, RNase-free (Thermo Fisher Scientific, USA).
14. Bovine albumin fraction (BSA) V, 7.5% solution (Thermo Fisher Scientific, USA).
15. Separation buffer: add 2 mL of 0.5 M EDTA and 38 mL of 7.5% BSA to 500 mL PBS. Store at 4 °C.

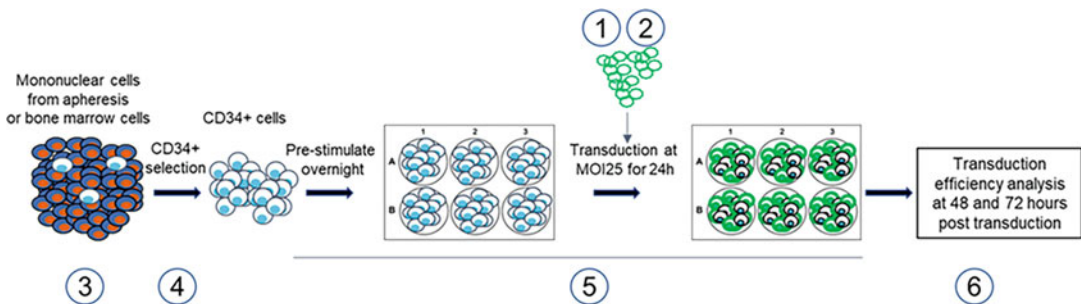
2.4 Transduction
Reagents and Supplies

1. 6-well plates (Corning Costar, USA)
2. 12-well plates (Corning Costar, USA)

3. RetroNectin®: recombinant human fibronectin (FN) fragment (Takara, USA).
4. Protamine sulfate (Sigma, USA).
5. 2.5% HEPES (Corning Cellgro, USA) in HBSS (Corning Cellgro, USA) buffer
6. X-Vivo10 serum-free hematopoietic cell medium (Lonza, USA).
7. Human recombinant stem cell factor (SCF), (Miltenyi Biotec, USA).
8. Human recombinant FMS-related tyrosine kinase 3 ligand: (FLT3L), (Miltenyi Biotec, USA).
9. Human recombinant thrombopoietin (TPO), (Miltenyi Biotec, USA).
10. Human serum albumin (HSA), (Grifols Biologicals, USA).

3 Methods

Figure 1 summarizes the overall workflow. Detailed procedures are described in Subheadings 3.1, 3.2, 3.3, 3.4, 3.5.



Workflow:

- 1-2: Lentiviral vector production and titration.
- 3: NHP HSPCs collection.
- 4: CD34⁺ HSPCs immunoselection.
- 5: Transduction of NHP CD34⁺ HSPCs.
- 6: Transduction efficiency analysis.

Fig. 1 Schematic of workflow for NHP CD34⁺ HSPCs column enrichment and ex vivo LV transduction. Numbers ① to ⑥ label the procedures/steps in this workflow, and detailed protocols are described in Subheading 3 Methods. ① and ②: preparation of LV for transduction, ③ and ④: mononuclear cell purification and positive immunoselection for CD34⁺ HSPCs. ⑤: HSPCs ex vivo lentivirus transduction. ⑥: analysis of transduction efficiency in HSPCs following transduction

3.1 *Lentivirus* *Production via* *Transient Transfection*

The χ HIV (HIV-1 Gag/Pol-plus-sCA) chimeric HIV/SIV packaging plasmid is substituted for a standard HIV-based plasmid during production of LV vector particles to be used for transduction of macaque HSPCs to avoid TRIM5 α -restriction and improve transduction efficiency. Any standard HIV-1-based vector can be produced using this 4 plasmid transfection system. The amount of vector required for autologous transplantation of a RM will need to be calculated based on expected CD34⁺ cell dose and the desired multiplicity of infection (MOI) defined as the ratio of vector particles to target CD34⁺ cells. We use an MOI of 25, but this can be adjusted based on desired transduction efficiency and small-scale testing of vector preparations. The protocol below is based on producing at least enough vectors for a single macaque transduction and transplantation experiment. For example, if we aim to transplant a RM with 30 million HSPCs (or a dose of five million CD34⁺ cells/kg for a 6 kg young adult animal) at a transduction MOI of 25, a total of 7.5×10^8 LV particles will be needed. This will require setting up approximately 25 triple flasks, given that one triple-layer flask produces an average of 3×10^7 vector particles when working with a vector of average size and conventional design. Larger vectors or those with transgenes in reverse orientation may be more difficult to produce at high titer.

1. Day 0 (9:00 am): Plate Nunc triple flasks with 293 T cells.
Plate 50 million 293 T cells in 70 mL I10 medium per each Nunc triple flask. Seeding smaller numbers of cells farther in advance is also feasible and may assure better cell adhesion: 35–40 million cells plated on day –1. Plate as many as flasks as needed based on how many vector particles are required, that is, for small scale in vitro studies versus an actual transplantation experiment.
2. Day 1 (5:00 pm): Transfect 293 T cells (the cells should be at approximately 80% confluency).
 - (a) For each triple flask, combine CaCl₂, the four vector and helper plasmids, and water in a 50 mL Falcon conical tube to create a “plasmid/CaCl₂ mix” (amounts listed in Table 2). The total volume produced can be adjusted based on the cell culture surface if alternate-sized flasks or dishes are used to culture 293 T cells (*see Note 1*).
 - (b) Measure volume of 2X HBS equal to the volume of the plasmid/CaCl₂ mix and transfer into a second 50 mL Falcon tube.
 - (c) (*see Note 2*). Set the discharge rate to “fast” on one pipette aid, connect a sterile 5 mL pipette, place into the 2X HBS 50 mL Falcon tube, and gently bubble air through the solution.

Table 2
Transfect solution preparation

	Plasmid size (kb)	Concentration (ug/uL)	DNA per triple flask (ug)	Volume per triple flask (ml)
Lentivirus vector plasmid	7.8	1.00	150	0.150
χ HIV Gag-Pol plasmid	12.3	1.00	90	0.090
HIV-1/Rev-Tat plasmid	4	1.00	30	0.030
pCAGGS-VSV-G plasmid	7.9	1.00	30	0.030
CaCl ₂		2 M		4.6
Water				5.6
Subtotal				
2X HBS				5.6

- (d) Set the discharge rate on a second pipette aid to “slow,” connect a sterile 5 mL pipette, draw up the plasmid/CaCl₂ mix, and carefully drip the solution drop by drop into the bubbling 2X HBS mixture.

Note: As the two solutions mix, the mixture should become cloudy due to formation of the expected fine particulate precipitate. If the rate of dripping is too fast, larger particles will form that are less efficient in transfection of 293 T cells.

- (e) Incubate the plasmid/CaCl₂/HBS mixture at room temperature for 30 min.
- (f) Vortex the plasmid/CaCl₂/HBS mixture well to break up any large precipitates that may have formed.
- (g) Combine the plasmid/CaCl₂/HBS mixture with I10 media without antibiotics to reach a total volume of 70 mL per triple flask of 293 T cells to be transfected.
- (h) Aspirate the old culture media from the 293 T-containing flasks and then gently add the transfection media 70 mL per triple flask without disturbing the cell layer.
3. **Day 2 (9:00 am, 16–18 hours posttransfection):** Remove transfection media and replace with 70 mL of fresh I10 media for each triple flask.
4. **Day 3–5 (9:00 am daily):** Collect vector-containing media 24 h, 48 h, and 72 h post addition of fresh media following transfection. Each day remove media from the cells, filter through 0.45 μ m filter, and store at 4 °C. Add fresh 70 mL of I10 media to each triple flask on days 3 and 4 after collecting

media, then discard the flasks at day 5 after collecting the final vector-containing supernatant.

5. **Day 5:** Collect and then concentrate vector by ultracentrifugation.
 - (a) Combine all the filtered vector-containing supernatants and transfer into sterile 250 mL ultracentrifuge bottles.
 - (b) Centrifuge the bottles in a JLA 10.5 rotor at maximum speed ($18,600\times g$), at maximum acceleration with deceleration off for 2 h at 4 °C.
 - (c) Carefully discard all supernatant into a biological/chemical waste container, carefully avoiding disturbance of the pellet.
 - (d) Pipette 250 μ L of X-Vivo10 media directly onto each vector pellet.
 - (e) Place the bottle(s) onto wet ice in a Styrofoam container or cooler, oriented so that the X-Vivo 10 is covering the pellet (complete coverage is critical), and place the container on a shaker (140 bpm/min) for 30 min.
 - (f) Pipette the liquid up and down to make sure the virus pellet is dissolved, and combine all the vector from each of the bottles into a 15 mL Falcon tube.
 - (g) Aliquot vector into 1.5 mL tubes for storage. First, transfer 9 μ L into a 1.5 mL microcentrifuge tube for titration. Aliquot the rest vector into 1.5 mL tube at 0.5 mL per tube. Freeze and store at -80 °C long term.

3.2 Vector Titration Using HeLa Cells

1. **Day 0 (9:00 am):** Seed HeLa cells at 100,000/well in all wells of a 12 well plate in 1.5 mL D10 medium per well. Swirl plate gently to ensure cells are well distributed within each well. Incubate overnight.
2. **Day 1 (5:00 pm):** Transduction of HeLa cells with vector preparation to be titrated.
 - (a) Prepare transduction media: D10 with 4 μ g/mL protamine sulfate.
 - (b) Trypsinize, count, and record the cell number from wells C1–4 (*see* Fig. 3, or any wells not being used for titration dilutions). The average cell number per well will be needed for titer calculations.
 - (c) Prepare serial dilutions of vector: In the first tube, mix a known amount (e.g., 9 μ L) of virus with 1.5 mL transduction medium, fill the rest of dilution tubes with 600 μ L transduction medium, and then perform serial dilutions by mixing the first tube and transferring 600 μ L transduction solution (virus+ transduction medium) to the next

tube. Continue for a total of at least 7 tubes (more if expect very high titer vector), as diagramed in Fig. 2.

- (d) Remove media from the HeLa cells plated in the 12 well plate, and transfer 500 μ L from each of the serial dilution tubes onto a well in the plate as shown in Fig. 3. The negative control well should have 500 μ L of D10 media added (*see Note 3*).
- (e) Place the plate of cells back in the cell culture incubator.

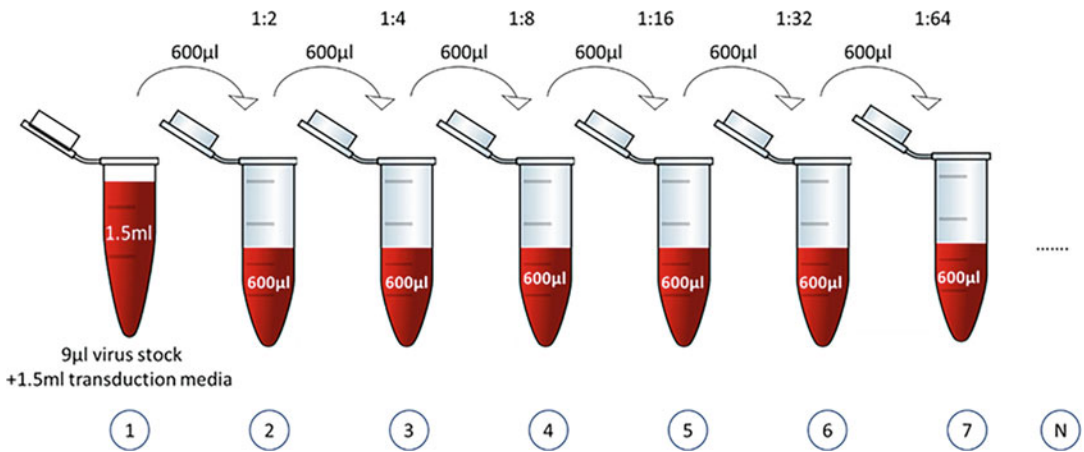


Fig. 2 Schematic of lentiviral vector serial dilution titration. Nine μ l virus stock is diluted in 1.5 ml transduction medium, then a serial 1:2 dilution is carried out over a total of 8 tubes, including a negative control without virus. Detailed procedures are described in Subheading 3.2, **step 2(c)**

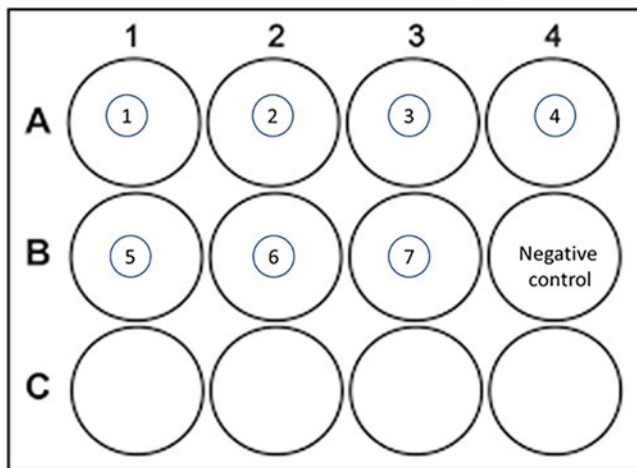


Fig. 3 Layout of a viral vector titration cell plate. Each well contains the same number of plated HeLa cells for transduction. Detailed procedures are described in Subheading 3.2, **step 2(b and d)**

Table 3
An example calculation to compute the vector titer in the original vector preparation

			Starting number of HeLa cells at day 1	
Well C1			240,000	
Well C2			220,000	
Well C3			190,000	
Well C4			200,000	
Average cell number			212,500	

Dilutions	Vector stock in each well (μL)	%GFP+	Starting vector particle number = (%GFP+ – Background)*average cell number	Vector particle/mL = Starting vector particle number/starting vector stock volume
1	3.000	96.3	204,425	6.81E+07
2	1.500	90.4	191,888	1.28E+08
3	0.750	70.2	148,963	1.99E+08
4	0.375	50.7	107,525	2.87E+08
5	0.188	35.4	75,013	4.00E+08
6	0.094	17.7	37,400	3.99E+08
7	0.047	8.9	18,700	3.99E+08
Negative (background)	0	0.1		
			Average titer (only take average from the linear change dilutions, such as 5–7 here)	3.99E+08

3. **Day 3:** Remove the transduction media from the titration plate and add 1.5 mL fresh D10 media to each well.
4. **Day 5:** Trypsinize the cells in each well and analyze by flow cytometry for GFP or another cell surface gene present in the vector (*see Note 4*).
5. Compute the vector titer in the original vector preparation, as shown in Table 3 in a sample calculation:

3.3 Purification of CD34⁺ HSPCs

1. Ficoll separation of mononuclear cells from mobilized peripheral blood cells or bone marrow.
 - (a) Transfer aliquots of ~10 mL of heparinized blood or marrow to 50 mL Falcon tubes and add PBS to reach a total volume of 35 mL per tube (i.e., for a 40 mL

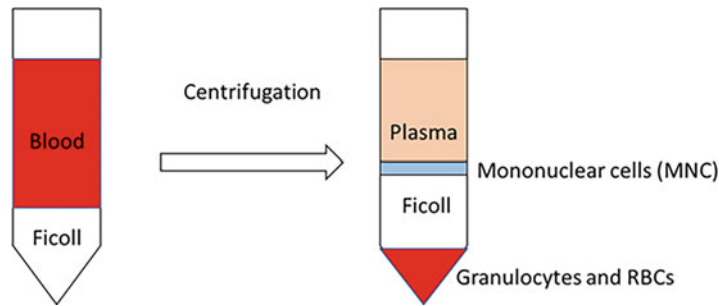


Fig. 4 Schematic of density sedimentation separation of mononuclear cells from red blood cells and granulocytes contained in a mobilized peripheral blood collection or a bone marrow aspiration. A cell suspension is layered onto Ficoll and following centrifugation, mononuclear cells are carefully collected from the interface between the Ficoll and the plasma layer, and granulocytes from the cell pellet

collection, transfer 10 mL blood or marrow and add 25 mL PBS to each of four 50 mL tubes.)

- (b) Add 15 mL Ficoll to each of an equal number of empty 50 mL Falcon tubes. Slowly pipette the 35 mL of diluted blood or marrow to each tube containing Ficoll.
 - (c) Centrifuge at 1600 rpm for 30 min at room temperature (RT).
 - (d) After centrifugation, the following components can be visualized from top to bottom as shown in Fig. 4.
 - (e) Carefully aspirate and discard the top layer (plasma) from the top of each tube, being careful not to disturb the MNC layer.
 - (f) Carefully aspirate with a pipette the MNC layer from each of four tubes and pool the layers into 2 new 50 mL tubes.
 - (g) Add PBS to the MNC tube to reach a total volume of 50 mL.
 - (h) Centrifuge at 1600 rpm at RT for 10 min.
 - (i) Aspirate the supernatant and leave 1 mL in the tube, being careful to not disturb the MNC pellet (*see Note 5*).
2. RBC lysis.
- (a) Resuspend pellet by pipetting up and down in the remaining 1 mL fluid, add 49 mL Red Cell Lysis solution to each tube.
 - (b) Incubate at RT for 30 min.
 - (c) Centrifuge at 1600 rpm for 10 min at RT.
 - (d) Aspirate all but ~1 mL of the supernatant.

- (e) Combine the remaining cells into one 50 mL tube and bring to 50 mL with PBS.
 - (f) Let the cell suspension run through a 100 μ m cell strainer.
 - (g) Count the cells.
 - (h) Centrifuge at 1600 rpm for 10 min at RT.
 - (i) Resuspend cells in 20 mL of PBS containing 2% BSA.
3. Antibody labelling.
- (a) Add 100 μ g of the anti-CD34 (clone 12.8) antibody (sufficient for up to 5×10^9 MNCs).
 - (b) Incubate the antibody-cell suspension for 30 min at RT on a rocker or with mild agitation.
 - (c) Wash to remove excess antibody by bringing the volume to 50 mL with PBS containing 2% BSA, centrifuge at 1600 rpm for 10 min at RT, and aspirate the supernatant.
 - (d) Resuspend cells in 20 mL of PBS containing 2% BSA.
 - (e) Add 2 mL IgM microbeads, mix well, and incubate for 30 min at RT on a rocker or with mild agitation.
 - (f) Add 30 mL of PBS containing 2% BSA, centrifuge at 1600 rpm for 10 min, and aspirate the supernatant.
 - (g) Resuspend the cells in 20 mL of separation buffer.
 - (h) Run the cell suspension through a 40 μ m cell strainer to remove cell clumps that could clog the separation columns.
4. CD34⁺ cell MACS separation.
- (a) Place one MACS LS separation column in the magnetic field of the VarioMACS Separator.
 - (b) Place a 50 mL collection tube under the column.
 - (c) Prime the column with 3 mL of separation buffer.
 - (d) Add 5 mL of the cell suspension with the total cell number up to 2×10^9 MNCs to the column.
 - (e) Allow the cell suspension to run through and collect the effluent as the CD34-negative fraction.
 - (f) Wash the column with 5 mL of separation buffer and collect a second CD34-negative fraction.
 - (g) Remove the column from the separator and place above a new collection tube labelled "stage 1 CD34⁺ cells."
 - (h) Apply 5 mL of separation buffer to the reservoir of the column and firmly flush out cells using the plunger supplied with the column. Discard the used column.

- (i) Repeat steps 3.3.4.1 to 8 if more than 2×10^9 MNCs were collected and need CD34⁺ immunoselection by using more LS columns (each column can hold up to 2×10^9 MNCs).
- (j) To increase the purity of CD34⁺ cells, the “stage 1 CD34⁺ cells” will be immunoselected again over a second column.
- (k) Place a new column in the separator.
- (l) Prime the column with 3 mL of separation buffer.
- (m) Apply all the collected “stage 1 CD34⁺ cells” to the column and allow the cell suspension to run through and collect the effluent as negative fraction.
- (n) Wash columns with 5 mL of separation buffer and collect the effluent as CD34-negative cells.
- (o) Remove the column from the separator and place on a new collection tube. Label this tube as “Stage 2 CD34⁺ cells.”
- (p) Apply 5 mL of separation buffer to the reservoir of the column and firmly flush out cells using the plunger supplied with the column. Discard the used columns.
- (q) Count the “stage 2 CD34⁺ cells.”
- (r) The purity of the CD34⁺ cells can be checked by removing an aliquot of 100,000 cells, adding 4 μ L of the Mouse Antihuman CD34-PE (Clone 563) antibody and performing flow cytometry (*see Note 6*).

3.4 Lentiviral Transduction of RM CD34⁺ HSPCs

The following protocol is our standard, utilized for the majority of macaques transplanted in our facility. With most vectors of reasonable titer, this protocol results in vector copy numbers of 0.1–0.4 in circulating myeloid, B lymphoid, and natural killer cells long term, following transplantation into autologous macaques conditioned with 900–1000 rads of total body irradiation. T cell vector copy number is lower, due to slow and incomplete naïve T cell production following thymic damage from irradiation. However, specific experimental conditions or goals may govern alternative transduction approaches, including omission of cytokine prestimulation to shorten *ex vivo* culture, higher density culture and/or higher MOI if high titer vector is available and/or higher copy number is desired, and use of transduction enhancers [19, 20].

1. Day 0 (5:00 pm): Prestimulation of CD34⁺ HSPCs.
 - (a) Prepare sufficient prestimulation: X-Vivo 10 + 1% HSA + recombinant human cytokines (Flt-3 L, SCF, and TPO each at a final concentration of 100 ng/mL) (*see Note 7*).

2. Prepare fibronectin-coated plates.
 - (a) Prepare fibronectin (FN) solution:
 - (b) Dilute stock 1 mg/mL RetroNectin to a concentration of 100 $\mu\text{g}/\text{mL}$ by adding 2.5 mL to 22.5 mL of PBS.
 - (c) Sterilize through a 0.22 micron filter into a 50 mL filter unit.
3. Coating plates with FN.
 - (a) Add 2 mL of FN 100 $\mu\text{g}/\text{mL}$ solution to each well of a 6-well tissue culture plate. Prepare as many plates as needed for the expected CD34⁺ cell number (three million cells per well).
 - (b) Incubate at room temperature for at least 2 h.
 - (c) Sterilely remove the FN after 2 h using a pipette and refreeze at $-20\text{ }^{\circ}\text{C}$ (*see Note 8*).
 - (d) Add 500 μL of 2.5% HEPES/HBSS buffer to the coated wells of the 6-well tissue culture plates, then suction the liquid out. Use immediately or wrap in foil and store at $4\text{ }^{\circ}\text{C}$ overnight or for up to 1 week before use.
4. Plating of CD34⁺ cells in prestimulation media:
 - (a) Aliquot two wells of a 12-well plate (not FM-coated) with 1×10^5 CD34⁺ and culture in 1 mL of prestimulation media until needed on day 3 and 5. These cells will serve as negative control “mock” transduced cells for transduction efficiency assays at 48 and 72 h post transduction and will not be manipulated on Day 1 or Day 2.
 - (b) Plate the remainder of the CD34⁺ cells at a concentration of $1 \times 10^6/\text{mL}$ in a total volume of 3 mL prestimulation media per well on the previously prepared FN-coated 6-well plates.
 - (c) Incubate overnight at $37\text{ }^{\circ}\text{C}$ with 5% CO_2 .
5. Day 1 (9:00 am): Transduction of CD34⁺ cells:
 - (a) The volume of vector required depends on the desired MOI, the vector titer, and the number of CD34⁺ cells to be transduced. We typically target an MOI of 25, and find that transduction of rhesus macaque HSPCs at an MOI of greater than 25 does not achieve higher transduction efficiencies with most vector preparations. Assume the cell number per well will not have changed during prestimulation and thus will remain at $1 \times 10^6/\text{mL}$. Calculate the amount of vector that will need to be thawed for the number of CD34⁺ cells to be transduced. Thaw vector preparation on ice and add to transduction media (warmed to room temperature). For an MOI of 25, the final concentration of vector in the media should be

2.5×10^7 particles/mL, with a total volume of 3 mL X the number of wells. Since the vector stock includes only X-Vivo10 media without HSA or cytokines, the volume of the vector preparation added needs to be considered, and additional HSA and cytokines will need to be added to adjust the final concentrations to 1% HSA and 100 ng/mL of each cytokine if the vector preparation makes up more than 10% of the total volume. Finally, add protamine sulfate to reach a concentration of 4ug/mL in the final transduction solution.

- (b) Remove 6-well FN-coated plates containing CD34⁺ cells from the incubator. Gently pipette the contents of each well into separate 15 mL conical tubes. Some cells will remain attached to the wells – do not vigorously try to dislodge these cells. Add 1 mL transduction solution to each well to prevent cells adhered to the FN from drying.
 - (c) Centrifuge the tubes at 1600 rpm for 15 min at room temperature.
 - (d) Gently remove media from the 15 mL tube, being careful not to disturb the cell pellet.
 - (e) Resuspend each pellet in 2 mL transduction solution and transfer back to the original FN-coated wells. Each well should now contain 3×10^6 CD34⁺ cells and 3 mL transduction solution containing 7.5×10^7 vector particles.
 - (f) Incubate the plates for 24 h at 37 °C in the presence of 5% CO₂ (*see Note 9*).
6. Day 2 (9:00 am): Collection of transduced CD34⁺ cells:
- (a) 24 h following transduction, dislodge the CD34⁺ HSPCs in each well using a cell scraper (*see Note 10*).
 - (b) Transfer the contents of all wells to a 50 mL conical tube. Wash each well twice with 0.5–1 mL of X-Vivo10 and add the washes to the same 50 mL tube.
 - (c) Confirm that virtually no cells remain attached in the wells by observation under the microscope. Scrape and wash again as needed.
 - (d) Measure volume of media and cells in the 50 mL tube.
 - (e) Count the cells and calculate the total cell number present in the tube.
 - (f) Aliquot two wells of 1×10^5 transduced cells per well in a 12-well plate, culture the cells in prestimulation media at 37 °C with 5% CO₂. These cells will be used for transduction efficiency analysis (see below). Additional culture is

required to allow for transgene expression and loss of nonintegrated vector.

- (g) The remainder of the cells can be centrifuged at 1600 rpm for 10 min and resuspended in transplantation solution (PBS + 2% FBS + 10 U/mL heparin) for immediate transplantation, or in CryoStor™CS10 at ten million cells/mL in 2 mL cryopreservation tubes for storage in liquid nitrogen if transplantation will not occur on the same day.

7. Analysis of transduction efficiency.

Day 3: Analysis of CD34⁺ HSPC transduction efficiency in vitro at 48 h post transduction.

- (a) Collect one well of pre- and posttransduction cells from the 12-well plate by vigorously pipetting with a P1000 pipette. Place in sterile Eppendorf tubes (tapered bottom with screw cap, 1 tube per condition).
- (b) Wash each well by adding 250 μ L of prestimulation media to each well and scrape the bottom of the wells with the tip. Transfer to the Eppendorf tubes.
- (c) Repeat wash step. Make sure no cells remain attached to the wells by observation under the microscope. Repeat wash if needed.
- (d) Centrifuge cells at 1600 rpm for 10 min at RT.
- (e) Gently remove supernatant using a P1000 pipette and resuspend the cell pellets in 500 μ L prestimulation media.
- (f) Analyze transduction efficiency by flow cytometry (e.g., GFP fluorescence) or extract DNA and perform qPCR for vector copy number.

Day 5: Analysis of transduction efficiency in vitro at 72 h post transduction. Follow the same procedure as on day 3.

3.5 Summary

In this chapter, we provide a detailed protocol to transduce mobilized RM HSPCs with HIV-1-based LVs. We include methodologies for purification of CD34⁺ RM HSPCs, lentivirus production using a χ HIV Gag/Pol package system (critical for high transduction efficiencies in NHP HSPCs), transduction and assessment of gene transfer efficiency. These methods are critical for establishing NHP HSCT models to study HSPC biology and conduct preclinical studies. However, due to the different aims of individual experiments, the transduction conditions cannot be fully standardized, and some amount of optimization is needed for each experimental design.

4 Notes

1. The amount (μg) of the lentiviral vector plasmid used per transfection mixture may need to be adjusted based on the size of the vector to achieve the same relative ratio of plasmids.
2. These next steps require 2 electric pipette aids.
3. Add solutions gently to the wells and only minimally disturb the cells in the well via discharging the pipette on the wall of each well.
4. If there is no marker protein encoded by the vector, the vector copy number of the transduced HeLa cells will need to be determined via qPCR.
5. The granulocyte and RBC lowest layer can be discarded or stored as a source of untransduced control DNA.
6. Negative fraction cells can be counted and frozen for future use.
7. StemSpan™ Serum-Free Expansion Medium (SFEM, STEM-CELL Technologies, Canada) has also been developed for culture and expansion of NHP HSPCs. A preclinical human cord blood HSPC expansion study reported higher yields of primitive HSPCs with SFEM; however, X-Vivo 10 supported more robust megakaryocytic lineage output [38]. These two different base medias have not been rigorously compared for RM HSPCs.
8. The FN 100 $\mu\text{g}/\text{mL}$ solution can be reused (frozen/thawed) a total of 5 times.
9. If high copy vector number is required in preclinical NHP study, transduction efficiency can be increased by modifying the transduction conditions based on recently published studies. These modifications have not been rigorously tested on macaque HSPCs, but we have preliminary data supporting improved efficiency:
 - (a) Increase cell density to up to $4 \times 10^6/\text{mL}$ if viral titer permits while maintaining MOI [20].
 - (b) Add adjuvants into transduction media, such as.
 - (i) Poloxamer 407(P407, Sigma Aldrich, Catalog #:62035, 100 $\mu\text{g}/\text{mL}$) and Prostaglandin E2(PGE2, R&D, Catalog # 2296/10, 10 μM) to the transduction media [20].
 - (ii) LentiBOOST Lentivirus Transduction Enhancer Solution(SIRION Biotech) has been suggested to significantly enhance transduction efficiency in human HSCs and T cells [19, 39, 40]. We have tested that the transduction efficiency increased two-fold by adding

LentiBOOST(1:100) when $MOI = 5-10$ is used in NHP HSPCs.

- (c) Increase MOI: $MOI = 100$ has been tested in NHP HSPCs with high transduction efficiency and minimal toxicity.
- (d) Two rounds of transduction: transduction media with virus can be washed off after the first transduction and followed with a second transduction.

10. Do not use trypsin to dissociate the cells.

Acknowledgments

We are grateful to Idalia Yabe, Xing Fan, and Stefan Cordes for their helpful discussions and critical reading and to Naoya Uchida, John Tisdale, Robert Donahue, So Gun Hong, Aylin Bonifacino, Stephanie Sellers, and many others within the laboratory and the primate facility for their contributions to development of rhesus macaque transplantation and gene transfer methodologies. We acknowledge funding from the NHLBI Division of Intramural Research.

References

1. Dunbar CE et al (2018) Gene therapy comes of age. *Science* 359(6372):eaan4672
2. Larochelle A, Dunbar CE (2013) Hematopoietic stem cell gene therapy: assessing the relevance of preclinical models. *Semin Hematol* 50:101–130
3. Shepherd BE, Kiem H-P, Lansdorf PM et al (2007) Hematopoietic stem-cell behavior in nonhuman primates. *Blood* 110:1806–1813
4. Radtke S, Adair JE, Giese MA et al (2017) A distinct hematopoietic stem cell population for rapid multilineage engraftment in nonhuman primates. *Sci Transl Med* 9(414):eaan1145
5. Sestak K, Scheiners C, Wu XW et al (2007) Identification of anti-human CD antibodies reactive with rhesus macaque peripheral blood cells. *Vet Immunol Immunopathol* 119:21–26
6. Larochelle A, Savona M, Wiggins M et al (2011) Human and rhesus macaque hematopoietic stem cells cannot be purified based only on SLAM family markers. *Blood* 117:1550–1554
7. Trobridge G, Beard BC, Kiem HP (2005) Hematopoietic stem cell transduction and amplification in large animal models. *Hum Gene Ther* 16:1355–1366
8. Donahue RE, Dunbar CE (2001) Update on the use of nonhuman primate models for pre-clinical testing of gene therapy approaches targeting hematopoietic cells. *Hum Gene Ther* 12:607–617
9. Wu C, Li B, Lu R et al (2014) Clonal tracking of rhesus macaque hematopoiesis highlights a distinct lineage origin for natural killer cells. *Cell Stem Cell* 14:486–499
10. Koelle SJ, Espinoza DA, Wu C et al (2017) Quantitative stability of hematopoietic stem and progenitor cell clonal output in rhesus macaques receiving transplants. *Blood* 129:1448–1457
11. Wu C, Espinoza DA, Koelle SJ et al (2018) Clonal expansion and compartmentalized maintenance of rhesus macaque NK cell subsets. *Sci Immunol* 3(29):eaat9781
12. Yabe IM, Truitt LL, Espinoza DA et al (2018) Barcoding of macaque hematopoietic stem and progenitor cells: a robust platform to assess vector genotoxicity. *Mol Ther Methods Clin Dev* 11:143–154
13. Naldini L (2015) Gene therapy returns to centre stage. *Nature* 526:351–360

14. Naldini L, Trono D, Verma IM (2016) Lentiviral vectors, two decades later. *Science* 353: 1101–1102
15. Hematti P, Hong B-K, Ferguson C et al (2004) Distinct genomic integration of MLV and SIV vectors in primate hematopoietic stem and progenitor cells. *PLoS Biol* 2:e423
16. Baum C, Modlich U, Gohring G et al (2011) Concise review: managing genotoxicity in the therapeutic modification of stem cells. *Stem Cells* 29:1479–1484
17. Moritz T, Patel VP, Williams DA (1994) Bone marrow extracellular matrix molecules improve gene transfer into human hematopoietic cells via retroviral vectors. *J Clin Invest* 93:1451–1457
18. Ingraio D, Majdoud S, Seye AK et al (2014) Concurrent measures of fusion and transduction efficiency of primary CD34+ cells with human immunodeficiency virus 1-based lentiviral vectors reveal different effects of transduction enhancers. *Hum Gene Ther Methods* 25: 48–56
19. Schott JW, Leon-Rico D, Ferreira CB et al (2019) Enhancing lentiviral and Alpharetroviral transduction of human hematopoietic stem cells for clinical application. *Mol Ther Methods Clin Dev* 14:134–147
20. Uchida N, Nassehi T, Drysdale CM et al (2019) High-efficiency lentiviral transduction of human CD34(+) cells in high-density culture with Poloxamer and prostaglandin E2. *Mol Ther Methods Clin Dev* 13:187–196
21. Trobridge GD, Wu RA, Beard BC et al (2009) Protection of stem cell-derived lymphocytes in a primate AIDS gene therapy model after in vivo selection. *PLoS One* 4:e7693
22. Verhoeven E, Relouzat F, Cambot M et al (2012) Stem cell factor-displaying simian immunodeficiency viral vectors together with a low conditioning regimen allow for long-term engraftment of gene-marked autologous hematopoietic stem cells in macaques. *Hum Gene Ther* 23:754–768
23. Sakuma R, Noser JA, Ohmine S et al (2007) Inhibition of HIV-1 replication by simian restriction factors, TRIM5alpha and APO-BEC3G. *Gene Ther* 14:185–189
24. Uchida N, Washington KN, Hayakawa J et al (2009) Development of a human immunodeficiency virus type 1-based lentiviral vector that allows efficient transduction of both human and rhesus blood cells. *J Virol* 83:9854–9862
25. Uchida N, Hargrove PW, Lap CJ et al (2012) High-efficiency transduction of rhesus hematopoietic repopulating cells by a modified HIV1-based lentiviral vector. *Mol Ther J Am Soc Gene Ther* 20:1882–1892
26. Evans ME, Kumkhaek C, Hsieh MM et al (2014) TRIM5alpha variations influence transduction efficiency with lentiviral vectors in both human and rhesus CD34(+) cells in vitro and in vivo. *Mol Ther* 22:48–58
27. Hematti P, Tuchman S, Laroche A et al (2004) Comparison of retroviral transduction efficiency in CD34+ cells derived from bone marrow versus G-CSF-mobilized or G-CSF plus stem cell factor-mobilized peripheral blood in nonhuman primates. *Stem Cells* 22: 1062–1069
28. Donahue RE, Kirby MR, Metzger ME et al (1996) Peripheral blood CD34+ cells differ from bone marrow CD34+ cells in Thy-1 expression and cell cycle status in nonhuman primates mobilized or not mobilized with granulocyte colony-stimulating factor and/or stem cell factor. *Blood* 87:1644–1653
29. Donahue RE, Kuramoto K, Dunbar CE (2005) Chapter 22: Large animal models for stem and progenitor cell analysis. In: Coligan JE (ed) *Current protocols in immunology: Unit 22A.1*. Wiley, New York. <https://doi.org/10.1002/0471142735.im22a01s69>
30. Haynes LD, Coonen J, Post J et al (2017) Collection of hematopoietic CD34 stem cells in rhesus macaques using Spectra Optia. *J Clin Apher* 32:288–294
31. Garofalo M, Bennett A, Farese AM et al (2014) The delayed pulmonary syndrome following acute high-dose irradiation: a rhesus macaque model. *Health Phys* 106:56–72
32. Uchida N, Weitzel RP, Shvygyn A et al (2016) Total body irradiation must be delivered at high dose for efficient engraftment and tolerance in a rhesus stem cell gene therapy model. *Mol Ther Methods Clin Dev* 3:16059
33. Uchida N, Nassehi T, Drysdale CM et al (2019) Busulfan combined with immunosuppression allows efficient engraftment of gene-modified cells in a rhesus macaque model. *Mol Ther* 27:1586–1596
34. Palchadhuri R, Saez B, Hoggatt J et al (2016) Non-genotoxic conditioning for hematopoietic stem cell transplantation using a hematopoietic-cell-specific internalizing immunotoxin. *Nat Biotechnol* 34:38–45
35. Chhabra A, Ring AM, Weiskopf K et al (2016) Hematopoietic stem cell transplantation in immunocompetent hosts without radiation or chemotherapy. *Sci Transl Med* 8:351ra105
36. Kustikova OS, Wahlers A, Kuhlcke K et al (2003) Dose finding with retroviral vectors: correlation of retroviral vector copy numbers

- in single cells with gene transfer efficiency in a cell population. *Blood* 102:3934–3937
37. Yee JL, Vandeford TH, Didier ES et al (2016) Specific pathogen free macaque colonies: a review of principles and recent advances for viral testing and colony management. *J Med Primatol* 45:55–78
 38. Lam AC, Li K, Zhang XB et al (2001) Preclinical ex vivo expansion of cord blood hematopoietic stem and progenitor cells: duration of culture; the media, serum supplements, and growth factors used; and engraftment in NOD/SCID mice. *Transfusion* 41:1567–1576
 39. Delville M, Soheili T, Bellier F et al (2018) A nontoxic transduction enhancer enables highly efficient lentiviral transduction of primary murine T cells and hematopoietic stem cells. *Mol Ther Methods Clin Dev* 10:341–347
 40. Simon B, Harrer DC, Thirion C et al (2019) Enhancing lentiviral transduction to generate melanoma-specific human T cells for cancer immunotherapy. *J Immunol Methods* 472: 55–64

Part III

Cellular Isolation and Characterization



Identification of Nonhuman Primate Hematopoietic Stem and Progenitor Cells

Stefan Radtke and Hans-Peter Kiem

Abstract

The preclinical development of hematopoietic stem cell (HSC) gene therapy/editing and transplantation protocols is frequently performed in large animal models such as nonhuman primates (NHPs). Similarity in physiology, size, and life expectation as well as cross-reactivity of most reagents and medications allows for the development of treatment strategies with rapid translation to clinical applications. Especially after the adverse events of HSC gene therapy observed in the late 1990s, the ability to perform autologous transplants and follow the animals long-term make the NHP a very attractive model to test the efficiency, feasibility, and safety of new HSC-mediated gene-transfer/editing and transplantation approaches.

This protocol describes a method to phenotypically characterize functionally distinct NHP HSPC subsets within specimens or stem cell products from three different NHP species. Procedures are based on the flow-cytometric assessment of cell surface markers that are cross-reactive in between human and NHP to allow for immediate clinical translation. This protocol has been successfully used for the quality control of enriched, cultured, and gene-modified NHP CD34⁺ hematopoietic stem and progenitor cells (HSPCs) as well as sort-purified CD34 subsets for transplantation in the pig-tailed, cynomolgus, and rhesus macaque. It further allows the longitudinal assessment of primary specimens taken during the long-term follow-up post-transplantation in order to monitor homing, engraftment, and reconstitution of the bone marrow stem cell compartment.

Key words Hematopoietic Stem Cells, Progenitor cells, Nonhuman Primate, Transplantation and Gene Therapy, CD34, CD90

1 Introduction

The development of HSC-mediated gene therapy/editing and transplantation approaches is commonly performed with CD34⁺ cell fractions. However, CD34⁺ HSPCs are knowingly a very heterogeneous pool of cells predominantly containing lineage-committed progenitor cells and only very few true HSCs with long-term multilineage engraftment potential *in vivo* [1–4]. Consequently, available gene therapy and editing approaches are significantly limited in their ability to reliably target HSCs [5–8], modification of CD34 cells requires large quantities of costly

reagents (e.g., lentiviral vectors or nucleases) [9–11], and current CD34-targeted approaches increase the risk for side effects in modified non-HSCs such as insertional mutagenesis for lentivirus-based approaches [12–18]. These hurdles currently limit the translation of this technology to the clinical setting. Thus, HSC gene therapy would greatly benefit from the ability to isolate, target, and modify a more HSC-enriched subset that provides short-term reconstitution as well as long-term multilineage engraftment.

For more than 5 decades, the phenotype of functionally distinct human CD34 subsets has been investigated. Continuously improving technology and the availability of more comprehensive ex vivo as well as in vivo read-outs allowed scientists to define dozens of cell surface markers on functionally defined HSCP subsets [1, 2, 19–30], investigate the relationship among these phenotypes [1, 25, 29, 31–42], and get closer to the identity of the most primitive multipotent HSCs. Described as $\text{lin}^- \text{Rho}^{\text{lo}} \text{CD38}^{\text{low}/-} \text{CD34}^+ \text{CD135}^+ \text{CD45RA}^- \text{CD90}^{+/-} \text{CD49f}^+$ cells, Notta et al. reported the currently most refined phenotype to purify multipotent long-term engrafting human HSCs [1].

While the cell surface marker for human HSCs and functionally distinct progenitors are well investigated, conservation of phenotypes and expression patterns between human and NHP are less well known. The lack of literature on cross-reactive antibody clones and the limited research aiming to close this gap are significantly hindering the development of HSC-targeted gene therapy and transplantation approaches in this preclinical large animal model.

Recognizing this discrepancy, we invested significant effort to identify cross-reactive antibodies that enable the identification of phenotypically defined and functionally distinct NHP HSPCs that are conserved between humans and NHPs [3]. We identified antibody clones for CD45RA, CD90, CD117, and CD123 that were marking CD34 subsets that are similarly enriched for functionally distinct HSPCs as previously described for human stem cell sources. Combining all 6 antibodies (CD34, CD45, CD45RA, CD90, CD117, and CD123), we were able to distinguish up to 9 phenotypically distinct CD34 subsets with unique differentiation potential ex vivo and in vivo. In addition, a simplified panel of only 4 antibodies (CD34, CD45, CD45RA, and CD90) allows to reliably enrich for an HSC-enriched CD34 subpopulation that reduced the number of target cells for HSC gene therapy up to 20-fold and was exclusively required for rapid short-term recovery onset as well as robust multilineage long-term engraftment with immediate translational potential for HSC gene therapy [3, 4, 43]. Here, we provide a detailed protocol for the most comprehensive as well as the simplified assessment of NHP HSPCs by flow cytometry.

2 Materials

2.1 Reagents

1. Heparin or ethylenediaminetetraacetic acid (EDTA) collection tubes.
2. Hemolytic buffer: 150 mM Ammonium chloride, 12 mM sodium bicarbonate, 0.1 mM EDTA, in double-distilled water (ddH₂O).
3. Wash/staining buffer: 0.5% Bovine serum albumin (BSA), 2 mM EDTA (optional, recommend for flow-sorting), in phosphate-buffered saline (PBS) pH 7.2.
4. Fluorochrome-conjugated antibodies (*see* Table 1).
5. Compensation beads. (any commercially available spherical particles with the binding ability of antibodies listed in Table 1).

2.2 Equipment

1. 15/50 mL Polypropylene tubes
2. 5 mL polypropylene tubes for flow cytometry with and without cell strainer (this item can be company/vendor specific depending on the flow-cytometer or cell-sorter)
3. Filtered pipette tips.
4. Cell strainer filter (70 μ m).
5. Cell counter (Neubauer Hemocytometer or other automated systems).
6. Centrifuge for 5 mL, 15 mL, and 50 mL tubes with swing-out rotor.
7. Vortex mixer.
8. Flow-cytometer (*see* Note 1).

Table 1
Fluorochrome-conjugated antibodies for flow cytometry

Antigen	Fluorochrome	Clone
CD34	PECF594 (Phycoerythrin-cyan-Fluor-594)	563
CD45	BV421 (Brilliant Violet 421)	D058-1283
CD45RA	APC-Cy7 (Allophycocyanin-cyanine7)	5H9
CD90	PE (Phycoerythrin)	5E10
CD117	BV711 (Brilliant Violet 711)	104D2
CD123	PerCP-Cy5.5 (Peridinin Chlorophyll Protein Complex-cyanine5.5)	7G3

3 Methods

3.1

Sample Collection and Processing

1. Collect your specimen in tubes containing either citrate dextrose solution (ADC-A) or heparin (20USP/mL) (*see Note 2*).
2. To hemolyze the sample, divide it into multiple 50 mL conical tubes (10–12 mL each tube).
3. Add hemolytic buffer up to 50 mL. Gently vortex the cell/buffer mix.
4. Incubate the cell/buffer mix at room temperature (RT) for up to 7 min.
5. Centrifuge cell/buffer mix at $800\times g$ for 5 min.
6. Carefully aspirate the supernatant from the pellet.
7. Resuspend the pellet in 15 mL of hemolytic buffer. Gently vortex the cell/buffer mix.
8. Filter the cell/buffer mix through a 70 μm cell strainer to remove tissue fragments and clots.
9. Add hemolytic buffer up to 50 mL. Gently vortex the cell/buffer mix (*see Note 3*).
10. Incubate cell/buffer mix at RT for up to 7 min.
11. Centrifuge at $800\times g$ for 5 min.
12. Aspirate the supernatant from the pellet.
13. Resuspend the pellet in 10 mL staining buffer and count the cells on a hemocytometer or automated cell counter to determine the total white blood cell (WBC) count.

3.2 Preparation of Samples for Flow Cytometry

1. Adjust the cell suspension to $1e7$ WBCs/mL based on the previous cell count and transfer 100 μL of the cell suspension into 2 polypropylene tubes (Tube 1 + 2) (*see Table 2*).

Table 2

Staining panel of NHP WBCs for flow cytometry (*see Notes 4 and 5*)

Tube	CD34	CD45	CD45RA	CD90	CD117	CD123	
1	–	–	–	–	–	–	WBCs
2	+	+	+	+	+	+	WBCs
3	+	–	–	–	–	–	Comp. Beads
4	–	+	–	–	–	–	Comp. Beads
5	–	–	+	–	–	–	Comp. Beads
6	–	–	–	+	–	–	Comp. Beads
7	–	–	–	–	+	–	Comp. Beads
8	–	–	–	–	–	+	Comp. Beads

2. Add the recommended test volume of each fluorochrome-conjugated antibody to Tube 2, vortex the cell/antibody mix, and incubate cells at 4 °C in the dark.
3. In parallel, prepare single stained compensation beads for each individual fluorochrome-conjugated antibody according to the manufacturer's instructions (Tubes 3–9) (*see* Table 2).
4. After 20 min, fill up all tubes with 3 mL staining buffer.
5. Centrifuge at $800\times g$ for 5 min.
6. Aspirate the supernatant from the pellet.
7. Resuspend cells and compensation beads in 100 μ L staining buffer.

3.3 Analysis of Samples on Flow-Cytometer

1. Generate a protocol with 5 plots as illustrated in Fig. 1.
2. Run unstained WBCs (Tube 1, Table 2) to adjust the voltage on the FSC (forward-scatter), SSC (side-scatter), and all fluorescence channels. Record a minimum of 50,000 WBCs.
3. Run all single stained compensation beads (Tubes 3–8, Table 2) to adjust the compensation in between channels. If the signal for individual fluorochrome-conjugated antibodies exceeds the upper detection limit of the flow-cytometer, reduce the voltage on the channel and restart with the protocol at step 2. Record a minimum of 5000 beads (*see* Note 6).
4. Run the fully stained sample (Tube 2, Table 2) when adjustment of voltages and compensation is complete (*see* Note 7).
5. Record a minimum of 500,000 WBCs or 5000 CD34⁺ cells (*see* Note 8).

3.4 Flow-Cytometric Data Analysis – Comprehensive/High Resolution (See Fig. 1 and Table 3)

1. Visualize WBCs in a plot showing SSC-W on the x-axis versus SSC-H on the y-axis or FSC-W on the x-axis versus SSC-H on the y-axis (first plot).
2. Draw a polygon gate around the single cells and exclude doublets.
3. Name the gate “Singlets.”
4. Visualize Singlets in a plot showing FSC-A on the x-axis versus SSC-A on the y-axis (2nd plot).
5. Draw a polygon gate around the cells and exclude debris (lower left corner) as well as dead cells (upper left section).
6. Name the gate “Scatter.”
7. Visualize Scatter cells in a plot showing CD45 on the x-axis versus CD34 on the y-axis (3rd plot).

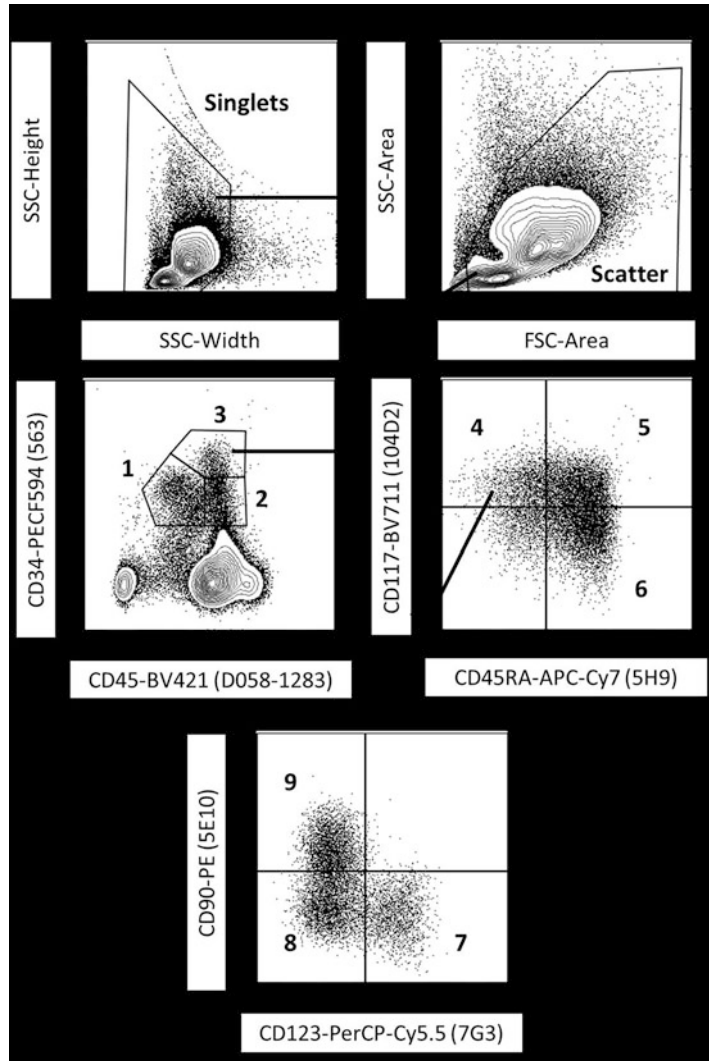


Fig. 1 Flow-cytometric gating strategy (comprehensive) for NHP HSPCs. Doublets are excluded using the SSC (side scatter)-Width vs. SSC-Height (top left plot). Single cells are plotted for size (FSC (forward scatter)-Area) vs. granularity (SSC-Area) to exclude debris and dead cells (top right plot). Cells in the Scatter gate are subdivided plotting CD45 vs. CD34 (middle left plot). CD34⁺ cells can be separated based on the level of CD34 and CD45 expression into three populations (population 1–3). CD34^{high}CD45^{int} cells (population 3) are further subdivided plotting CD45RA vs. CD117 separating three different subsets (populations 4–6, middle right plot). Finally, cells from population 4 are analyzed for CD123 and CD90 expression identifying populations 7–9 (bottom plot)

Table 3
Phenotype and functional characteristics of NHP CD34 subsets (comprehensive/high resolution)

Surface marker	1	2	3	4	5	6	7	8	9
CD45	Low	Int	Int	Int	Int	Int	Int	Int	Int
CD34	Int	Int	High	High	High	High	High	High	High
CD117				+	+	–	+	+	+
CD45RA				–	+	+	–	–	–
CD123							+	–	–
CD90							–	–	+
Differentiation potential									
Granulocytes	–	+	+	+	+	+	–	+	+
Monocytes	+	+	+	+	+	+	+	+	+
Erythrocytes	+	–	+	+	–	–	–	+	+
Megakaryocytes	–	–	+	+	–	–	+	+	+
T cells	n.d.	–	+	+	+	–	–	+	+
NK cells	n.d.	–	+	+	+	–	–	+	+
CAFCs	n.d.	–	–	n.d.	–	–	–	+	+
Sec CFCs	–	+	+	+	–	–	–	–	+

n.d.: not determined

8. Cells expressing CD34 on the surface will show three populations with different levels of CD34 as well as CD45 expression. Gate and name the following three populations:
 - (a) CD34^{low}-expressing cells are CD45^{int} (Population 1).
 - (b) CD34^{int}-expressing cells are CD45^{low} (Population 2).
 - (c) CD34^{high}-expressing cells are CD45^{int} (Population 3).
9. Visualize CD34^{high}CD45^{int} cells (Population 3) in a plot showing CD117 on the x-axis versus CD45RA on the y-axis (4th plot).
10. Gate and name three distinct populations:
 - (a) CD117⁺CD45RA[–] cells (Population 4).
 - (b) CD117⁺CD45RA⁺ cells (Population 5).
 - (c) CD117[–]CD45RA⁺ cells (Population 6).
11. Visualize CD117⁺CD45RA[–] cells (Population 4) in a plot showing CD123 on the x-axis versus CD90 on the y-axis (5th plot).

12. Gate and name three distinct populations (*see Note 9*):

- (a) CD123⁺CD90⁻ cells (Population 7).
- (b) CD123⁻CD90⁻ cells (Population 8).
- (c) CD123⁻CD90⁺ cells (Population 9).

3.5 Flow-Cytometric Data Analysis – Short/Low Resolution (See Fig. 2 and Table 4)

1. Visualize WBCs in a plot showing SSC-W on the x-axis versus SSC-H on the y-axis or FSC-W on the x-axis versus SSC-H on the y-axis (1st plot).
2. Draw a polygon gate around the single cells and exclude doublets.
3. Name the gate “Singlets.”
4. Visualize Singlets in a plot showing FSC-A on the x-axis versus SSC-A on the y-axis (2nd plot).
5. Draw a polygon gate around the cells and exclude debris (lower left corner) as well as dead cells (upper left section).

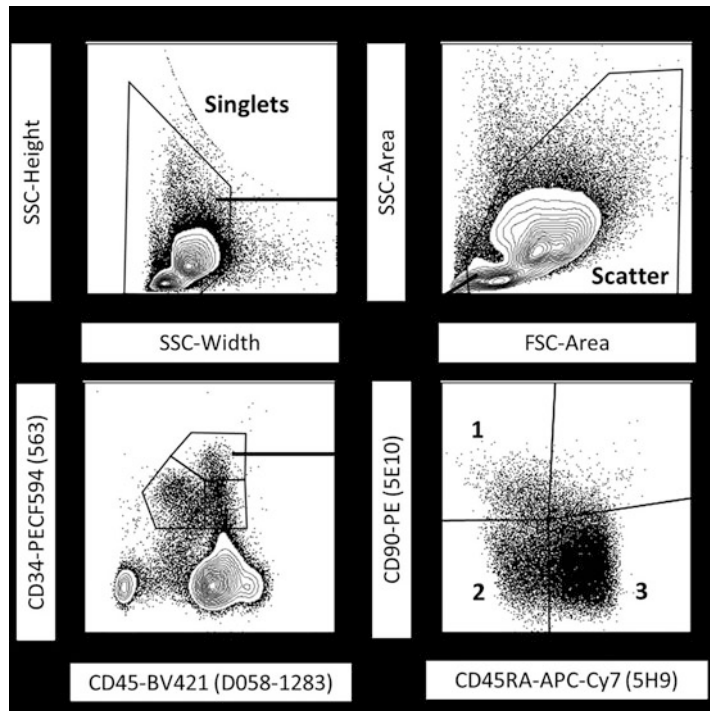


Fig. 2 Flow-cytometric gating strategy (short) for NHP HSPCs. Doublets are excluded using the SSC (side scatter)-Width vs. SSC-Height (top left plot). Single cells are plotted for size (FSC (forward scatter)-Area) vs. granularity (SSC-Area) to exclude debris and dead cells (top right plot). Cells in the Scatter gate are subdivided plotting CD45 vs. CD34 (bottom left plot). CD34^{high}CD45^{int} cells are further subdivided plotting CD45RA vs. CD90 separating three different subsets (populations 1–3, bottom right plot)

Table 4
Phenotype of NHP CD34 subsets (low resolution)

Surface marker	1	2	3
CD45	Int	Int	Int
CD34	High	High	High
CD45RA	–	–	+
CD90	+	–	–

6. Name the gate “Scatter.”
7. Visualize Scatter cells in a plot showing CD45 on the x-axis versus CD34 on the y-axis (3rd plot).
8. Gate the CD34^{high}CD45^{int} cells.
9. Visualize CD45^{int}CD34^{high} cells in a plot showing CD45RA on the x-axis versus CD90 on the y-axis (4th plot).
10. Gate and name three distinct populations (*see Note 9*):
 - (a) CD90⁺CD45RA[–] cells (Population 1).
 - (b) CD90[–]CD45RA[–] cells (Population 2).
 - (c) CD90[–]CD45RA⁺ cells (Population 3).

4 Notes

1. Flow-cytometers need to be equipped with lasers and filters to detect the recommended fluorochromes listed in Table 1. Systems with at least 3 lasers (405 nm, 488 nm, and 633 nm or similar specifications) are feasible; however, 4-laser machines (405 nm, 488 nm, 523 nm, and 633 nm or similar specifications) are recommended to minimize compensation and improve excitation/emission of fluorochromes.
2. This protocol has been tested for the following species and cell sources:
 - (a) Pig-tailed macaque (*Macaca nemestrina*).
 - (i) Steady-state bone marrow.
 - (ii) GCSF-/SCF-primed bone marrow.
 - (iii) Umbilical cord blood.
 - (b) Rhesus macaque (*Macaca mulatta*).
 - (i) Steady-state bone marrow.
 - (ii) GCSF-/SCF-primed bone marrow.

- (iii) GCSF mobilized peripheral blood stem cells.
 - (iv) AMD3100 mobilized peripheral blood stem cells.
 - (c) Cynomolgus (*Macaca fascicularis*).
 - (i) Steady-state bone marrow.
3. For small samples below 15 mL, the second hemolysis step can be skipped to reduce the stress and cell loss if the cell pellet after the first hemolysis does not show any red shade any longer. Alternatively, if light redness is visible, the second lysis step can be performed with only 25 mL hemolytic buffer for 5–7 min and the reaction stopped by adding 25 mL wash buffer right before centrifugation.
 4. Due to the limited availability of cross-reactive antibody clones with nonhuman primate HSPCs, inclusion of classical live/dead cell marker such as DAPI, PI, or 7AAD is very challenging in the recommended flow panel. If the acquisition of a live/dead marker is required, specialized dyes excited by the 375 nm UV laser are recommended to avoid overlap with the recommended fluorochrome-conjugated antibodies. Alternatively, individual cell surface marker can be dropped with the exception for CD34, CD45, CD45RA, and CD90 in the short/low-resolution panel. Rotation of antibody fluorochromes is possible but not recommended, since the panel has been optimized for the intensity of each cell surface antigen to enable best discrimination.
 5. The shown combination of fluorochrome-conjugated antibodies is designed to keep channels available for green fluorescent protein (GFP), mCherry, and/or mCerulean, three common proteins delivered by lentiviral vectors or mRNA for tracing and tracking of cells. All three channels can be occupied with alternative fluorochrome-conjugated antibodies and/or live/dead cell marker if necessary and available.
 6. Compensation can be either performed manually or fully automatic with integrated compensation tools in the acquisition software. The use of this software should be performed according to the manufacturer's instructions. Retrospective compensation is not advised to prevent data loss during acquisition and guarantee correct collection of data.
 7. If you plan to run your samples on a cell sorter, add EDTA to the staining buffer to prevent cell clotting and clogging of the machine. Filter your samples through 70 μ M cell strainer before running them on the cell sorter.
 8. The average frequency of CD34⁺ hematopoietic stem and progenitor cells varies based on the cell source [3]. In order to guarantee high-quality data, the number of WBCs recorded should be determined based on the frequency of CD34⁺ cells.

For optimal data analysis, at least 5000 CD34⁺ cells should be recorded in order to allow reliable gating of all phenotypically defined CD34 subsets listed in Tables 3 and 4.

9. Only CD34⁺CD90⁺CD45RA⁻ cells are responsible for rapid short-term and robust long-term hematopoietic recovery upon autologous transplantation in the nonhuman primate large-animal model [3] or in xenograft transplants in the sublethally irradiated MISTRG mouse model [4]. This HSC-enriched CD34 subset can easily be sort-purified, gene-modified with lentiviral vectors or nucleases (e.g., CRISPR/Cas9), and successfully be transplanted following our previously published protocols [3, 4, 43, 44].

References

1. Notta F, Doulatov S, Laurenti E et al (2011) Isolation of single human hematopoietic stem cells capable of long-term multilineage engraftment. *Science* 333:218–221
2. Doulatov S, Notta F, Eppert K et al (2010) Revised map of the human progenitor hierarchy shows the origin of macrophages and dendritic cells in early lymphoid development. *Nat Immunol* 11:585–593
3. Radtke S, Adair JE, Giese MA et al (2017) A distinct hematopoietic stem cell population for rapid multilineage engraftment in nonhuman primates. *Sci Transl Med* 9(414):eaan1145
4. Radtke S, Chan YY, Sippel TR et al (2019) MISTRG mice support engraftment and assessment of nonhuman primate hematopoietic stem and progenitor cells. *Exp Hematol* 70: 31–41
5. Peterson CW, Haworth KG, Burke BP et al (2016) Multilineage polyclonal engraftment of Cal-1 gene-modified cells and in vivo selection after SHIV infection in a nonhuman primate model of AIDS. *Mol Ther Methods Clin Dev* 3:16007
6. Peterson CW, Wang J, Norman KK et al (2016) Long-term multilineage engraftment of autologous genome-edited hematopoietic stem cells in nonhuman primates. *Blood* 127: 2416–2426
7. Wang J, Exline CM, DeClercq JJ et al (2015) Homology-driven genome editing in hematopoietic stem and progenitor cells using ZFN mRNA and AAV6 donors. *Nat Biotechnol* 33: 1256–1263
8. Genovese P, Schirotti G, Escobar G et al (2014) Targeted genome editing in human repopulating haematopoietic stem cells. *Nature* 510: 235–240
9. Naldini L (2015) Gene therapy returns to Centre stage (review). *Nature* 526:351–360
10. Morrison C (2015) \$1-million price tag set for Glybera gene therapy. *Nat Biotechnol* 33:217–218
11. Melchiorri D, Pani L, Gasparini P et al (2013) Regulatory evaluation of Glybera in Europe – two committees, one mission. *Nat Rev Drug Discov* 12:719
12. Baldo A, van den Akker E, Bergmans HE et al (2013) General considerations on the biosafety of virus-derived vectors used in gene therapy and vaccination (review). *Curr Gene Ther* 13: 385–394
13. Basner-Tschakarjan E, Mingozzi F (2014) Cell-mediated immunity to AAV vectors, evolving concepts and potential solutions (review). *Front Immunol* 5:350
14. Raper SE, Chirmule N, Lee FS et al (2003) Fatal systemic inflammatory response syndrome in a ornithine transcarbamylase deficient patient following adenoviral gene transfer. *Mol Genet Metab* 80:148–158
15. Hacein-Bey-Abina S, von Kalle C, Schmidt M et al (2003) LMO2-associated clonal T cell proliferation in two patients after gene therapy for SCID-X1. *Science* 302(5644):415–419; Erratum in *Science* (2003) 302:568
16. Stein S, Ott MG, Schultze-Strasser S et al (2010) Genomic instability and myelodysplasia with monosomy 7 consequent to EVI1 activation after gene therapy for chronic granulomatous disease. *Nat Med* 16:198–204
17. Braun CJ, Boztug K, Paruzynski A et al (2014) Gene therapy for Wiskott-Aldrich syndrome—long-term efficacy and genotoxicity. *Sci Transl Med* 6:227ra233
18. Braun CJ, Witzel M, Paruzynski A et al (2014) Gene therapy for Wiskott-Aldrich Syndrome—Long-term reconstitution and clinical benefits, but increased risk for leukemogenesis. *Rare Dis* 2:e947749

19. Six EM, Bonhomme D, Monteiro M et al (2007) A human postnatal lymphoid progenitor capable of circulating and seeding the thymus. *J Exp Med* 204:3085–3093
20. Galy A, Travis M, Cen D et al (1995) Human T, B, natural killer, and dendritic cells arise from a common bone marrow progenitor cell subset. *Immunity* 3:459–473
21. Civin CI, Strauss LC, Brovall C et al (1984) Antigenic analysis of hematopoiesis. III. A hematopoietic progenitor cell surface antigen defined by a monoclonal antibody raised against KG-1a cells. *J Immunol* 133:157–165
22. Katz FE, Tindle R, Sutherland DR et al (1985) Identification of a membrane glycoprotein associated with haemopoietic progenitor cells. *Leukemia Res* 9:191–198
23. Terstappen LW, Huang S, Safford M et al (1991) Sequential generations of hematopoietic colonies derived from single nonlineage-committed CD34+CD38- progenitor cells. *Blood* 77:1218–1227
24. Lansdorp PM, Sutherland HJ, Eaves CJ (1990) Selective expression of CD45 isoforms on functional subpopulations of CD34+ hemopoietic cells from human bone marrow. *J Exp Med* 172:363–366
25. Notta F, Zandi S, Takayama N et al (2016) Distinct routes of lineage development reshape the human blood hierarchy across ontogeny. *Science* 351:aab2116
26. Murray L, DiGiusto D, Chen B et al (1994) Analysis of human hematopoietic stem cell populations. *Blood Cells* 20:364–369; discussion 369–370
27. Solar GP, Kerr WG, Zeigler FC et al (1998) Role of c-mpl in early hematopoiesis. *Blood* 92: 4–10
28. Gunji Y, Nakamura M, Osawa H et al (1993) Human primitive hematopoietic progenitor cells are more enriched in KITlow cells than in KIThigh cells. *Blood* 82:3283–3289
29. Manz MG, Miyamoto T, Akashi K et al (2002) Prospective isolation of human clonogenic common myeloid progenitors. *Proc Natl Acad Sci U S A* 99:11872–11877
30. Yin AH, Miraglia S, Zanjani ED et al (1997) AC133, a novel marker for human hematopoietic stem and progenitor cells. *Blood* 90: 5002–5012
31. Doulatov S, Notta F, Laurenti E et al (2012) Hematopoiesis: a human perspective. *Cell Stem Cell* 10:120–136
32. Majeti R, Park CY, Weissman IL (2007) Identification of a hierarchy of multipotent hematopoietic progenitors in human cord blood. *Cell Stem Cell* 1:635–645
33. Gorgens A, Radtke S, Horn PA et al (2013) New relationships of human hematopoietic lineages facilitate detection of multipotent hematopoietic stem and progenitor cells. *Cell Cycle* 12:3478–3482
34. Giebel B, Zhang T, Beckmann J et al (2006) Primitive human hematopoietic cells give rise to differentially specified daughter cells upon their initial cell division. *Blood* 107:2146–2152
35. Akashi K, Traver D, Miyamoto T et al (2000) A clonogenic common myeloid progenitor that gives rise to all myeloid lineages. *Nature* 404: 193–197
36. Kondo M, Weissman IL, Akashi K (1997) Identification of clonogenic common lymphoid progenitors in mouse bone marrow. *Cell* 91:661–672
37. Kawamoto H, Ikawa T, Masuda K et al (2010) A map for lineage restriction of progenitors during hematopoiesis: the essence of the myeloid-based model. *Immunol Rev* 238:23–36
38. Adolfsson J, Mansson R, Buza-Vidas N et al (2005) Identification of Flt3+ lympho-myeloid stem cells lacking erythro-megakaryocytic potential a revised road map for adult blood lineage commitment. *Cell* 121:295–306
39. Goardon N, Marchi E, Atzberger A et al (2011) Coexistence of LMPP-like and GMP-like leukemia stem cells in acute myeloid leukemia. *Cancer Cell* 19:138–152
40. Carrelha J, Meng Y, Kettyle LM et al (2018) Hierarchically related lineage-restricted fates of multipotent haematopoietic stem cells. *Nature* 554:106–111
41. Rodriguez-Fraticelli AE, Wolock SL, Weinreb CS et al (2018) Clonal analysis of lineage fate in native haematopoiesis. *Nature* 553:212–216
42. Pei W, Feyerabend TB, Rossler J et al (2017) Polylox barcoding reveals haematopoietic stem cell fates realized in vivo. *Nature* 548: 456–460
43. Humbert O, Radtke S, Samuelson C et al (2019) Therapeutically relevant engraftment of a CRISPR-Cas9-edited HSC-enriched population with HbF reactivation in nonhuman primates. *Sci Transl Med* 11(503):eaaw3768
44. Radtke S, Perez AM, Venkataraman R et al (2019) Preparation and gene modification of nonhuman primate hematopoietic stem and progenitor cells. *J Vis Exp* 144. <https://doi.org/10.3791/58933>



Isolation and Characterization of Fetal Liver Hematopoietic Stem Cells

Diego A. López and Anna E. Beaudin

Abstract

Hematopoietic stem cells (HSCs) are responsible for the generation and maintenance of pools of multipotent precursors that ultimately give rise to all fully differentiated blood and immune cells. Proper identification and isolation of HSCs for functional analysis has greatly facilitated our understanding of both normal and abnormal adult hematopoiesis. Whereas adult hematopoiesis in mice and humans is driven by quiescent HSCs that reside almost exclusively within the bone marrow (BM), developmental hematopoiesis is characterized by a series of transient progenitors driving waves of increasingly mature hematopoietic cell production that occur across multiple anatomical sites. These waves of hematopoietic cell production are also responsible for the generation of distinct immune cell populations during development that persist into adulthood and contribute uniquely to adult immunity. Therefore, methods to properly isolate and characterize fetal progenitors with high purity across development become increasingly important not only for defining developmental hematopoietic pathways, but also for understanding the contribution of developmental hematopoiesis to the immune system. Here, we describe and discuss methods and considerations for the isolation and characterization of HSCs from the fetal liver, the primary hematopoietic organ during fetal development.

Key words Hematopoietic stem cells, HSC, Fetal liver, Dissection, Characterization, Transplantation

1 Introduction

During development, fetal hematopoiesis occurs in overlapping waves of hematopoietic cell production. The long-standing view is that of two primary waves: primitive hematopoiesis that initiates in the extraembryonic yolk sac and generates primarily primitive erythroid and megakaryocytic cells [1], and definitive hematopoiesis that initiates with the generation of definitive HSCs from hemogenic endothelium in the developing aorta [2]. Definitive HSCs that arise in the developing aorta enter the bloodstream and immediately migrate to the fetal liver [3] and soon thereafter undergo massive expansion within the fetal liver. The fetal liver then becomes the primary niche that supports hematopoietic stem cell

expansion and hematopoiesis prior to maturation of the bone marrow microenvironment [4].

Proper isolation and characterization of embryonic and fetal HSCs across ontogeny is critical for defining the mechanisms and factors that underlie the establishment of hematopoiesis during development. Most of what we know about isolation of HSCs from the fetal liver comes from isolation of adult HSCs from the bone marrow (BM). The isolation of adult HSCs is being continuously refined and can now be deduced not only by the use of many cell surface markers for negative and positive selection but also with highly specific molecular markers and genetic reporter models [5]. We also now appreciate that the adult HSC compartment is considerably more heterogeneous than previously considered [6]. Given the dynamic nature of fetal hematopoiesis, the fetal HSC compartment has to necessarily be even more heterogeneous. The fetal HSC compartment is likely to contain both definitive HSCs, some subset of which persist into adulthood, as well as transient progenitors that exist during early development [7–9].

Here, we focus on isolation of mouse HSCs from the fetal liver at embryonic day (E)14.5 as this is the most well-characterized stage of fetal hematopoiesis. It is also the stage from which it is possible to isolate the most fetal progenitors in terms of both quantity and diversity. With the advent of more sophisticated lineage tracing and transplantation approaches, we now appreciate that fetal hematopoiesis is driven by many discrete transient progenitors with increasingly diverse lineage potential that give rise to overlapping waves of hematopoietic cell generation. We also now know that these waves are responsible for the generation of distinct subsets of immune cells during development that persist into adulthood and play critical roles in tissue establishment, tissue homeostasis, and the first line of immunity [10–12]. Therefore, methods to properly isolate and characterize specific progenitors across development become increasingly important. The purpose of this chapter is to provide the most comprehensive information on isolation, identification, and characterization of fetal HSCs from the liver during mid-gestation.

2 Materials

2.1 Mice

Much of our understanding of HSC characterization and function has been derived from work utilizing laboratory mouse strains. Given that (1) HSCs are a rare population in the adult mouse, (2) we have less information regarding fetal HSC cell surface markers and identity during development and (3) relatively fewer genetic tools specific for fetal HSC isolation are available, it is imperative to select a mouse strain with access to multiple genetic tools to facilitate proper isolation of functional HSCs in the fetal

liver. For these reasons, in our laboratory, we typically utilize 8–12-week-old female mice on the C57Bl/6 J background for fetal HSC isolation and characterization experiments. Because strain-specific differences do exist among commercially available mice, we advise that appropriate considerations be taken into account when using mice other than those on a C57BL/6 J background.

2.2 Reagents and Supplies

Necessary reagents and supplies are determined on a per-need basis and may be adjusted depending on your specific setup. Rather than provide a comprehensive list, here we aim to provide some useful supplies and reagents that we use regularly in our laboratory for fetal HSC isolation. These same reagents are referenced in the subsequent methods section.

2.2.1 Supplies

1. 10× Dulbecco's phosphate-buffered saline, no calcium, no magnesium (DPBS –/–) (Cat #: 14200-075, Gibco)
2. 1× DPBS –/– (Cat #: 14190-144, Gibco)
3. Fetal bovine serum (FBS) (Cat #: 26140-079-500mL, Gibco).
4. Ethylenediaminetetraacetic acid disodium salt dihydrate (Cat #: E-5134, Sigma-Aldrich).
5. Collagenase Type IV (Cat #: LS004189, Worthington-Biochemical Corp.)
6. CD117 (cKit) enrichment beads, mouse (Cat #: 130-091-224, Miltenyi Biotec).
7. 100 × 20 mm tissue culture dish (Cat #: 353003, Falcon Corning)
8. 35 × 10 mm petri dish (Cat #: 351008, Falcon Corning)
9. 12-well tissue culture plate (Cat #: 10861-556, VWR)
10. 5 mL FACS polystyrene round-bottom tube (Cat #: 352008, Falcon Corning)
11. 50 mL Conical Tubes (Cat #: 05-539-13, Fisher Scientific)
12. 15 mL Conical Tubes (Cat #: 352196, Falcon Corning)
13. Stericup 500 mL Durapore 0.22 μm PVDF (Cat #: SCGVU05RE, EMD Millipore Corp.)
14. 70 μm Nylon mesh (Cat #: U-CMN-70-C, Component Supply Co.)
15. LS Columns (Cat #: 130-042-401).
16. MACS MultiStand (Cat #: 130-042-303).

2.2.2 0.5 M EDTA

1. Add 186.1 g EDTA to 800 mL of diH₂O.
2. While stirring, slowly add ~20 g of NaOH (Cat #: S8045-500G, Sigma-Aldrich) to bring pH to 8.0.

3. Filter through a 0.2 μm filter into an autoclaved glass container.
4. Keep at 4 °C for 2–3 months.

2.2.3 Staining Media
(5 mM EDTA + 1 \times DPBS –/
– + 2% FBS)

1. To 10 mL of 0.5 M EDTA solution, add 100 mL 10 \times DPBS –/–.
2. Bring volume up to 1000 mL using diH₂O and stir for 15–20 min.
3. Vacuum filter solution with a Stericup-GV (Cat #: SCGVU05RE, EMD Millipore Corp.) into autoclaved glass bottles.
4. Keep sealed at 4 °C for 2–3 months.
5. On day of use: supplement with FBS (Cat #: 26140-079-500 mL, Gibco) to achieve a 2% FBS by volume solution. Use within 1 week of preparation.

2.2.4 10 \times ACK
(Ammonium-Chloride-
Potassium) Lysis Buffer

1. To 800 mL of diH₂O add 82.8 g NH₄Cl (Cat #: A2037, TCI America), 10 g KHCO₃ (Cat #: 0889-500G, VWR), and 372 mg Na₂EDTA (Cat #: BP120-1, Fisher Scientific Company) and stir to mix.
2. Adjust pH to 7.2–7.4 using 1 N HCl (Cat #: A144-212, Fisher Scientific Company).
3. Bring final volume to 1 L using diH₂O and filter through 0.2 μm filter. Store at 4 °C for up to 1 year.
4. Keep 1 \times working stock at room temperature for up to 30 days.

2.2.5 Digestion Buffer

1. To 20 mLs of 1 \times DPBS add 4 mg of Collagenase Type IV and vortex gently until fully dissolved.
2. Supplement with FBS to achieve a 2% FBS by volume solution. Use immediately upon preparation.

3 Methods

3.1 Timed Mating

To minimize variability and maintain reproducibility across our experiments, we only utilize virgin 8–12-year-old females for timed matings. Breeding pairs are set up overnight and the female is checked early the next morning for the presence of a copulatory plug. This time point can be considered as 0.5 days postcoitum, at which point the female should be housed separately from the male. We recommend that males used for timed matings be replaced at 6–7 months of age, as we have observed a decrease in reliable pregnancies from timed matings once males age beyond this point.

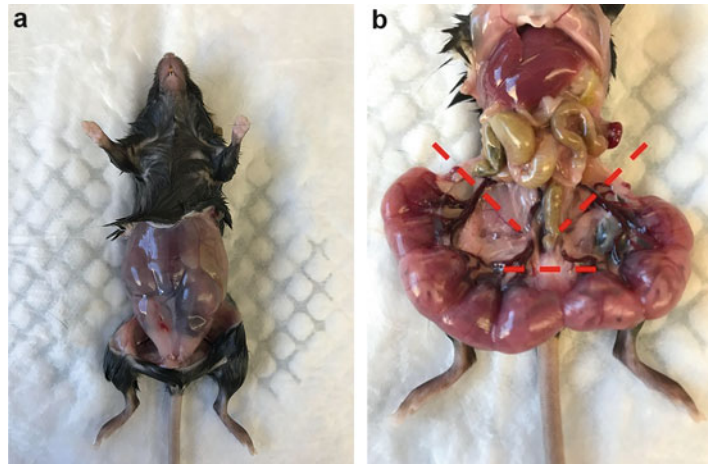


Fig. 1 Accessing embryos for fetal liver isolation. Images depicting a pregnant C57BL/6 female at E14.5. (a) Exposed abdominal wall after opening and retracting skin. To remove the entire uterine horn with intact embryos, detach at ovaries and at the cervix by cutting along the indicated lines (b). Promptly place extracted uterine horn in a tissue culture dish containing ice-cold staining media

3.2 Embryo Isolation

1. At E14.5, the pregnant dam should be euthanized according to your IACUC-approved euthanasia method, hereafter, via CO₂ inhalation. This process should be monitored and followed by approved secondary measures of euthanasia. After euthanasia, place mouse, ventral side up, on dissection tray or absorbent pad and spray down using 70% EtOH.
2. Using curved forceps, lift skin near the middle of the abdomen and make an incision at the skin using scissors. Use forceps to pull apart at the incision toward the head and tail to expose the abdominal wall as shown in Fig. 1a.
3. Carefully cut through the abdominal wall to expose embryos attached to the bicornuate uterus. Gently move aside any obstructing organs from view to allow free access.
4. Remove the entire uterus from the mouse by cutting and detaching at the left and right ovaries and at the base of the cervix as shown in Fig. 1b and place in a tissue culture dish with ice-cold staining media.
5. Separate each embryo using dissecting scissors by making an incision between the embryonic sacs, being careful to avoid damaging the embryo within.
6. Using forceps, carefully tear an opening near the placenta to release the fetus from the embryonic sac. Carefully cut away the fetus from the umbilical cord and gently rinse in a separate tissue culture dish with ice-cold staining media.
7. Transfer each fetus onto a 12-well tissue culture plate containing approximately 2 mLs of staining media and keep over ice.

3.3 Fetal Liver Isolation and Processing

Careful attention should be placed on dissecting the entire liver from the fetus without premature trituration, as this can impede whole-tissue quantification. When homogenizing the tissue, it is important to consider whether to use mechanical versus enzymatic trituration and, depending on the intended downstream analysis, RBC lysis, in order to maximize both HSC recovery and viability. In our hands, both mechanical and enzymatic trituration methods equally facilitate breaking down tissue structure for homogenization. We'd like to caution that high concentrations of collagenase with greater tryptic activity (i.e., collagenase type I-III), in combination with prolonged exposure during incubation, can result in cell surface marker degradation, thereby negatively impacting flow cytometric analysis. Therefore, if enzymatic trituration is utilized, we highly recommend use of collagenase type IV due to its low tryptic activity. For this reason, in our laboratory, we prefer to utilize mechanical trituration as our primary form of fetal liver homogenization. We suggest both methods be tested side-by-side in your laboratory to compare efficiency and reproducibility of results before deciding on the most appropriate technique.

1. Using fine tip forceps, gently create an opening into the abdominal cavity of the fetus to expose the liver.
2. Protrude the liver outside the cavity by applying gentle pressure on the fetus using the inner edges of the forceps while encompassing the liver as shown in Fig. 2.

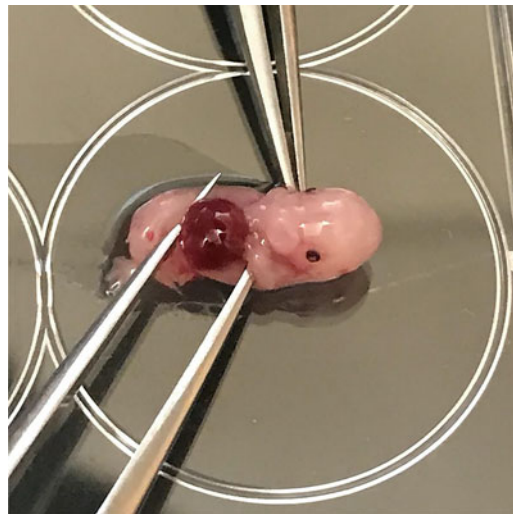


Fig. 2 Fetal liver isolation. Create an opening into the abdominal cavity of the fetus using fine forceps to expose the liver. Gently protrude the liver from the cavity by applying pressure on the fetus while simultaneously using the inner edges of the forceps to encompass the liver. Apply direct pressure against the fetus while gently clasping underneath the liver and lifting upward to effectively remove it

3. Apply direct pressure against the fetus while gently clamping it underneath the liver. Lifting will effectively remove the liver with minimal damage and tearing.
4. Place liver in a 35×10 mm petri dish with 1–1.5 mLs of ice-cold staining media and inspect the tissue for wholeness (*see Note 1*).

3.3.1 Manual Trituration

- (a) *For E14.5 and earlier fetal liver trituration:* use a 1000 μ L pipette tip to carefully triturate the liver. Avoid creating bubbles while homogenizing the tissue, as this decreases cell viability. To further maximize HSC yield, conserve tips used for homogenization and reuse during subsequent washes.
- (b) *For E16.5 and later fetal liver trituration:* use two glass slides to position the liver a third of the way up between the slides by flanking the tissue between the ends of the glass slides. Proceed to gently crush the liver by closing the gap between the two slides 2–3 times. Using a 1000 μ L pipette tip, rinse off any adhering tissue from the slides before completing the trituration process mechanically.
- (c) Filter homogenate into a 5 mL FACS tube through a $70 \mu\text{m}$ mesh or filter top. Wash petri dish twice, using the same pipette tip, with 1–1.5 mLs of ice-cold staining media and filter into the same FACS tube.
- (d) Centrifuge at $300 \times g$ for 5 min at 4°C and keep cells on ice.

3.3.2 Enzymatic Digestion

- (a) Place liver in a 12-well tissue culture plate containing 2 mLs of digestion solution. This digestion solution should be made fresh on the day of intended use.
 - (b) Using dissection scissors, cut the liver into ~2-mm size pieces and place the 12-well plate in a 37°C incubator for 30 min.
 - (c) After incubation, place the 12-well tissue culture plate on ice and allow it to cool before using a 1000 μ L pipette to carefully mechanically triturate the fetal liver.
 - (d) Filter homogenate into a 5 mL FACS tube through a $70 \mu\text{m}$ mesh or filter top. Wash the well two times, using the same pipette tip, with 1–1.5 mLs ice-cold staining media and filter into the same 5 mL FACS tube.
 - (e) Centrifuge at $300 \times g$ for 5 min at 4°C and keep cells on ice.
5. *For fetal liver analysis (no FACS):* Discard supernatant and add 500 μ Ls of $1 \times$ ACK lysis buffer and gently resuspend. Incubate on ice for ~45–60 s and immediately top off with staining media to stop cell lysis. Centrifuge at $300 \times g$ for 5 min at 4°C . Take a small aliquot for cell counting.

6. *For fetal liver HSC FACS:* Do not ACK lyse and instead discard supernatant, resuspend cells in 500–600 uLs of staining media, and keep cells on ice. Take a small aliquot for cell counting, then proceed to the c-Kit enrichment step.

3.4 HSC Enrichment Techniques

Fetal HSCs represent less than 0.01% of total cells in an E14.5 fetal liver. This results in a challenging and time-consuming process to reliably isolate purified HSCs in sufficient numbers for cell culture and transplantation assays. To optimize fetal liver HSC isolation and reduce FACS time, we have utilized both positive (CD117 enrichment) and negative selection (lineage depletion) techniques to enrich for hematopoietic stem and progenitor cells (HSPCs). While both techniques are suitable to enrich for cells of interest, we have had the best success using positive selection via CD117 (c-Kit) enrichment beads (Miltenyi Biotec) in combination with fluorescently labeled anti-CD117. It is important to note that neither positive nor negative selection techniques should be used if cellularity analysis is to be performed, as both techniques will skew cell number and frequency, preventing accurate quantification of cellular compartments.

3.4.1 C-Kit Enrichment

1. To 500–600 uL of fetal liver homogenate, add 12.5 uLs of CD117 (cKit) enrichment beads and gently mix by flicking the tube 2–3 times (*see Note 2*).
2. Incubate on ice for 25 min, flicking the tube 3–4 times halfway through the incubation period.
3. Wash cells with 2–3 mLs of ice-cold staining media and centrifuge at $300\times g$ for 5 min at 4 °C.
4. Prepare MACS magnetic MultiStand by attaching LS columns and prerinse the columns with 2–3 mLs of staining media over 70 μ m mesh, collecting volume in a 15 mL conical.
5. Discard supernatant and resuspend pelleted cells in 1.5 mLs of staining media and add to Miltenyi LS column in 500 uL increments over the filter. Wash 5 mL FACS tube with 4 mLs of staining media two times and add to column over filter in 1 mL increments. Do not allow the column to run dry.
6. Remove column from magnet, place in a clean 5 mL FACS tube, and add 4 mLs of staining media. Allow 2–3 drops of flow through to collect inside the FACS tube and swiftly expunge the remaining volume. Centrifuge at $300\times g$ for 5 min at 4 °C.

3.5 Cell Surface Markers and Flow Cytometry for Fetal HSCs

In the adult BM, numerous cell surface markers have been identified that can be reliably used for both positive and negative selection of primitive HSC populations, including but not limited to cKit, Sca1 [13], SLAM-family markers including CD150 and CD48 [14], CD34 [15, 16], Flt3 (also known as Flk2) [17],

ePCR [18], ESAM [19, 20], CD41 [21], and exclusion of dye [22]. Although many of these same markers identify HSCs in the fetal liver, it is important to note that in several cases, some HSC activity has also been observed outside of conventional marker definitions [23]. Additionally, there are some surface markers that are selective for adult HSCs but not fetal HSCs, including CD34 [24], Cd11b [25], and Flk2 [17]. Whether differences in HSC phenotype reflect maturation of the HSC pool across ontogeny, or shifts in more transient populations during the first few weeks of life, remains to be determined. However, these differences warrant caution when using stringent or conventional adult phenotypic definitions to isolate fetal HSCs at any stage.

3.5.1 Antibody Cocktail Preparation

We highly recommend that the antibody titer used for HSC identification be titrated to both optimize efficiency of cellular labelling as well as minimize reagent costs. Our laboratory uses antibody manufacturer's recommendations for cell staining volumes as a starting point and sets the titers for individual antibodies as works best in our own hands.

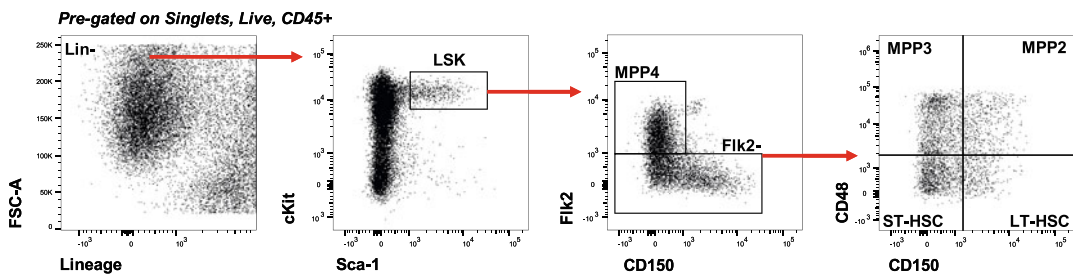
1. Prepare primary and secondary antibody cocktails in staining media accounting for 100–200 μ L staining volume per fetal liver sample as shown in Table 1.
2. Discard supernatant from samples and resuspend cells with 100–200 μ Ls of primary antibody cocktail. Allow to stain on ice, protected from direct light source, for 20 min.
3. Wash samples with staining media and centrifuge at $300\times g$ for 5 min at 4 °C.
4. Repeat **steps 2** and **3** with secondary antibody stain (Table 1).
5. Prepare viability stain (i.e., propidium iodide, 1 mg/mL stock used at 1:5000) in staining media to be used to resuspend cells just before sort or analysis.

3.5.2 Fetal HSC Gating Strategy

A representative gating strategy to identify and isolate fetal HSCs is shown in Fig. 3. As described in the previous section, there has been considerable effort to refine phenotypic isolation of adult HSCs using surface cell markers, and much of this work has been extended, at least in practice, to fetal hematopoiesis. There are some important exceptions to be noted: CD11b should always be excluded from the lineage markers, as it marks fetal HSCs [25]. There is also some HSC activity noted in CD150^{lo} and Flk2-negative populations within the fetal liver [8, 17, 23]. Because more detailed examination of fetal HSPC populations has not yet been performed to yield the level of clarity for phenotypic isolation as it has for adult populations, it's important to be cautious when drawing gates and isolating populations that are not yet as well characterized.

Table 1
Primary and secondary antibodies for HSC identification

Antibody:	Clone:	Cat #:	Manufacturer:
CD16/32 PGP (Fc Block)	93	101302	Biolegend
CD3 ϵ Biotin	145-2C11	100304	Biolegend
CD4 Biotin	GK1.5	100404	Biolegend
CD5 Biotin	53-7.3	13-0051-85	eBioscience
CD8a Biotin	53-6.7	100704	Biolegend
CD19 Biotin	6D5	115504	Biolegend
NK1.1 Biotin	PK136	108704	Biolegend
CD11c Biotin	N418	117304	Biolegend
Gr-1 Biotin	RB6-8C5	30-5931-U500	eBioscience
F4/80 Biotin	BM8	123106	Biolegend
Fc ϵ RI α Biotin	MAR-1	134304	Biolegend
Ter119 Biotin	TER-119	116204	Biolegend
CD117 (cKit) APC-Cy7	2B8	105826	Biolegend
CD150 (SLAM) PE-Cy7	TC15-12F12.2	115914	Biolegend
Ly6-A/E (Sca-1) Pacific Blue	E13-161.7	122520	Biolegend
CD48 Brilliant Violet 605	HM48-1	103441	Biolegend
CD135 (Flk2) APC	A2F10	135310	Biolegend
CD45.2 Brilliant Violet 785	104	109839	Biolegend
^a Streptavidin PE-Cy5	–	405205	Biolegend

^aSecondary antibody**Fig. 3** Example fetal liver HSC gating strategy using flow cytometry. Representative flow cytometry plot of pre-gated singlet, live, CD45+ cells from an E14.5 fetal liver. Staining conditions (number of cells, volume, antibody concentration, etc.) were consistent with those described above, with data acquisition performed the same day of cell preparation. Of note, the red-arrow gating schematic shown is indicative of known HSC and MPP gating strategies described in adult BM [29]

3.6 Fetal HSC Function in Transplantation

HSC function has historically been characterized both by *ex vivo* culture and by transplantation. While *ex vivo* culture has proven valuable to ascertain absolute lineage potential, these experiments are much harder to perform with fetal cells that are both fewer in number and also proliferate rapidly in culture. Given how little information we have regarding the fetal niche and how a fetal niche supports fetal hematopoiesis, it is harder to replicate those conditions *ex vivo*. For these reasons, in our laboratory, we have found that transplantation and other *in vivo* assays are much more valuable means to assess fetal HSC function.

3.6.1 Recipients

In our laboratory, we ensure fetal liver HSC transplant recipients are 8–12 weeks of age at the time of irradiation. While we typically utilize male recipients due to greater availability within our colonies, female recipients can be indiscriminately used as well. Sex differences in HSC transplantation efficiencies have been previously described for certain commercially available humanized mouse lines [26] and should be considered when using these particular mouse strains. Similarly, it is important to consider the impact of niche differences on transplanted HSC long-term multilineage reconstitution (LTMR) among adult, neonatal, and fetal recipients. In particular, examination of reconstitution potential of transplanted HSCs should be placed in the context of whether the recipient niche supports their regeneration, as certain subsets of immune cells, specifically those that arise during early development such as innate-like lymphocytes, may not be capable of being regenerated upon transplantation in certain settings [8, 27].

3.6.2 Irradiation

The gold-standard of HSC functionality is that, upon transplantation into an irradiated host, they are able to reconstitute blood and immune cell production for the lifespan of the recipient. Irradiation dose and timing can be manipulated to assess HSC functionality under competitive and noncompetitive conditions, each having implications on downstream analysis of engraftment and donor chimerism. Under lethal irradiation conditions (900–1100 Gy), competitive transplants utilizing whole bone marrow and HSC equivalents aid in both maximizing survival of recipients and dissociating technical error due to improper injection from *bona fide* changes to HSC functionality. In our laboratory, we utilize both lethal (900 Gy, split dose 4 h apart) and sublethal (450 Gy) doses of irradiation to assess isolated HSC functionality, but have found sublethal irradiation particularly useful for two reasons: (1) it does not require cotransplantation of HSC-equivalent BM cells to ensure survival of the recipient and (2) it aids to prevent an early “ceiling effect” in HSC chimerism resulting from engraftment of donor HSCs in a completely ablated BM niche, leading to a loss in resolution of HSC output potential upon transplantation. We

therefore recommend your laboratory test both lethal and sublethal irradiation methods to determine which is best suited to address your questions of interest and optimize downstream analysis. We also recommend irradiated mice be transplanted with donor cells within 24 h after last irradiation dose.

3.6.3 Cell Numbers and Transplantation

Just as varying irradiation doses and conditions can influence the interpretation of HSC functionality upon transplantation, transplanted cell numbers and purity will also necessarily influence BM chimerism and can impact the interpretation of immune cell regeneration dynamics post transplantation. As described in an earlier section, fetal liver HSCs represent a very small percentage of all liver cells during fetal development and, despite the use of enrichment and/or lineage depletion techniques, sorting sufficient number of fetal HSCs for transplantation remains a challenging feat. Moreover, the lack of defined fetal-specific HSC cell surface markers makes isolating true HSC populations within conventional gating strategies all the more difficult. To circumvent these issues, we sort fetal HSCs from cKit-enriched samples as Lin⁻ cKit⁺ Sca1⁺ (LSK) CD150^{mid/hi} to maximize total HSC yield and improve successful LTMR in recipient mice. We typically aim to sort 200 CD150⁺ LSK cells per transplant into sublethally irradiated adults, with cotransplantation of lethally irradiated adults with 500,000 WBM cells. It is important to note that this sort and gating strategy will also include short-lived MPP subsets that can also contribute to the initial readout of immune cell generation, up to 1–2 months post transplantation [28], and thus should be taken into account when interpreting readout potential.

1. Add FBS to a 10% concentration in staining media (sort collection media) and add 2 mLs per 5 mL FACS collection tube.
2. Resuspend cKit enriched samples in 2–3 mLs of staining media containing propidium iodide (if not already treated with viability stain previously) and sort fetal HSCs, as shown in Fig. 3, no faster than 2500 events/sec (*see Note 3 and 4*).
3. After sorting, immediately centrifuge collection tubes at $300\times g$ for 5 mins at 4 °C. While postsort purity analysis is essential to determine potential contamination within your sorted cells, it is not a feasible assay to perform with fetal HSC sorts due to extremely low cell yields. We therefore use an alternative sort gate to perform a postsort purity analysis as a proxy for our sorted cell population of interest.
4. Carefully remove supernatant and resuspend cells to appropriate cell concentration per 100–150 uLs. Transfer cells to 1.5 mL microtube and keep on ice until transplanted. We find this volume to be ideal for retro-orbital delivery using a 27G 0.5 mL tuberculin syringe.

5. Following your IACUC-approved anesthesia protocol, ensure recipient mice are unresponsive to paw-pinch before proceeding with retro-orbital injection.
6. Gently protrude the right or left eye by carefully retracting the skin toward the body of the mouse and insert the needle at a 45° into the medial canthus to access the retro-orbital sinus behind the eye and slowly inject the cells.
7. Observe the mouse for 10–15 mins posttransplantation for normal, active behavior.
8. Chimeric analysis can be performed every 4 weeks for the next 16 weeks using blood samples collected via tail bleeds or facial vein puncture, according to your IACUC-approved protocol. Similarly, antibiotic treatment may be required for recipient mice post irradiation and should be monitored by veterinarian staff for health status changes within the first 4–6 weeks post transplantation.

4 Notes

1. When isolating the fetal liver, it is possible to overestimate and remove extra tissue beyond the fetal liver. It is critical to remove any contaminating tissue once it is excised and transferred prior to homogenization.
2. The manufacturer recommends adding a specific volume of beads based on the cell concentration, which we have generally observed to be more beads than necessary to acquire proper enrichment. We recommend titering the specific number of beads based on cell concentration for your specific experimental needs.
3. To improve HSC viability during cell sorting, we maintain a slow sort rate and use a 100 µm nozzle on the BD FACSAria™ II and III sorters. It is important to test and standardize these parameters to best fit your experimental needs.
4. Proper care should be taken to ensure that the sort process is as gentle on the fetal HSCs as possible. Ensure that sort streams are directly centered into the sorting FACS tubes, as we've observed decreased viability in sorted fetal liver HSCs when sort streams enter too closely to FACS tube walls.

References

1. Palis J (2016) Hematopoietic stem cell-independent hematopoiesis: emergence of erythroid, megakaryocyte, and myeloid potential in the mammalian embryo. *FEBS Lett* 590: 3965–3974
2. Muller AM, Medvinsky A, Strouboulis J et al (1994) Development of hematopoietic stem cell activity in the mouse embryo. *Immunity* 1:291–301

3. Gekas C, Dieterlen F, Orkin S et al (2005) The placenta is a niche for hematopoietic stem cells. *Dev Cell* 8:365–375
4. Mahony CB, Bertrand JY (2019) How HSCs colonize and expand in the fetal niche of the vertebrate embryo: an evolutionary perspective. *Front Cell Dev Biol* 7:34
5. Upadhaya S, Reizis B, Sawai CM (2018) New genetic tools for the in vivo study of hematopoietic stem cell function. *Exp Hematol* 61:6–35
6. Haas S, Trumpp A, Milsom MD (2018) Causes and consequences of hematopoietic stem cell heterogeneity. *Cell Stem Cell* 22:627–638
7. Crisan M, Kartalaei PS, Neagu A et al (2016) BMP and hedgehog regulate distinct AGM hematopoietic stem cells ex vivo. *Stem Cell Rep* 6:383–395
8. Beaudin AE, Boyer SW, Perez-Cuninham J et al (2016) A transient developmental hematopoietic stem cell gives rise to innate-like B and T cells. *Cell Stem Cell* 19:768–783
9. Böiers C, Carrelha J, Lutteropp M et al (2013) Lymphomyeloid contribution of an immune-restricted progenitor emerging prior to definitive hematopoietic stem cells. *Cell Stem Cell* 13:535–548
10. Ginhoux F, Guillems M (2016) Tissue-resident macrophage ontogeny and homeostasis. *Immunity* 44:439–449
11. Montecino-Rodriguez E, Dorshkind K (2006) New perspectives in B-1 B cell development and function. *Trends Immunol* 27:428–433
12. Vantourout P, Hayday A (2013) Six-of-the-best: unique contributions of gammadelta T cells to immunology. *Nat Rev Immunol* 13:88–100
13. Okada S, Nakauchi H, Nagayoshi K et al (1992) In vivo and in vitro stem cell function of c-kit- and Sca-1-positive murine hematopoietic cells. *Blood* 80:3044–3050
14. Kiel MJ, Yilmaz OH, Iwashita T et al (2005) SLAM family receptors distinguish hematopoietic stem and progenitor cells and reveal endothelial niches for stem cells. *Cell* 121:1109–1121
15. Osawa M, Hanada K, Hamada H et al (1996) Long-term lymphohematopoietic reconstitution by a single CD34-low/negative hematopoietic stem cell. *Science* 273:42–45
16. Krause DS, Ito T, Fackler MJ et al (1994) Characterization of murine CD34, a marker for hematopoietic progenitor and stem cells. *Blood* 84:691–701
17. Christensen JL, Weissman IL (2001) Flk-2 is a marker in hematopoietic stem cell differentiation: a simple method to isolate long-term stem cells. *Proc Natl Acad Sci U S A* 98:14541–14546
18. Kent DG, Copley MR, Benz C et al (2009) Prospective isolation and molecular characterization of hematopoietic stem cells with durable self-renewal potential. *Blood* 113:6342–6350
19. Ooi AG, Karsunky H, Majeti R et al (2009) The adhesion molecule esam1 is a novel hematopoietic stem cell marker. *Stem Cells* 27:653–661
20. Yokota T, Oritani K, Butz S et al (2009) The endothelial antigen ESAM marks primitive hematopoietic progenitors throughout life in mice. *Blood* 113:2914–2923
21. Ferkowicz MJ, Starr M, Xie X et al (2003) CD41 expression defines the onset of primitive and definitive hematopoiesis in the murine embryo. *Development* 130:4393–4403
22. Goodell MA, Brose K, Paradis G et al (1996) Isolation and functional properties of murine hematopoietic stem cells that are replicating in vivo. *J Exp Med* 183:1797–1806
23. Kim I, He S, Yilmaz OH et al (2006) Enhanced purification of fetal liver hematopoietic stem cells using SLAM family receptors. *Blood* 108:737–744
24. Matsuoka S, Ebihara Y, Xu M et al (2001) CD34 expression on long-term repopulating hematopoietic stem cells changes during developmental stages. *Blood* 97:19–25
25. Morrison SJ, Hemmati HD, Wandycz AM et al (1995) The purification and characterization of fetal liver hematopoietic stem cells. *Proc Natl Acad Sci U S A* 92:10302–10306
26. Notta FS, Doulatov S, Dick JE (2010) Engraftment of human hematopoietic stem cells is more efficient in female NOD/SCID/IL-2Rgc-null recipients. *Blood* 115:3704–3707
27. Ikuta K, Kina T, MacNeil I et al (1990) A developmental switch in thymic lymphocyte maturation potential occurs at the level of hematopoietic stem cells. *Cell* 62:863–874
28. Duran-Struuck R, Dysko RC (2009) Principles of bone marrow transplantation (BMT): providing optimal veterinary and husbandry care to irradiated mice in BMT studies. *J Am Assoc Lab Anim Sci* 48:11–22
29. Pietras EM, Reynaud D, Kang Y-A et al (2015) Functionally distinct subsets of lineage-biased multipotent progenitors control blood production in Normal and regenerative conditions. *Cell Stem Cell* 17:35–46



Utilizing CyTOF to Examine Hematopoietic Stem and Progenitor Phenotype

Safa F. Mohamad and Maegan L. Capitano

Abstract

Regulation of hematopoiesis is dependent upon interactions between hematopoietic stem/progenitor cells and niche components, requiring a highly diverse array of different cell-cell interactions and cell signaling events. The overwhelming diversity of the components that can regulate hematopoiesis, especially when factoring in how the cell surface and intracellular protein expression profiles of hematopoietic stem/progenitor cells and niche components differ between homeostatic conditions and stressed conditions such as aging and irradiation, can make utilizing techniques like flow cytometry daunting, particularly while examining small cell populations such as hematopoietic stem cells (HSCs). Due to the complexity of the hematopoietic system, high-dimensional single-cell genomics and proteomics are constantly performed to understand the heterogeneity and expression profiles within this system. This chapter describes one such single-cell assay, which utilizes mass cytometry Time of Flight (CyTOF) technology to determine differences in expression profile within HSC, using changes in HSC populations due to gender and aging.

Key words Hematopoietic Stem Cell (HSC), Bone marrow, Single-cell proteomics, Mass cytometry, CyTOF

1 Introduction

The complexity of the hematopoietic system demands the use of high-dimensional single-cell approaches to fully understand the process of hematopoiesis. These approaches both at the single-cell genomics and proteomics level have helped increase our knowledge about the heterogeneity within the hematopoietic system. One such single-cell approach is the use of mass cytometry Time of Flight technology, also called CyTOF. When utilizing CyTOF, element isotopes tagged to antibodies are used to create a detailed response profile of the system in question. The antigens, if present on single cells, are bound to these metal-tagged antibodies, which are recognized via atomic mass spectrometric analysis. Moreover, antibodies bound to both surface and intracellular antigens can be recognized at the same time. CyTOF thus combines flow

cytometry with mass spectrometry to create this high-dimensional approach capable of analyzing differential protein expression at the single-cell level. The advantage of using CyTOF over flow cytometry is the absence of single color and fluorescent minus one (FMO) controls required to perform multicolor flow cytometric analysis, and the absence of compensation issues involved in flow cytometry. Furthermore, a higher number of parameters, almost 35+, can currently be analyzed with greater sensitivity in comparison to flow cytometry [1–3]. CyTOF also allows the use of complex algorithms such as VisNE, SPADE, and FlowSOM to understand the heterogeneity within populations in a more efficient manner. These algorithms convert high-dimensional data into simple two-dimensional data, making it easy to visualize (details mentioned in Subheading 3.5).

Since its discovery, several groups have utilized single-cell CyTOF to examine hematopoiesis. Bendall et al. performed CyTOF to demonstrate immune signaling in healthy human hematopoiesis [1]. Furthermore, the same group has published a paper profiling myelodysplastic syndrome utilizing patient samples to perform CyTOF [4]. Severe et al. used mass cytometry to determine the heterogeneity within bone marrow stromal cells in the hematopoietic niche, identifying the differential expression patterns within these subsets in homeostatic and stressed conditions [5]. Our group has utilized CyTOF to determine differential expression changes between osteomacs and bone-marrow-derived macrophages within the hematopoietic niche [6], and to determine molecular mediators through which megakaryocyte-stimulated osteomacs regulate hematopoietic function (*S.F. Mohamad and E.F. Srouf, manuscript in preparation*). We have also utilized CyTOF to examine expression changes of various signaling molecules in hematopoietic stem cells (HSCs) when isolating mouse bone marrow in hypoxia versus ambient air [7]. In this chapter, in order to fully understand how CyTOF works, we will demonstrate how to examine changes in mouse bone marrow HSC populations with gender and age.

2 Materials

Each section of the protocol is unique and requires its own set of reagents and supplies. For the sake of convenience, we are mentioning all the materials required for each individual section. Also, we isolated and analyzed bone marrow cells for our CyTOF experiments. However, any cell source may be used to perform the procedures outlined in this chapter.

2.1 Conjugation of Metal-Tagged Antibodies

1. Panel Designer V2 Software (Fluidigm; CA).
2. Maxpar Antibody Labeling Kit (Cat. # 201169B; Fluidigm; CA).
Contents of the kit include the following:
 - (a) Lanthanide Metal solution.
 - (b) Maxpar Polymer.
 - (c) R-Buffer.
 - (d) C-Buffer.
 - (e) W-Buffer.
 - (f) L-Buffer.
3. Antibodies (100 µg) to be labelled (From various vendors) (*see Note 1*).
4. TCEP-R-Buffer: Mix 8 µL of 0.5 M Tris(2-carboxyethyl) phosphine hydrochloride solution (TCEP) stock (Cat. # 646547; Millipore Sigma) with 992 µL of R-buffer.
5. Antibody stabilizer (Cat. # 130 050; CANDOR Bioscience; Germany).
6. Sodium azide (Cat. # S2002; Millipore Sigma).
7. Amicon[®] Ultra-0.5 Centrifugal Filter Unit, 0.5 mL V-bottom, 8-pack (Millipore Sigma).
 - Cat. # UFC500308 (3 kDa).
 - Cat. # UFC505008 (50 kDa).
8. 1.5 mL Microcentrifuge tubes.
9. Water bath at 37 °C.
10. Two table-top microcentrifuges (Room Temperature).
11. Nanodrop (Thermo Scientific).

2.2 Isolation of Lineage-Depleted Bone Marrow Cells

1. Mouse for isolation of lineage-depleted bone marrow cells.
2. Phosphate Buffer Saline (PBS) (Cat. # MB-008; Rockland Immunochemicals).
3. Iscoves's Modified Dulbecco's Medium (IMDM) complete: In 445 mL of IMDM, add 50 mL of heat-inactivated fetal bovine serum and 5 mL of penicillin-streptomycin, then filter the medium.
4. Lineage depletion buffer: Prepare a solution containing 0.5% bovine serum albumin (BSA) and 2 mM ethylenediaminetetraacetic acid (EDTA) in phosphate-buffered saline (PBS).
5. Direct lineage depletion cocktail (Cat. # 130-110-470; Miltenyi Biotec).
6. LS Columns (Cat. # 130-042-401; Miltenyi Biotec).

7. MidiMACS separator magnetTM (Cat. # 130-042-302; Miltenyi Biotec).
8. Sterile surgical scissors.
9. Sterile forceps.
10. Sterile gauze sponge.
11. 10 mL syringe.
12. 70 μ m cell strainers.
13. 25G, 5/8 in. needle.
14. 50 mL tubes.
15. 15 mL tubes.
16. Centrifuge.

2.3 Reagents for Cell Surface and Intracellular Staining

1. PBS (Cat. # MB-008; Rockland Immunochemicals).
2. CyTOF Stain Wash: 2.5 mL of 10X PBS + 0.025 gm of BSA (Cat. # A3059; Sigma Aldrich) 0.025 gm of sodium azide (Cat. # S-2002; Sigma Aldrich) + 100ul of EDTA (Cat. # E7889; Sigma Aldrich). Make up to 25 mL using MilliQ Water (*see Note 2*).
3. Brefeldin A (Cat. # B7651; Millipore Sigma).
4. Cell-IDTM Cisplatin (Cat. # 201064; DVS Sciences; Fluidigm).
5. Fc-Receptor Block (Cat. # 101320; Biolegend).
6. 1.6% Formaldehyde: 16% Formaldehyde (Cat. #18814-10; Polysciences) diluted with PBS.
7. Maxpar[®] Perm-S Buffer (Cat. # 201066; DVS Sciences; Fluidigm).
8. Maxpar[®] Fix and Perm Buffer (Cat. #201067; DVS Sciences; Fluidigm).
9. Cell-IDTM Intercalator-Ir (Cat. # 201192A (125 μ M) or 201192B (500 μ M); DVS Sciences; Fluidigm).
10. 10X EQ Calibration Beads (Cat. #201078; DVS Sciences; Fluidigm).
11. MilliQ Water.
12. 37 °C incubator.
13. 15 mL Tubes.
14. Polystyrene or Polypropylene Round-bottom Tubes with Cell-Strainer Cap, 5 mL capacity, 12 \times 75 mm.
15. CyTOF 2 Mass Cytometer (Fluidigm).
16. Cytobank Software (Beckman Coulter).
(Follow **Note 2** for specifications on reagents.)

3 Methods

3.1 Conjugation of Metal-Tagged Antibodies

To design a panel, we begin by choosing the antigens of which we want to determine the expression on our cell population. The list of antibodies chosen for the panel demonstrated in this book chapter along with their clones is provided in Table 1. To determine which metal tag should be attached to which antibody, we used the Panel Designer software present on the Fluidigm website. Metal isotopes ranging from ^{141}Pr to ^{176}Yb can be conjugated to antibodies. The general rule is that antigens that are assumed to be high in expression should have their antibodies tagged with lower metal isotopes. Isotopes 159–169Da are tuned for optimal delivery of metals and are tagged to antibodies, which bind antigens that are assumed to be low in expression. Moreover, background signal overlap from metal tags bleeding into other channels is also seen in mass cytometry. This overlap is minimal, constant, and measurable and can be avoided with a well-designed panel. The Panel Design software helps reduce background to a minimum based on the selection of channels. Antibody titration to determine the volume of individual antibodies also helps reduce background signal.

The first place to find metal-conjugated antibodies is the Fluidigm website. Fluidigm has a wide array of pre-conjugated antibodies targeting human and mice antigens. They also offer custom conjugation of antibodies, as well as antibody labeling kits for self-conjugation. We tried all three options and reached the conclusion that ordering pre-conjugated antibodies and conjugating antibodies in-house are the most feasible options. The Maxpar Antibody Labeling kit (Fluidigm) was purchased to conjugate antibodies and the protocol was followed according to manufacturer's instructions. The main components of the kit were the lanthanide solution, which consisted of the metal that is needed to be conjugated to the antibody, and the Maxpar Polymer, which formed the link between the metal and the antibody. Antibodies were purchased from various vendors (Table 1) based on the criteria mentioned in **Note 1**:

1. Retrieve the polymer from the $-20\text{ }^{\circ}\text{C}$. Thaw only the number of polymer tubes that are required; this will avoid moisture condensation. Centrifuge the polymer for 10 s before use. Resuspend the polymer with 95 μL of L-buffer. Next, add 5 μL of lanthanide metal solution to the same tube and incubate at $37\text{ }^{\circ}\text{C}$ for 30–40 min in a water bath. This tube now contains both the polymer and lanthanide metal solution.
2. Simultaneously, add 100 μg of the desired antibody in up to 400 μL of R-buffer to a 50 kDa column filter. Centrifuge at $12,000 \times g$ for 10 min at room temperature. Discard the flow-

Table 1
List of CyTOF antibodies

	Antibody	Label	Clone	Company
Extracellular	Lineage Cocktail FITC (Lin; includes markers CD3/Gr-1/CD11b/B220/Ter-119) Anti-FITC	160Gd	145-2C11; RB6-8C5; RA3-6B2; Ter119; M1/70 FIT-22	Biologend Fluidigm
Extracellular	CD150 APC (Signaling Lymphocytic Activation Molecule or SLAM) Anti-APC	176Yb	TC15- 12F12.2 APC003	Biologend Fluidigm
Extracellular	Sca-1 PE (Stem cell antigen-1/ Ly6a) Anti-PE	145Nd	E13-161.7 PE001	Biologend Fluidigm
Extracellular	CD166 (Activated Leukocyte Cell Adhesion Molecule, ALCAM)	151Eu	eBioALC48	eBiosciences
Extracellular	CD117 (ckit/ Stem Cell Factor receptor)	166Er	2B8	Fluidigm
Extracellular	CD48	156Gd	HM48.1	Fluidigm
Intracellular	Octamer-Binding Transcription Factor 3/4 (Oct 3/4, POU5f1)	165Ho	40/Oct-3	Fluidigm
Intracellular	Tumor Necrosis Factor α (TNF α)	162Dy	MP6-XT22	Fluidigm
Intracellular	Transforming Growth Factor β (TGF β)	164Dy	TW716B4	Fluidigm
Intracellular	Insulin-Like Growth Factor 1 (IGF1)	174Yb	M23	Thermo Fisher
Intracellular	Platelet-Derived Growth Factor β (PDGF β)	169Tm	Polyclonal	Abcam
Intracellular	Runt-Related Transcription Factor 1 (Runx1)	170Er	3H2L6	Invitrogen
Intracellular	cMyC	175Lu		Invitrogen
Intracellular	CCAAT/Enhancer-Binding Protein β (CEBP β)	141Pr	1H7	Biologend
Intracellular	GATA-Binding Protein 1 (GATA1)	149Sm	234737	R&D Systems
Intracellular	Notch1	171Yb	HMN1-12	Biologend
Intracellular	Growth Factor-Independent 1 Transcriptional Repressor (Gfi1)	168Er	Polyclonal	Invitrogen
Intracellular	SMAD family member 4 (SMAD4)	159Tb	4G1C6	Invitrogen
Intracellular	Phosphoinositide 3-kinase p85 α (PI3K)	150Nd	6G10	NOVUS
Intracellular	Mammalian Target of Rapamycin (Ser2448) (a.k.a. pmTOR)	143Nd	A17024A	Biologend
Intracellular	pAkt (S473)	152Sm	D9E	Fluidigm
Intracellular	pStat3 (Y705)	158Gd	4/P- STAT3	Fluidigm
Intracellular	pERK 1/2 (T202/Y204)	167Er	D13.14.4E	Fluidigm

through and add 100 μL of 4 mM TCEP-R-buffer to the antibody in the filter. Incubate at 37 °C for 30 min in a water bath (DO NOT EXCEED 30 min). This step will partially reduce the antibody.

3. Add 200 μL of L-buffer to a 3 kDa filter. The tube from **step 1**, which contained the polymer and lanthanide solution, was transferred to the same 3 kDa filter. Centrifuge at $12,000 \times g$ for 25 min at room temperature; wash with 400 μL of C-buffer and centrifuge at $12,000 \times g$ for an additional 30 min.
4. Retrieve the 50 kDa filter containing the partially reduced antibody and wash the filter twice with 400 μL of C-buffer at $12,000 \times g$ for 10 min at room temperature.

It is imperative that steps 3 and 4 are completed at the same time (see Note 3).

5. Resuspend the lanthanide-loaded polymer in 60 μL of C-buffer and transfer to the 50 kDa filter containing the partially reduced antibody. To let the conjugation occur, incubate the filter at 37 °C for 90 min.
6. Wash the conjugation mixture a total of 4 times using 400 μL of W-buffer. After the final wash, add 80 μL of W-buffer to the 50 kDa filter. This will dilute the conjugate, which should be approximately 20 μL in volume.
7. Determine the yield of the conjugated antibody using a nanodrop.
8. Centrifuge the 50 kDa filter at $12,000 \times g$ for 10 min to remove the W-buffer. Resuspend the antibody at a final concentration of 0.5 $\mu\text{g}/\mu\text{L}$ in antibody stabilizer with 0.05% sodium azide. Invert the 50 kDa filter over a clean 1.5 mL collection tube and centrifuge the inverted filter/collection tube at $1000 \times g$ for 2 min to transfer the resuspended metal-tagged antibody to the collection tube.

3.2 Titration of Metal-Tagged Antibodies

Metal-tagged antibodies conjugated in the previous section were titrated to reduce background signal. To titrate antibodies:

1. Make groups of 4–5 antibodies from the main panel. Antibodies within each group should be tagged to metals that are not within 1–2 channels of each other. Also, the +16 channel from the metal-tagged antibody should be avoided to prevent background signal due to oxidation.
2. Isolate lineage-depleted bone marrow cells following Subheading 3.3. For each group of antibodies, make 3 tubes of $3\text{--}3.5 \times 10^6$ lineage-depleted bone marrow cells. Label the tubes from 1 to 3 for each group.
3. Stain the cells according to Subheading 3.4. In the tube labeled 1, add 0.5 μL of each antibody within that group; in the tube

labeled 2, add 1 μL of each antibody; and in the tube labeled 3, add 2 μL of each antibody.

4. Collect 400,000–500,000 cells on the CyTOF2 (Equivalent to 1 injection on the CyTOF, which is 500 μL of the resuspended sample).
5. Analyze cells on cytobank following Subheading 3.5. For each antibody, determine which volume of antibody gave optimal signal with minimal background in adjacent channels.

3.3 Isolation of Lineage-Depleted Bone Marrow Cells

Lineage-negative bone marrow cells were isolated from mice. The detailed protocol for bone marrow isolation has been previously published [7, 8].

1. Isolate femurs and/or tibias from mice. Strip the tissue and muscle from the bone using a sterile gauze sponge. Keep the bones in a sterile culture plate containing IMDM complete.
2. Collect IMDM complete in a 10 mL syringe with a 25G needle and flush the bones.

To flush the bones, cut as little of the epiphyseal ends as possible to insert the tip of the needle into the bone. If difficult, cut the bone into half and flush both halves. Once flushed, bones will appear pale in color. Collect the bone marrow in a sterile 50 mL tube and centrifuge at $500 \times g$ for 5 min. Discard the supernatant, and count the cells.

3. Resuspend the cell pellet in 80 μL of lineage depletion cell buffer per 20×10^6 cells.
4. Use the direct lineage cell depletion cocktail obtained from Miltenyi Biotec to label lineage-positive cells with magnetic beads. Add 20 μL of cocktail per 20×10^6 cells. Incubate for 10 min, and proceed to the lineage depletion step.
5. Place LS column in the MACS separator magnet. Prepare the column by rinsing with 3 mL of lineage depletion cell buffer. Apply the incubated cells into the column. Collect unlabeled cells in a 15 mL tube (*see Note 4*).
6. Wash the column 3X with 3 mL and collect the unlabeled cells. Centrifuge the unlabeled cells $500 \times g$ for 5 min. Discard the supernatant, and count the cells (*see Note 5*). Resuspend the cells in complete IMDM at 1×10^6 cells/mL.

3.4 Staining Protocol for Cell Surface and Intracellular Antibodies

The next step is to stain the lineage-depleted bone marrow cells with surface and intracellular antibodies. Make sure to use presterilized filtered tips for all steps. Do not use any autoclaved tips or autoclaved reagents for any of the procedures (*see Note 2*).

1. Plate $3\text{--}3.5 \times 10^6$ lineage-depleted bone marrow cells in a sterile 6-well plate. Treat the cells with 10 $\mu\text{g}/\text{mL}$ of Brefeldin A in a 37°C incubator for 3 h to inhibit protein transport. An

alternate to using Brefeldin A is 10 $\mu\text{g}/\text{mL}$ of Monensin or a combination of 5 $\mu\text{g}/\text{mL}$ of Brefeldin A and 5 $\mu\text{g}/\text{mL}$ of Monensin. This step is important for intracellular staining, since Brefeldin A inhibits protein transport between the endoplasmic reticulum and the golgi, whereas Monensin inhibits trans-golgi function.

2. Following stimulation with Brefeldin A, transfer cells to a 15 mL tube. Add 10 mL of PBS to wash the cells at $500 \times g$ for 5 mins. Resuspend in PBS (10^7 cells/mL). Since we started with 3.5×10^6 cells, cells were resuspended in 400 μL of PBS, and transferred to a 5 mL round bottom tube to stain for cell viability.
3. Stain with 0.4 μL of Cell-ID Cisplatin viability dye for 2 min at room temperature. If needed, a titration can be performed to determine the ideal time required to stain for Cisplatin. Our titration results indicated an incubation time of 2 min for mouse bone marrow cells.
4. Wash cells at $500 \times g$ for 5 min at 4°C using 2 mL of CyTOF stain wash. Discard the supernatant and add 1 μL of Fc-Receptor-blocking solution to the cell pellet. Vortex and incubate for 10 min at room temperature.
5. Following Fc block, stain cells with a master mix of primary fluorophore antibodies (refer to Table 1). Gently vortex and incubate at 4°C for 20 min. Following incubation, wash cells using 2 mL CyTOF stain wash. Discard the supernatant and resuspend the pellet in the residual volume left after the wash.
6. Next, stain cells with a master mix containing extracellular/surface metal-labeled antibodies (refer Table 1) at 4°C for 30 min. The master mix is a combination of surface antibodies, which are added in an amount determined by your previous titrations (Refer to Subheading 3.2). Make the master mix volume to 100 μL using CyTOF stain buffer.
7. After surface staining, wash cells using 2 mL CyTOF stain wash and fix with 1 mL of 1.6% formaldehyde for 30 min at room temperature (*see Note 6*).
8. To permeabilize cells, perform two 10-min washes with Maxpar Perm-S Buffer.
9. Next, stain cells with a master mix containing intracellular metal-labeled antibodies (refer to Table 1) at 4°C for 30 min. The master mix consisted of pretitrated intracellular antibodies made to a volume of 100 μL with CyTOF stain wash.
10. Following incubation, wash cells using 2 mL CyTOF stain wash and incubate overnight in 1 mL of 1:1000 Cell-ID

Intercalator-Ir diluted in Maxpar Fix and Perm buffer (*see Notes 7 and 8*).

11. The next day, wash cells once with CyTOF stain wash and twice with MilliQ water. Filter cells twice, once before the last wash and once after. This prevents clogging of the CyTOF.
12. Resuspend cells in 1X EQ Calibration beads. The EQ Calibration beads arrive in a 10X solution. Shake the bottle vigorously for 2 min before dilution.
13. Samples are acquired on a CyTOF 2 mass cytometer. Use the bead signature to normalize raw CyTOF data before analysis on Cytobank software.

3.5 Data Analysis

Cytobank software was used to analyze normalized data. FlowJo is an alternate software that can be used for basic CyTOF data analysis. However, Cytobank offers several options for data representation, which is not the case for FlowJo. Furthermore, Cytobank also offers a useful feature to analyze heterogeneity within populations based on the antibody panel.

1. Exported files are gated on singlet viable cells based on DNA labeling with iridium (Ir191/193), event length, and cisplatin (Pt195). Detailed gating is shown in Fig. 1.
2. Gating on Ir191/193 (X-axis) with any of the EQ bead channels 140Ce/151Eu/165Ho/175Lu (Y-axis) excludes any beads, which mistakenly were attached to the cells (*see Note 9*). The next gating is based on Ir191/193 on the X-axis and event length on the Y-axis. This gating allows us to exclude doublet cells. The third basic gating required for CyTOF is cisplatin (Pt195) on the X-axis versus event length on the Y-axis, which allows us to exclude cisplatin+ dead cells.

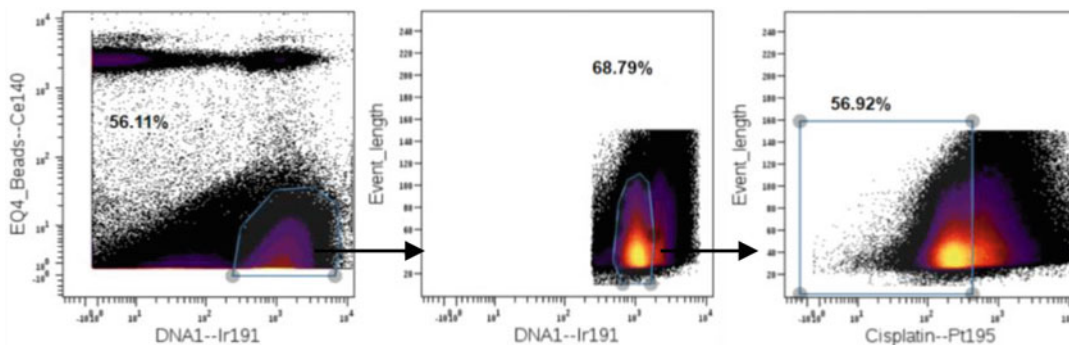
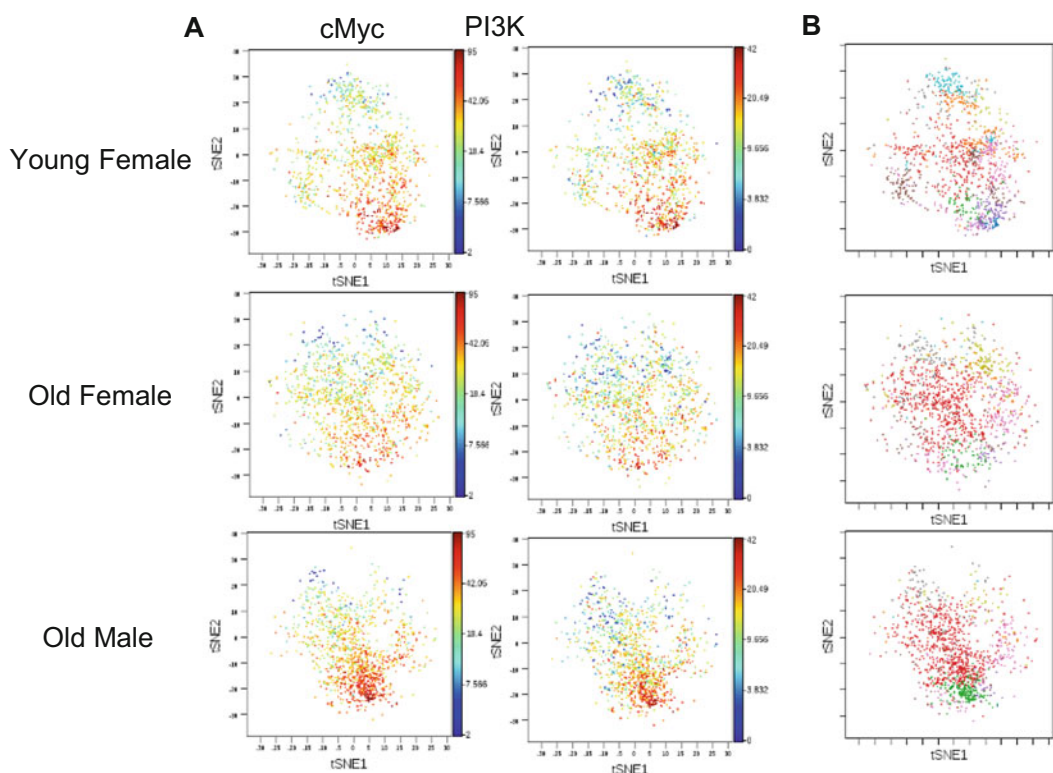


Fig. 1 Initial gating strategy for CyTOF samples. Lineage-depleted bone marrow was subjected to surface and intracellular staining. Cells were put through a mass cytometry Time of Flight machine (CyTOF) to collect data for protein expression profiling. Initial data analysis included gating on EQ4 beads and DNA Ir191 (left plot) to get rid of the EQ4 beads in the sample. The next was on event length vs. DNA Ir191 (middle plot) to isolate singlet cells. Finally, cells were gates on Cisplatin Pt195-negative cells to identify live cells

3. After the initial clean-up, lineage-depleted samples are gated on chosen cell population. For example, lin-Sca+ckit+CD48-CD150+ can be used for long-term HSC. You can then use the gated long-term HSC to make viSNE plots, heatmaps, and FlowSOM plots on Cytobank software.
4. ViSNE Plots: ViSNE is a powerful tool that reduces high-parametric data into simple two-dimensional dot plots. It is based on the t-Distributed Stochastic Neighbor Embedding (t-SNE) algorithm. Each antibody from the panel can be annotated on the resulting 2D plots to determine which cluster of cells express the antigen (Fig. 2a). These ViSNE plots can also be used to make FlowSOM plots described below.
5. FlowSOM Plots: FlowSOM is an algorithm that forms Self-Organizing Maps (SOMs) based on the similarities and differences between cells. The subsets thus formed are based on the clustering channels, which we choose from our antibody panel. This algorithm shows population abundance and most importantly identifies heterogeneity within cell populations. An example of a FlowSOM plot is shown in Fig. 2b and the figure legend for the plot is shown in Fig. 2c.
6. Heat Maps: Cytobank also has a feature to make heat maps based on the expression intensity of the antigens present within the panel (Fig. 3).

4 Notes

1. Antibodies used for metal conjugation should be carrier-free and should NOT contain bovine serum albumin (BSA), glycerol, gelatin, etc. Sodium azide is fine. BSA removal kits may be used to get rid of the antibody of BSA; however, it is not highly recommended. Avoid using antibodies of hamster origin, since they do not conjugate well. Several companies now sell CyTOF-ready antibodies for easy conjugation to metal isotopes.
2. Reagents:
 - Do not store the CyTOF stain wash and the MilliQ water for over a week.
 - Do not use any other PBS besides Rockland Immunochemicals to avoid background during data collection.
 - Do not use any autoclaved tips or autoclaved plasticware to avoid background. Use presterilized filter tips.
 - None of the glassware should be washed in a dishwasher or with soap to avoid metal contamination. To clean glassware, wash with MilliQ water.



C





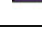
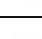
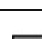



Color	Subpopulation #	Phenotype
	1	CD150 ⁺ cMyc ⁺ IGF1 ⁺ Runx1 ⁺ PDGFβ ^h Gfi1 ^h TGFβ ^h TNFα ⁺ BMP4 ⁺ pAkt ⁺ PI3K ^h pmTOR ^h CEBPβ ^h
	2	CD150 ^h cMyc ⁺ IGF1 ⁺ Runx1 ⁺ PDGFβ ^h Gfi1 ^h pErk ⁺ TGFβ ^h BMP4 ⁺ pAkt ⁺ PI3K ^h pmTOR ^h CEBPβ ⁺
	3	CD150 ^h cMyc ⁺ IGF1 ⁺ Runx1 ⁺ PDGFβ ^{low} Gfi1 ^h pErk ^{low} TGFβ ⁺ BMP4 ⁺ PI3K ^h pmTOR ^h CEBPβ ^h
	4	CD150 ⁺ cMyc ⁺ IGF1 ⁺ Runx1 ⁺ PDGFβ ⁺ Gfi1 ^h pErk ⁺ TGFβ ^h BMP4 ⁺ pAkt ⁺ PI3K ^h pmTOR ^h CEBPβ ⁺
	5	CD150 ⁺ cMyc ⁺ IGF1 ⁺ Gfi1 ^h TGFβ ^h PI3K ⁺ pmTOR ⁺
	6	CD150 ⁺ cMyc ⁺ IGF1 ⁺ Gfi1 ^h pErk ^{low} TGFβ ⁺ BMP4 ⁺ pAkt ⁺ PI3K ⁺ pmTOR ⁺
	7	CD150 ^h IGF1 ⁺ Gfi1 ^{low} PI3K ⁺ pmTOR ⁺
	8	CD150 ^h cMyc ⁺ IGF1 ^{low} Gfi1 ⁺ TGFβ ^{low} BMP4 ⁺ PI3K ⁺ pmTOR ⁺
	9	CD150 ⁺ cMyc ^{low} IGF1 ^{low} Gfi1 ⁺ TGFβ ^{low} BMP4 ^{low} PI3K ⁺ pmTOR ⁺
	10	CD150 ⁺ cMyc ⁺ IGF1 ^{low} Gfi1 ⁺ TGFβ ^{low} BMP4 ⁺ PI3K ⁺ pmTOR ⁺

Fig. 2 CyTOF analysis of gated LT-HSCs differing in age and gender. BM from a young female and old male and female C57BL/6 donor mice was collected and processed as described in Subheading 3.3. Samples were stained with the indicated antibodies conjugated to metal (Table 1) and then analyzed with a CyTOF 2 mass

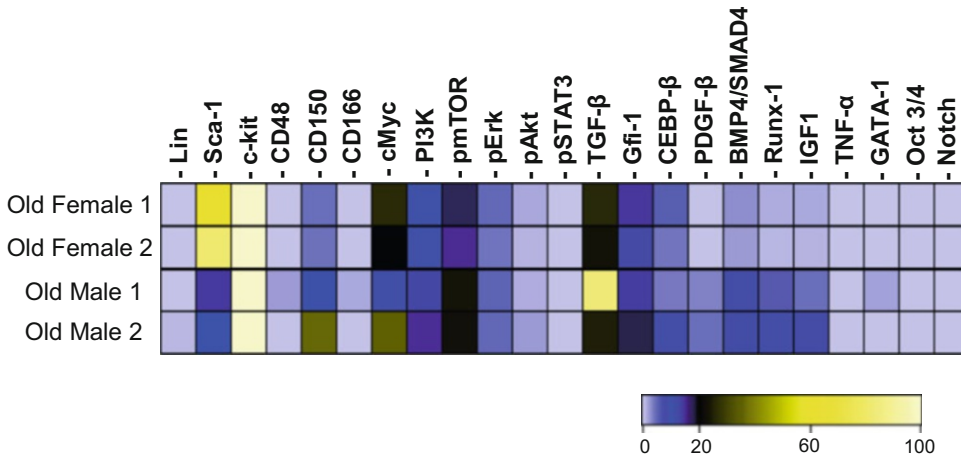


Fig. 3 Heat maps generated using gated LT-HSCs differing in gender. Samples processed and analyzed in Fig. 2 were used to generate heat maps using the Cytobank software

- Buffers should be calcium- and magnesium-free. Avoid reagents such as Ficoll, since they contain iodine.
 - Always make fresh 1.6% paraformaldehyde.
3. It is imperative that **steps 3** and **4** of the antibody conjugation be completed at the same time. To accomplish this, we started **step 2** around 20–25 min after the tube in **step 1** was incubated in the water bath. Using two table-top microcentrifuges is also helpful to complete **steps 3** and **4** at the same time. The conjugation will fail if **steps 3** and **4** are not completed within a maximum of 5 min of each other.
 4. Do not add more than $150\text{--}200 \times 10^6$ cells per LS column. The depletion works better with around 150×10^6 cells.
 5. Be careful not to include lineage-positive magnetically bound cells. Magnetic beads clog the CyTOF and interfere with the collection of data. Therefore, positive selection kits CANNOT be used in combination with CyTOF.
 6. Make sure to use fresh 1.6% paraformaldehyde for every experiment. The fixation step is very important for CyTOF. If cells are not fixed properly, there will be further cell loss, which can be seen during upcoming washes where the pellet size will reduce. Also, inefficient fixation can lead to increased background due to debris while acquiring data.

Fig. 2 (continued) cytometer and Cytobank software. (a) cMyc and PI3K levels within gated LSK CD48⁻CD150⁺ plots using viSNE analysis. Scales indicate the mean marker intensity of arcsinh-transformed values. (b–c) Gated LSK CD48⁻CD150⁺ LT-HSCs were used to make FlowSOM plots, where different colors indicate the subpopulations explored. *t*-SNE1,-2, *t*-distributed stochastic neighbor embedding

7. As an alternative, cells can be incubated for 1 h at room temperature. However, overnight incubation gives cleaner data. Also, since the protocol is long, it is better to carry out the experiment over two days.
8. Cells can be left at 4 °C in the intercalation solution for up to 48 h. For longer storage for up to a week, make fresh intercalation buffer and mix in a 1:1 ratio with PBS. However, storage for longer times shifts signal intensity.
9. For cleaner looking data, gating Ir191/193 (X-axis) with multiple of the EQ bead channels (Y-axis) may be considered.

References

1. Bendall SC, Simonds EF, Qiu P et al (2011) Single-cell mass cytometry of differential immune and drug responses across a human hematopoietic continuum. *Science* 332:687–696
2. Cheung RK, Utz PJ (2011) CyTOF—the next generation of cell detection. *Nat Rev Rheumatol* 7:502–503
3. Maecker HT, Nolan GP, Fathman CG (2010) New technologies for autoimmune disease monitoring. *Curr Opin Endocrinol Diabetes Obes* 17:322–328
4. Behbehani GK, Finck R, Samusik N et al (2020) Profiling myelodysplastic syndromes by mass cytometry demonstrates abnormal progenitor cell phenotype and differentiation. *Cytometry B Clin Cytom* 98:131–145
5. Severe N, Karabacak NM, Gustafsson K et al (2019) Stress-induced changes in bone marrow stromal cell populations revealed through single-cell protein expression mapping. *Cell Stem Cell* 25:570–583
6. Mohamad SF, Gunawan A, Blosser R et al (2021) Neonatal osteomacs and bone marrow macrophages differ in phenotypic marker expression and function. *J Bone Miner Res* 36:1580–1593
7. Capitano ML, Mohamad SF, Cooper S et al (2021) Mitigating oxygen stress enhances aged mouse hematopoietic stem cell numbers and function. *J Clin Invest* 131:e140177
8. Ghosh J, Mohamad SF, Srouf EF (2019) Isolation and identification of Murine bone marrow-derived macrophages and osteomacs from neonatal and adult mice. *Methods Mol Biol* 2002:181–193



Hematopoietic Stem Cell Identification Postirradiation

Andrea M. Patterson, Christie M. Orschell, and Louis M. Pelus

Abstract

Radiation exposure is particularly damaging to cells of the hematopoietic system, inducing pancytopenia and bone marrow failure. The study of these processes, as well as the development of treatments to prevent hematopoietic damage or enhance recovery after radiation exposure, often require analysis of bone marrow cells early after irradiation. While flow cytometry methods are well characterized for identification and analysis of bone marrow populations in the nonirradiated setting, multiple complications arise when dealing with irradiated tissues. Among these complications is a radiation-induced loss of c-Kit, a central marker for conventional gating of primitive hematopoietic populations in mice. These include hematopoietic stem cells (HSCs), which are central to blood reconstitution and life-long bone marrow function, and are important targets of analysis in these studies. This chapter outlines techniques for HSC identification and analysis from mouse bone marrow postirradiation.

Key words Bone marrow, Irradiation, Flow cytometry, Hematopoiesis, c-Kit, FGD5, Pelvic bones, Spine, SLAM, Autofluorescence

1 Introduction

Hematopoietic stem cells (HSCs) are able to self-renew and repopulate blood-forming cells for a lifetime. But these important cells are easily compromised by radiation exposure, which can lead to bone marrow failure. Hematopoietic tissues comprise the most sensitive cells to radiation, and the study of HSCs postirradiation is pivotal to the development of treatments for acute and long-term radiation effects on hematopoiesis. However, irradiated tissues are not always amenable to analysis techniques developed in the nonirradiated setting, and often come with a new set of challenges; HSCs are no exception.

1.1 Radiation-Induced Marker Changes

One of the biggest challenges in HSC analysis postirradiation is HSC gating by flow cytometry. Widely established gating strategies for HSCs from mouse bone marrow begin with an LSK gate (Lineage⁻ (*see Note 1*), Sca-1⁺, c-Kit⁺), which contains HSCs as well as their earliest progeny [1–4]. From here, further HSC

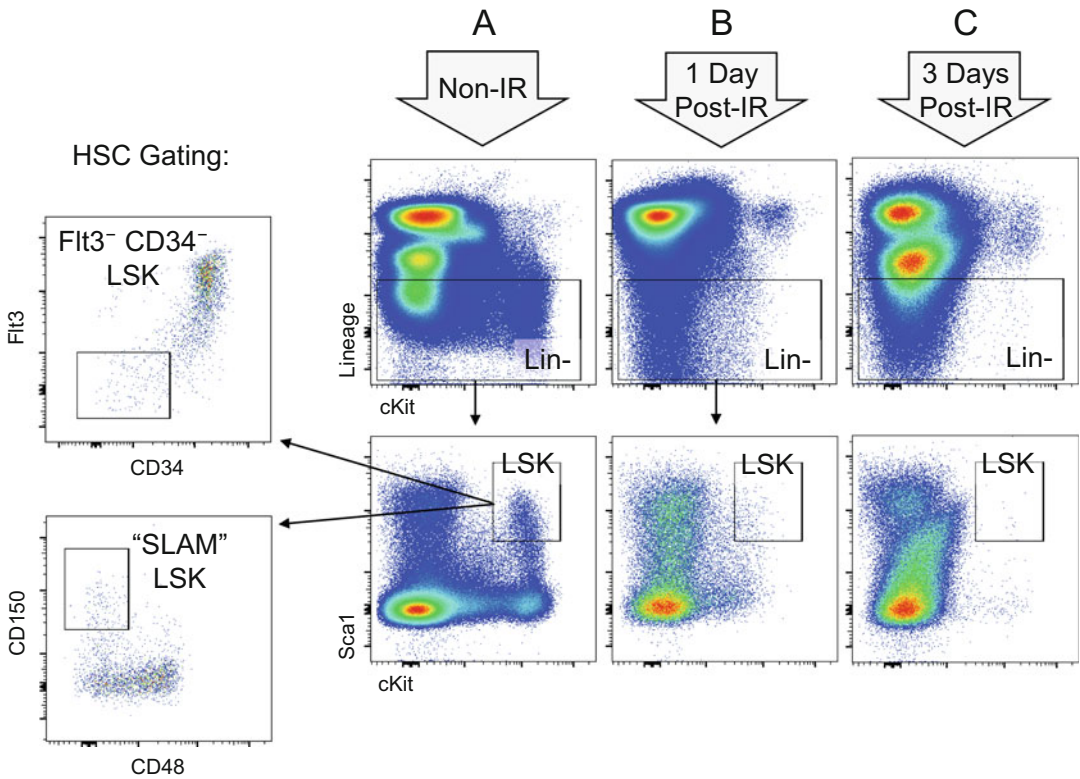


Fig. 1 (a) Classical HSC gating strategies for nonirradiated (non-IR) bone marrow. (b–c) Bone marrow cells progressively lose the central LSK population as shown at 1 and 3 days postirradiation (post-IR) (here, 8.53 Gy)

enrichment is accomplished with either a CD34⁻/Flt3⁻ gate [5–8], or a CD150⁺/CD48⁻ SLAM marker gate (SLAM-LSK) [9, 10] (*see* Fig. 1a). If fixation is not required, the unique efflux capacity of HSCs also potentiates identification by Hoechst-low “side population” (SP) gating, though this method requires high technical expertise and typically still uses LSK markers to ensure a pure HSC population [11, 12].

Following irradiation, however, the LSK marker c-Kit virtually disappears from bone marrow cells, precluding the routine flow cytometry analysis of HSC (*see* Fig. 1b–c). Some c-Kit⁺ subsets may be preferentially dying from irradiation, thus contributing to the disappearance of c-Kit⁺ cells in the bone marrow, but we and others have found that persisting HSCs are in fact losing surface c-Kit expression. One study showed that two days after total body irradiation, SP-gated cells had adopted a temporary c-Kit-low phenotype but retained HSC repopulating capacity [13]. We have confirmed and further elucidated this phenomenon, tracking HSCs with ZsGreen fluorescence in FGD5-transgenic mice postirradiation (Jackson Laboratories 027788). These mice have ZsGreen in place of one allele of FGD5, a gene with specific expression in

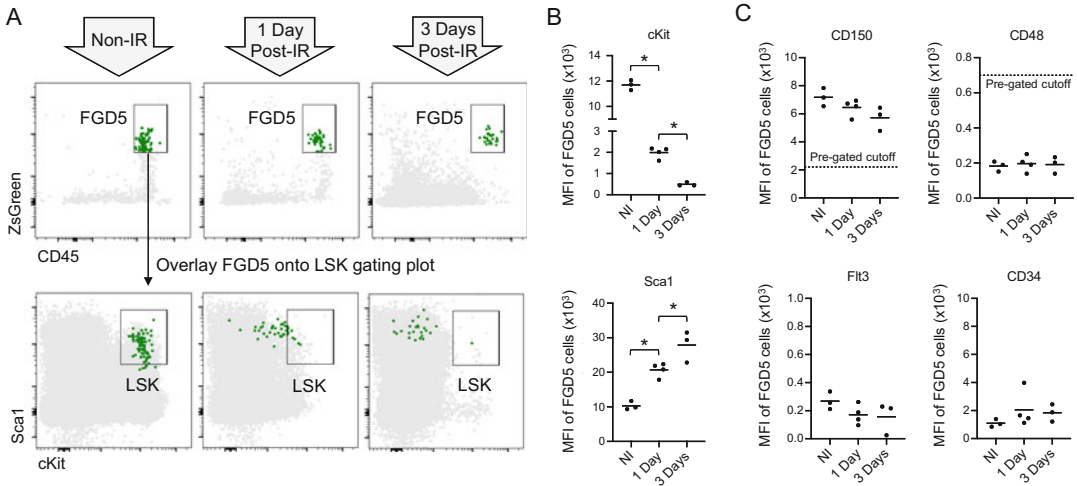


Fig. 2 FGD5-defined HSCs are still present 1 and 3 days post-IR in a c-Kit-low state. FGD5 mice were exposed to 8.53 Gy gamma irradiation 1 or 3 days prior to sacrifice or left nonirradiated (NI) ($n = 3-4$ mice per group). BM was harvested from femurs, tibias, and pelvic bones, and stained with the indicated HSC markers for flow cytometry. (a) ZsGreen fluorescence was used to identify FGD5-expressing HSCs (top, green), and this gate was overlaid onto the classical LSK plot (bottom). FGD5 plots are pregated on Lin⁻ CD48⁻ CD150⁺, and LSK plots are pregated on CD45⁺ Lin⁻. (b) Median fluorescence intensity (MFI) of the FGD5 population for c-Kit and Sca-1 as visualized in (a). (c) MFI of the FGD5 population for other HSC markers does not change substantially post-IR. * $p < 0.05$, one-way ANOVA

HSCs within the hematopoietic compartment as confirmed through transplant studies [14]. Gating on FGD5⁺ HSCs illustrates their shift over time to a c-Kit-low and Sca-1-high gating position in the LSK plot (*see* Fig. 2). In this chapter, we describe a modified gating strategy for HSCs in the absence of normal c-Kit expression postirradiation, with minimal loss of HSC purity (*see* Fig. 3).

1.2 Radiation-Induced Debris and Autofluorescence

Flow cytometry gating after irradiation can also be confounded by cellular remnants and debris that now accompany the bone marrow cells of interest, much of which may not be excluded by a given live/dead dye. These may obscure the scatter plot and tend to have high autofluorescence, which can also obscure markers for gating and analysis. In this chapter, we provide simple measures for obtaining “cleaner” HSC analyses in the irradiated setting. In addition to live/dead discrimination, we describe multiple scatter gates, special considerations for compensation, and the inclusion of CD45 as a bright marker to pull cells of interest away from low-to-mid autofluorescing noise.

Irradiation may also increase autofluorescence within the viable HSCs under analysis. We characterized the background fluorescence in live HSCs over time postirradiation in the FITC and PE channels and found that fluorescence intensity in both channels increased over 24 h (*see* Fig. 4). Here the effect was more

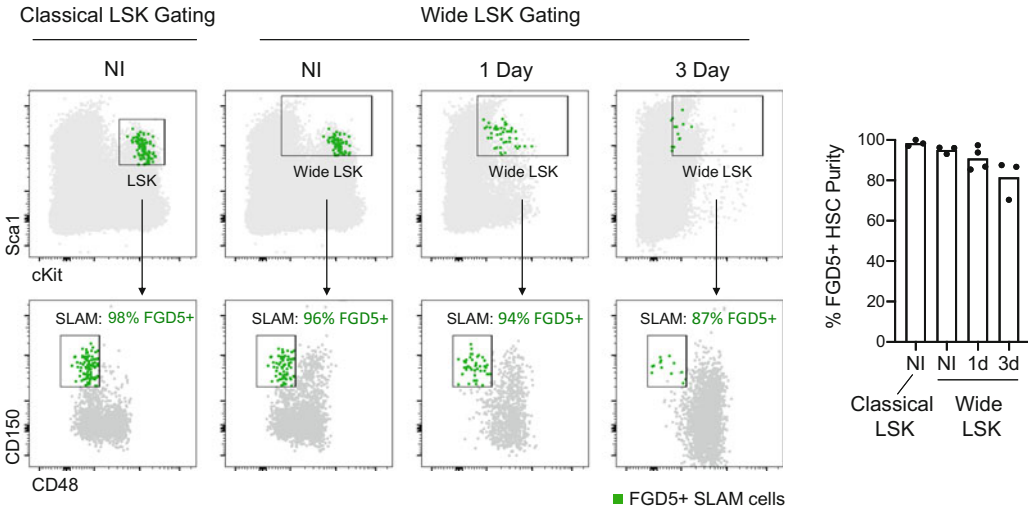


Fig. 3 Wide LSK gating followed by SLAM markers allows HSC identification in the absence of normal c-Kit expression post-IR, with minimal loss of FGD5-defined HSC purity. FGD5 mice were treated as in Fig. 2. Classical SLAM-LSK gating of NI cells (far left plots and first bar in bar graph) produces a highly pure HSC population, which is ~98% positive for FGD5 expression. Use of a wide LSK gate with SLAM gating still produces a highly pure HSC population in NI bone marrow, which is ~96% positive for FGD5 (next plots and bar). At 1 day and 3 days post-IR (here, 8.53 Gy), wide LSK gating is able to capture c-Kit-low HSCs, while subsequent SLAM gating remains >90% and >80% positive for FGD5, respectively (remaining plots and bars); n = 3-4 mice per time point

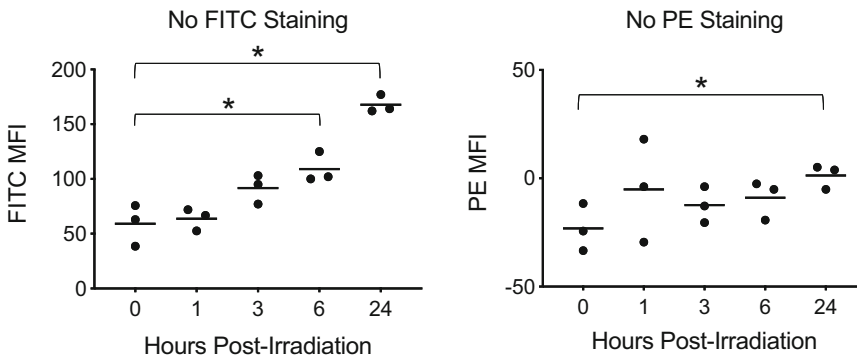


Fig. 4 Irradiation can increase HSC autofluorescence. BM cells taken from C57BL6 mice at the indicated time points post-IR (8.72 Gy) were stained for HSC markers with the FITC and PE channels left open. All colors were fully compensated against the FITC and PE channels in addition to each other. HSCs were gated with a wide LSK gate and SLAM markers. Median fluorescence intensity (MFI) of gated HSCs was measured in the empty FITC and PE channels; n = 3 mice per time point

pronounced in the FITC channel than the PE channel, but these effects may vary depending on the specific flow cytometer, voltage settings, and various other factors. This underscores the importance of including “fluorescence minus one” (FMO) controls for individual samples, or at least one per treatment group, for any

colors in which potentially low fluorescence levels will be statistically compared between groups. An FMO control is a separate tube of the same cells, stained with all colors but one, and is used either to subtract background from fluorescence intensity values or to accurately set negative versus positive gating. Without sufficient FMO controls, radiation-induced background fluorescence could be mistaken for changes in a low frequency antigen in a given channel. Thus, the use of individual FMO controls is included in this protocol.

1.3 Limiting Numbers of Bone Marrow Cells

Cell numbers become limiting in studies of high-dose radiation in which loss of >90% of total nucleated bone marrow cells can be expected, and it can become critical to maximize the available bone marrow from each mouse. Long bones such as femurs and tibiae are the most common bones harvested for marrow studies, but the challenge of low cell numbers postirradiation often requires harvesting more bones such as the pelvis and spine among others. Pelvic bones are flat bones, which contain about as much marrow as femurs [15], and are fairly straightforward to extract and clean. The spine contains approximately 1/3 of the total bone marrow in a mouse [15], but is more difficult to work with due to many small vertebrae and intercalating tissues. Also, while flushing of bone marrow is often routine for long bones, marrow from both pelvis and spine is most easily extracted by crushing with mortar and pestle. This chapter describes the extraction and use of these additional bones in the mouse, which may not be routine for many hematopoiesis labs.

Overall, this chapter provides detailed methods and best practices for HSC identification and analysis from mouse bone marrow following radiation exposure.

2 Materials

1. Dissection and bone cleaning tools: scissors, forceps, gauze, (optional: razor blade).
2. 70% ethanol in diH₂O.
3. Phosphate-buffered saline (PBS).
4. Cell buffer: PBS, 2% FBS, 2 mM EDTA.
5. Mortar and pestle.
6. 40 μ m cell strainers fit to 50 mL conical tubes.
7. Trypan blue.
8. Manual hemacytometer.
9. Live/Dead Fixable Dead Cell Stain Kit (*see* Table 1).
10. ArC Amine Reactive Compensation Bead Kit, Invitrogen.

Table 1
Suggested 10-color flow panel for HSC analysis

#	Marker	Fluor/color channel	Clone	Vendor
1	Live/dead	“Yellow” (BV605 channel)	N/A	ThermoFisher
2	Lineage	APC	Various	BD Biosciences
3	Sca-1	PerCP/Cy5.5	D7	Biolegend
4	c-Kit	BV785	2B8	Biolegend
5	CD150	PE/Cy7	TC15-12F12.2	Biolegend
6	CD48	APC/Cy7	HM48-1	Biolegend
7	CD45	FITC	30-F11	Biolegend
8	DAPI/other	(Pac Blue/BV421 channel)	Other targets of interest	
9	Other	PE		
10	Other	Alexa Fluor 700		

11. UltraComp Compensation beads, Invitrogen.
12. Fluorophore-conjugated antibodies to HSC markers (*see* Table 1).
13. Other antibodies of interest with compatible fluorophores (*see* Table 1).
14. 40 μ m filter-top flow tubes (5 mL).
15. (Optional) 4% Paraformaldehyde (PFA).
16. (Optional) Cytotfix/Cytoperm buffer and Perm/Wash buffer, BD Biosciences.
17. (Optional) DAPI.
18. Flow cytometer such as the BD LSRFortessa with sufficient lasers and filters for the fluorophores in use.

3 Methods

3.1 Extraction of Multiple Bone Types

Removal of long bones including femurs, tibias, and humeri is routine for most hematopoiesis groups. Here we will describe the additional extraction of pelvic bones and spine. Depending on the irradiation dose and time point, and the number of cells needed for analysis, long bones alone may be sufficient. If more cells are needed, we recommend adding pelvic bones first and crushing them altogether with the long bones. If still more cells are needed, continue with dissection of the spine and crush separately before combining together all filtered marrow.

1. Place fully euthanized mouse under a laminar flow hood and soak all fur in 70% ethanol to increase sterility and minimize fur interference.
2. Make a small incision in the skin layer over the abdomen and pull apart to remove all skin from the body. Continue to pull away skin until all limbs are exposed.
3. Cut away the major muscles surrounding the tibia and femur and continue exposing slightly beyond the femur at the hip joint.
4. Carefully disconnect the femur from the hip joint. Locate the empty hip socket and grip here with forceps. This is the center of the pelvic bone. Cut around the bone to release it. The pelvic bone is long and flat on the anterior side of the joint and forms a fan on the posterior side.
5. Demuscle all long bones and pelvic bones with gauze and place directly into a tube with 3 mL chilled cell buffer on ice (*see Note 2*).
6. To remove the spine, begin at the base of the tail and cut along the spine on both sides toward the head, cutting through the ribs close to the spine. Continue cutting along all sides to release the spinal column, which remains encased in tissues.
7. Using a razor blade, shave away as much tissue as possible along the outside of the column, while leaving the spine intact. Tissue will remain in between and around vertebrae, and this will not preclude analysis.
8. Cut spine into 3–4 sections and place into a separate tube of 3 mL chilled cell buffer on ice.

3.2 Crushing to Release Bone Marrow Cells

1. Long bones and pelvic bones can be crushed together.
2. Dump the bones and buffer into a prechilled mortar (*see Notes 2 and 3*).
3. Crush with pestle in a circular motion for ~20 s.
4. Decant fluid from mortar into a 40 μm filter placed in a 50 mL conical tube.
5. Add cell buffer to the mortar and repeat crush, targeting red areas of bone. Decant fluid into the same filter/tube.
6. If adding spine, crush separately. Repeat **steps 2–5** and combine with other cells after filtration.
7. Centrifuge at $500 \times g$ for 10 min at 4 °C (precooled; *see Note 2*).
8. Decant supernatant, resuspend to 2 mL in cell buffer, and take a small sample for RBC lysis and manual counting with Trypan blue (*see Notes 4 and 5*).

3.3 Surface Staining Bone Marrow Cells for Flow Cytometry

The staining panel should include live/dead discrimination and CD45 in addition to the HSC markers and any other parameters being evaluated. Here we use a fixable amine-reactive live/dead dye (*see Note 6*), which is available in multiple excitation/emission wavelengths. An example staining panel is provided in Table 1.

1. Remove the vials of amine-reactive live/dead dye and DMSO from the freezer to come to room temperature.
2. Aliquot 2×10^6 cells per sample (*see Note 7*) into a tube for full panel staining, and an equivalent number of cells per sample into a separate tube for each necessary FMO control (*see Note 8*).
3. Remember to aliquot cells for an unstained control tube. However, compensation beads are recommended for all single-color compensation controls (*see Note 9*).
4. Optional: If using DAPI for cell cycle (not reactive with compensation beads), aliquot another tube of control cells for DAPI single color compensation.
5. Centrifuge all at $500 \times g$ for 5 min at 4 °C, and then decant supernatant.
6. Reconstitute a vial of amine-reactive live/dead dye by adding 50 μ L DMSO and vortex well.
7. Add ≤ 1 μ L dye to one drop of reactive ArC beads, vortex, and incubate covered at RT.
8. Dilute the rest of the dye (~ 49 μ L) into 50 mL PBS.
9. Add 1 mL diluted live/dead dye per sample, vortex, and incubate covered at 4 °C for 20 min.
10. Centrifuge all tubes, including the ArC beads, at $500 \times g$ for 5 min at 4 °C.
11. Create the surface antibody cocktail in cell buffer (e.g., Table 1 markers 2–7 plus any additional surface markers of interest). Be sure to create a separate antibody cocktail lacking the color of interest for any relevant surface marker FMO tubes.
12. Decant and resuspend sample tubes directly in 100 μ L of surface antibody cocktail or FMO cocktail.
13. For the ArC bead control tube, resuspend in cell buffer, and add one drop of ArC-negative beads.
14. Also add ≤ 1 μ L of each undiluted surface antibody to one drop of UltraComp compensation beads in separate single-color control tubes.
15. Vortex all and incubate covered at 4 °C for 30 min.
16. Add 1 mL cell buffer to each tube and centrifuge all at $500 \times g$ for 5 min at 4 °C.

17. If no intracellular staining is required and same-day flow cytometry will be performed, resuspend in 300 μ L cell buffer and skip to Subheading 3.5.
18. If performing immediate intracellular staining and same-day flow cytometry, skip to Subheading 3.4 *and proceed directly to step 2* (*see Note 10*).
19. For fixation and storage, resuspend with 300 μ L 4% PFA and incubate covered at 4 °C for 30 min.
20. Add 1 mL cell buffer and centrifuge at 1000 $\times g$ (*see Note 11*) for 5 min at 4 °C.
21. Resuspend in 300 μ L cell buffer.
22. Samples can now be stored at 4 °C in the dark (*see Note 12*). If no intracellular staining is required, skip to Subheading 3.5.

3.4 Intracellular Staining

1. Remove tubes from storage and directly centrifuge at 1000 $\times g$ for 5 min at RT.
2. Decant and resuspend in 300 μ L Cytofix/Cytoperm buffer.
3. Incubate covered for 30 min. Keep at 4 °C for this step if not previously fixed, or optionally at RT if previously fixed and stored.
4. Add 1 mL 1X Perm/Wash buffer (ensure diluted from 10X to 1X with dH₂O), vortex, and centrifuge at 1000 $\times g$ for 5 min at RT.
5. Decant and resuspend directly in intracellular antibody diluted in 1X Perm/Wash buffer.
6. Incubate covered at RT for 30 min.
7. Add 1 mL 1X Perm/Wash buffer and centrifuge at 1000 $\times g$ for 5 min.
8. Resuspend in 300 μ L 1X Perm/Wash buffer.
9. Optional: If using DAPI for cell cycle analysis after fixation and permeabilization, add ~0.1 μ g/mL final DAPI concentration in 1X Perm/Wash buffer.
10. Proceed to flow cytometry (*see Note 10*).

3.5 Flow Cytometry Analysis of HSCs Postirradiation

Using FGD5 mice to track ZsGreen fluorescent HSCs, we confirmed literature [10, 16] that SLAM markers can enrich HSCs to virtually the same purity with or without c-Kit, and found that this holds true postirradiation (*see Fig. 3*). In addition, shifting the gate higher for Sca-1 can give cleaner SLAM gating after irradiation without losing irradiated HSCs (*see Figs. 2 and 3*). Finally, the inclusion of CD45 helps to gate away from CD45⁻ “junk,” which arises after irradiation. Recommended gating strategies are represented in Figs. 5 and 6.

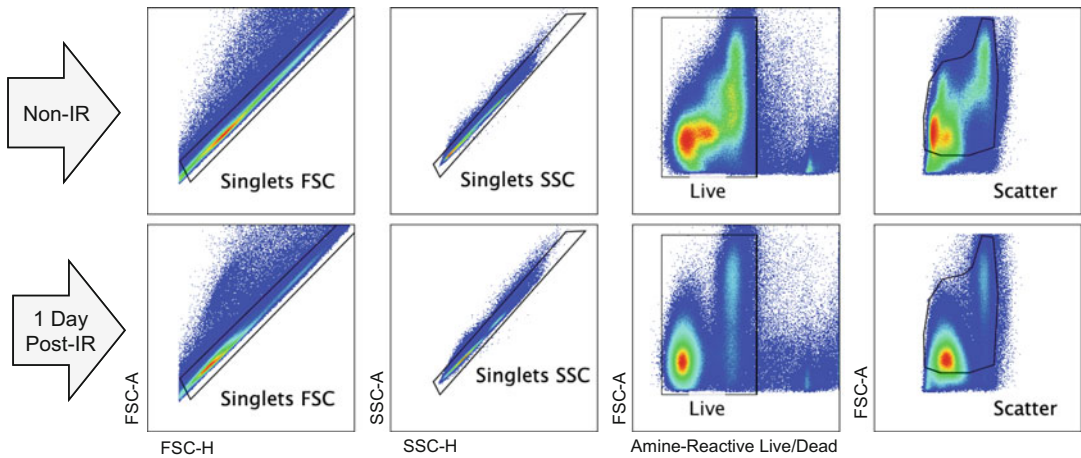


Fig. 5 Example scatter and live/dead gating. Shown is bone marrow from a non-IR mouse (top) and from a mouse 1 day post-IR (8.53 Gy; bottom)

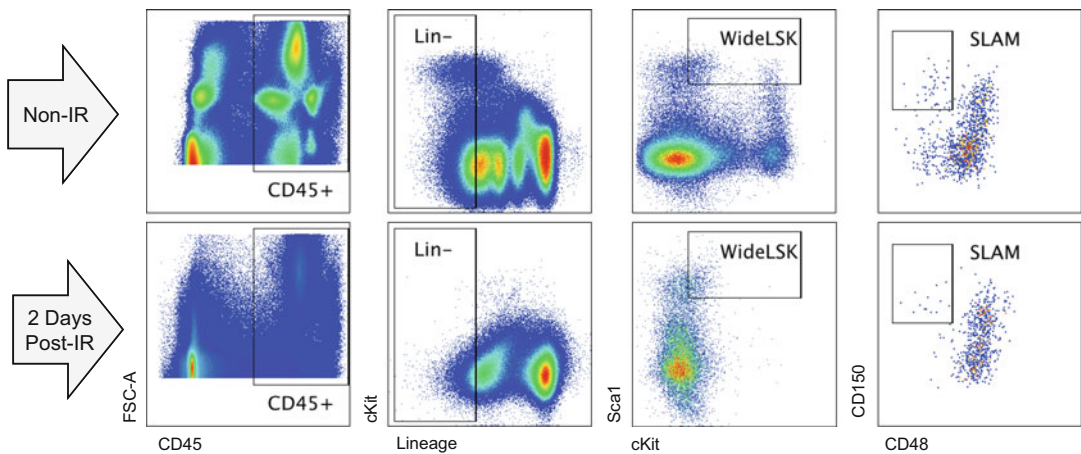


Fig. 6 Example CD45 and wide LSK + SLAM gating. Shown is bone marrow from a non-IR mouse (top) and from a mouse 2 days post-IR (8.53 Gy; bottom)

1. Immediately prior to flow cytometry, refilter all cells through 40 μ m filter-top flow tubes.
2. In the flow cytometer settings, be sure to include FSC-H and SSC-H in addition to FSC-A and SSC-A.
3. Set appropriate voltages using the unstained control and a full stained sample and perform compensation with the single-color control beads (*see Note 9*).
4. Set an FSC threshold cutoff above the majority of the irradiation-induced debris (*see Note 13*).
5. Gate for diagonal singlets using both the FSC-A/FSC-H plot and the SSC-A/SSC-H plot in succession (*see Fig. 5*).

6. Then gate on live cells with low amine-reactive dye staining, followed by tight overall scatter gating around the major cell populations in an FSC-A/SSC-A plot (*see* Fig. 5).
7. Then gate the bright CD45+ cells away from further background noise and continue with the wide LSK and SLAM gating (*see* Fig. 6).
8. Collect enough events to visualize sufficient HSCs (*see* Notes 14 and 15).

4 Notes

1. “Lineage” denotes an antibody cocktail of hematopoietic lineage markers for labeling mature blood cells in the bone marrow. An example lineage cocktail includes anti-mouse CD3, clone 17A2; anti-mouse Ly-6G/Ly-6C, clone RB6-8C5; anti-mouse CD11b, clone M1/70; anti-mouse CD45R/B220, clone RA3-6B2; anti-mouse TER-119, clone Ter-119.
2. Keep cells as cold as possible to prevent a metabolic response to extraction from the bone marrow niche, such as oxygen shock [17]. It is very important to keep bones and extracted marrow cells on ice at all times, and prechill components such as the cell buffer, mortar, and centrifuge.
3. Crushing bones in the same cell buffer in which they were stored can help prevent cell loss from possible bone marrow leakage.
4. Based on our experience, we recommend manual counts, as radiation-induced dead cells and debris can skew the counts of automated hemocytometers. However, if available, an automated cell counter with fluorescent discrimination of live nucleated cells via Acridine Orange and Propidium Iodide (AO/PI) is ideal for this application.
5. When using the spine, keep in mind that the total cell count will include extra cells from the spinal cord as well as cells sloughed off from intervertebral tissues during the crush. This becomes more important following irradiation; as hematopoietic cells are rapidly depleted, residual nonhematopoietic cells from spine crushing will make up a higher percentage of the total. This is another reason to include CD45 in the staining panel, ensuring only hematopoietic cells are being analyzed.
6. This dye reacts with free amines at the cell surface, but can enter through the damaged membrane of dead/dying cells to react with amines inside the cell and produce much higher fluorescence for dead cell discrimination.

7. It may be advantageous to stain a higher number of bone marrow cells per sample ($5\text{--}10 \times 10^6$) for an assay such as cell cycle analysis, in which only a small subset of HSCs are expected to have positive staining for the parameter of interest. It may be necessary to collect several million events on the flow cytometer to visualize sufficient positive HSCs. Increase all volumes accordingly when staining a higher number of cells.
8. Best practice is to create individual FMO tubes for each “color of interest,” for which fluorescence will be directly compared between groups, particularly for low-intensity markers. This does not need to include colors used simply for population gating such as SLAM-LSK markers, particularly since these are relatively strong markers. If limited by cell numbers, reagents, or time, one FMO *per group* for a given color may be sufficient. In this case, combine cells from each sample in a given group into the group FMO tube, ideally totaling the same number of cells per sample to give the most representative background measurement. Do not use a single FMO across all groups, as irradiation can differentially affect background fluorescence with radio-mitigating treatments or other variables under analysis.
9. Use of compensation beads as opposed to cells is highly recommended for single-color controls in analysis of bone marrow populations, particularly in the irradiated setting. Uniform negative and positive populations are essential for accurate compensation, but heterogeneous bone marrow populations have differing background fluorescence levels at steady state and become further skewed by irradiation. If cells must be used for compensation, it would be best to use nonirradiated cells for all control tubes. However, some markers of interest may only appear with irradiation. These complications are circumvented by the use of compensation beads, provided the beads are stained with the same antibody lot and staining conditions (including exposure to the same reagents for fixation, permeabilization, etc.).
10. Intracellular staining can be performed immediately, or after fixation and storage, but should be performed on the same day as flow cytometry for best results.
11. Increase centrifugation speed after fixation due to increased cell buoyancy.
12. Next day use is best, or as soon as possible. We do not recommend storing for more than one week prior to flow cytometry, particularly with tandem dyes.
13. Set the FSC threshold as high as possible without losing cells of interest. This is advantageous to exclude large amounts of low-scatter irradiation debris from the total event count. It

may be helpful to back-gate some Live/CD45⁺ cells onto the scatter plot to help determine this cutoff.

14. A rough goal of ~50 HSCs will likely require collection of millions of total events, depending on irradiation dose and time point, and may take up to ~15 min per sample. This should be considered when planning time for flow cytometry.
15. Alternatively, a “lineage depletion” step (magnetic depletion of lineage⁺ cells) can be performed prior to staining (not described here; EasySep™ Mouse Hematopoietic Progenitor Cell Isolation Kit, StemCell Technologies). This adds ~1 h of time in cell preparation, as well as the cost of the kits (1 kit covers only ~5 mice when using all bones) but allows collection of more HSCs in a shorter time frame on the flow cytometer. This is necessary when sorting HSCs for further analysis like RNA sequencing and allows collection of ~5000 HSCs from a single nonirradiated mouse in 30–45 min. In our experience, 24 h after a lethal irradiation dose of ~8.5 Gy, > 1000 HSCs per mouse can still be sorted using the modified gating strategy described herein.

Acknowledgments

This work was supported by DOD partnering grant W1XWH-15-1-0254/0255, NIH grant HL096305, and NIH T32 training grant HL007910. Flow cytometry was conducted in the Indiana University Melvin and Bren Simon Comprehensive Cancer Center (IUSCCC) Flow Cytometry Resource Facility (FCRF), funded in part by NCI grant P30 CA082709, NIDDK grant U54 DK106846, NIH instrumentation grant 1S10D012270, and the Center of Excellence Grant in Molecular Hematology grant PO1 DK090948.

References

1. Spangrude GJ, Heimfeld S, Weissman IL (1988) Purification and characterization of mouse hematopoietic stem cells. *Science* 241: 58–62
2. Ikuta K, Weissman IL (1992) Evidence that hematopoietic stem cells express mouse c-kit but do not depend on steel factor for their generation. *Proc Natl Acad Sci U S A* 89: 1502–1506
3. Okada S, Nakauchi H, Nagayoshi K et al (1992) In vivo and in vitro stem cell function of c-kit- and Sca-1-positive murine hematopoietic cells. *Blood* 80:3044–3050
4. Osawa M, Nakamura K, Nishi N, Takahasi N, Tokuomoto Y, Inoue H, Nakauchi H (1996) In vivo self-renewal of c-Kit⁺ Sca-1⁺ Lin(low/-) hemopoietic stem cells. *J Immunol* 156: 3207–3214
5. Osawa M, Hanada K, Hamada H, Nakauchi H (1996) Long-term lymphohematopoietic reconstitution by a single CD34-low/negative hematopoietic stem cell. *Science* 273:242–245
6. Adolfsson J, Borge OJ, Bryder D, Theilgaard-Monch K, Astrand-Grundstrom I, Sitnicka E, Sasaki Y, Jacobsen SE (2001) Upregulation of Flt3 expression within the bone marrow Lin(-) Sca1(+)-c-kit(+) stem cell compartment is

- accompanied by loss of self-renewal capacity. *Immunity* 15:659–669
7. Christensen JL, Weissman IL (2001) Flk-2 is a marker in hematopoietic stem cell differentiation: a simple method to isolate long-term stem cells. *Proc Natl Acad Sci U S A* 98: 14541–14546
 8. Yang L, Bryder D, Adolfsson J, Nygren J, Mansson R, Sigvardsson M, Jacobsen SE (2005) Identification of Lin(-)Sca1(+)-kit(+) CD34(+)-Flt3- short-term hematopoietic stem cells capable of rapidly reconstituting and rescuing myeloablated transplant recipients. *Blood* 105:2717–2723
 9. Forsberg EC, Prohaska SS, Katzman S, Heffner GC, Stuart JM, Weissman IL (2005) Differential expression of novel potential regulators in hematopoietic stem cells. *PLoS Genet* 1(3): e28
 10. Kiel MJ, Yilmaz OH, Iwashita T, Yilmaz OH, Terhorst C, Morrison SJ (2005) SLAM family receptors distinguish hematopoietic stem and progenitor cells and reveal endothelial niches for stem cells. *Cell* 121:1109–1121
 11. Ergen AV, Jeong M, Lin KK, Challen GA, Goodell MA (2013) Isolation and characterization of mouse side population cells. *Methods Mol Biol* 946:151–162
 12. Mayle A, Luo M, Jeong M, Goodell MA (2013) Flow cytometry analysis of murine hematopoietic stem cells. *Cytometry A* 83: 27–37
 13. Simonnet AJ, Nehme J, Vaigot P, Barroca V, Leboulch P, Tronik-Le Roux D (2009) Phenotypic and functional changes induced in hematopoietic stem/progenitor cells after gamma-ray radiation exposure. *Stem Cells* 27:1400–1409
 14. Gazit R, Mandal PK, Ebina W, Ben-Zvi A, Nombela-Arrieta C, Silberstein LE, Rossi DJ (2014) Fgd5 identifies hematopoietic stem cells in the murine bone marrow. *J Exp Med* 211:1315–1331
 15. Boggs DR (1984) The total marrow mass of the mouse: a simplified method of measurement. *Am J Hematol* 16:277–286
 16. Oguro H, Ding L, Morrison SJ (2013) SLAM family markers resolve functionally distinct subpopulations of hematopoietic stem cells and multipotent progenitors. *Cell Stem Cell* 13:102–116
 17. Mantel CR, O’Leary HA, Chitteti BR, Huang X, Cooper S, Hangoc G, Brustovetsky N, Srour EF, Lee MR, Messing-Graham S, Haas DM, Falah N, Kapur R, Pelus LM, Bardeesy N, Fitamant J, Ivan M, Kim KS, Broxmeyer HE (2015) Enhancing hematopoietic stem cell transplantation efficacy by mitigating oxygen shock. *Cell* 161:1553–1565

Part IV

The Hematopoietic Niche and Accessory Cells



Intravital Microscopy for Hematopoietic Studies

Myriam L. R. Haltalli and Cristina Lo Celso

Abstract

The bone marrow (BM) is home to numerous cell types arising from hematopoietic stem cells (HSCs) and nonhematopoietic mesenchymal stem cells, as well as stromal cell components. Together they form the BM microenvironment or HSC niche. HSCs critically depend on signaling from these niches to function and survive in the long term. Significant advances in imaging technologies over the past decade have permitted the study of the BM microenvironment in mice, particularly with the development of intravital microscopy (IVM), which provides a powerful method to study these cells *in vivo* and in real time. Still, there is a lot to be learnt about the interactions of individual HSCs with their environment – at steady state and under various stresses – and whether specific niches exist for distinct developing hematopoietic lineages. Here, we describe our protocol and techniques used to visualize transplanted HSCs in the mouse calvarium, using combined confocal and two-photon IVM.

Key words Bone marrow, Hematopoietic stem cell, Transplantation, Bone marrow microenvironment, Niche, Intravital imaging, Confocal and Multiphoton microscopy, 3-dimensional image analysis

1 Introduction

The BM is a highly dynamic environment, in which the generation of billions of mature blood cells arising from proliferating hematopoietic progenitors takes place each day prior to their release into the circulation. This tissue is home to a range of complex and specialized microenvironments, or niches, characterized by various stromal cell compartments including endothelial cells [1–3], perivascular cells [4–7], and osteoblasts [8–11]. HSCs maintain the process of hematopoiesis and reside within the BM where they critically rely on interactions with these niches to survive, self-renew, and differentiate. Understanding HSC-niche interactions is critical for the development of improved regenerative medicine approaches and to prevent disease.

By measuring the multilineage output of cells, colony-forming assays *in vitro* and transplantation assays *in vivo* have facilitated the identification and study of HSCs. However, while informative, these methods require significant periods of time and a true stem

cell can only be identified retrospectively, at which point it no longer exists to be assayed further or visualized. Two-dimensional histological analyses on BM sections have been performed to assess the position of HSCs in various tissues and at high imaging resolution [1]. While sectioning the bone to generate 3-dimensional (3D) reconstructions of the tissue has been used with some success [6, 12–15], it is technically difficult and preprocessing methods used to decalcify the bone can alter tissue morphology, protein antigenicity, and may result in the loss of intrinsic fluorescence or increased autofluorescence. The main disadvantage, however, is the lack of a temporal dimension – necessary to accurately analyze interactions of cells with and within the BM microenvironment.

Over the past decade, the use of *in vivo* confocal and multiphoton microscopy of the BM has dramatically advanced our knowledge of cellular dynamics taking place during hematopoiesis [16, 17], hematopoietic cell mobilization [18, 19], HSC homing, and early engraftment [11, 20–22], as well as the spatiotemporal activity of malignant cells as they invade and occupy the niche [23, 24]. IVM can accurately capture dynamic events and allows the investigation of specific HSC-niche interactions, the timescales of biological processes (i.e., the length of time required for a cell to divide and differentiate), and cell behaviors (i.e., whether a cell is immotile or migratory, directionality within the niche and speed). With the growing interest in understanding the spatial organization of HSCs in the BM and how cell-cell interactions vary both at steady state and under stress, there is a greater need to use IVM in order to directly visualize these phenomena as they happen *in vivo*.

The development of genetically modified mouse models coupled with a vast selection of injectable fluorophore-conjugated antibodies, dyes, and reagents has enhanced the study of murine phenotypic HSCs and niche components by IVM (*see* Table 1). In contrast to the challenges faced by imaging the long bones – including mechanical stress caused by thinning of the bone by shaving prior to imaging – the calvarium (skull cap) bone plate is thin and the BM cavity can be imaged after a minimally invasive surgery to implant a specially designed headpiece.

In this chapter, we provide a technical overview of the procedures we use for imaging interactions of transplanted HSCs in the calvarium BM in the days following injection. We provide tips for the isolation and enrichment of HSCs, subsequent IVM of transplanted cells in the BM niche, and, finally, image processing for data analysis. We indicate alternative options that we know would not preclude the generation of results and may be relevant to addressing specific questions.

Table 1
Summary of reporter animal models and other labeling methods for visualizing HSPCs and BM niche components by IVM

Cell type	Reporter mice available	Other labelling methods
HSC	Hoxb5-Tri-mCherry [25] α -catulin – GFP [14] vWF-eGFP [26, 27] Tie2-GFP [28] Fgd5 ^{mCherry/+} [29] Mds1 ^{GFP/+} Flt3 ^{Cre} [17]	Lipophilic carbocyanine membrane dyes (e.g., Vybrant DiO, DiI, DiD and DiR from Life Technologies) [22]. FACS sort HSCs from mice expressing fluorescence in all tissues and cell types (e.g., mT/mG [30]).
Hematopoietic cells	mT/mG [30] H2B-eGFP [31] LifeAct-GFP [32]	<i>In vivo</i> administration of anti-CD45 antibody (<i>see Note 1</i>) BM chimeras in which hematopoietic cells and stroma express different fluorescent proteins [24] (<i>see Note 2</i>)
Vasculature	Flk1-GFP [33] Tie-2 Cre [3] VECad-Cre [34] Fgd5 ^{mCherry/+}	<i>In vivo</i> administration of anti-CD31, anti-Endomucin antibody (<i>see Note 1</i>), or fluorescently conjugated lectins Vascular dyes, for example, FITC-, TRITC- or Cy5-dextran, nontargeted quantum dots or angiosense probes
Bone, Osteoblasts, and Perivascular cells	Col2.3GFP [35] and CFP [36] Osterix-EGFP-Cre [37] Nestin-GFP [6] Prx1-Cre [38, 39] CXCL12-GFP [40] and dsRed [41] LepR-Cre;Rosa26-tdTomato [42] NG2-dsRed [43]	OsteoSense for newly formed bone [44] Calcium-binding reagents such as tetracycline or calcein blue or alizarin red (Sigma) [17] Cathepsin K for osteoblasts and osteoclasts [17, 45] Second harmonic generation (typically 840nm excitation and 415–445 nm detection) [46, 47]

2 Materials

2.1 Mice

Any strain of mouse can be used provided appropriate genetically compatible donors and recipients are selected to avoid graft-versus-host disease upon reconstitution of the immune system after transplantation of cells. We standardly use mouse strains derived from C57BL/6 (Charles River Laboratories or Jackson Laboratory). Depending on the specific investigation, care should be taken to minimize fluorescence signal overlap with reporters, antibodies, dyes, or reagents used (*see Note 3*). Typically, mice aged 6–16 weeks are used, and it is important to remain consistent

between experimental repeats. Mice older than 16 weeks may have larger skulls; however, this may compromise depth of imaging due to increased bone thickness.

2.2 Reagents, Supplies, and Equipment

2.2.1 HSC Sort and Transplant

1. Dissection tools (scissors and forceps).
2. Phosphate-buffered saline (PBS) without calcium and magnesium.
3. Fetal bovine serum (FBS).
4. FACS buffer: PBS supplemented with 2% FBS.
5. Red cell lysis buffer: 0.001 g/mL Potassium bicarbonate, 0.008 g/mL ammonium chloride, 20 mM EDTA, and 5% (v/v) FBS made up in Milli-Q® water.
6. Fluorescently conjugated antibodies for HSC isolation (*see* [24] for a comprehensive list of antibodies used by our research group for this).
7. (*Optional*—if using wild-type mice as donors and depending on the experiment) Lipophilic carbocyanine membrane dyes: Vybrant DiO, DiI, DiD, DiR (Life Technologies) or other appropriate fluorescent dyes.
8. Fluorescence-Activated Cell Sorter, for example, the BD FACS Aria (BD Biosciences).
9. Cell incubator set at 37 °C (if using lipophilic carbocyanine membrane dyes for labelling HSCs postsort).
10. Centrifuge and/or microcentrifuge.
11. General lab supplies including sterile mortar and pestle, collection tubes of various volumes, 40 µm cell strainers, pipettes, etc.
12. Supplies for the lineage depletion of BM cells, for example, the MACS microbeads, magnetic columns, and stand with magnet (Miltenyi Biotec).
13. Gamma Irradiator. For our work, we have access to a Gamma-cell 40 Exactor (MDS Nordion).
14. Disposable insulin syringes (ideally 29 G × 12.7 mm and 0.5 mL or 1 mL, as required).
15. Heat box and mouse restrainer to facilitate intravenous (i.v.) injections.

2.2.2 Surgery and Intravital Microscopy

1. A biological safety cabinet that ensures sterility and the containment of allergens.
2. Anesthesia drugs, for example, isoflurane (*see* Note 4).
3. Gas anesthesia vaporizer and scavenging system (if using isoflurane).

4. Heatpad to keep the mouse warm during surgery as well as on the stage of the microscope, best equipped with body temperature probe (e.g., the ThermoStar Homeothermic Monitoring System).
5. Sterile surgical tools (scissors and forceps).
6. Cotton buds.
7. Specially designed headpieces that attach to the skull of the mouse and fit into a lock and key mechanism on the microscope stage. This may vary depending on the specific IVM mouse-holding setup available to you.
8. Dental cement (we use Diamond Carve from Kemdent.).
9. Lacri-Lube or equivalent eye ointment to lubricate and protect the animal's eyes from drying while anaesthetized.
10. Lubricant to facilitate inserting the rectal temperature probe connected to the heatpad.
11. PBS and plastic Pasteur pipettes.
12. Microscope – for example, we use a Zeiss LSM 780 upright confocal/two-photon hybrid microscope equipped with Argon (458, 488, and 514 nm), a diode-pumped solid-state 561 nm, a Helium-Neon 633 nm, and a tuneable infrared multiphoton laser (Spectraphysics Mai Tai DeepSee 690–1020 nm), 4 non-descanned detectors (NDD), and an internal spectral detector array (*see Note 5*). Signal is visualized using a Zeiss W Plan-Apochromat 20X DIC water immersion lens (1.0 NA).
13. Vascular dyes and other antibodies or injectable reagents for the specific IVM experiment to be carried out.
14. (*Optional* – for recovery imaging) Intrasite gel, plasters, and analgesic for pain relief during recovery.

2.2.3 Image Analysis

1. A powerful workstation, for example (and at minimum), an Intel-Core i5-3427U processor at 1.80 GHz and 4.0 GB RAM, running the 64-bit Windows 7 operating system
2. FIJI/Image J
3. (*Optional*) Further software including Imaris, Matlab, and R packages

3 Methods

3.1 Bone Marrow Transplant

3.1.1 Conditioning of BM Recipients

At steady state in healthy animals, the BM space is occupied with hematopoietic and stromal cells, which provide a challenge to newly transplanted cells attempting to engraft. To facilitate this, recipient animals are irradiated with a sublethal dose (6 Gy total) or a lethal dose (11 Gy total) up to 24 h before transplanting donor HSCs

using a Caesium-137 source (*see Note 6*). We typically split the dose into two and administer the two irradiations at least three hours apart (i.e., two doses of 5.5 Gy for lethal irradiation).

3.1.2 HSC Preparation and Injection

Standard protocols may be followed to isolate HSCs. Our protocol will be briefly described here (*see Note 7*).

1. Sacrifice the donor mice, harvest tibias, femurs, and ileac bones, and clean away the attached muscle tissue. If a large number of cells are required, the sternum and spine can also be collected, cleaned, and processed.
2. Isolate BM cells by gently crushing the bones in FACS buffer with a mortar and pestle using circular and rocking movements of the pestle and until only white bone chips remain at the bottom.
3. Resuspend the cells to break any clumps and pass them through a 40 μm strainer into a 50 mL Falcon tube and centrifuge cells ($500 \times \text{g}$, 5 min).
4. Resuspend the pellet in at least 10 mL of red cell lysis buffer, incubate at room temperature for 2 min, top up the tube with FACS buffer, and centrifuge.
5. Lineage-deplete the BM cell suspension using a lineage cell depletion kit. In our lab, we use the MACS system (Miltenyi Biotec) (*see Note 8*).
6. Stain the depleted fraction of cells with the remaining antibodies required to identify the HSC population by FACS and subsequently with an appropriate viability dye prior to sorting.
7. Prepare labelled 1.5 mL tubes for collecting the sorted HSCs containing PBS + 10% FBS and take the sample and collection tubes to be sorted (*see Note 9*).
8. After the sort, immediately centrifuge the cells in a microcentrifuge ($500 \times \text{g}$, 5 min) and verify that a small pellet has formed at the bottom of the tube. At this point, if follow-up of donor HSC behavior with IVM is to be carried out in the short term (within 1 week) and nonfluorescent mice have been used as donors, the HSCs can be labelled with carbocyanine membrane dyes (*see Note 10*).
9. Carefully remove the supernatant and resuspend in PBS at the desired concentration for i.v. injection into appropriately conditioned recipient mice (*see Note 11*).

3.2 Intravital Microscopy

3.2.1 Microscope Considerations for In Vivo Imaging

1. Microscopes for *in vivo* imaging should include a stage and a holder that secures the animal in a steady but comfortable position, which will minimize movement from breathing and heartbeat during imaging. Multiple variations of this setup are now available; thus, this protocol may need to be adjusted depending on your specific system. The microscope should

also have a means of keeping the mouse warm, such as a heatpad and rectal probe thermometer for measuring and adjusting body temperature throughout. If using Isoflurane for anesthesia, the mechanism of delivery to the animal, as well as a scavenging system to protect users, would also be necessary.

2. When planning your experiments, ensure the microscope to be used will have the capacity to allow multichannel setup in order to capture and record information from the fluorescent probes that are labelling your cells of interest, as well as any reference structures within the BM space. Ideally, and to help with navigating around the calvarium, the bone can be imaged by the endogenous second harmonic generation (SHG) signal from bone collagen through two-photon excitation.
3. Autofluorescence from BM cells can cause false positives when identifying fluorescently labelled cells *in vivo* (see Fig. 1).

The intensity of this signal varies from cell to cell and from mouse to mouse and can be particularly strong within the blue to red wavelengths. To deal with this, it is useful to know your sample and understand the spectra of the autofluorescence in your experiment, for example, by using spectral lambda scanning. This will allow you to optimize your fluorophore choices and select those with spectra as far away as possible from the background noise. Selecting fluorophores with narrow excitation and emission spectra makes it easy to specifically acquire signal from your cell or structure of interest. If your microscope can detect them, far-red dyes are also a very good way to avoid issues with autofluorescence as these wavelengths are not usually found in biological samples. Furthermore, if your experimental setup permits it, an autofluorescence channel can be included during *in vivo* imaging, which does not overlap with those used to detect other fluorophores. During acquisition, this channel can share the same detection setup as any other channel of interest but with the excitation laser turned off. If your cell of interest is still bright compared to neighboring cells when the excitation laser is off, it can be considered to be another cell with high autofluorescence.

3.2.2 Surgery

1. If using fluorescent probes, such as antibodies, for *in vivo* labelling of BM components, these can be injected i.v. prior to inducing anesthesia and commencing surgery to allow time for labelling.
2. The following steps are carried out while the animal is under anesthesia, for example, using isoflurane and oxygen mixed in a vaporizer (4% in 4 L/min oxygen for induction and 1–2.5% in 1 L/min oxygen for maintenance) and delivered through a nose cone with an appropriate scavenging system in place.

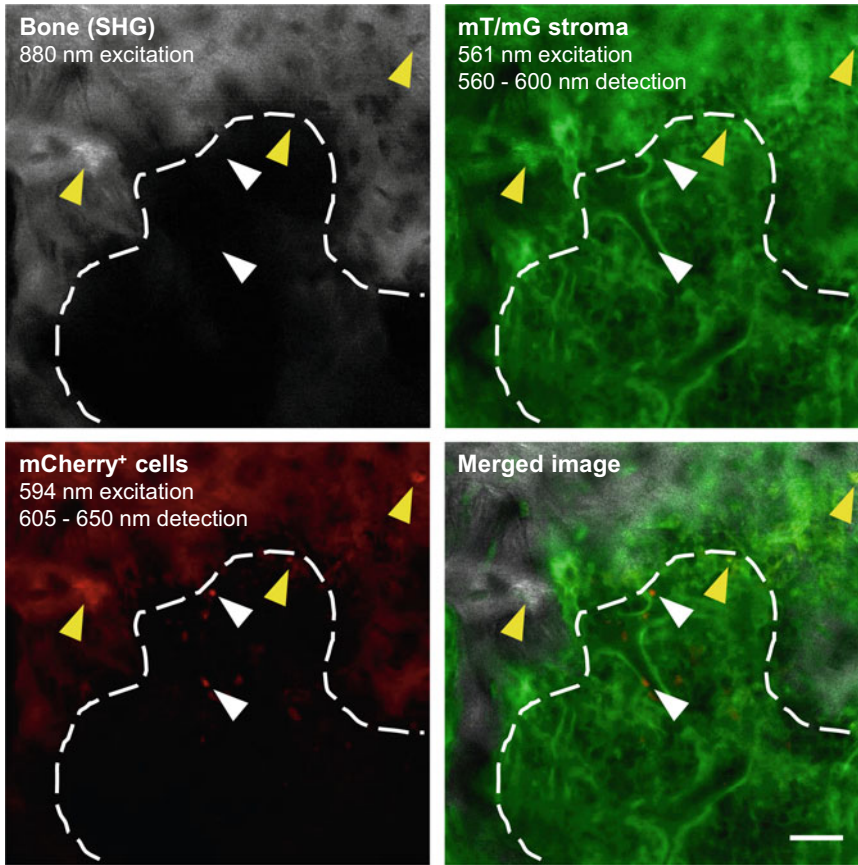


Fig. 1 An image acquired of $mCherry^+$ cells (red) acquired from an mT/mG mouse calvarium where the BM stroma can be visualized (green). The bone was imaged using SHG (gray) and is outlined with the white dashes in each panel. The white arrows indicate true cells as they appear brightly only in the $mCherry$ channel. The yellow arrows indicate examples of autofluorescent cells. Structures, which appear bright in the $mCherry$ channel but can also be seen in the tomato and/or SHG channel, therefore, is likely to exhibit autofluorescence and can be excluded from analysis. Details of the setup for each channel are provided within the images. Scale bar represents 100 μm

The breathing rate of the animal should be constantly monitored and maintained at approximately 1 breath per second, and anesthesia adjusted as necessary. The mouse should be placed on a heatpad for the duration of surgery and body temperature monitored.

3. To expose the calvarium for imaging, the fur on the scalp is first dampened with ethanol. Using forceps, the skin between the ears is raised and a small incision is made using surgical scissors. One side of the scissors can then be inserted under the skin to make two long incisions toward the nose of the mouse. A rectangular flap of skin can subsequently be removed by cutting horizontally behind the nose, resulting in a rectangular window to the bone (*see* Fig. 2a, left panel). Care should be taken

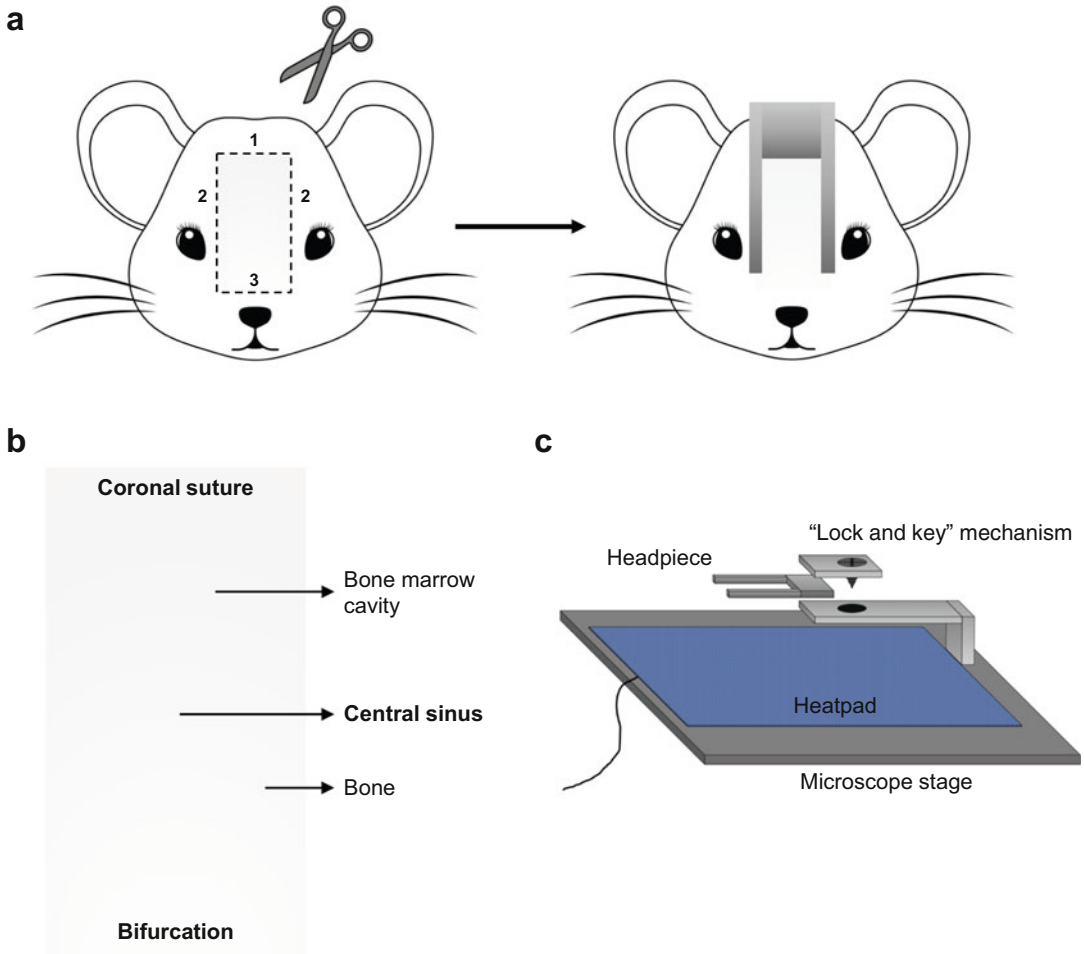


Fig. 2 (a) A schematic detailing an example of an optimal method for removing the scalp to create a sufficiently large imaging window so that the headpiece can be placed directly onto the bone of the skullcap, with the main landmarks of the calvarium clearly in view. These are highlighted in (b). (c) depicts an example of a “lock and key” mechanism that can be used to attach the headpiece to the microscope stage. The screw must be tightened well to avoid movement of the head during image acquisition. The mouse is laid onto a heatpad to control its body temperature throughout the procedure

to avoid trimming the mouse’s whiskers, especially if planning to recover it after imaging.

4. Clean, dry cotton buds should be used consistently to wipe away all fur from the exposed area of bone (hair is highly autofluorescent under the microscope, therefore should be eliminated as much as possible during preparation). The exposed area of the skull should be large enough for the metal headpiece to sit on the bone itself and not the skin and fur (the latter would likely lead to the detachment of the headpiece during imaging) (see Fig. 2a, right panel). The opening made at this stage should be measured against the

headpiece and adjusted accordingly by making further incisions and removing extra skin to widen the window, if required.

5. The headpiece can be attached to the mouse using dental cement. A firm paste is formed and applied to all edges of the base of a clean headpiece. Using forceps and a steady hand, the headpiece is placed on the exposed skull, ensuring that it is level on the bone. It is also useful to leave the coronal suture uncovered and ensure that the central vein can be seen running through the middle of the exposed area and parallel to the sides of the headpiece (*see* Fig. 2b). The cement is left to fully dry.
6. If using fluorescent vascular dyes to visualize vasculature, these can be injected i.v. prior to mounting the mouse onto the microscope to ensure it will last through image setup and acquisition.

3.2.3 Mounting the Mouse onto the Stage

1. The anaesthetized animal is transferred to the heatpad on the microscope stage and the headpiece is secured into the “lock and key” positioning brace mechanism (*see* Note 12 and Fig. 2c). A rectal probe is inserted to monitor the animal’s body temperature during imaging, using a lubricant to avoid causing discomfort to the mouse, and Lacri-Lube placed on the eyes.
2. PBS is applied to the imaging window using a Pasteur pipette.
3. Using a cotton bud, clean away the membrane that covers the bone to increase image quality (*see* Note 13).
4. Lower the lens onto fresh PBS on the calvarium. Using the bright-field setup and shining a white light over the calvarium, locate the sagittal suture and move to locate its intersection with the coronal suture, which has a characteristic curvature and striations, which can be seen in the bone. This is a prominent landmark of the calvarium, which serves as a helpful orientation guide while imaging and for keeping each imaging session between animals as consistent as possible.

3.2.4 Locating and Imaging HSCs

1. Once the lens is positioned appropriately, turn on the excitation source for the bone (e.g., using SHG) and adjust the Z-axis until the bone surface comes into focus in the imaging software.
2. The transplanted HSCs will present in very low numbers; therefore, it is important to take time to search the calvarium thoroughly for these cells. Switch on the relevant excitation sources and detection channels for the cells of interest and carry out a quick scan of the whole imaging area to observe the abundance of visible HSCs and the general environment. This time can also be used to adjust the power of your excitation

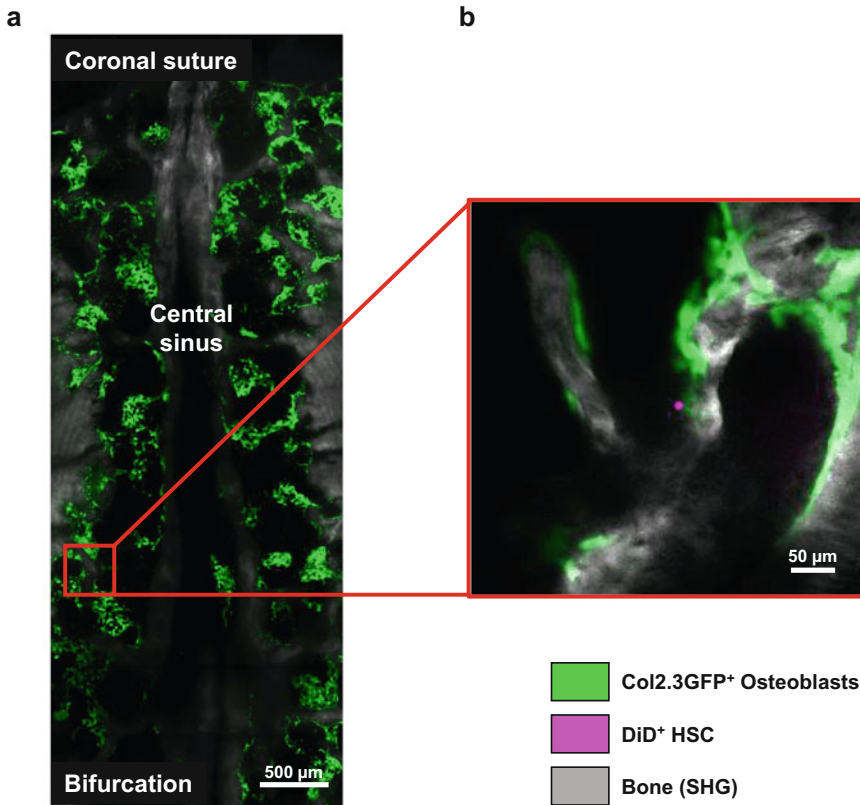


Fig. 3 (a) Individual 3D z-stacks are acquired and stitched together to build a 3D tile scan, allowing whole tissue visualization of the calvarium BM with single-cell resolution as seen in (b). Positions for subsequent time-lapse imaging can be selected from the tilescan overview, for example, when locating transplanted HSCs. These images were obtained from a Col2.3-GFP mouse, in which the osteoblasts express GFP (green), injected with DiD-labelled HSCs (magenta). The bone was imaged using SHG

source and the gain of the detection channels to ensure it is optimal for all the features you wish to capture.

3. It can be useful to acquire a tilescan image (individual tiles stitched together to form a composite) of the calvarium, which provides you with a detailed 3D overview of the BM cavity in your experiment (*see* Fig. 3a). A number of components can be visualized simultaneously by setting up the appropriate excitation and detection parameters. A typical tilescan captures the area between the coronal suture and the bifurcation of the central sinus (*see* Note 14). Using the motorized, precision stage control of the microscope, select the area where overlapping Z-stacks are to be captured (*see* Note 15). These can be stitched together postacquisition to create one image of the calvarium BM. It is recommended, in order to get a good stitching effect, to have at least 10% tile overlap.

4. Once the tilescan has been acquired, it can be used to specifically locate HSCs within the calvarium BM and to select positions and set Z-stacks for time-lapse imaging of the cells (*see Note 16* and Fig. 3b). The time interval should be selected based on the cell type you are imaging, the specific experimental question, and the potential for bleaching the fluorophore in question. For transplanted HSCs, in our hands, we have found that taking an image every 3 min is sufficient for capturing mobilization, interactions with the niche, and cell division events (*see Note 17*).
5. The main limitations to the *in vivo* imaging sessions are time constraints imposed due to animal welfare concerns and the gradual loss of fluorescence signals. The mice may remain continuously anesthetized; however, they will, over time, suffer from dehydration. Hydration and nutrients should be supplied for imaging sessions lasting longer than 8 h and longer than 6 h if followed by recovery. The gradual loss of fluorescence is unavoidable as fluorescent probes will be cleared from the animal's circulation over time, or by photobleaching of the fluorophore themselves, but can be managed by reinjecting some dyes and careful setup of excitation parameters.

3.2.5 Recovery of the Mouse for Re-imaging

For following cells over the course of a few days, for example, the mice can be recovered and reimaged when necessary (*see Note 18*). The calvarium will need to be covered postimaging each time to reduce the buildup of scar tissue and dehydration of the bone. Local expertise from veterinary surgeons should be sought for devising the most appropriate experimental protocol that will ensure animal welfare.

1. With the mouse still under anesthesia, the headpiece and imaging window should be dried thoroughly with a cotton bud, cleaned, and enough intrasite gel should be evenly applied to cover the entirety of the exposed calvarium in the imaging window.
2. Once the gel is dry, a piece of plaster should be cut to the size of the headpiece, laid over the gel, and secured in place.
3. The mouse is then placed in a heated recovery box with appropriate analgesic. Once the animal begins to exhibit normal behavior, it can be placed in its cage, ensuring that any cage enrichment that the headpiece could get entwined with is removed. Extra analgesic for pain relief can be placed in the cage or in the water, as required. Animals should be monitored frequently over the following days.
4. For subsequent imaging sessions, anesthesia should be induced, the plaster removed, and the gel cleaned away. The headpiece is then immediately ready to be attached to the

microscope and the imaging session can readily commence. As long as the headpiece has been attached well and does not fall off postrecovery, the main advantage of this method is that the exact positions imaged previously can be imported from the metadata of previous imaging sessions and reimaged again.

3.3 Image Processing and Analysis

For stitching 3D BM tilescans, we generally use ZEN black software (Zeiss, Germany) as it is the same used for image acquisition. However, stitching can also be done using FIJI/ImageJ. We use ImageJ to visualize and process raw data using various tools including bleach correction and maximum projections (*see Note 19*). Tilescans will often contain a large amount of autofluorescent signal obtained during acquisition and it helps with visualization and quantification of these images to manually crop that signal out using ImageJ (*see Fig. 4*). Macros can be designed to aid with the process; however, a full automation of this step is challenging. Often, time-lapse images may shift or tilt due to movement of the animal or of the headpiece during image acquisition. The registration tool in ImageJ [48] can be used to rectify this. Cell tracking can be performed in ImageJ using plugins such as TrackMate or in other analysis software such as Imaris or R packages. Ultimately, the processing and analysis of images obtained by IVM will mainly be driven by the specific research questions. Despite the tricky and lengthy protocol, the power of IVM lies in the vast amount of information that can be extracted from each image obtained, not forgetting how impactful it is to achieve direct visualization of cells within the BM.

4 Notes

1. For *in vivo* labelling with antibodies, we inject 5–10 µg i.v. via the tail vein before starting surgery to give the antibody at least 30 min to circulate and label the appropriate cells. This should be optimized based on the specific antibody used. As an example, for labelling endothelial cells *in vivo*, we have found anti-CD31, clone 390, to work best.
2. BM chimeras can be made, for example, by transplanting whole BM (approx. 1×10^6 cells) from mT/mG donor mice into lethally irradiated C57BL/6 wild-type recipients (11 Gy total, usually split into two doses administered at least 3 h apart, up to 24 h prior to transplantation). In this specific case, hematopoietic cells will be labelled with mTomato fluorescence protein and all stroma will remain dark. The opposite combination can be performed, which will allow IVM of stromal components (which will in this case be mTomato⁺) and their interactions *in vivo*.

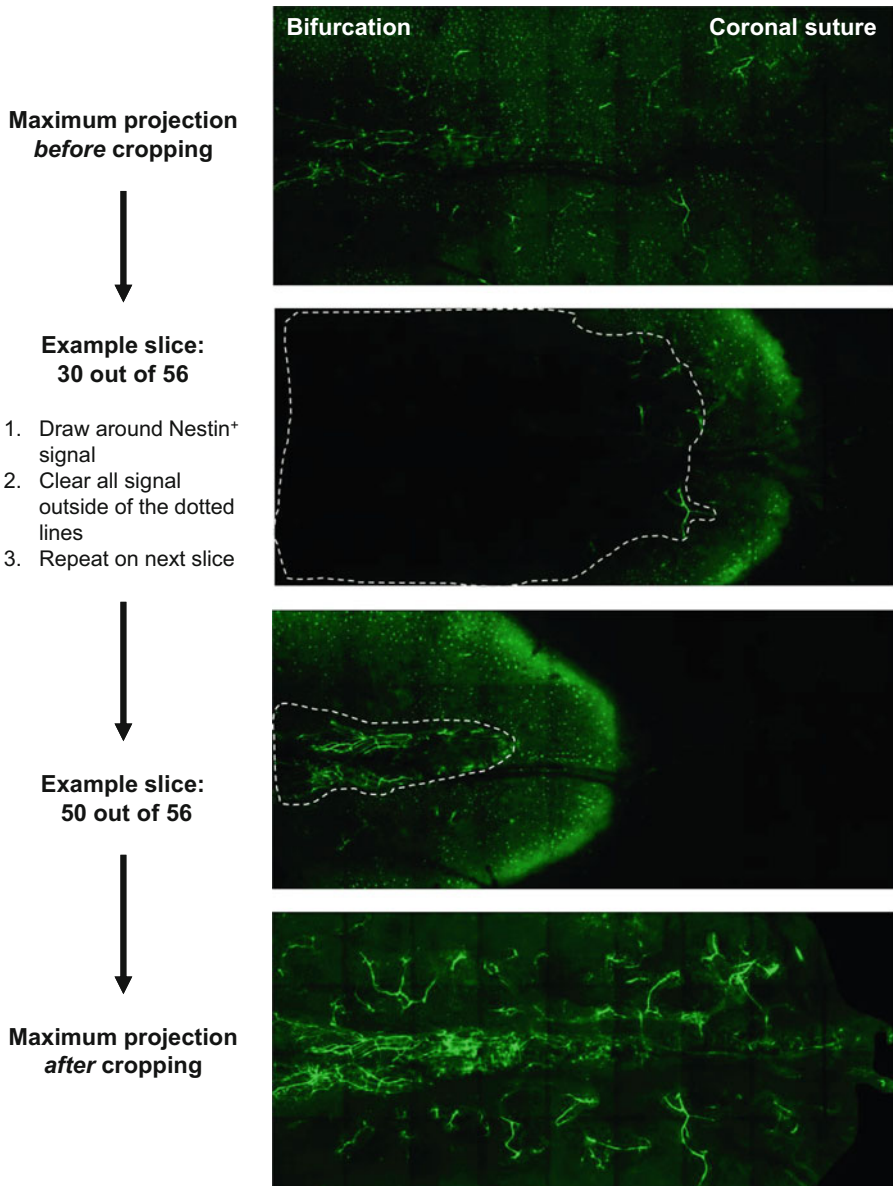


Fig. 4 An example of the impact that manually cropping tilescons acquired by IVM can have on the final image. This image represents the calvarium of a Nestin-GFP mouse, which labels perivascular cells. High levels of autofluorescence can be seen. Cropping was carried out on each slice of the tilescan in ImageJ following the steps detailed above and the striking difference can be seen in the final maximum projection, clearly depicting the distribution of Nestin⁺ cells in the calvarium BM

3. For HSC isolation and transplantation, we prefer using donors that carry fluorescent proteins within their cells (e.g., mT/mG or H2B-eGFP expressed under the control of ubiquitin or actin promoters) as this eliminates the requirement to carry out subsequent staining steps post sorting. This helps to minimize

the stress caused to sorted HSCs and allows direct injection of cells to the recipient mice. A further advantage is that one can subsequently follow repopulation of the niche and measure chimerism over time as all the progeny will also be marked by the fluorescent protein. Various niche reporters may be used as recipients, if available, for investigating interactions of the cells with stromal components labelled in the mouse. This provides contrast for the imaging and allows easy maneuvering around the calvarium to locate transplanted cells. *See* Table 1 for a comprehensive list of reporter mice and other labelling approaches currently available for these studies.

4. In our experience, isoflurane is more labor intensive than injectable anesthetics as it requires continuous monitoring of the animal's breathing and adjusting anesthesia and oxygen levels throughout surgery and imaging; however, it is advantageous in that it is more controllable and better in the long term for the mouse – especially if the experiment involves recovery and reimaging at a later timepoint.
5. Single two-photon or single confocal microscopes are also suitable for carrying out IVM. We find that two-photon is ideal to detect signal from the bone, therefore allowing visualization of the BM cavities edges; however, it is limited in identifying very weak signal. Confocal provides generally less penetration and resolution but allows the maximum signal collection. For example, weakly labelled cells can be identified using the confocal modality with a wide pinhole and then imaged optimally with two photons.
6. Bear in mind that irradiation is not an absolute requirement and there are other conditioning regimens that can be used. It is well known that irradiation triggers significant damage to the BM microenvironment [49], including the acute loss of endothelial cells and increased vessel dilation and permeability [50]. If it is important for your project to keep the microenvironment intact, there are mouse models, which can facilitate HSC long-term engraftment without conditioning such as mice bearing mutations in the receptor tyrosine kinase Kit (WBB6F1/J-Kit^W/Kit^{W-v}, Kit^{W/W^v} or Kit^{W41/W41}) [51–54].
7. While this protocol describes the isolation and transplantation of HSCs specifically, it can be adapted and applied to other cell populations such as early progenitor cells (Lineage⁻ c-Kit⁺ Sca-1⁺), multipotent progenitor cells, whole BM, T-cells, etc.
8. If staining with mouse anti-CD34 to isolate multipotent progenitor or HSC subpopulations by FACS, we advise staining prior to adding and incubating with the lineage cocktail. In our hands, in these conditions, antibody clone RAM34 used at a dilution of 1:50 works best.

9. Fluorescence minus one (FMO) controls should be made for each fluorophore in the panel in order to ensure confident and reliable gating at the machine. It is also useful to have an undepleted, fully stained control to determine whether the lineage depletion worked well and to accurately set the lineage negative/low gate.
10. For labelling cells with carbocyanine membrane dyes (e.g., we have used Vybrant[®] 1,1'-dioctadecyl-3,3,3'-tetramethylindodicarbocyanine perchlorate (DiD)), once cells have been pelleted, up to 100,000 cells should be resuspended in 100 μ L PBS and 0.5 μ L DiD added followed immediately by vortexing to minimize the lipophilic dye exiting the solution and not labelling the cells and incubated for 10 min at 37 °C. Cells are then immediately washed and resuspended in PBS at the desired concentration for i.v. injection into appropriately conditioned recipient mice. To avoid injecting debris from the DiD tubes, which can often also be visualized during imaging, centrifuge at maximum speed the tube of DiD before use.
11. In our experiments, to visualize HSCs in the calvarium, we have found that injecting 10,000 cells per mouse will allow visualization of between 1 and 10 cells up to 2 days post transplant. For successful i.v. injections, and to minimize the loss of precious cells, use an animal restrainer to restrict mouse movements and use a heat box to facilitate locating and injecting into the vein. Insulin syringes allow injecting their entire content, again, minimizing cell loss.
12. It is extremely important to secure the mouse well at this stage as any small movements due to loosening of the headpiece from the brace can have drastic (and often unsalvageable) effects on image acquisition. Ensure that the screw holding the headpiece in place (if applicable in your setup) is tightened well. It may also be beneficial to change the screw between imaging sessions to avoid blunting of the head, which will impede tightening of the screw.
13. If, while cleaning away the membrane, the mouse starts to bleed, stop wiping. Instead, gently press with the cotton bud and allow the bleed to air-dry and clot before wiping away the clotted blood with PBS and a fresh cotton bud prior to imaging. If blood is present on the calvarium during imaging, it will not allow the lasers to penetrate through to the tissue and will obstruct image acquisition.
14. When setting up tilescans for a cohort of mice within an experiment, it is useful to keep the images as consistent as possible and aiming for a similar number of Z-stacks horizontally and vertically. This becomes important at the stage of

image quantification to ensure that bias is not introduced due to variability in the surface area of BM imaged each time. Optimal positioning of the imaging window contributes to maximizing reproducibility of the images.

15. The interval between each image acquired in each Z-stack should be set to ensure that there are no gaps in your acquisition while avoiding oversampling, which could lead to bleaching due to excessive illumination. Generally, intervals of up to 5 μm are fine. A 3–5- μm step is usually sufficient for capturing the locations of HSCs. Smaller steps can allow acquisition of the fine details of the BM microarchitecture, if required.
16. Averaging helps to improve the image by increasing the signal-to-noise ratio. The higher the averaging, the more time image acquisition takes and the higher the risk of photobleaching. Therefore, a balance between the number of positions to image, the number of channels to be acquired, and averaging should be found to ensure you are able to image all cells located in the calvarium for the desired time.
17. If a particular cell you are tracking moves deeper into the marrow or out of frame, you can stop the current time-lapse at the end of a cycle, save the movie, readjust the Z-axis or position, and restart the movie. It is important to keep track of time to maintain the selected time intervals between each frame. These resultant movies can be concatenated using ImageJ postacquisition.
18. If you are planning to carry out recovery imaging, it is best to work as quickly and efficiently as possible to minimize the time that the mouse is under anesthesia in order to ensure effective recovery each time.
19. When generating projections of acquired tilescans or time-lapse positions, you may want to consider using different projection types for different channels, depending on the data you are trying to represent. For example, maximum projection is preferable for viewing structures and cells deeper within the calvarium BM. However, if this is applied to the channel used to acquire the bone, for example, it can mask all other channels as the signal intensity is extremely bright at the highest point of the calvarium. To overcome this, split the channels and do not include the bone channel when merging them again to create a maximum projection of your channels of interest. For the bone, you can create a *median* projection, which will result in a clear outline of the central bone structures as seen in Fig. 3a. These two projections can subsequently be merged together to create a final composite image.

Acknowledgments

We are grateful to the Imperial College London Central Biomedical Services and Sir Francis Crick Institute Biological Research Facility for their support with *in vivo* experimental models. Thanks to Andreas Bruckbauer and Steve Rothery from the Imperial College Facility for Imaging by Light Microscopy for their advice on image acquisition and particularly analysis. This work was funded by the Wellcome Trust (Investigator award 212304/Z/18/Z to C.L.C. and PhD studentship 105398/Z/14/Z to M.L.R.H.), Cancer Research UK (Programme Foundation award C36195/A26770 to C.L.C.), the ERC (Starting grant 337066 to C.L.C.), and BBSRC (grant BB/L023776/1 to C.L.C.).

References

1. Kiel MJ, Yilmaz ÖH, Iwashita T et al (2005) SLAM family receptors distinguish hematopoietic stem and progenitor cells and reveal endothelial niches for stem cells. *Cell* 121: 1109–1121
2. Kiel MJ, Radice GL, Morrison SJ (2007) Lack of evidence that hematopoietic stem cells depend on N-Cadherin-mediated adhesion to osteoblasts for their maintenance. *Cell Stem Cell* 1:204–217
3. Ding L, Saunders TL, Enikolopov G, Morrison SJ (2012) Endothelial and perivascular cells maintain haematopoietic stem cells. *Nature* 481:457
4. Katayama Y, Battista M, Kao W-M et al (2006) Signals from the sympathetic nervous system regulate hematopoietic stem cell egress from bone marrow. *Cell* 124:407–421
5. Méndez-Ferrer S, Lucas D, Battista M, Frenette PS (2008) Haematopoietic stem cell release is regulated by circadian oscillations. *Nature* 452:442
6. Méndez-Ferrer S, Michurina TV, Ferraro F et al (2010) Mesenchymal and haematopoietic stem cells form a unique bone marrow niche. *Nature* 466:829
7. Pinho S, Lacombe J, Hanoun M et al (2013) PDGFR α and CD51 mark human Nestin⁺ sphere-forming mesenchymal stem cells capable of hematopoietic progenitor cell expansion. *J Exp Med* 210:1351–1367
8. Calvi LM, Adams GB, Weibrecht KW et al (2003) Osteoblastic cells regulate the haematopoietic stem cell niche. *Nature* 425:841
9. Zhang J, Niu C, Ye L et al (2003) Identification of the haematopoietic stem cell niche and control of the niche size. *Nature* 425:836
10. Arai F, Hirao A, Ohmura M et al (2004) Tie2/Angiopoietin-1 signaling regulates hematopoietic stem cell quiescence in the bone marrow niche. *Cell* 118:149–161
11. Lo Celso C, Fleming HE, Wu JW et al (2009) Live-animal tracking of individual haematopoietic stem/progenitor cells in their niche. *Nature* 457:92
12. Nombela-Arrieta C, Pivarnik G, Winkel B et al (2013) Quantitative imaging of haematopoietic stem and progenitor cell localization and hypoxic status in the bone marrow microenvironment. *Nat Cell Biol* 15:533
13. Kusumbe AP, Ramasamy SK, Adams RH (2014) Coupling of angiogenesis and osteogenesis by a specific vessel subtype in bone. *Nature* 507:323
14. Acar M, Kocherlakota KS, Murphy MM et al (2015) Deep imaging of bone marrow shows non-dividing stem cells are mainly perisinusoidal. *Nature* 526:126
15. Coutu DL, Kokkalis KD, Kunz L, Schroeder T (2017) Multicolor quantitative confocal imaging cytometry. *Nat Methods* 15:39–46
16. Itkin T, Gur-Cohen S, Spencer JA et al (2016) Distinct bone marrow blood vessels differentially regulate haematopoiesis. *Nature* 532:323
17. Christodoulou C, Spencer JA, Yeh S-CA et al (2020) Live-animal imaging of native haematopoietic stem and progenitor cells. *Nature* 578:278–283
18. Köhler A, Filippo KD, Hasenberg M et al (2011) G-CSF-mediated thrombopoietin release triggers neutrophil motility and mobilization from bone marrow via induction of Cxcr2 ligands. *Blood* 117:4349–4357

19. Beck TC, Gomes A, Cyster JG, Pereira JP (2014) CXCR4 and a cell-extrinsic mechanism control immature B lymphocyte egress from bone marrow. *J Exp Med* 211:2567–2581
20. Sipkins DA, Wei X, Wu JW et al (2005) In vivo imaging of specialized bone marrow endothelial microdomains for tumour engraftment. *Nature* 435:969–973
21. Adams GB, Alley IR, Chung U-I et al (2009) Haematopoietic stem cells depend on Galpha (s)-mediated signalling to engraft bone marrow. *Nature* 459:103–107
22. Rashidi NM, Scott MK, Scherf N et al (2014) In vivo time-lapse imaging shows diverse niche engagement by quiescent and naturally activated hematopoietic stem cells. *Blood* 124: 79–83
23. Hawkins ED, Duarte D, Akinduro O et al (2016) T-cell acute leukaemia exhibits dynamic interactions with bone marrow microenvironments. *Nature* 538:518
24. Duarte D, Hawkins ED, Akinduro O et al (2018) Inhibition of endosteal vascular niche remodeling rescues hematopoietic stem cell loss in AML. *Cell Stem Cell* 22:64–77
25. Chen JY, Miyanishi M, Wang SK et al (2016) Hoxb5 marks long-term haematopoietic stem cells and reveals a homogenous perivascular niche. *Nature* 530:223
26. Sanjuan-Pla A, Macaulay IC, Jensen CT et al (2013) Platelet-biased stem cells reside at the apex of the haematopoietic stem-cell hierarchy. *Nature* 502:232–236
27. Pinho S, Marchand T, Yang E et al (2018) Lineage-biased hematopoietic stem cells are regulated by distinct niches. *Dev Cell* 44: 634–641.e4
28. Ito K, Turcotte R, Cui J et al (2016) Self-renewal of a purified *Tie2*⁺ hematopoietic stem cell population relies on mitochondrial clearance. *Science* 354:1156–1160
29. Gazit R, Mandal PK, Ebina W et al (2014) *Fgd5* identifies hematopoietic stem cells in the murine bone marrow. *J Exp Med* 211: 1315–1331
30. Muzumdar M, Tasic B, Miyamichi K et al (2007) A global double-fluorescent Cre reporter mouse. *genesis* 45:593–605
31. Hadjantonakis A-K, Papaioannou VE (2004) Dynamic in vivo imaging and cell tracking using a histone fluorescent protein fusion in mice. *Bmc Biotechnol* 4:33
32. Schachtner H, Li A, Stevenson D et al (2012) Tissue inducible Lifeact expression allows visualization of actin dynamics in vivo and ex vivo. *Eur J Cell Biol* 91:923–929
33. Ishitobi H, Matsumoto K, Azami T et al (2010) Flk1-GFP BAC Tg Mice: an animal model for the study of blood vessel development. *Exp Anim Tokyo* 59:615–622
34. Alva JA, Zovein AC, Monvoisin A et al (2006) VE-Cadherin-Cre-recombinase transgenic mouse: A tool for lineage analysis and gene deletion in endothelial cells. *Dev Dynam* 235: 759–767
35. Kalajzic Z, Liu P, Kalajzic I et al (2002) Directing the expression of a green fluorescent protein transgene in differentiated osteoblasts: comparison between rat type I collagen and rat osteocalcin promoters. *Bone* 31:654–660
36. Paic F, Igwe JC, Nori R et al (2009) Identification of differentially expressed genes between osteoblasts and osteocytes. *Bone* 45:682–692
37. Liu Y, Strecker S, Wang L et al (2013) Osterix-Cre labeled progenitor cells contribute to the formation and maintenance of the bone marrow stroma. *PLoS One* 8:e71318
38. Logan M, Martin JF, Nagy A et al (2002) Expression of Cre recombinase in the developing mouse limb bud driven by a *Prxl* enhancer. *Genesis* 33:77–80
39. Greenbaum A, Hsu Y-MS, Day RB et al (2013) CXCL12 in early mesenchymal progenitors is required for haematopoietic stem-cell maintenance. *Nature* 495:227
40. Sugiyama T, Kohara H, Noda M, Nagasawa T (2006) Maintenance of the hematopoietic stem cell pool by CXCL12-CXCR4 chemokine signaling in bone marrow stromal cell niches. *Immunity* 25:977–988
41. Ding L, Morrison SJ (2013) Haematopoietic stem cells and early lymphoid progenitors occupy distinct bone marrow niches. *Nature* 495:231
42. Comazzetto S, Murphy MM, Berto S et al (2019) Restricted hematopoietic progenitors and erythropoiesis require SCF from leptin receptor+ niche cells in the bone marrow. *Cell Stem Cell* 24:477–486.e6
43. Zhu X, Bergles DE, Nishiyama A (2008) NG2 cells generate both oligodendrocytes and gray matter astrocytes. *Development* 135:145–157
44. Lassailly F, Foster K, Lopez-Onieva L et al (2013) Multimodal imaging reveals structural and functional heterogeneity in different bone marrow compartments: functional implications on hematopoietic stem cells. *Blood* 122: 1730–1740
45. Kozloff KM, Quinti L, Patntirapong S et al (2009) Non-invasive optical detection of cathepsin K-mediated fluorescence reveals osteoclast activity in vitro and in vivo. *Bone* 44:190–198

46. Ambekar R, Chittenden M, Jasiuk I, Toussaint KC (2012) Quantitative second-harmonic generation microscopy for imaging porcine cortical bone: comparison to SEM and its potential to investigate age-related changes. *Bone* 50:643–650
47. Houle M-A, Couture C-A, Bancelin S et al (2015) Analysis of forward and backward second harmonic generation images to probe the nanoscale structure of collagen within bone and cartilage. *J Biophotonics* 8:993–1001
48. Preibisch S, Saalfeld S, Schindelin J, Tomancak P (2010) Software for bead-based registration of selective plane illumination microscopy data. *Nat Methods* 7:418
49. Batsivari A, Haltalli MLR, Passaro D et al (2020) Dynamic responses of the haematopoietic stem cell niche to diverse stresses. *Nat Cell Biol* 22:7–17
50. Chen Q, Liu Y, Jeong H-W et al (2019) Apelin + endothelial niche cells control hematopoiesis and mediate vascular regeneration after myeloablative injury. *Cell Stem Cell* 25: 768–783.e6
51. Russell ES (1979) Hereditary anemias of the mouse: a review for geneticists. *Adv Genet* 20: 357–459
52. Nocka K, Tan JC, Chiu E et al (1990) Molecular bases of dominant negative and loss of function mutations at the murine c-kit/white spotting locus: W37, Wv, W41 and W. *Embo J* 9:1805–1813
53. Migliaccio AR, Carta C, Migliaccio G (1999) In vivo expansion of purified hematopoietic stem cells transplanted in nonablated W/Wv mice. *Exp Hematol* 27:1655–1666
54. Waskow C, Madan V, Bartels S et al (2009) Hematopoietic stem cell transplantation without irradiation. *Nat Methods* 6:267–269



Laser Micromachining of Bone as a Tool for Studying Bone Marrow Biology

Christa Haase, Dmitry Richter, and Charles P. Lin

Abstract

The bone marrow (BM) has traditionally been a difficult tissue to access because it is embedded deep within the bone matrix. It is home to the hematopoietic stem cells (HSCs) that give rise to all blood cells in the body. It is also the site of origin for malignant blood cells such as leukemia and multiple myeloma, as well as a frequent site of metastasis for many solid tumors including prostate and breast cancer. The following chapter describes how laser micromachining of bone can be used to improve both optical and physical access to the BM. For example, laser thinning of the overlying bone can improve optical access, enabling deeper imaging into the BM as well as enhancing optical resolution by reducing scattering and aberration. Laser micromachining can also be used to provide physical access into the BM by creating access ports for micropipette insertion and delivery of cells to precise locations in the BM, as well as for the extraction of BM cells and interstitial fluid, all under image guidance. This chapter provides a detailed protocol for installing a laser-micromachining capability for users with an existing multiphoton microscope. Additionally, we briefly outline how such a system improves the optical resolution during imaging as well as its potential use to study injury response.

Key words Hematopoietic stem cell, Stem cell transplantation, Leukemia, Plasma-mediated laser ablation, Intravital microscopy

1 Introduction

The bone marrow (BM) is home to the hematopoietic stem cells (HSCs) that sit at the apex of all blood and immune cell production. It is also home to hematologic malignancies like leukemia, myelodysplastic syndrome, and multiple myeloma, as well as a frequent site of metastasis for many solid tumors, including prostate and breast cancer. Intravital microscopy, in combination with transgenic mice and fluorescent labeling strategies, has provided important insights into the basic biology of normal and malignant hematopoiesis [1–11]. It has also been used to study the homing and engraftment of HSCs in the BM after transplantation [12, 13]. The imaging depth, however, remains limited due to

the highly scattering bone matrix which restricts the ability to reconstruct the 3D spatial organization of BM tissue *in vivo*.

In this chapter, we describe how laser micromachining of bone can be used to improve imaging depth and resolution. Moreover, we describe how to generate small defects in the bone as a methodology for studying injury response. These defects can also be used as access ports for insertion of a micropipette, allowing for the delivery of cells to the BM under image guidance, as well as the isolation of cells from precise anatomical locations [14, 15]. As a central part of this experimental strategy, plasma-mediated laser ablation is used to etch bone tissue away with a precisely defined geometry. Plasma, a highly ionized state of matter, is generated when the energy of femtosecond laser pulses (typically kept below 1 nJ for multiphoton microscopy) exceeds a few nJ, generating electric fields at the focal point that are sufficiently strong (~ 100 MV/m in our system) to initiate tunneling and multiphoton ionization [16] which leads to a dense region of ions and electrons. Because of the short laser pulses and the tight-focusing geometry, the plasma is tightly confined in space and time, with a dimension of $\sim 1 \mu\text{m}^3$ that collapses after termination of the laser pulse. This removes a $\sim 1\text{-}\mu\text{m}^3$ volume of bone with each laser pulse while imparting minimal thermal damage to the surrounding tissue. If the ablation is performed under fluid immersion, as in most high-resolution multiphoton imaging applications, each pulse is accompanied by a cavitation bubble that expands and collapses on the timescale of $\sim 1 \mu\text{s}$. In essence, this is a highly precise microsurgery procedure that limits tissue damage within $<20 \mu\text{m}$ of the surgery (ablation) site. It is sometimes referred to as a “laser scalpel” and is used clinically in ophthalmic surgery [17]. In the following, we describe how to integrate a plasma-mediated laser ablation setup into a conventional multiphoton microscope (Subheading 3.1) and provide a detailed protocol for bone thinning (Subheading 3.2) and the generation of bone defects (Subheading 3.3). Laser bone thinning provides greater imaging depth by reducing the bone thickness and concomitant scattering [18]. On top of that, this has the added benefit of improving optical resolution. With some modifications, the technology can be used for cell delivery to the BM [19, 20] as well as the extraction of BM cells [18, 19] and interstitial fluid.

2 Materials

2.1 Materials and Supplies for Installation of the Ablation Capability

We organize the components necessary for installing the ablation capability on the multiphoton microscope into two categories: optics and mechanical components. Whenever necessary, we provide information on the quantity of the required items. We assume the ablation capability is being integrated into a functioning

multiphoton microscope (including an imaging laser, scanning optics, and objective lens) and therefore do not provide information on these components.

2.1.1 Optical Components

1. A femtosecond laser source with a repetition rate of ~ 1 MHz (e.g., Satsuma; central wavelength, 1030 ± 5 nm; *see Note 1*).
2. Mirrors M1–M4 (*see Fig. 2*): Round, protected aluminum mirrors (Thorlabs, PF10-03-g01, qt. 4) with corresponding mirror mounts (Thorlabs, KM100, qt. 4).
3. Lens L1 and L2 (*see Fig. 2*): Mounted achromatic doublet lens ($f = 75$ mm) (Thorlabs, AC254-075-AB-ML, qt. 2) with corresponding lens mount (Thorlabs, CP35, qt. 4), attached to a post and holder (*see Note 2*). Lens L2 is mounted on a translation stage (Thorlabs, MS1S) to facilitate its positioning along the laser propagation axis (needed to optimize collimation; *see Note 3*).
4. For combining imaging and ablation beam (*see Note 4*): Dichroic mirror (DC) 950-nm cutoff (Thorlabs, DMSP950R, short pass) or 980-nm BrightLine® single-edge laser-flat dichroic beamsplitter (Semrock, BLP01-980R-25). Corresponding mount (Thorlabs, FFM1 (Filterholder) and B4C (Platform), along with C6WR (Cage Cube)). The cage cube can be fixed to a regular post and holder but helps ensure a 45° angle with respect to both the imaging and ablation beam.
5. Apertures for the intermediate image plane (*see Note 5*).
6. For characterizing beam diameter: CMOS camera, Zelux monochrome (Thorlabs, CS165MU). Only required for troubleshooting (*see Note 7*).
7. For measuring laser power (if not already purchased for the multiphoton microscope): Slim Photodiode Power Sensor (Thorlabs, S130C) and Compact Power and Energy Meter Console, Digital 4" LCD (Thorlabs, PM100D).
8. Alignment disk for beam alignment (Thorlabs, VRC4CPT, qt. 2).

General Comments

- We recommend using either imperial or metric-sized components. Do not mix and match.
- All mounts should be connected to a post (Optical Post, SS, 8-32 Setscrew, $\frac{1}{4}$ "-20 Tap, L=4", Thorlabs, TR4, qt. ~ 20) inserted into a post holder (Post Holder, Spring-Loaded Hex-Locking Thumbscrew, L=3", Thorlabs, PH3, qt. ~ 20) and fixed to the optical table by clamping forks (Thorlabs, CF175, qt. ~ 20) with M6 screws (Thorlabs, SH6MS16V, qt. ~ 30). If

the space on your optical table is limited, we recommend using short clamping forks (e.g., Thorlabs, CF038 or CF125C).

- As a general recommendation, it is advised to install optical components/mounts in a way that leaves room for translation and optimizing their positioning.
- To maintain a consistent experimental performance level, it is strongly recommended to mark the position of the laser beam at multiple locations throughout the optical system by installing irises (Thorlabs, SM1D25) along with their mounts (post, post holder, clamping fork). As part of the daily alignment, you can check the laser position with respect to the irises and make any necessary adjustments.

2.1.2 Mechanical Components

- (a) Motorized Micromanipulator (Sutter Instrument, MPC-385). The MPC-385 System consists of the MPC-200 controller and one to four MP-285 micromanipulators.
- (b) A post and holder, used to mount the sample on the micromanipulator. A right-angle clamp (Thorlabs, RA90) or rotation stage (Thorlabs, PR005) can be used to obtain greater flexibility in sample positioning.

2.2 Materials and Supplies for Laser Ablation

To obtain high-quality ablation geometries with a water immersion objective lens (used on most multiphoton microscopes), it is necessary to generate a continuous stream of water or saline across the sample (flushing), removing gas and debris that is generated during the ablation procedure (*see* Fig. 3). In the following we have listed all relevant components that are required for setting up a flushing system:

1. Peristaltic pump, MPM REGLO ICC 2CHNL 6RLR (Cole-Parmer, EW-78001-58), and tubing (L = 16", D = 1.85 mm, ISMATEC, 95714-24) for controlling flow speed.
2. 2 Male Luer Lock to Hose Barb Adapters, 1/16" (Cole Parmer, UX-45513-00).
3. Blunt-tip needles (22G, 2", Grainger, 5FVC4, 2x) that are positioned at the tip of the objective lens and attached to the tubing of the peristaltic pump with the adapters.
4. Falcon[®] 50-mL High Clarity PP Centrifuge Tube (CORNING, 352098, qt. 10), that is filled with PBS (Thermo Fisher Scientific, #10010002).
5. Rubber-Cal Neoprene Sheet (0.5 in thick × 12 in wide × 24 in length, Lowes, #2696930). This is used to install the flushing system needles onto the objective lens (*see* Fig. 4).
6. A Hamilton needle (Luer Lock, 22G, Thermo Fisher Scientific, 14-815-412).

7. An excised piece of bone that can be mounted to a glass slide (BoliOptics, SL39101003) with Krazy Glue (#457099, Staples) or a mouse (see below).

General Comment

While we describe using a piece of rubber to fix the needles on the objective lens, we typically use a custom-designed, 3D-printed holder (drawing available upon request).

2.3 Materials for In Vivo Imaging

1. General supplies: Deionized water, molecular biology grade (Boston BioProducts, WT-035), isopropanol (CVS, 152074), lens tissue (Thorlabs, MC-5) for cleaning optics, Ethilon 6-0 suture, 18" (Zogo Medical, ETH-1956G), Curad triple antibiotic ointment (Curad, CUR001231H), PBS (Thermo Fisher Scientific, #10010002), and Qtracker 655 vascular labels (Thermo Fisher Scientific, Q21021MP).
2. Mice: C57BL6/J #000664 (Jackson Laboratories) or a fluorescent reporter mouse of your choice.
3. Mouse surgical kit (Kent Scientific, INSMOUSEKIT). When autoclaving your instruments, please familiarize yourself with the manufacturer's specifications.
4. Sterile, individually, wrapped transfer pipettes (Thermo Fisher Scientific, 13-711-20).
5. Q-tips (Thorlabs, CTA10, qt. 10). Sterilize by autoclave.
6. Anesthesia: Isoflurane (Piramal Critical Care) and vaporizer (WPI, EZ-155). We recommend the SomnoFlo starter kit that includes an induction chamber and tubing (Kent Scientific, SF-MSEKIT) *or* ketamine/xylazine (Sigma-Aldrich, K113-10ML) as an alternate anesthetic.
7. Analgesics such as bupivacaine, buprenorphine and Tylenol. Administer analgesics in accordance with your institution's IACUC policy, and consult an OAR/IACUC veterinarian.

3 Methods

3.1 Installing a Laser Ablation Capability on Your Multiphoton Microscope

All laser-scanning multiphoton microscopes have a built-in device that translates the laser beam along the x and y dimensions of the microscope field of view (FOV) (termed xy-scan), thereby generating a 2D image (*see* Fig. 1). This device can be a combination of two galvo mirrors, a resonant galvo and galvo mirror, or a scanning polygon and a galvo mirror (we use the latter on our home-built microscope). However, most commercial 2P imaging systems have a galvo-galvo scanner implemented. The same scanning device can be used to translate the ablation beam across the field of view (FOV), achieved by co-propagating the imaging beam and the ablation beam with the help of a dichroic mirror (DC; *see* Fig. 1).

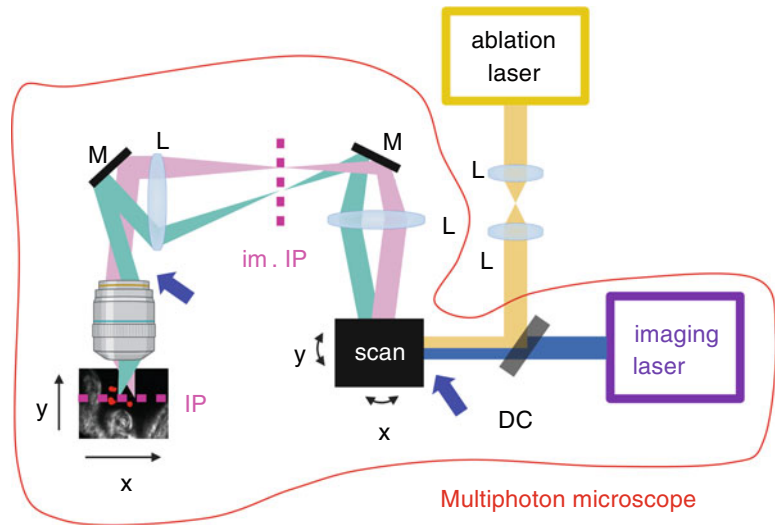


Fig. 1 Co-propagation of ablation and imaging beams in the multiphoton microscope. The ablation beam is overlapped with the imaging beam using a dichroic mirror (DC). Both beams are steered across the microscope field of view using scanning optics. *M* mirror, *L* lens, *IP* image plane, *im. IP* intermediate IP. Blue arrows mark the entrance of the scanning optics and back aperture of the objective lens, respectively

3.1.1 Installation of the Ablation Laser Unit

1. Fix the ablation laser to the breadboard of the microscope table using screws of the appropriate dimensions (typically M6 screws).
2. Turn on the ablation laser, and measure its output power to ensure that it is functioning as advertised. Reduce its power to ~10 mW, and proceed with the alignment. *As a safety precaution, laser alignment should “never” be performed at full power. Additionally, we advise the operator to wear appropriate laser safety glasses as the operating wavelength of the ablation laser (1030 nm) is beyond the visible spectrum and therefore cannot be seen by the human eye. It can cause severe damage to the retina if operated inappropriately.*
3. Using the alignment disk, visualize the laser propagation axis. Mark its height with respect to the table surface using an iris, adjusting the iris height so that the beam passes through the center of the iris. Install mirror M1 and M2 (see Fig. 2) by placing them at the correct height and at a 45° angle with respect to the propagation direction of the laser beam. Ensure that the height of the laser beam remains constant as it propagates from M1 to M2 and beyond using the iris. *Never place an optical element such as a lens or prism at the position of M1.* These elements have a reflective surface that is perpendicular to the propagation direction of the laser and can reflect part of the beam back into the laser head, damaging its function.

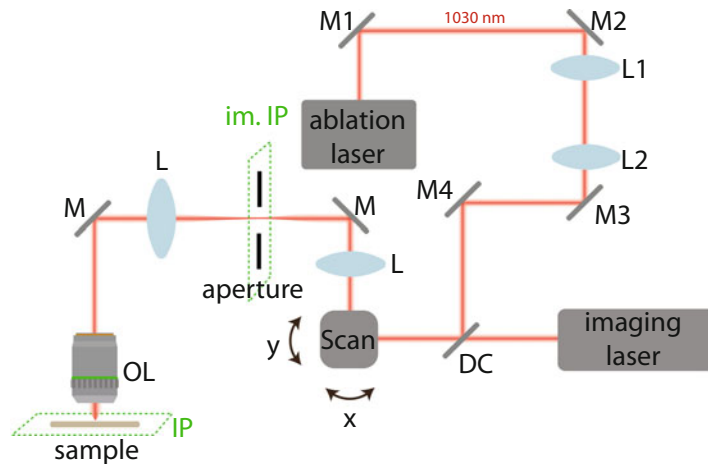


Fig. 2 Detailed optical diagram for installation of the ablation beam. *M1–M4* mirrors 1–4, *L1,2* lens 1,2, *DC* dichroic needed for overlapping the ablation beam and imaging beam, *M* mirror, *L* lens, *OL* objective lens, *IP* image plane, *im. IP* intermediate IP

4. Install lens L1 (focal length 75 mm) into the beam path, ensuring that it is perpendicular to the propagation direction and that the beam passes through its center. For this, install short cage rods (Thorlabs, ER1) into the lens mount, and use the alignment disk for positioning.
5. Place L2 (focal length 75 mm) onto a mount, and fasten it to a translation stage, placing it roughly at a 150-mm distance from L1. Use the translation stage to fine-tune the distance between L1 and L2. Proper positioning is ascertained by testing the collimation of the beam that exits L2 (*see Note 3*). If the beam is divergent, the distance between the lenses needs to be increased. If it is convergent, the distance needs to be decreased.
6. Install the 950-nm short-pass dichroic (DC) while ensuring that both laser beams have a 45° angle with respect to it.
7. Overlap the imaging with the ablation beam by adjusting M3 and M4 as follows: use M3 to overlap the two beams at the dichroic. Use M4 to overlap the beams before entry to the scanning optics. Repeat iteratively until the two beams overlap completely at all positions between these two points.
8. Unscrew the objective lens, and ensure that the two beams overlap at its back aperture, tweaking the alignment of M3 and M4 if necessary. Measure the transmission of the imaging beam through the microscope by measuring its power at the scanning optics and at the back aperture (blue arrows in Fig. 1). Compare its transmission to that of the ablation beam to further confirm proper alignment (*see Note 7*).

3.1.2 Installation of Flushing System

To perform plasma-mediated laser ablation of bone using a water immersion objective lens, it is necessary to flow a steady stream of PBS, saline, or water across the sample, thereby removing any gas and debris that is created during the procedure. Install the flushing system by proceeding as follows:

1. Install tubing on your peristaltic pump, and attach a Luer Lock to Hose Adapter at one end of each hose, screwing the blunt-tip needles into place (*see* Fig. 3). Place the other end of the hose into a Falcon tube filled with PBS (*see* Fig. 3). Turn on the peristaltic pump, and verify flow from the needle on channel 1, as well as suction into the needle on channel 2 (*see* Fig. 3).
2. Take the neoprene rubber slab, and cut out a circle with the correct dimensions, fitting it around the objective lens (OL; *see* Fig. 4). Advance a sharp-edged needle (same gauge as blunt) along the cone of the OL, and slowly stencil a hole into the rubber slab (*see* Fig. 4). Stencil a second hole directly opposite, and thread the two blunt-tip needles through the respective openings, positioning them as shown (*see* Fig. 4). Turn on the peristaltic pump, setting channel 1 (efflux) to 62 rpm and channel 2 (influx) to 75 rpm.
3. Position an excised piece of bone in the image plane of the OL, adjusting the flow rate of influx/efflux to achieve a liquid cone with the correct dimensions (*see* Fig. 5).

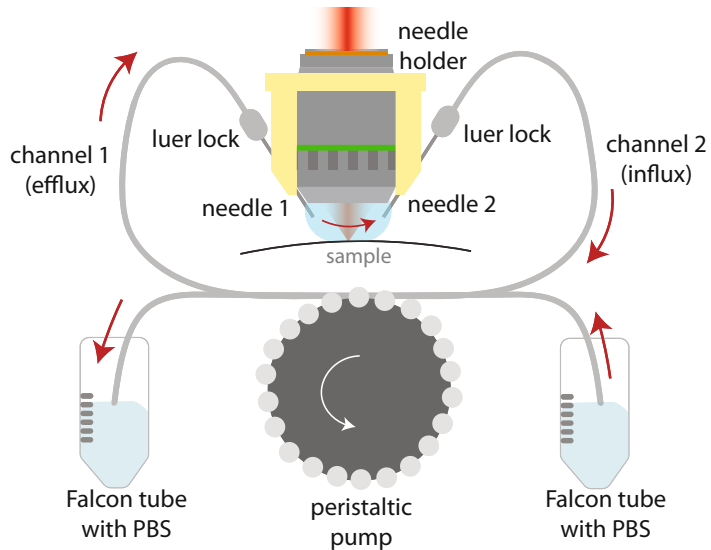


Fig. 3 Flushing system. A peristaltic pump is used to flow a continuous stream of PBS, saline, or water across the sample. Flow directions marked by red arrows

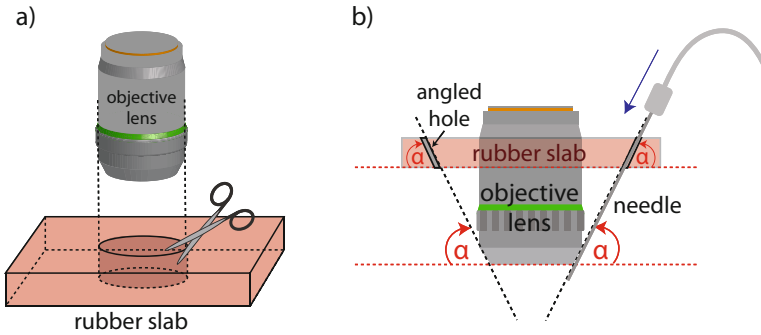


Fig. 4 Preparation of rubber slab to become a needle holder. Flushing requires a holder for the needles that can be prepared as shown here. **(a)** Remove a circular piece with dimensions of the objective lens. **(b)** Etch small holes into the rubber fitting, so that needles can be positioned at the tip of the objective lens

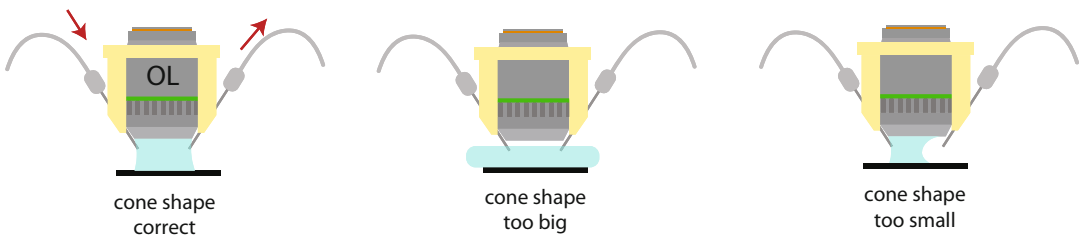


Fig. 5 Diagram showing correct flow rate. When influx and efflux are matched, a PBS cone with the correct dimensions is observed (left). If influx is too high (middle), PBS overflows the sample and dripping is observed. If influx is too low, the cone is too small, and it is impossible to generate a plasma due to the air interface (right)

4. Use your imaging software to perform laser ablation by taking a z-stack and adjusting the pulse energy of the ablation laser to ~ 12 nJ in the image plane. Set the step size along z to $0.25 \mu\text{m}$, frame average to 10, and the number of z-slices according to the ablation depth that you would like to achieve, i.e., for an ablation depth of $20 \mu\text{m}$, you would need $20 \mu\text{m} / 0.25 \mu\text{m} = 80$ z-slices. Your ablation geometry should be smooth (*see Note 6*).
5. To obtain an arbitrary ablation shape, adjust the scan geometry of your galvo mirrors in the microscope imaging software. Alternatively, if your system does not provide this function (*see Note 5*), insert a mask in the intermediate image plane (im. IP in Figs. 1 and 2). Optimal dimensions will vary depending on the magnification of your microscope, and it could be necessary to custom-design your mask (*see Note 9*).

3.2 Laser Bone Thinning to Improve Image Quality

Intravital microscopy of the skull BM is typically limited to depths of ~ 100 – $150 \mu\text{m}$ due to strong scattering and absorption of UV/Vis and NIR wavelengths by bone and BM tissue. Bone

thinning presents one method for improving imaging depth. However, mechanical thinning produces rough surface quality along with low precision and proclivity for thermal damage. Laser thinning of bone has been shown to improve imaging depth, while only minimally damaging the surrounding tissue, and results in flat bone surfaces that maintain high image quality [18, 21].

3.2.1 Perform Skin Flap Surgery

Place the mouse into an induction chamber, start the oxygen flow, and set the isoflurane to 3%. Alternatively, you can use ketamine/xylazine at a dose of 100 mg/kg (IP) to anesthetize the mouse. Administer analgesics in accordance with your institution's animal care and use committee's (IACUC) policy. Sterile equipment should be used throughout the procedure:

1. Set the isoflurane to 2%, and place the mouse into a mouse holder, ensuring that the skull is securely fixed (*see Note 10*).
2. Shave the mouse's head hair using a blade or scissors, then disinfect it first with an alcohol and then an iodine wipe. Using a pair of tweezers, pull the mouse skin away from the skull, and cut a half-elliptic shape with dimensions of $\sim 3 \times 5$ mm (*see Fig. 6a*), making sure to point the scissor tips upward to avoid damaging the skull or eyes.
3. Fold the skin flap toward the back of the skull, and gently secure it in place with a drop of antibiotic ointment. Using a sterile transfer pipette, place a drop of sterile saline onto the mouse skull, and gently remove the periosteum using two Q-tips, drawing the periosteum back from the skull center in a unified motion (*see Fig. 6b*). Use an additional Q-tip, and rub it across the mouse skull while applying a good amount of pressure, thereby removing any further periosteal tissue (*see Note 11*).

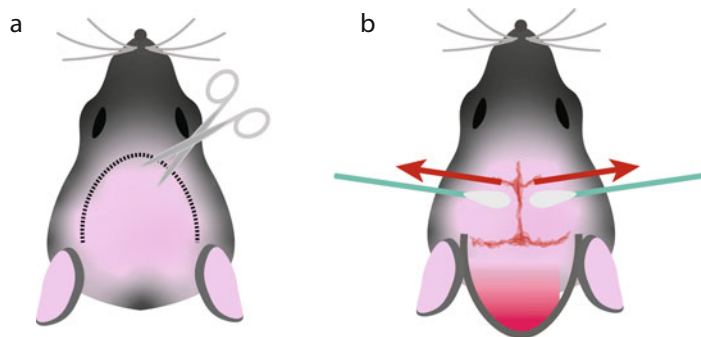


Fig. 6 Skin flap surgery for in vivo imaging. (a) Incision site for skin flap surgery. After folding the skin flap backward (b), moving two Q-tips from the skull center outward in a concerted motion (arrows) leads to removal of the periosteum

4. Add a fresh drop of sterile saline onto the skull, and set the isoflurane to 1.5%. Ensure that the mouse is breathing at a rate of ~once every 1–2 s, adjusting the isoflurane if necessary. If using ketamine/xylazine, re-inject the mouse every ~40 min with 100 mg/kg (IP) to maintain anesthesia. Transfer the mouse to the multiphoton microscope.

3.2.2 Perform In Vivo Multiphoton Microscopy

1. Turn on the microscope's photomultiplier tubes, set your imaging laser to the correct wavelength for two-photon excitation, and adjust its power to ~40 mW (*see Note 12*). You should also ensure that the correct set of dichroic mirrors and filters is in place in order to visualize your fluorophores (*see Note 13*).
2. Bring the mouse skull into focus by adjusting either the mouse or the microscope along the z dimension (*see Note 14*). Record the x, y, and z position of lambda, bregma, and bifurcation on the mouse skull (*see Fig. 7*). These anatomical landmarks are most readily visualized by the second harmonic generation of bone (generated by your imaging laser or ablation laser at half the emission wavelength). Recording the position of your in vivo images with regard to these landmarks will allow you to compare results from different mice, as well as to identify

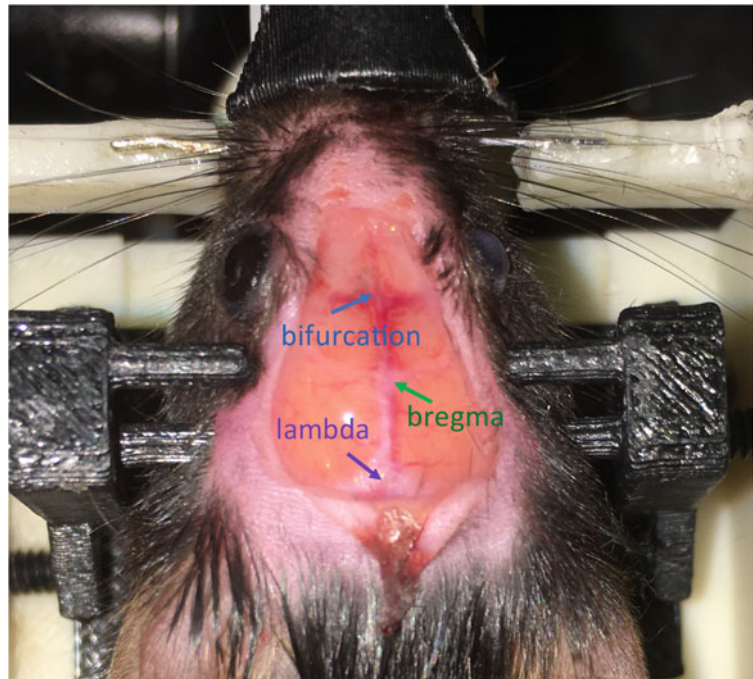


Fig. 7 Mouse skull with anatomical landmarks. Position of bifurcation, bregma, and lambda shown by arrows

sites from previous experiments when doing longitudinal imaging experiments.

3. Translate the mouse/scope along the x/y/z dimension, and identify sites of interest for intravital imaging. Record a z-stack by setting the step size to between 1 and 5 μm and averaging at least ten imaging frames. You can record z-stacks in multiple, adjacent locations that can later be stitched together to generate a larger, tiled image.

3.2.3 Perform Bone Thinning

To perform bone thinning during intravital imaging, turn on the flushing system, and set the ablation pulse energy to ~ 12 nJ, the step size along z to 0.25 μm and the frame average to 10. You can thin multiple, adjacent regions and stitch individual microscope fields of view to create tiled, high-depth images of larger bone marrow regions.

3.3 Generation of Bone Defects

Laser ablation is not only a precise method for thinning bone tissue and improving imaging depth and resolution; it can also be used to generate small defects in the bone and track the injury response by in vivo imaging [21]. In combination with fluorescent reporter mice for specific cell populations, this can provide important insights into wound healing and immune function.

3.3.1 Perform Skin Flap Surgery, Multiphoton Microscopy, and Laser Injury

Perform skin flap surgery and in vivo imaging as detailed in Subheadings 3.2.1 and 3.2.2, respectively:

1. Inject a vascular contrast agent such as Qtracker prior to imaging. This can be done either retro-orbitally or by tail vein injection.
2. If applicable, insert an iris/mask into the intermediate image plane of the microscope. Set the ablation pulse energy to ~ 12 nJ, the step size along z to 0.25 μm , and the frame average to 10.
3. Ablate a cone-shaped crater (*see Note 8*), and gently perforate the BM at its tip, taking care to avoid rupturing underlying blood vessels. Slowly close the iris as the sample/scope moves along the z dimension to further minimize collateral damage (*see Ref. [21]* for details).

3.3.2 Survival Surgery

1. Once you have completed the imaging and injury generation procedure, remove the mouse from the microscope, and gently rinse the calvarium with ~ 10 mL of sterile saline.
2. Fold the skin flap back onto the skull, and suture it in place using an Ethilon suture. The spacing between individual sutures should be no more than 2 mm. Apply triple antibiotic ointment onto the freshly sutured skin and administer analgesics in accordance with your institution's IACUC policy. Allow the mouse to recover from anesthesia.

3.3.3 Follow-Up Imaging

The procedure for follow-up imaging is the same as in Subheadings 3.2.1 and 3.2.2, although it can become necessary to rub the skull vigorously after the skin flap surgery to remove small amounts of scar tissue that has begun forming ~1 week after the first imaging session.

4 Notes

1. *Using a low repetition rate laser.* We recommend operating the laser at a repetition rate of 1 MHz for two reasons:
 - A. At relatively low repetition rates such as 1 MHz (compared to the maximum possible rep. rate of 40 MHz for Satsuma laser), the average power of the laser will leave less thermal damage behind as opposed to higher laser rep. rates.
 - B. The interval between two laser pulses is long enough for a plasma-induced cavitation bubble to collapse before the next laser pulse hits the sample, thereby maintaining a high ablation efficiency.
2. *Changing the beam diameter.* Depending on the objective lens that is used, the diameter of the ablation beam will need to be adjusted to fill out its back aperture. This can be done by installing two lenses in a 4f arrangement. This leads to a beam magnification of $M = f_2/f_1$, where f_1 is the focal length of L1 and f_2 is the focal length of L2, respectively.
3. *Measuring collimation.* One method for testing collimation is by using a commercially available laser beam profiler. These can be quite expensive, however, and we have found that a simpler method can also be used and delivers high-quality ablation geometries. Insert the alignment disk into your laser beam, and use a pencil to mark its circumference and beam center. Install a mirror at this position, and shoot the laser beam along the length of your optical table. If possible, extend the distance to the nearest wall. Move the alignment disk along the newly generated beam path (which is, ideally, several meters in length), and check to make sure that the beam doesn't focus at any point between the mirror and the wall. Compare the geometry of the laser beam at the wall to the markings on the alignment disk. If it is smaller, the beam is convergent, and the distance between the two lenses needs to be increased. If it is larger, the beam is divergent, and the distance needs to be reduced.
4. *Choice of dichroic mirror.* Depending on the existing imaging beam path set by the 2P microscope, the implementation of an ablation arm can be realized in two ways:

- A. The ablation beam is merged with the imaging beam by a short-pass dichroic mirror (*see* Fig. 2).
 - B. The ablation beam is merged with the imaging beam by a long-pass dichroic mirror (DM). In this case, the imaging beam is deflected into the 2P microscope, while the ablation beam passes through the DM and enters the microscope scanning optics. In essence, this would correspond to switching ablation laser and imaging laser in Fig. 2.
5. *Aperture in intermediate plane.* Most commercial 2P microscopes have a programmable scanning area. Therefore, these types of systems do not need an aperture in the intermediate image plane. However, for the sake of completeness, an aperture has been included in this protocol in case your system does not have a programmable galvo–galvo scanner.
 6. *Troubleshooting:* The ablation geometry is highly irregular. If the ablation beam is well aligned, the ablation quality should be good. However, here are some common reasons why the ablation has poor quality:
 - A. Alignment needs to be tweaked. Move the sample below the image plane, and turn on the flushing system and ablation beam. The emission of the ablation plasma should be visible (in our images this looks like tiny bubbles or speckles) and should fill the entire FOV (*see* Fig. 8). If not, adjust the tilt angles of M4 to optimize the ablation plasma.
 - B. The flushing needle is too far from the ablation plasma, and therefore the flow rate does not suffice to remove gas/debris. This becomes noticeable because large bubbles form during the ablation procedure, and they scatter the ablation beam, thereby preventing plasma generation. Move the needle closer to the image plane, advancing it along the cone of the OL, while paying attention not to block the imaging/ablation beams with the needle.
 - C. An ablation step of 0.25 μm with ten passes per plane (ten-frame average) yields optimal results on our system. You may need to adjust these values if the scanning optics on your system or the NA of your objective lens are different (our NA is 1.0).
 7. *Troubleshooting the transmission efficiency of the ablation beam.* If the ablation and imaging beams are well overlapped, their transmission efficiency should be similar, unless the beam diameters differ significantly. You can check the specs of the imaging laser to determine its diameter or measure it using an inexpensive CMOS camera (e.g., Zelux monochrome (#CS165MU, available from Thorlabs). If necessary, adjust the diameter of the ablation beam by installing two lenses with proper magnification.

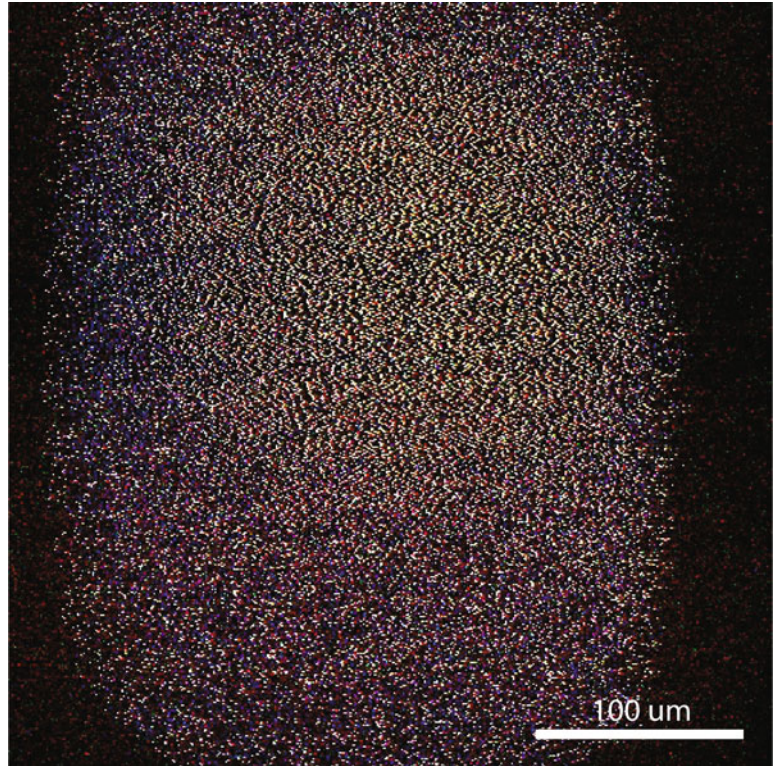


Fig. 8 Ablation plasma. Image of the ablation plasma, which fills the entire imaging FOV, if correctly aligned. The plasma emission is visible as tiny specks or bubbles

8. *Ablation crater shape.* The shape of the ablation crater is determined by the focusing geometry of the objective lens. Ideally, the angle of the crater wall takes the value of the focusing angle of the objective lens (given by its NA).
9. *Determining the magnification.* The fastest and most reliable way of doing this is by inserting an aperture of *known* geometry into the intermediate image plane. The same geometry should be visible in the multiphoton images, and calculation of the ratio between the two sizes will yield the magnification (*see* Fig. 9).
10. *Mouse holder.* We use a 3D-printed mouse holder for our imaging and ablation experiments. The SolidWorks file is available upon request. Discussing its design and fabrication is beyond the scope of this chapter. Please consult the *in vivo* imaging chapter in this book for information on alternate mouse holders.
11. *Bleeding.* Slight bleeding is often observed when removing the periosteum and can reduce image and ablation quality. The bleeding will generally stop if you put a fresh drop of saline

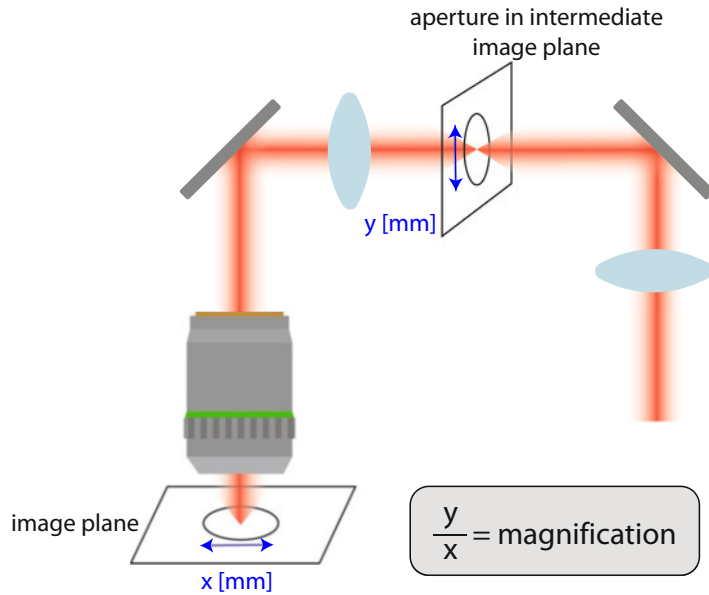


Fig. 9 Insertion of an aperture into the intermediate image. Comparing to the aperture dimensions in the image plane of your microscope makes it possible to calculate your microscope's magnification

onto the mouse skull and wait for a few minutes. Once bleeding has stopped, use fresh Q-tips to gently remove coagulated blood, and add a fresh drop of saline to the skull.

12. *Two-photon excitation frequency and laser power.* We recommend using one of the following resources to determine the two-photon excitation frequency of your fluorophore:
 - A. <https://www.bioimaging.bmc.med.uni-muenchen.de/manuals-protocols/multiphoton/index.html>
 - B. https://www.drbio.cornell.edu/cross_sections.html
 - C. <https://www.thermofisher.com/us/en/home/references/molecular-probes-the-handbook/technical-notes-and-product-highlights/fluorescent-probes-for-two-photon-microscopy.html>

The optimal power for in vivo multiphoton microscopy depends on the repetition rate of your laser. For a repetition rate of 80 MHz, we recommend using ~40 mW for bone marrow imaging. This value is obtained by measuring the laser power in the image plane. Note that at the bone surface lower powers are recommended.

13. *Dichroic mirrors and filters.* The optimal set of dichroics and filters will depend on the different fluorophores you are planning to excite. We recommend using Thermo Fisher's Fluorescence SpectraViewer [22] to help guide your choices

since the emission spectra for one- and two-photon excitation are typically similar.

14. *X, Y, and Z positioning.* Depending on your system, this will entail either moving the microscope or the sample (mouse) along the x, y, and z dimensions.

Acknowledgments

This work is supported in part by NIH R01 CA194596, R01 DK115577, R01 DK123216, and P01 HL142494.

References

1. Christodoulou C, Spencer JA, Yeh S-CA et al (2020) Live-animal imaging of native haematopoietic stem and progenitor cells. *Nature* 578:278–283
2. Itkin T, Gur-Cohen S, Spencer J et al (2016) Distinct bone marrow blood vessels differentially regulate haematopoiesis. *Nature* 532:323–328
3. Spencer JA, Ferraro F, Roussakis E et al (2014) Direct measurement of local oxygen concentration in the bone marrow of live animals. *Nature* 508:269–273
4. Carlson AL, Fujisaki J, Wu J et al (2013) Tracking single cells in live animals using a photo-convertible near-infrared cell membrane label. *PLoS One* 8:e69257
5. Sipkins DA, Wei X, Wu J et al (2005) In vivo imaging of specialized bone marrow endothelial microdomains for tumour engraftment. *Nature* 435:969–973
6. Tjin G, Flores-Figueroa E, Duarte D et al (2019) Imaging methods used to study mouse and human HSC niches: current and emerging technologies. *Bone* 119:19–35
7. Duarte D, Hawkins E, Akinduro O et al (2018) Inhibition of endosteal vascular niche remodeling rescues hematopoietic stem cell loss in AML. *Cell Stem Cell* 22:64–77
8. Hawkins ED, Duarte D, Akinduro O et al (2016) T-cell acute leukaemia exhibits dynamic interactions with bone marrow microenvironments. *Nature* 538(7626):518–522
9. Bixel MG, Kusumbe AP, Ramasamy SK et al (2017) Flow dynamics and HSPC homing in bone marrow microvessels. *Cell Rep* 18:1804–1816
10. Lawson MA, McDonald MM, Kovacic N et al (2015) Osteoclasts control reactivation of dormant myeloma cells by remodelling the endosteal niche. *Nat Commun* 6:8983
11. Zehentmeier S, Roth K, Cseresnyes Z et al (2014) Static and dynamic components synergize to form a stable survival niche for bone marrow plasma cells. *Eur J Immunol* 44:2306–2317
12. Lo Celso C, Fleming H, Wu J et al (2009) Live-animal tracking of individual haematopoietic stem/progenitor cells in their niche. *Nature* 457:92–96
13. Fujisaki J, Wu J, Carlson AL et al (2011) In vivo imaging of T reg cells providing immune privilege to the haematopoietic stem-cell niche. *Nature* 474:216–220
14. Haase C, Gustafsson K, Mei S et al (2021) Spatial transcriptomics reveals DPP4 as novel marker of a more proliferative phenotype in early AML progression. *Blood* 138:3310–3310
15. Haase C, Gustafsson K, Yeh S-C et al (2020) 3012 – probing hematopoietic-stromal cross-talk by spatially-resolved single-cell RNA-seq. *Exp Hematol* 88:S41
16. Vogel A, Noack J, Hüttman G et al (2005) Mechanisms of femtosecond laser nanosurgery of cells and tissues. *Appl Phys B* 81(8):1015–1047
17. Huhtala A, Pietilä J, Mäkinen P et al (2016) Femtosecond lasers for laser in situ keratomileusis: a systematic review and meta-analysis. *Clin Ophthalmol* 10:393–404
18. Turcotte R, Alt C, Mortensen LJ et al (2014) Characterization of multiphoton microscopy in the bone marrow following intravital laser osteotomy. *Biomed Opt Express* 5:3578–3588
19. Turcotte R, Alt C, Rannels JM et al (2017) Image-guided transplantation of single cells in the bone marrow of live animals. *Sci Rep* 7(1):1–9
20. Ito K, Turcotte R, Cui J et al (2016) Self-renewal of a purified Tie2+ hematopoietic

- stem cell population relies on mitochondrial clearance. *Science* 354:1156–1160
21. Mortensen LJ, Alt C, Turcotte R et al (2015) Femtosecond laser bone ablation with a high repetition rate fiber laser source. *Biomed Opt Express* 6:32
 22. Fluorescence SpectraViewer. <https://www.thermofisher.com/order/fluorescence-spectraviewer#!/>



MSC and HSPC Coculture: Mimicking Ex Vivo Bone Marrow Niche

Pratibha Singh

Abstract

Mesenchymal stromal cells (MSCs) are the crucial component of the hematopoietic stem and progenitor cell (HSPC) niche in the bone marrow. Therefore, an ex vivo culture system that recapitulates the marrow microenvironment is important to understanding the niche's regulatory role on HSPC function and improving ex vivo HSPC expansion for clinical transplantation. Herein, a procedure for ex vivo expansion of MSCs from human bone marrow cells and their identification and characterization is described. In addition, a protocol for MSC and HSPC coculture assay is presented. This MSC-HSPC coculture assay can be used for ex vivo expansion of HSPC. Furthermore, this assay is also useful for qualitative analysis of MSCs capable of supporting hematopoiesis.

Key words MSC, HSPC, Bone marrow microenvironment, CFU-F, MSC trilineage differentiation

1 Introduction

Hematopoietic stem and progenitor cells (HSPCs) generate all blood and immune cells throughout adult life. The majority of HSPCs reside in a highly complex cellular microenvironment/niche in the bone marrow (BM) composed of vasculature and perivascular mesenchymal stromal cell (MSC) [1–3]. Mesenchymal stromal cells are multipotent cells that have the potential to self-renew and differentiate into several lineages, including osteoblasts, chondrocytes, adipocytes, and neurons [4, 5]. In vivo, MSC supports HSPC maintenance and retention in the BM and promotes hematopoietic regeneration by producing several cytokines/growth factors such as stromal-derived factor-1 (SDF-1), stem cell factor (SCF), angiopoietin, and interleukin-7 [2, 6, 7]. The ease by which MSCs can be isolated from the BM and other tissues and ex vivo expanded has led to extensive investigations exploring their regenerative potential, tissue preservation capabilities, and anti-inflammatory properties. Recent studies show that ex vivo MSC can support HSPC extensive expansion without compromising

HSPC self-renewal property [2, 8]. In this book chapter, I describe protocols for human BM MSC purification and ex vivo expansion and MSC-HSPC coculture, which can be used to study the niche supporting function of MSC and to enhance ex vivo HSPC expansion for transplantation.

2 Materials

1. Human bone marrow (Lonza Bioscience or STEMCELL Technologies)
2. CD45 MicroBeads and Ter119 MicroBeads (Miltenyi Biotec)
3. Magnets and magnetic columns (Miltenyi Biotec)
4. MesenCult™-ACF Plus Medium (STEMCELL Technologies) or StemPro® MSC SFM (Thermo Fisher Scientific)
5. MesenCult™-SF Attachment Substrate (STEMCELL Technologies) or fibronectin
6. Animal Component-Free Cell Dissociation Kit (STEMCELL Technologies)
7. Lymphoprep™ (STEMCELL Technologies) or Ficoll-Paque Plus (GE Healthcare)
8. Cell buffer: PBS, 2% FBS, 2-mM EDTA
9. 0.4% trypan blue solution or 3% acetic acid with methylene blue
10. Hemacytometer
11. Alizarin Red S
12. Oil Red O
13. Alcian blue
14. Pre-separation filters
15. Fluorochrome-conjugated antibodies for MSC and HSPC evaluation
16. Flow cytometer cell analyzer with a minimum of three lasers

3 Methods

Steps involved in MSC and HSPC coculture assay.

3.1 MSC Isolation and Ex Vivo Expansion

The BM, adipose-derived tissue, and umbilical cord are the primary sources of MSC. In this chapter, I describe the isolation and expansion of MSC from human BM. But the same procedure can be used for the isolation and expansion of MSC from other sources.

Procedure

1. Freshly isolated unprocessed human BM cells can be purchased from Lonza Biologics and STEMCELL Technologies. The following protocol is for isolating MSC-rich cells from 25-mL freshly isolated human BM. If other volumes of BM are used, adjust the amount of the reagents accordingly. Bone marrow should be processed within 3–4 h of arrival to the lab to obtain good MSC recovery. An outline of MSC enrichment from human BM and its ex vivo expansion is described in Fig. 1a.

MSC enrichment and expansion

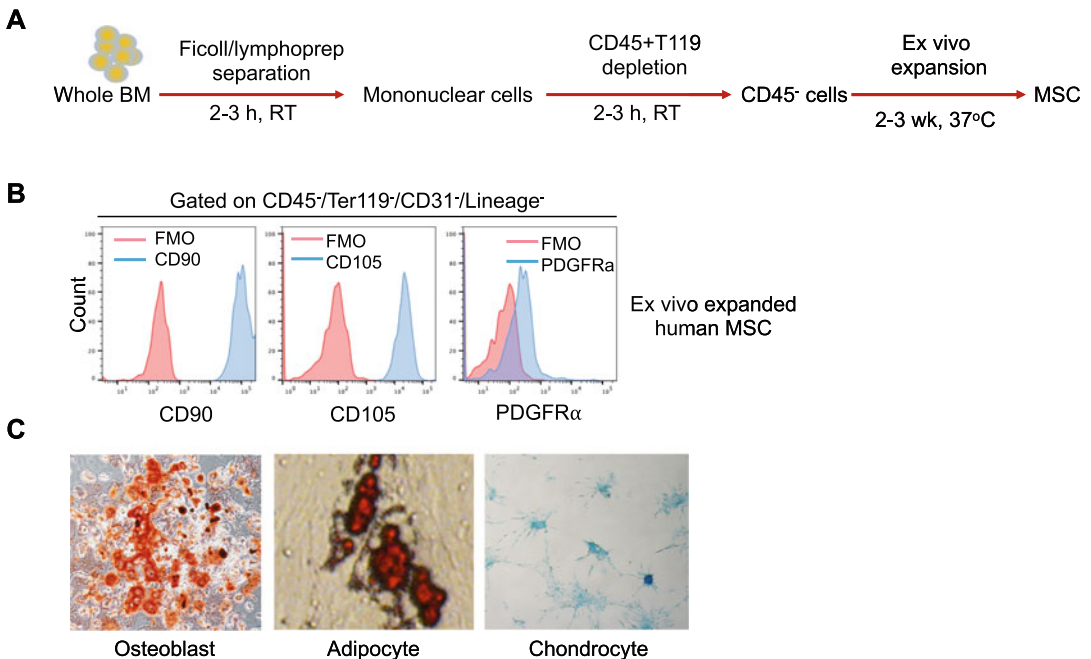


Fig. 1 Ex vivo human BM MSC expansion and characterization. **(a)** Schematic of human BM MSC enrichment and their ex vivo expansion. For the ex vivo MSC expansion, whole BM cells should first enrich for mononuclear cells using Ficoll-Paque or Lymphoprep™, followed by depletion of hematopoietic cells using magnetic beads-conjugated anti-CD45 anti-Ter119 antibodies. **(b)** Flow cytometry plots showing CD51, CD105, and PDGFR α expression on ex vivo expanded human BM MSC. To enrich MSC, whole BM cells were depleted for leukocytes and erythrocytes using Lymphoprep™ and anti-CD45 and anti-Ter119 microbeads. MSC-enriched BM cells were cultured for 3 weeks in an incubator at 37 °C with 5% O₂ and 5% CO₂. Ex vivo expanded MSCs were stained with anti-CD45, anti-Ter119, anti-CD31, anti-CD51, anti-CD105, and anti-PDGFR α and analyzed by flow cytometry. **(c)** Evaluation of ex vivo expanded MSC trilineage differentiation ability. Ex vivo expanded human BM MSCs were cultured in StemXVivo Osteogenic, Adipogenic or chondrogenic differentiation media for 2 weeks in an incubator at 37 °C and 5% CO₂. Osteogenic differentiation was determined by staining for mineralization of extracellular matrix and calcium deposits using Alizarin Red S. Cells were fixed with 4% paraformaldehyde (PFA) for 30 min, rinsed in distilled water, and stained with 40-mM Alizarin Red S solution at pH 4.2. Adipocytes were identified by the typical production of lipid droplets using Oil Red O staining. Alcian blue staining of glycosaminoglycans determined chondrocyte differentiation

3.1.1 Isolation of Mononuclear Cells

The first step of MSC purification from the BM sample is isolating mononuclear cells (MNCs) using a density-gradient medium. Several density-gradient media are commercially available, including Lymphoprep™ (STEMCELL Technologies) and Ficoll-Paque Plus (GE Healthcare). By exploiting the differences in cell density of the leukocytes, the density-gradient medium separates neutrophils and erythrocytes from MNCs during centrifugation. Following is the protocol for MNC isolation from human whole BM samples:

1. Count nucleated cells in the BM sample using 3% acetic acid with methylene blue or 0.4% trypan blue solution.
2. Split the BM sample into two 50-mL tubes (i.e., 12.5 mL of BM sample per tube).
3. Add 22.5-mL phosphate-buffered saline (PBS) containing 2% fetal bovine serum (FBS) and 2-mM EDTA per tube.
4. Prepare three new 50-mL tubes, and add 17 mL of Lymphoprep™ to each tube (*see Note 1*). Other density-gradient medium such as Ficoll-Paque can be substituted for Lymphoprep.
5. Carefully layer 23 mL of the BM suspension (from **step 3**) on top of the Lymphoprep™ in each tube. Centrifuge tubes at $800 \times g$ for 20 min, with the brake off.
6. Collect the MNC layer, at the plasma: Lymphoprep™ interface, and place in a single new 50-mL tube (*see Note 2*). Wash MNCs with PBS containing 2% FBS plus 2-mM EDTA.
7. Centrifuge the tube at $300 \times g$ for 10 min with the brake on. Discard the supernatant, and resuspend the cell pellet in PBS containing 2% FBS plus 2-mM EDTA (*see Note 3*).
8. Count MNCs using 3% acetic acid with methylene blue or 0.4% trypan blue solution.

3.1.2 Enrichment of MSCs

The MNCs isolated from the whole BM contain lymphocytes, erythrocytes (1–5%), and MSCs. Knowing that MSC lacks cell surface markers exclusively on hematopoietic origin cells, including CD45 (CD45 expresses on all hematopoietic cells except erythrocyte) and Ter119 (Ter119 expresses on erythrocytes), these cells could be enriched from MNCs by depleting CD45- and Ter119-positive cells. Several techniques are available to enrich/sort MSCs without affecting their viability and function. One of these techniques is the use of magnetic beads-conjugated CD45 and Ter119 antibodies. These antibodies are available from Miltenyi Biotec and STEMCELL Technologies. In a standard procedure for MSC enrichment, magnetic beads-conjugated anti-human CD45 and Ter119 antibodies are simultaneously added to the single-cell suspension of MNCs and incubated according to the respective separator user manual. When these labeled cells with the entire mixed-

cell population are placed into a magnetic separation system, the CD45- and Ter119-positive cells are attracted by the magnetic field to the tube wall or magnetic column, resulting in depletion of hematopoietic origin cells. I usually enrich MSCs from MNCs using CD45 and Ter119 microbeads and LS columns from Miltenyi Biotech (*see Note 4*). This procedure depletes 95% of hematopoietic cells from the MNC population, and I get MSC-enriched 4–5 million CD45⁻ and Ter119⁻ cells from 50 million MNCs.

3.1.3 In Vivo Expansion of MSCs

To accomplish MSCs ex vivo expansion, the MSC-enriched BM cells (CD45 and Ter119 depleted) should be cultured in media containing chemically defined constituents that support the attachment and proliferation of primary and passaged MSCs while maintaining their repopulation and trilineage differentiation properties (i.e., ability to differentiate into osteogenic, chondrogenic, and adipogenic lineages). Human MSC expansion media can be purchased from STEMCELL Technologies (MesenCult™-ACF Plus Medium), Thermo Fisher Scientific (StemPro® MSC SFM), and R&D Systems (StemXVivo Serum-Free Human MSC Expansion Media). These serum-free media are specifically formulated for the growth and expansion of human MSCs. We found that MesenCult™-ACF Plus Medium provides superior human MSC growth and increased consistency compared to classical serum-supplemented medium (DMEM + 10% FBS). Using MesenCult™-ACF Plus Medium, human MSCs can be expanded beyond five passages while still maintaining their trilineage mesoderm differentiation potential. The abovementioned media can be prepared and used for MSC expansion using respective user manual. The following protocol is for human MSC expansion using MesenCult™-ACF Plus Medium in a single T-25 flask. If using other cultureware, adjust cell numbers and volumes accordingly:

1. Prepare the complete MesenCult™-ACF Plus Medium (catalog # 05448) according to the user manual.
2. Coat a T-25-cm flask with animal component-free cell attachment substrate (STEMCELL Technologies) or another equivalent substrate such as fibronectin.
3. In the coated flask, seed freshly isolated MSC-enriched BM cells (depleted for CD45⁺ and Ter119⁺ cells) in 6 mL of MesenCult™-ACF Plus Medium. The cell density at $4\text{--}10 \times 10^3$ cells/cm ($1\text{--}2.5 \times 10^5$ cells per T-25-cm flask) gives optimal MSC expansion.
4. Incubate at 37 °C in a humidified incubator having 5% CO₂ and 5% O₂ until cells are approximately 80–90% confluent. It takes 2–3 weeks. Every 4–5 days, replace half medium with pre-warmed fresh medium (aspirate 3 mL of medium, and add

3 mL of complete of MesenCult™-ACF Plus Medium per flask.

5. Subculture the cells as needed using Animal Component-Free Dissociation Kit (Catalog # 05426) according to the user manual (*see* **Note 5**).

3.1.4 MSC Evaluation

Mesenchymal and Tissue Stem Cell Committee of the International Society for Cellular Therapy (ISCT) proposed minimal criteria to define human MSCs: (1) able to adhere to the plastic surface and form colony-forming unit-fibroblast (CFU-F) during *ex vivo* culture; (2) express CD105, CD73, and CD90 and lack hematopoietic markers such as CD45, CD34, and CD11b on the cell surface; and (3) able to *ex vivo* differentiate into osteoblasts, chondrocytes, and adipocytes.

The routine method for the evaluation of MSC cell surface markers is flow cytometry. The antibodies used for the MSC evaluation (as described above) are commercially available from BioLegend, eBioscience, and BD Biosciences. To identify the MSC surface markers, *ex vivo* expanded MSCs should be first detached from the flask/tissue culture plates at passage 2–3 using Animal Component-Free Cell Dissociation Kit (Stem Cell Technologies) or Trypsin EDTA (0.25%). Then, these cells should be labeled with fluorochrome-conjugated antibodies against CD45, CD34, CD11b, CD105, CD90, and PDGFR α and acquired by flow cytometry as I previously described [9]. The unstained cells, isotype-stained cells, and fluorescence minus one (FMO)-stained cells should be used as controls for flow cytometry data acquisition and analysis. I use FlowJo Software for MSC phenotypic analysis. The cell surface expression of CD90, CD105, and PDGFR α on *ex vivo* expanded human MSC is shown in representative flow cytometry plots in Fig. 1b.

Ex vivo cultured MSCs can differentiate into three mesodermal cell types, including adipocytes, osteoblasts, and chondrocytes, under specific culture conditions. MSC differentiation-inducing media are commercially available from R&D Systems, STEMCELL Technologies, and Invitrogen. The trilineage differentiation ability of *ex vivo* expanded MSCs can be examined by culturing these cells with differentiation-inducing culture media (osteoblast-, adipocyte-, or chondrocyte-specific medium) in 5% O₂ and 5% CO₂ for 2–3 weeks as we described [9]. Osteogenic differentiation can be determined by staining for mineralization of extracellular matrix and calcium deposits using Alizarin Red S. Adipocytes is identified by the typical production of lipid droplets using Oil Red O. Chondrocyte differentiation can be identified by Alcian blue staining of glycosaminoglycans. MSC differentiation into osteoblast, adipocyte, and chondroblast is shown in Fig. 1c.

3.2 Isolation of HSPC-Enriched Human CD34+ Cells

The membrane antigen CD34 predominantly expresses on human HSPCs. The magnetic beads coated with a primary CD34 antibody are commercially available from Miltenyi Biotec, STEMCELL Technologies, and Thermo Fisher Scientific. CD34+ HSPC can be isolated from unprocessed human BM using a two-step procedure including (1) purification of MNCs from whole BM using Lymphoprep™ or Ficoll-Paque™ as described above for MNC isolation for MSC enrichment and (2) labeling of CD34+ cells with micromagnetic beads-conjugated CD34 antibody and placing with the labeled cells into a magnetic field according to the specific manual instruction. Always use fresh BM samples (within 30 h of withdrawal) for CD34+ cell isolation. Human CD34+ cells can also be purchased from Lonza Bioscience (Bend, OR) or AllCells (Alameda, CA).

3.3 MSC and HSPC Coculture

To evaluate the impact of human MSCs on CD34+ HSPC expansion, freshly isolated human CD34+ cells should be cultured on ex vivo expanded MSC monolayers for 2 weeks. Ex vivo HSPC expansion should be evaluated by measuring the recovery of the total nucleated cell, CD34+ cell, and colony-forming unit cell after MSC-HSPC coculture. The following is the protocol for ex vivo expansion of HSPC with MSC coculture:

1. At 24–48 h before MSC-HSPC coculture, subculture ex vivo expanded MSCs, seed 1–2-million cells in per well of six-well plates in MesenCult™-ACF Plus Medium (4 mL), and culture at 37 °C with 5% CO₂ and 5% O₂.
2. Before the initiation of MSC-HSPC coculture assay, make sure that the MSC layers are 85–95% confluent. Remove one half of the MesenCult™-ACF Plus Medium, and replace it with StemSpan SFEM medium (STEMCELL Technologies, # 09650) supplemented with StemSpan CC100 (STEMCELL Technologies, # 02690).
3. Add 0.5–1.0-million freshly isolated CD34+ cells per well over the MSC monolayer, and coculture at 37 °C in the presence of 5% CO₂ and 5% O₂ for 2 weeks in humidified incubator. Throughout the MSC-HSPC coculture, MesenCult™-ACF Plus Medium and StemSpan SFEM medium should be used in 1:1 ratio.
4. Replenish one-half of the coculture media (2 mL) every 4 days without disturbing the MSC monolayers and the HSPCs. Collect media from the wells in 10-mL tubes, and spin down at 2000 rpm for 5 min at room temperature to avoid loss of HSPCs during media change. Resuspend in 2.0 mL of fresh coculture media, and gently add back to the wells, so that each well has a total of 4 mL of coculture media.

5. On day 15 post-MS-C-HSPC coculture, collect non-adherent HSPCs from the plates by gentle pipetting, and measure the recovery of total hematopoietic cells and HSPC. Count total cell numbers using hemocytometer counts with trypan blue for dead cell exclusion. To measure the HSPC number, stain cells with antibodies against CD34, CD38, CD90, lineage, and CD45RA, and evaluate Lineage⁺CD34⁺CD90⁺CD38⁻CD45RA⁻ HSPC-enriched cells using flow cytometry. HSPC clonal expansion can be tested by colony-forming unit cell (CFU-C) assay. To examine the HSPCs attached to MSC monolayers, harvest the adherent cells from the MSC-HSPC coculture plates by trypsinization, and evaluate the MSC monolayers adherent to CD34⁺ cells by flow cytometry.

4 Notes

1. Bring Lymphoprep™ or Ficoll-Paque to room temperature (15–20 °C), and mix thoroughly before use.
2. Sometimes it is difficult to see the cells at the interface. In this situation, removing some of the Lymphoprep™ along with the enriched cells will maximize cell recovery.
3. Density-gradient isolated MNC fraction may contain 1–5% erythrocytes.
4. For optimal enrichment of MSC, it is crucial to obtain a single-cell suspension before magnetic separation. Pass cells through 30-µm nylon mesh (Pre-Separation Filters, Miltenyi Biotec, #130-041-407) to remove cell clumps which may clog the magnetic column. Wet filter with buffer before use. Add CD45 and Ter119 microbeads together to simultaneous depletion of lymphocytes and erythrocytes.
5. To avoid the MSCs from sticking to the tubes during subculture, use polypropylene tubes (15 mL). To break up possible cell clumps, use 1-mL pipettor to gently pipette the cell pellet up and down a couple of times. Only use tissue culture-treated cultureware.

References

1. Ding L, Saunders TL, Enikolopov G et al (2012) Endothelial and perivascular cells maintain haematopoietic stem cells. *Nature* 481:457–462
2. Mendez-Ferrer S, Michurina TV, Ferraro F et al (2010) Mesenchymal and haematopoietic stem cells form a unique bone marrow niche. *Nature* 466:829–834
3. Morrison SJ, Scadden DT (2014) The bone marrow niche for haematopoietic stem cells. *Nature* 505:327–334
4. Caplan AI, Correa D (2011) The MSC: an injury drugstore. *Cell Stem Cell* 9:11–15
5. Crisan M, Yap S, Casteilla L et al (2008) A perivascular origin for mesenchymal stem cells in multiple human organs. *Cell Stem Cell* 3: 301–313

6. Abbuehl JP, Tatarova Z, Held W et al (2017) Long-term engraftment of primary bone marrow stromal cells repairs niche damage and improves hematopoietic stem cell transplantation. *Cell Stem Cell* 21:241–255.e6
7. Pinho S, Lacombe J, Hanoun M et al (2013) PDGFRalpha and CD51 mark human nestin+ sphere-forming mesenchymal stem cells capable of hematopoietic progenitor cell expansion. *J Exp Med* 210:1351–1367
8. Iscove NN, Nawa K (1997) Hematopoietic stem cells expand during serial transplantation in vivo without apparent exhaustion. *Curr Biol* 7: 805–808
9. Singh P, Fukuda S, Liu L, Chitteti BR, Pelus LM (2018) Survivin is required for mouse and human bone marrow mesenchymal stromal cell function. *Stem Cells* 36(1):123–129. <https://doi.org/10.1002/stem.2727>



Isolation of Thymus Stromal Cells from Human and Murine Tissue

Karin Gustafsson and David T. Scadden

Abstract

T cells go through most of their maturation in the thymus, and the stromal constituents of the thymus are therefore essential for T cell differentiation. The thymic stroma secretes the factors that recruit and sustain T cell progenitors, and they also partake in the shaping of a functional and tolerant T cell receptor repertoire. The damage incurred to the thymic stromal compartment by bone marrow conditioning regimens as well as by the natural aging process impairs T cell production. Yet little is known of how to prevent or reverse this damage. The development of high-throughput, single-cell analysis technologies has enabled better characterization of thymic stromal cells. This does however require tissue dissociation protocols optimized for stromal cell isolation. In this chapter, we detail the methodology of harvesting thymus stromal cells from human and murine tissue for downstream applications such as flow cytometric analysis and single-cell RNA sequencing.

Key words Thymus, Thymic stromal cells, Tissue dissociation, Thymus cell harvesting, Murine thymus stroma, Human thymus stroma

1 Introduction

The first evidence that thymic stromal cells contribute to the education of T lymphocytes came from work on T cell tolerance [1]. These early studies primarily implicated thymic epithelial cells as the stromal interaction partners of developing thymocytes [2, 3]. Since then, the scope of lymphostromal cross talk has broadened to include everything from supply of essential growth factors to expression and presentation of peripheral tissue self-antigens to ensure tolerance [4–6]. Other stromal cell types such as the endothelium, fibroblasts, and pericytes have also been demonstrated to be of significance to T cell maturation [7–9].

Preservation of thymic stromal cells is necessary for efficient T cell generation. After a bone marrow transplantation, thymic stroma is impaired by the cytotoxic conditioning as well as the ensuing graft-versus-host disease [10–12]. This in turn impairs

the secretion of the cytokines that recruit and expand T cell precursors, consequently leading to a delay in T cell reconstitution [8, 13]. The thymus is also one of the first organs to experience aging-related functional decline. Tolerance induction is impaired in aged individuals, the epithelial pool is diminished, and fat and fibrotic tissue replace the T cell supportive substrate [14–17]. The T cell repertoire is therefore contracted in the elderly, impairing vaccine responses, tumor surveillance, and peripheral tolerance maintenance [18]. The molecular underpinnings of thymic stromal cell sustainment and repair remain poorly understood. Single-cell analysis technologies have improved our understanding of thymic stromal cell populations in homeostasis [19, 20] but also necessitate stromal isolation protocols that yield quality preparations without sacrificing cell quantity. This is of particular importance when working with damaged or otherwise abnormal thymic tissue where obtaining a sufficient number of thymic stromal cells can be more challenging. In this chapter, we present protocols optimized for isolation of human and mouse thymic stroma in health and disease.

2 Materials

2.1 Isolation of Murine Thymus

1. Sterile surgical scissors
2. Sterile surgical forceps
3. Sterile spring scissors
4. Sterile blunt-ended forceps
5. Medium 199 supplemented with 2% fetal bovine serum (M199+)
6. Sterile six-well plate
7. Dissecting microscope

2.2 Dissociation of Murine Thymic Tissue

1. Sterile surgical scissors
2. 15-mL conical polypropylene centrifuge tube
3. Medium 199 supplemented with 2% fetal bovine serum (M199+)
4. Liberase TM
5. DNase I
6. Dissociation cocktail I: 0.5-WU/mL Liberase TM and 6.3-U/mL DNase I dissolved in M199+
7. Parafilm
8. Shaking water bath
9. 70- μ m cell strainer

10. 50-mL conical polypropylene centrifuge tube
11. Hemocytometer and microscope or automated cell counter

**2.3 Magnetic
Depletion of
Hematopoietic Cells**

1. 15-mL conical polypropylene centrifuge tube
2. Medium 199 supplemented with 2% fetal bovine serum (M199+)
3. Murine Fc Block
4. Biotinylated hematopoietic cell-specific antibodies (CD45, Ter119, CD3, CD8, CD11b, Gr-1, B220, CD19, and NK1.1)
5. Streptavidin magnetic microspheres
6. Orbital shaker
7. Magnet
8. Hemocytometer and microscope or automated cell counter

**2.4 Flow Cytometric
Analysis of Murine
Thymus Stromal Cells**

1. Sterile round-bottom polypropylene tubes
2. Medium 199 supplemented with 2% fetal bovine serum (M199+)
3. Murine Fc Block
4. Fluorescently tagged antibodies against CD45-APC/Cy7, Ter119-APC/Cy, CD31-BUV7373, EpCam-BV711, and Pdgfra-BV785
5. Viability dye (7AAD or DAPI)
6. Flow cytometry compensation beads
7. Sterile round-bottom polypropylene tubes with 40- μ m filter cap
8. Flow cytometer

**2.5 Dissociation of
Human Thymic Tissue**

1. Sterile surgical scissors
2. Sterile surgical forceps
3. Medium 199 (M199)
4. Bovine serum albumin (BSA)
5. Medium 199 supplemented with 2% fetal bovine serum (M199+)
6. STEMxyme
7. DNase I
8. 0.25% trypsin
9. Dissociation cocktail II: 2-mg/mL STEMxyme, 6.3-U/mL DNase I, and 1.5% BSA (w/v) dissolved in M199
10. Sterile 100-mm petri dish
11. 10-mL syringe

12. 50-mL conical polypropylene centrifuge tube
13. 50-mL tube rack
14. Parafilm
15. Shaking water bath
16. 70- μ m cell strainer
17. Hemocytometer and microscope or automated cell counter

2.6 Flow Cytometric Analysis of Human Thymus Stromal Cells

1. Sterile round-bottom polypropylene tubes
2. Medium 199 supplemented with 2% fetal bovine serum (M199+)
3. Human Fc Block
4. Fluorescently tagged antibodies against CD45-BV711, Cd235a-BV711, Lineage cocktail-FITC, CD8-APC/Cy7, CD31-PE/Dazzle, and EpCam-BV421
5. Viability dye (7AAD or DAPI)
6. Sterile round-bottom polypropylene tubes with 40- μ m filter cap
7. Flow cytometer

3 Methods

3.1 Isolation of Murine Thymus

1. Euthanize an 8–12-week-old mouse using CO₂ asphyxiation (*see Note 1*).
2. Open the chest cavity, and remove the thymus, placing it in a six-well plate with Medium 199 supplemented with 2% fetal bovine serum (M199+).
3. Under a dissecting microscope, carefully remove any extrathymic tissue using micro-spring scissors and blunt-ended forceps.

3.2 Dissociation of Murine Thymic Tissue

1. Place the thymus in the cap of a 15-mL tube, and cut it into small pieces using sterile surgical scissors.
2. Add 2 mL of dissociation cocktail I to the 15-mL tube, and attach the cap containing the finely minced thymus. Invert five times to ensure that all the thymic tissue is transferred from the cap to the dissociation cocktail I (*see Note 2*).
3. Wrap the cap with parafilm to prevent leakage, and place the tube horizontally into a 37 °C water bath shaking at 250 rpm. Incubate for 10 min.
4. Take the 15-mL tube containing the dissociated thymus, and place it in a rack to let the tissue pieces settle. Then carefully remove the supernatant, and filter this over a 70- μ m cell strainer into a 50-mL tube. Place on ice.

5. Repeat **step 2** twice for a total of three rounds of 10-min incubations, and collect the supernatant at each step. At the end of the digestion, the tissue should be mostly dissociated.
6. Wash the cells by adding 20 mL of M199+ and centrifuging at $500 \times g$ for 5 min at 4 °C.
7. Decant the supernatant and resuspend the pellet in 5 mL of M199+.
8. Count the cells.

3.3 Magnetic Depletion of Hematopoietic Cells

Magnetic depletion can sometimes be helpful when isolating large quantities of thymic stromal cells for flow cytometric sorting. The depletion step will cut down on sort time significantly and also reduces contamination of hematopoietic cells in the final preparation (*see* Fig. 1). An important factor to keep in mind though is that some of the cells of interest will be lost in the depletion. If the sample is derived from a treatment-naïve wild-type mouse, this is rarely an issue, but if working with tissue from an irradiated mouse or a mutant with impairments in T cell development, this excess loss of cells can be prohibitive of downstream applications. On the other hand, the starting material is usually much smaller than these mice, making sort time less of an issue:

1. Adjust the cell concentration to 10^8 cells/mL in a 15-mL conical tube.
2. Add biotinylated lineage-defining antibodies at a concentration of 5 µg/mL, and incubate for 10 min at room temperature on an orbital shaker.
3. Vortex streptavidin RapidSpheres, and add 25-µL/mL cell suspension. Incubate at room temperature on an orbital shaker for 5 min.
4. Place 15-mL conical tube in a magnet for 2.5 min, and then carefully decant the supernatant into a new 15-mL conical tube.
5. For improved purity add additional biotinylated lineage-defining antibodies at a concentration of 2.5-µg/mL cell suspension, and incubate for 10 min at room temperature on an orbital shaker.
6. Vortex streptavidin RapidSpheres and add 25-µL/mL cell suspension. Incubate at room temperature on an orbital shaker for 5 min.
7. Place 15-mL conical tube in a magnet for 2.5 min, and then carefully decant the supernatant into a new 15-mL conical tube.
8. Count the cells.

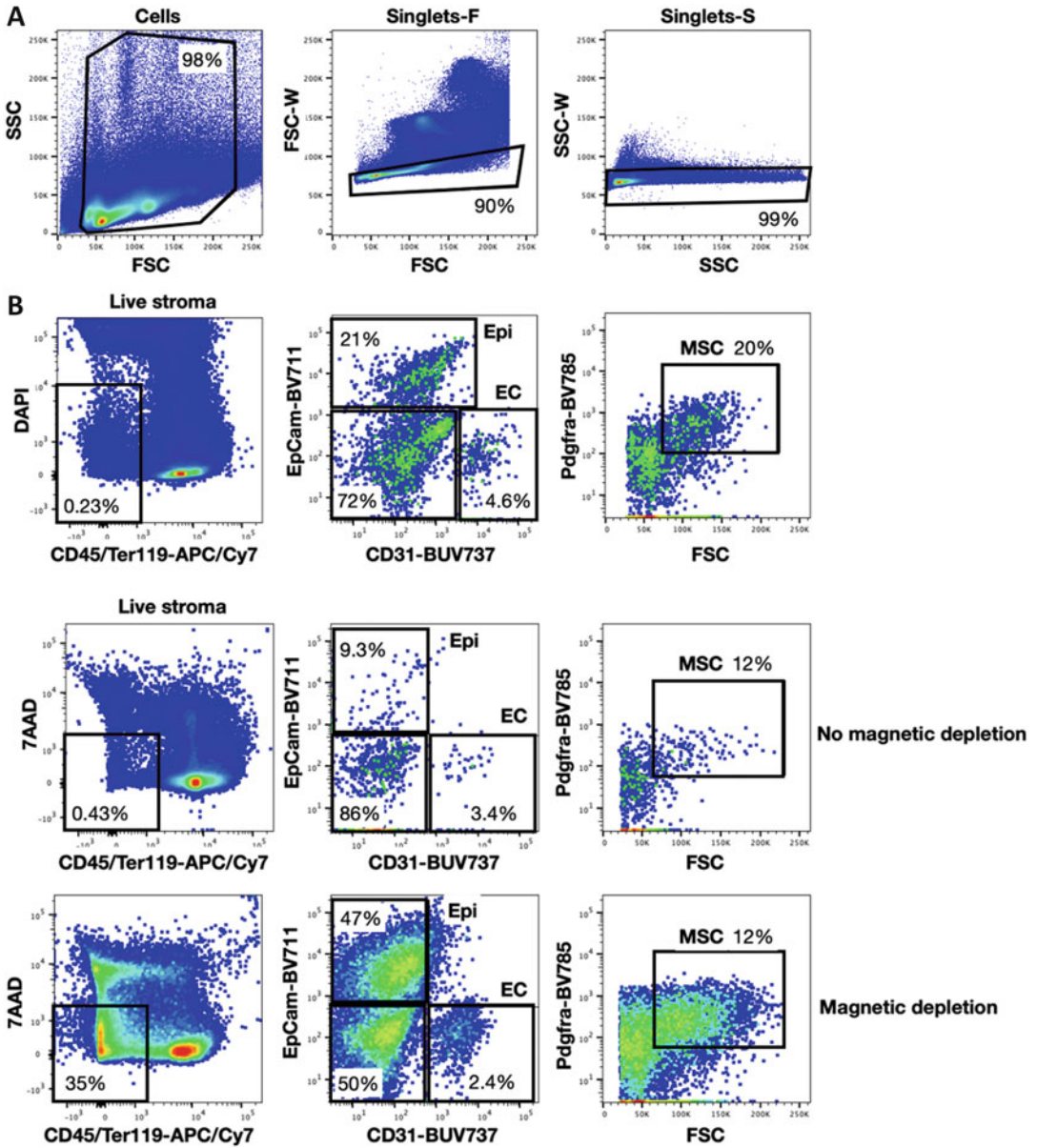


Fig. 1 (a) Gating strategy for flow cytometric analysis of murine thymus stroma. Percentages refer to percent of parent gate. (b) Representative flow plots showing the effect of depleting hematopoietic cells from thymic cell suspensions prior to cell sorting. The same number of total cells was collected for the depleted and non-depleted samples. Percentages refer to percent of parent gate. *Epi* epithelium, *EC* endothelial cells, and *MSC* mesenchymal stromal cells

3.4 Flow Cytometric Analysis of Murine Thymus Stromal Cells

1. Pellet the cells by centrifuging at 500 *g* for 5 min at 4 °C. Resuspend the cells at a concentration of 5 × 10⁷ cells/ml in M199+ in round-bottom polypropylene tubes.
2. Add murine Fc Block at a 10-μg/mL concentration, and incubate for 10 min at 4 °C.

3. Stain the cells with the following antibodies: CD45-APC/Cy, Ter119-APC/Cy7, CD31-BUV737, EpCam-BV711, and Pdgfra-BV785. Incubate for 30 min at 4 °C.
4. While the cells are stained, prepare the compensation control beads. Prepare one tube for each fluorescent color used, i.e.:
 - (a) APC/Cy7
 - (b) BUV737
 - (c) BV711
 - (d) BV785
5. Add one drop of flow cytometry compensation beads to each round-bottom polypropylene tube followed by 200 μ L M199. Add 0.1 μ g of fluorescent antibody to its corresponding tube.
6. Wash the stained cells by addition of 3 mL of M199+ followed by centrifugation at 500 *g* for 5 min at 4 °C.
7. Decant the supernatant, resuspend the cells in M199+ containing an appropriate viability dye like DAPI (5 μ g/mL) or 7AAD (1 μ g/mL), and proceed to analysis and cell sorting (*see* Fig. 1) (*see* **Note 3**).

3.5 Dissociation of Human Thymic Tissue

1. Collect the tissue in M199 on ice.
2. Place the thymus in a 10-mm petri dish with 10 mL of ice-cold M199. Start by carefully removing extrathymic tissue and any damaged thymic tissue using sterile surgical scissors and forceps (*see* **Note 4**).
3. Cut the thymus into 1-cm³ pieces. In order to reduce tissue volume in need of digestion to release stromal cells, use the plunger of a 10-mL syringe to press down on the thymic pieces. This will release hematopoietic cells into the medium, and collect the medium in a separate tube if the hematopoietic compartment is to be analyzed as well.
4. Weigh the lightly crushed tissue pieces. Transfer ~5 mg of the thymic tissue to the cap of a 50 ml conical tube and finely mince it using sterile surgical scissors.
5. Add 8 mL of dissociation cocktail II to the 50-mL tube, and attach the cap containing the finely minced human thymus. Invert five times to ensure that all the thymic tissue is transferred from the cap to the dissociation cocktail II (*see* **Notes 2 and 5**).
6. Wrap the cap with parafilm to prevent leakage, and place the tube horizontally into a 37 °C water bath shaking at 250 rpm. Incubate for 30 min.
7. Take the 50-mL tube containing the digesting human thymus, and place it in a rack to let the tissue pieces settle. Then carefully

remove the supernatant, and filter this over a 70- μ m cell strainer into a 50-mL tube placed on ice.

8. Add an additional 8 mL of dissociation cocktail II to the tissue remnants, and digest further for 30 min at 37 °C and 250 rpm.
9. Repeat **step 7**.
10. At this stage add 8 mL of dissociation cocktail II followed by 2 mL of 0.25% trypsin. Continue the digestion for an additional 30 min at 37 °C and 250 rpm (*see Note 6*).
11. Once the incubation is over, pass the remaining cell suspension and tissue fragments over a 70- μ m cell strainer into the 50-mL tube containing previous fractions. Add 3 mL of fetal bovine serum to break the trypsin reaction.
12. Count the cells.

3.6 Flow Cytometric Analysis of Human Thymus Stromal Cells

1. Pellet the human thymic cells by centrifuging at 500 *g* for 5 min at 4 °C. Resuspend the cells at a concentration of 5×10^7 cells/mL in M199+ in round-bottom polypropylene tubes.
2. Add human Fc Block at a 10- μ g/mL concentration, and incubate for 10 min at 4 °C.
3. Stain the cells with the following antibodies: CD45-BV711, CD235a-BV711, Lineage cocktail-FITC, CD8-APC/Cy7, CD31-PE/Dazzle594, and EpCam-BV421. Incubate for 30 min at 4 °C.
4. While the cells are stained, prepare the compensation control beads. Prepare one tube for each fluorescent color used, i.e.:
 - (a) BV711
 - (b) FITC
 - (c) APC/Cy7
 - (d) PE/Dazzle594
 - (e) BV421
5. Add one drop of flow cytometry compensation beads to each round-bottom polypropylene tube followed by 200- μ L M199. Add 0.1 μ g of fluorescent antibody to its corresponding tube.
6. Wash the stained cells by addition of 3 mL of M199+ followed by centrifugation at 500 *g* for 5 min at 4 °C.
7. Decant the supernatant, resuspend the cells in M199+ containing an appropriate viability dye like DAPI (5 μ g/mL) or 7AAD (1 μ g/mL), and proceed to analysis and cell sorting (*see Fig. 2a*) (*see Note 3*).

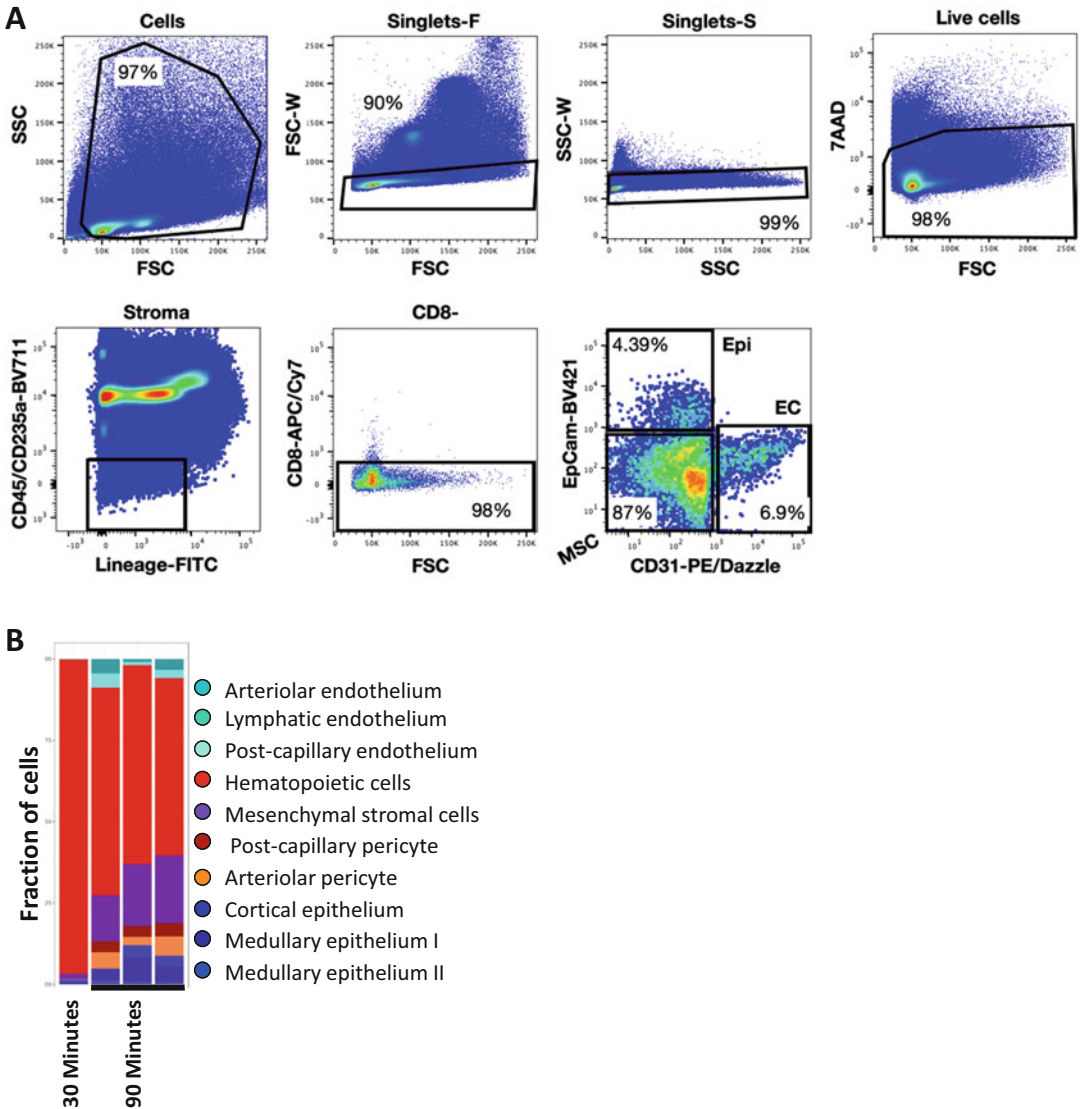


Fig. 2 (a) Gating strategy for flow cytometric analysis of human thymus stroma. Percentages refer to percent of parent gate. *Epi* epithelium, *EC* endothelial cells, and *MSC* mesenchymal stromal cells. **(b)** Bar graph showing the frequency of various cell types in the human thymus as determined by single-cell RNA sequencing

4 Notes

1. CO₂ asphyxiation is preferable to cervical dislocation when isolating thymus as the force of the dislocation sometimes causes hemorrhages around the thymus, thus making its complete removal more challenging. This is of particular importance when working with recently irradiated mice or mutants with abnormal T cell development. The thymus is often very

small in these mice, and excessive bleeding in the area can easily obscure most of the tissue.

2. Both murine and human CD4 are extremely sensitive to enzymatic digestion cleavage, and most commonly used dissociation cocktails will remove it from the cell surface. We have found that 1-mg/mL collagenase IV preserves CD4, but this will lead to lower stromal cell yields. It is therefore important to keep this in mind if analysis of the hematopoietic compartment of the thymus is to be done alongside analysis of stromal cell subsets.
3. When sorting stromal cells from any hematopoietic tissue, the sorted CD45 fraction will always have a significant fraction of contaminating hematopoietic cells (*see* Fig. 2b) [19–22]. This can be reduced somewhat by a magnetic depletion step prior to the flow cytometric sort, but the hematopoietic contamination can never be completely avoided. This is something to always have in mind when sorting thymic stromal cells for downstream applications.
4. The removal of human thymic tissue often leaves part of the tissue damaged by cauterization and general handling. Damaged tissue will have a darker color than the rest and should be removed.
5. It is essential that the protein source for dissociation cocktail II is not fetal bovine serum but bovine serum albumin since the final digestion step involves the use of trypsin which is inhibited by fetal bovine serum.
6. The digestion time for human thymic tissue is significantly longer than for murine thymus. The extended protocol is essential to obtain stromal cell populations. Human thymus stromal cell diversity as characterized by single-cell RNA sequencing is significantly diminished in shorter digestion protocols (*see* Fig. 2b).

References

1. Bevan MJ (1977) In a radiation chimaera, host H-2 antigens determine immune responsiveness of donor cytotoxic cells. *Nature* 269: 417–418
2. Anderson G, Jenkinson EJ, Moore NC, Owen JJ (1993) MHC class II-positive epithelium and mesenchyme cells are both required for T-cell development in the thymus. *Nature* 362:70–73
3. Ashton-Rickardt PG, Bandeira A, Delaney JR, Van Kaer L, Pircher HP, Zinkernagel RM, Tonegawa S (1994) Evidence for a differential avidity model of T cell selection in the thymus. *Cell* 76:651–663
4. Anderson MS, Venanzi ES, Klein L, Chen Z, Berzins SP, Turley SJ, von Boehmer H, Bronson R, Dierich A, Benoist C, Mathis D (2002) Projection of an immunological self shadow within the thymus by the aire protein. *Science* 298:1395–1401
5. Moore NC, Anderson G, Smith CA, Owen JJ, Jenkinson EJ (1993) Analysis of cytokine gene expression in subpopulations of freshly isolated thymocytes and thymic stromal cells using semiquantitative polymerase chain reaction. *Eur J Immunol* 23:922–927
6. Wiles MV, Ruiz P, Imhof BA (1992) Interleukin-7 expression during mouse thymus development. *Eur J Immunol* 22:1037–1042

7. Nitta T, Takayanagi H (2020) Non-epithelial thymic stromal cells: unsung heroes in thymus organogenesis and T cell development. *Front Immunol* 11:620894
8. Wertheimer T, Velardi E, Tsai J, Cooper K, Xiao S, Kloss CC, Ottmuller KJ, Mokhtari Z, Brede C, deRoos P, Kinsella S, Palikuqi B, Ginsberg M, Young LF, Kreines F, Lieberman SR, Lazrak A, Guo P, Malard F, Smith OM, Shono Y, Jenq RR, Hanash AM, Nolan DJ, Butler JM, Beilhack A, Manley NR, Rafii S, Dudakov JA, van den Brink MRM (2018) Production of BMP4 by endothelial cells is crucial for endogenous thymic regeneration. *Sci Immunol* 3:eaal2736
9. Zachariah MA, Cyster JG (2010) Neural crest-derived pericytes promote egress of mature thymocytes at the corticomedullary junction. *Science* 328:1129–1135
10. Na IK, Lu SX, Yim NL, Goldberg GL, Tsai J, Rao U, Smith OM, King CG, Suh D, Hirschhorn-Cymerman D, Palomba L, Penack O, Holland AM, Jenq RR, Ghosh A, Tran H, Merghoub T, Liu C, Sempowski GD, Ventevogel M, Beauchemin N, van den Brink MR (2010) The cytolytic molecules Fas ligand and TRAIL are required for murine thymic graft-versus-host disease. *J Clin Invest* 120:343–356
11. Fletcher AL, Lowen TE, Sakkal S, Reiseger JJ, Hammett MV, Seach N, Scott HS, Boyd RL, Chidgey AP (2009) Ablation and regeneration of tolerance-inducing medullary thymic epithelial cells after cyclosporine, cyclophosphamide, and dexamethasone treatment. *J Immunol* 183:823–831
12. Williams KM, Mella H, Lucas PJ, Williams JA, Telford W, Gress RE (2009) Single cell analysis of complex thymus stromal cell populations: rapid thymic epithelia preparation characterizes radiation injury. *Clin Transl Sci* 2:279–285
13. Zhang SL, Wang X, Manna S, Zlotoff DA, Bryson JL, Blazar BR, Bhandoola A (2014) Chemokine treatment rescues profound T-lineage progenitor homing defect after bone marrow transplant conditioning in mice. *Blood* 124:296–304
14. Aw D, Silva AB, Maddick M, von Zglinicki T, Palmer DB (2008) Architectural changes in the thymus of aging mice. *Aging Cell* 7:158–167
15. Steinmann GG, Klaus B, Muller-Hermelink HK (1985) The involution of the ageing human thymic epithelium is independent of puberty. A morphometric study. *Scand J Immunol* 22:563–575
16. Coder BD, Wang H, Ruan L, Su DM (2015) Thymic involution perturbs negative selection leading to autoreactive T cells that induce chronic inflammation. *J Immunol* 194:5825–5837
17. Yang H, Youm YH, Sun Y, Rim JS, Galban CJ, Vandanmagsar B, Dixit VD (2009) Axin expression in thymic stromal cells contributes to an age-related increase in thymic adiposity and is associated with reduced thymopoiesis independently of ghrelin signaling. *J Leukoc Biol* 85:928–938
18. Palmer S, Albergante L, Blackburn CC, Newman TJ (2018) Thymic involution and rising disease incidence with age. *Proc Natl Acad Sci USA* 115:1883–1888
19. Bornstein C, Nevo S, Giladi A, Kadouri N, Pouzolles M, Gerbe F, David E, Machado A, Chuprin A, Toth B, Goldberg O, Itzkovitz S, Taylor N, Jay P, Zimmermann VS, Abramson J, Amit I (2018) Single-cell mapping of the thymic stroma identifies IL-25-producing tuft epithelial cells. *Nature* 559:622–626
20. Park JE, Botting RA, Dominguez Conde C, Popescu DM, Lavaert M, Kunz DJ, Goh I, Stephenson E, Ragazzini R, Tuck E, Wilbrey-Clark A, Roberts K, Kedlian VR, Ferdinand JR, He X, Webb S, Maunder D, Vandamme N, Mahbubani KT, Polanski K, Mamanova L, Bolt L, Crossland D, de Rita F, Fuller A, Filby A, Reynolds G, Dixon D, Saeb-Parsy K, Lisgo S, Henderson D, Vento-Tormo R, Bayraktar OA, Barker RA, Meyer KB, Saecys Y, Bonfanti P, Behjati S, Clatworthy MR, Taghon T, Haniffa M, Teichmann SA (2020) A cell atlas of human thymic development defines T cell repertoire formation. *Science* 367:eaay3224
21. Baryawno N, Przybylski D, Kowalczyk MS, Kfoury Y, Severe N, Gustafsson K, Kokkaliaris KD, Mercier F, Tabaka M, Hofree M, Dionne D, Papazian A, Lee D, Ashenberg O, Subramanian A, Vaishnav ED, Rozenblatt-Rosen O, Regev A, Scadden DT (2019) A cellular taxonomy of the bone marrow stroma in homeostasis and leukemia. *Cell* 177:1915–1932.e16
22. Severe N, Karabacak NM, Gustafsson K, Baryawno N, Courties G, Kfoury Y, Kokkaliaris KD, Rhee C, Lee D, Scadden EW, Garcia-Robledo JE, Brouse T, Nahrendorf M, Toner M, Scadden DT (2019) Stress-induced changes in bone marrow stromal cell populations revealed through single-cell protein expression mapping. *Cell Stem Cell* 25:570–583.e7

Part V

Transplantation and In Vivo Models



Experimental Models of Mouse and Human Hematopoietic Stem Cell Transplantation

Scott H. Cooper, Maegan L. Capitano, and Hal E. Broxmeyer

Abstract

Experimental hematopoietic stem cell transplantation (HSCT) is an invaluable tool in determining the function and characteristics of hematopoietic stem cells (HSC) from experimental mouse and human donor groups. These groups could include, but are not limited to, genetically altered populations (gene knock-out/knockin models), ex vivo manipulated cell populations, or in vivo modulated cell populations. The basic fundamentals of this process involve taking cells from a mouse/human donor source and putting them into another mouse (recipient) after preconditioning of the recipient with either total body irradiation (TBI) for mouse donor cells or into sublethally irradiated immune-deficient mice for human donor cells. Then, at pre-determined time points post-transplant, sampling a small amount of peripheral blood (PB) and at the termination of the evaluation, bone marrow (BM) to determine donor contribution and function by phenotypic analysis. Exploiting the congenic mouse strains of C57BL/6 (CD45.1⁻ CD45.2⁺), BoyJ (CD45.1⁺ CD45.2⁻), and their F1-crossed hybrid C57BL/6 × BoyJ (CD45.1⁺ CD45.2⁺), we are able to quantify donor, competitor, and recipient mouse cell contributions to the engraftment state. Human donor cell engraftment (e.g., from the cord blood [CB], mobilized PB, or BM) is assessed by human cell phenotyping in sublethally irradiated immune-deficient mouse recipients (e.g., NOD *scid* gamma mice that are deficient in B cells, T cells, and natural killer cells and have defective dendritic cells and macrophages). Engraftment of cells from primary mouse recipients into secondary mice allows for an estimation of the self-renewal capacity of the original donor HSC. This chapter outlines concepts, methods, and techniques for mouse and human cell models of HSCT and for assessment of donor cells collected and processed in hypoxia versus ambient air.

Key words Hematopoietic stem cell transplantation, Engraftment, Homing, Hematopoietic stem (HSC), Hematopoietic progenitor cells (HPC)

1 Introduction

The BM provides a home and nursery for all stages of hematopoietic progenitor (HPC) and stem (HSC) cells [1, 2]. Functional colony assays to enumerate and define more mature progenitors have been described [3–12]. However, these colony assays utilize growth factors such as granulocyte-macrophage colony-stimulating factor (GM-CSF), interleukin (IL)-3, and stem cell factor (SCF)

which stimulate early and late progenitors to form quantifiable colonies in semi-solid media (methylcellulose or agar), but they do not enumerate the true stem cell. In addition, they fall short in their ability, compared to whole living animals, to regulate and control the renewal with proliferation of the true stem cell. These progenitors have a limited “self-renewal” capacity [13–15] which is essential to the long-term hematopoietic reconstitution of a host. Attempts to design in vitro culture methods, such as the “long-term initiating cell” (LT-CIC) [16] and Cobblestone Area cells [17], to enumerate this rare population of functional HSC with virtually limitless capacity for self-renew have not been very useful in defining the long-term repopulating HSC or the capacity of these cells. There are means to phenotypically identify mouse and human HSC [18, 19], but HSC phenotype does not always recapitulate the functional activities of these rare cells [20, 21]. The signals and switches required to keep these cells in a state of “stemness” while allowing them to multiply, “renew,” or differentiate are complex and poorly understood. Therefore, the only sure way to characterize and quantitate these totipotent HSCs is to allow the animal itself to control these steps in vivo. This is accomplished by transplanting mouse donor cells into recipient mice whose hematopoietic system has been obliterated or greatly reduced with a single or split dose of lethal, total body irradiation [22–27] or sublethal irradiation of immune-deficient mice for human donor cells [28–34]. After recipient mice have been conditioned, donor cells are infused, intravenously (IV). The cells of interest will then home to and engraft the bone marrow (BM) cavity and begin to proliferate.

We describe herein three types of HSC transplants: non-competitive and competitive mouse-mouse HSCT and human donor cell into immune-deficient mouse recipient xenograft HSCT. More detail will be given in each section, but common to all is the timeline summary described in Table 1. For general and competitive transplants of mouse cells, we utilize a congenic mouse model which allows analysis of and differentiation between donor, competitor, and recipient mice or mouse cells contributing to recovery and function. C57BL/6 mouse (CD45.1⁻ CD45.2⁺) BM is usually used for donor cells, and BoyJ (CD45.1⁻ CD45.2⁺) BM used for competitor cells with C57BL/6 × BoyJ F1 (CD45.1⁺ CD45.2⁺) used as recipients. (Please note that, currently, F1 mice are not available commercially. They are bred in our in-house mouse breeding facility.) But one can mix these congenic mice as donor, competitor, or recipients. The key is to be able to distinguish between the three using antibodies that recognize these congenic differences to determine contributions from donor, competitor, or recipient [22–27]. Xenograft transplants are useful in evaluating donor cells from off-strain (non-C57BL/6 background) or human HSC engraftment. We use sublethally irradiated NSG (NOD.Cg-Prkdc^{scid} Il2rg^{tm1Wjl}/SzJ) immune-compromised mice as recipients of human cell recipients [28–34].

Table 1
General transplant procedure/timeline

Time	Step/procedure	Target
-24 h	Recipient preconditioning: TBI Lethal ^a Single 950 cGy Split 700/400 cGy Sublethal ^b 300 cGy	Recipient
-1 h	Donor and/or competitor cell harvest	Donor (CD45.2 or other strains) Competitor (CD45.1) Human cells: PB, CB, BM
0	Infusion	Recipient
1, 2, 4, 6 months or later	Peripheral blood sampling	
6 months	1⁰ recipient bone marrow harvest/2⁰ transplant	2 ⁰ transplant into F1 or NSG recipients

^aLethal TBI used in congenic mouse model transplants

^bSublethal dose used for NSG/xenograft models (e.g., human donor cells)

2 General Transplant (Non-competitive)

2.1 Introduction

The need to evaluate the role of a single-gene deletion, the effects of ex vivo treatment of wild-type (WT) cells, or in vivo treatment of animals may only require a general transplant. Since the question is generally “how does my experimental group differ from my control group,” only one donor cell concentration is usually used. Additional donor concentrations can be included, but only if you think it has merit. This is discussed further in the “Notes” section. In addition, while we routinely use C57BL/6 mice as donor mice and C57BL/6 × BoyJ F1 as recipients, you could interchange any or all of these three strains for this type of transplant, as long as the donor cells are distinguishable from recipient cells. This is useful in cases of limited availability of one strain or another. Having two to three donor mice per WT and test group to create a pool of cells helps eliminate anomalies potentially present in a single mouse:

- Scenario 1: Evaluate the effects of a single-gene deletion “X” on engraftment and proliferation. This knockout is usually on a C57BL/6 background. Harvest donor BM and infuse per protocol. The control for the experiment would be WT C57BL/6 BM if the knockout is on a C57BL/6 mouse background.
- Scenario 2: Evaluate the effects of pretreatment ex vivo of WT donor cells with compound “A” on engraftment and proliferation. Harvest BM, treat ex vivo as desired, and infuse per

protocol. Depending on the treatment time and the possibility that “mock” treatment may actually cause a change, it may be necessary to include a second control; untreated/input cells (*see* “Notes”). Therefore, control(s) for this experiment would be untreated and/or mock-treated BM. Please note that in cases of *ex vivo* expansion transplantation analysis, one must have a pre-expansion group to compare to the expanded group so that one can assess output versus input of engraftment capability.

- Scenario 3: Evaluate the *in vivo* effects of compound “X” on WT donor cells on engraftment and proliferation. Inject or treat animals as desired. Harvest BM and infuse into recipient mice. Like in scenario 2, control(s) for this experiment would be BM from untreated mice and/or mock-treated mice.

2.2 Materials

2.2.1 General

1. Donor mice: usually three to six mice for one to three pools of two to three mice per test group, as many groups as you wish:
 - C57BL/6 (CD45.1⁻ CD45.2⁺) or BoyJ (CD45.1⁻ CD45.2⁺) or C57BL/6 × BoyJ F1 (CD45.1⁺ CD45.2⁺)
2. Recipient mice: minimum $n = 5$ mice per test group, usually 6–10-week-old, male or female mice:
 - C57BL/6 (CD45.1⁻ CD45.2⁺) or BoyJ (CD45.1⁻ CD45.2⁺) or C57BL/6 × BoyJ F1 (CD45.1⁺ CD45.2⁺)
 - The number of recipient mice needed is determined by the number of test groups evaluated. For example, in scenario 3, if you evaluated three concentrations of compound “A,” then you would have four groups (control, cells, e.g., treated with 2 μg, 5 μg, and 10 μg compound “A”) × five recipients per group. For this you would need 20 recipients.
3. Cesium 137 research irradiator.
4. Plexiglass pie, 12 place.
5. 70% ethanol (spray bottle).
6. Sterile surgical instruments (e.g., scissors and forceps).
7. “Buffer”; sterile 1× Dulbecco’s phosphate-buffered saline (DPBS) (DPBS) (Mg- and Ca-free) or sterile saline.
8. Sterile tubes: polyethylene (12–15 ml), snap, or screw.
9. Sterile syringes: 5 ml and 10 ml.
10. Needles: 26 gauge.
11. Centrifuge.
12. Hemacytometer/cell counter.

2.2.2 Infusion

1. Syringes: 1-ml tuberculin
2. Needles: 26 gauge
3. Mouse restraint device for tail vein injections

4. Heating device: Heat lamp or heating pad
5. Alcohol wipes

2.2.3 PB Collection and Analysis

1. 16-gauge needle or lancet
2. 70- μ l heparinized capillary tubes
3. Expulsion bulb
4. Heparin (1000 U/ml)—optional
5. 12 \times 75-mm polystyrene flow cytometry-compatible centrifuge tubes

2.2.4 Phenotype Staining Reagents

1. Red blood cell (RBC) lysis buffer: H₂O (800 ml), NH₄Cl (0.1544 M; 8.26 g), KHCO₃ (10.0 mM, 1 g), EDTA (0.1 mM, 32.7 mg), adjust pH to 7.2–7.4 with 1 N HCl. Add H₂O to 1 L. Filter-sterilize through a 0.2- μ m filter, and store at room temperature
2. Staining buffer (1 \times DPBS + 1% BSA)
3. Anti-mouse CD16/CD32 Fc blocking antibody—optional:
 - (a) When staining samples that contain cells that express Fc receptors (which can non-specifically bind the Fc component of antibodies), using Fc blocking agents will guard against false-positive staining.
4. Fluorochrome-conjugated monoclonal antibodies (anti-mouse CD45.1 and anti-mouse CD45.2):
 - (a) Optional additional antibodies can be used to determine myeloid and lymphoid cell numbers (e.g., anti-mouse CD3 [T cells], anti-mouse B220 [B cells], and anti-mouse CD11b and anti-mouse Gr-1 [myeloid cells]).
5. 1.5% paraformaldehyde—optional
6. 12 \times 75-mm tubes (polystyrene) flow cytometry compatible

2.3 Methods

- Note: All animal works should be conducted in accordance with the Institutional IACUC guidelines.

2.3.1 Obtain Recipient Mice

F1 hybrid (C57BL/6 \times BoyJ) animals should be on site no later than 14 days prior to transplant and allow them to acclimate to Laboratory Animal Resource Center (LARC) environment. At best, it is important to have all mice (donors and recipients) equilibrated in your animal room, especially those shipped from a distant place in order to reduce stress to the mice.

2.3.2 Start Recipient Prophylaxis

Seven days prior to transplant, place recipients on antibiotic feed (e.g., Uniprim, doxycycline) and treated water (e.g., acidified, Neosporin). Note: consult with your LARC veterinarian as to what is available at your site.

2.3.3 *Irradiate/
Precondition Recipient
Mice F1 Hybrid (C57BL/
6 × BoyJ)*

Eighteen to 24 h prior to infusion, mice are placed in a 12-place Plexiglass irradiation pie and a single dose of 950-cGy irradiation is administered via a cesium 137 research irradiator. (Alternatively, mice can receive a split dose of irradiation of 700/400 cGy.) Mice are then placed back in the original cages and rested until the following day.

2.3.4 *Donor BM Cell
Harvest*

1. Donor mice, for each group, are euthanized via CO₂ asphyxiation and verified via cervical dislocation.
2. The animal is then either submerged in or thoroughly wetted with 70% ethanol.
3. Using dissecting scissors and forceps, frequently dipped in 70% alcohol, excise one or two femurs by stripping fur and large muscles from the bone. Snip through the knee tendon and hip socket, releasing the femur.
4. While being careful to remove as little bone as possible, remove the distal and proximal ends of the femur (*see* Fig. 1).
5. Flush the marrow from the femur into a 12–15-ml sterile tube by gently inserting a 26-gauge needle attached to a 10-ml syringe containing 5-ml sterile DPBS buffer. As you gently flush, move the needle up and down inside the marrow cavity.
6. Repeat for the second femur.
7. Break up any marrow clumps with a 10-ml pipet or syringe with 18-gauge needle attached. Take care not to be too vigorous as this could lyse cells.
8. Repeat **steps 3–7** for each additional mouse for each group.
9. Wash cells by centrifugation at $400 \times g$ for 10 min at room temperature.
10. Resuspend each cell pellet in 5-ml DPBS using a 5-ml pipet.
11. Perform cell count manually or by mechanical cell counter, and keep at room temperature.

2.3.5 *Prepare Infusion
Dilutions*

We recommend infusing between 100–200 μ l per IV injection;

1. Based on the number of recipient mice used per group and number of cells infused (2×10^5 ; *see* “Notes”), dilute donor cells in sterile DPBS (or as mentioned previously sterile saline) to give the desired dose per injected volume. Always make extra (e.g., five recipients at 2×10^5 cells/0.2 ml/mouse; make 1.5 ml at 1×10^6 cells/ml).
2. Infuse within 1 h of preparing.

2.3.6 *Infusion*

Tail vein injections are the most difficult to master. Extensive practice before the actual transplant is essential. It is extremely difficult to hit these small, fragile veins and infuse any material without vasodilating the tail. Heat is the best, non-pharmaceutical

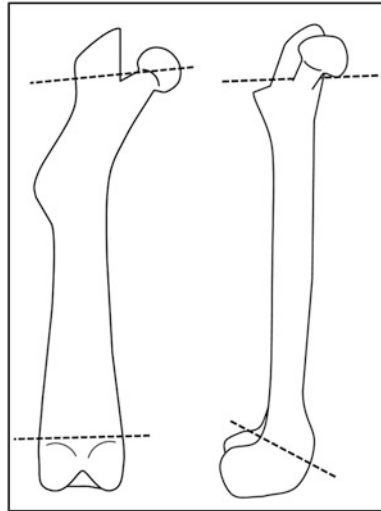


Fig. 1 Basic structure of the mouse femur and targeted cut lines to open marrow cavity and maximize bone marrow harvest

way to achieve this. However, it is best if possible to use heat as other agents may have unknown effects on the recipient mice. Depending on the scale, you can use a heat lamp directed at the cage or place the cage on a heating pad. Take care not to overheat the animals. See “Notes” for extended discussion on injection technique:

1. Clean the mouse restraint with 70% ethanol and dry thoroughly.
2. Draw 0.2–1.0 ml (*see* “Notes”) into a 1-ml tuberculin syringe fitted with 26-gauge needle.
3. Tap out bubbles to void embolisms.
4. Place mouse in restraint.
5. Gently clean the mouse tail with alcohol prep.
6. Hold the tail approximately 2/3 way down the tail between your thumb and middle finger.
7. Gently curve the tail over your second (pointer) finger (*see* Fig. 2a), and roll to the side to visualize one of the lateral veins (*see* Fig. 2b).
8. With bevel up, introduce the point into the tail vein with only a slight angle (almost parallel to the tail), and insert 3–5 mm or just passed the bevel (*see* Fig. 3).
9. Slowly infuse cells. About 200 μ l should take 2–3 s.
10. Withdraw the needle and apply pressure to the wound.

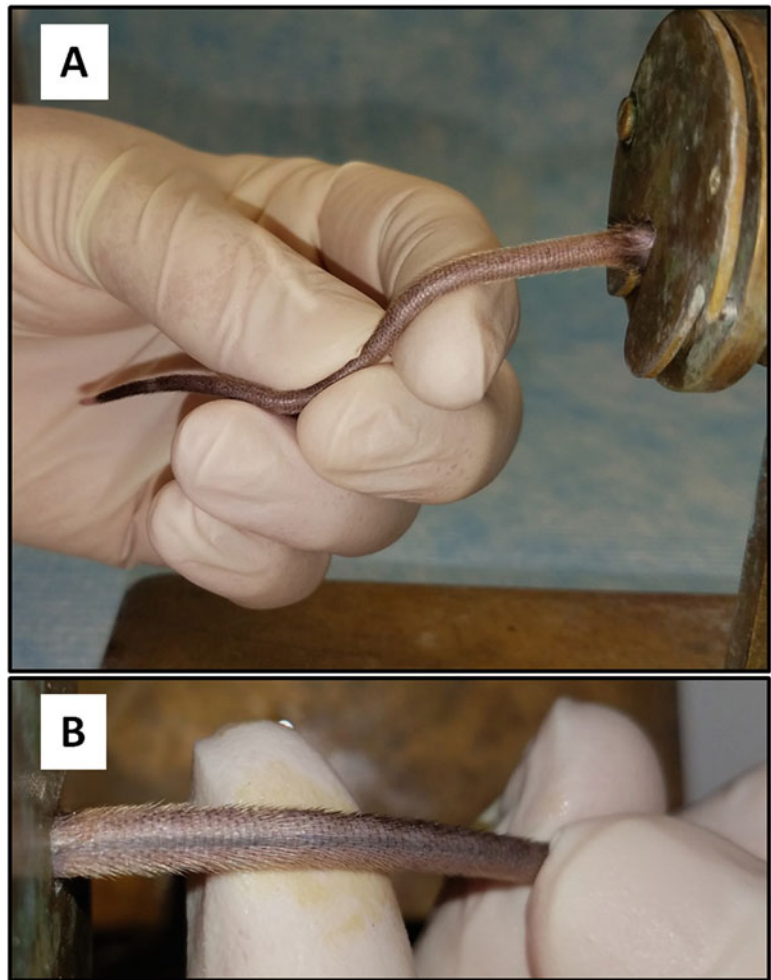


Fig. 2 (a) Show the correct position to hold the tail for injection; slightly bent over the pointer finger. (b) Roll the tail to either side to visualize the lateral veins

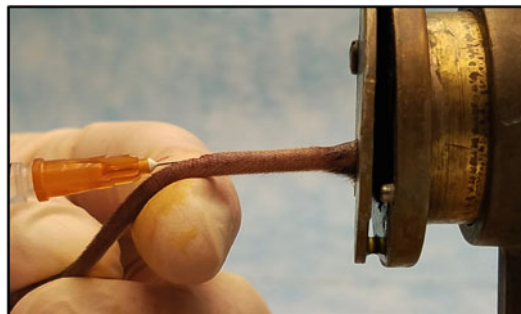


Fig. 3 The needle should be introduced, bevel up, almost parallel to the tail, and inserted just past the bevel

11. Either mark the tail (a marker may be used for this task) or place the mouse back in the cage (to distinguish from the un-injected mice), or place mouse in a new cage.
12. Once all mice are infused, return them to the animal facility.

2.3.7 Post-transplant PB Collection

Assessment of engraftment and functional proliferation is evaluated at 1, 2, 4, and 6 months or later with the last month time point terminating the experiment and possibly proceeding to a secondary transplant. About 30–50 μl of PB is collected from the submandibular facial vein of the mouse and processed for flow cytometry analysis. Approved bleeding technique may vary from institution to institution, and approved IACUC protocols should be followed. This procedure can be done by one person, but we find it to be easier and much faster with two persons, as person 1 can handle the mouse, while person 2 collects and manipulates the sample:

1. Grab the mouse securely by the scruff of the neck using a standard grip.
2. Introduce the point of a 16-gauge needle (or lancet) at the rear of the jaw and into the muscle.
3. Dip the tip of a capillary tube into heparin, resulting in 2–5 μl being drawn into the capillary.
4. Use the capillary tube to collect blood.
5. Place the capillary into the marked tube and expel blood with the bulb.
6. Release the mouse, and with a marker, mark the mouse's tail and return it to the cage.
7. Repeat for all test subjects.

2.3.8 Staining for Flow Cytometry Analysis

1. Add 1 ml of lysis buffer to each tube, vortex gently, then quickly add a second ml of lysis buffer to each tube.
2. Vortex gently and incubate for 5 min at room temperature. Quench reaction by adding 1 ml of staining buffer.
3. Centrifuge at $500 \times g$ for 5 min. Remove the supernatant.
4. Add 2–3 ml of wash buffer, and centrifuge at $500 \times g$ for 5 min. Remove the supernatant. Repeat.
5. Add an appropriate volume of Fc blocking reagents (use according to the manufacturer's instructions).
6. Add 2–3 ml of wash buffer, and centrifuge at $500 \times g$ for 5 min. Remove the supernatant. Repeat.
7. Add an appropriate volume of fluorochrome-conjugated monoclonal antibody (based on antibody manufacturer's recommendation or from titration results) to the cell pellet in a 12×75 -mm tube.

8. Vortex gently and incubate for 15 min in the dark at room temperature (20 °C to 25 °C).
 - (a) Can be done at 4 °C, but incubate for 20–30 min instead.
9. Add 2–3 ml of wash buffer, and centrifuge at $500 \times g$ for 5 min. Remove the supernatant. Repeat.
10. Two options for flow cytometry analysis: immediate or delayed analysis:
 - (a) Option 1: Resuspend cells in 500- μ l staining buffer, mixing thoroughly to avoid clumping. Perform flow cytometry analysis immediately (keeping cells in the refrigerator and in the dark until analysis is performed). If this is the option taken, cells must be analyzed within a few hours.
 - (b) Option 2: Resuspend cells in 1 ml of 1.5% paraformaldehyde, mixing thoroughly to avoid clumping. Incubate for 20–30 min at 4 °C keeping samples in the dark. Add 2–3 ml of wash buffer, and centrifuge at $500 \times g$ for 5 min. Remove the supernatant. Repeat. Perform flow cytometry analysis within 1–2 days.

2.3.9 Analysis by Flow Cytometry

Figure 4 shows illustrated analysis results for donor cell engraftment by flow cytometry. We recommend collecting 100,000 events at slow to medium collection speed. Percent engraftment is determined by gating on the population of donor cells in the PB at the indicated time points as determined by CD45 marker. For example, if C57BL/6 mice (CD45.1⁻ CD45.2⁺) are used as donor cells and C57BL/6 \times BoyJ F1 (CD45.1⁺ CD45.2⁺) are used as recipient mice, then percent engraftment would be determined by examining the percent CD45.1⁻ CD45.2⁺ cells that are present within the sample. One can also examine host recovery by examining the percent CD45.1⁺ CD45.2⁺ population that would have come from recovery of irradiated recipient C57BL/6 \times BoyJ F1 BM cells. Staining and flow analysis of these cells would be the same as with PB, but RBC lysis is an optional step. One can also stain for specific HSC and HPC cell numbers as reported [18, 19].

2.4 Notes

1. Mouse strain selection: These congenic mouse strains provide invaluable tools to evaluate each player's contribution to hematopoietic reconstitution. There is little evidence that the minor epitopic congenic disparity between CD45.1 and CD45.2 causes T cell recognition and, thus, may not apparently alter their function. Therefore, for all intents and purposes (unless future studies determine otherwise), they are all functionally identical and should behave as such. Because of this, one can use any one of the three strains as donor or recipient (or competitor, next section). This is useful when availability of one or another is limited. However, if, for example, C57BL/

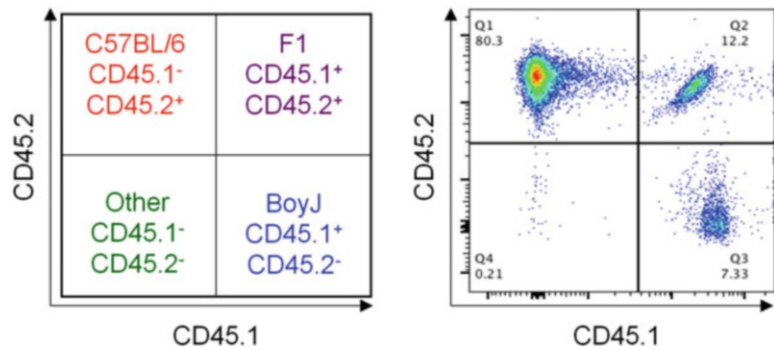


Fig. 4 Representative flow analysis for examining engraftment of C57BL/6 (CD45.2⁺) and BoyJ (CD45.1⁺) mouse bone marrow into lethally irradiated F1 hybrid (CD45.2⁺ /45.1⁺; C57BL/6 x BoyJ) recipient mice. The percentage of donor cells was determined by being single positive for the marker CD45.2 in the peripheral blood and/or bone marrow

6 mice are chosen to be used for donor cells, one should not compare to any experiments where Boy/J mice were used as donors.

2. Controls: This is simply a cautionary note that in some cases, ex vivo treatment may last for hours or days (e.g., during HSC expansion assays). This time delay alone may change your control-/mock-treated cells. In these cases, additional controls might be needed. This would be time 0, freshly isolated input BM, or human CB cells (*see* Subheading “Xenograft Transplant”). In order to use the same population of cells, this will require two transplant times: one on the day of harvest for the untreated cells and the second after the treatment.
3. Cell harvest/dilutions: Since it has been shown that CXCR4 is a major player in homing of stem cells [35] and exposure to lower temperatures may downregulate CXCR4 expression on donor cells [36], it is important to keep cells at room temperature to optimize homing. This creates a potential problem in that cells remain more biologically active at higher temperatures and may actually start to differentiate and mature. Therefore, the quicker you can go from harvest to infusion, the better chance of retaining a more accurate HSC picture of the donor BM cells.

When creating pools, it is good practice to combine an equal number, not volume, from each sample. Two femurs should yield $30\text{--}50 \times 10^6$ nucleated cells. So, two femurs resuspended in 5-ml buffer will allow sufficient dilution in this step. For example, if the cell volume for three donor mice is 8×10^6 cells/ml, 9×10^6 cells/ml, and 11×10^6 cells/ml, respectively, and the infusion cell concentration needs to be 1×10^6 c/ml (100,000 cells/0.2 ml), then you would want to

pool five to ten times more concentrated than that, $5\text{--}10 \times 10^6$ cells/ml. Therefore, take 5×10^6 cells from each mouse (15×10^6 cells total) in a final volume of 3.0 ml:

1. at 8×10^6 cells/ml, $5 \times 10^6 = 0.625$ ml
2. at 9×10^6 cells/ml, $5 \times 10^6 = 0.556$ ml
3. at 11×10^6 cells/ml, $5 \times 10^6 = 0.454$ ml

Adjust the final volume with buffer (3 ml total–1.635 ml cell mixture), and add 1.365-ml buffer.

Then when creating your infusion dilution(s), you use this pool knowing that you have equal representation from all mice in the pool.

4. Injections: Other than ensuring proper staining and analyzing techniques for flow cytometry analysis of engraftment, tail vein injections present the biggest obstacles to overcome for variation in engraftment. There are several things that can go wrong. For some unexplained reason, an injection can start perfectly, and then half way through the administration of the dose, the vein “shuts down” and you cannot get any more fluid to go in. At that point, you need to remove the needle, stop the bleeding, position the tail to the opposite side, and try to infuse the remaining dose in the contralateral vein. If this is unsuccessful, sometimes it is best to put that animal aside and not include them in that group as it will skew the results for that group. In our experience, the biggest misunderstanding by beginners is how very shallow these lateral tail veins are. Those who are inexperienced tend to angle too steeply and puncture right through the vein. Once the point of the needle breaks the skin and enters the vein, the needle should run almost parallel to the tail (*see* Fig. 3). One does not need to introduce the entire needle into the vein. Just insert it so the entire bevel is intravascular. The injection should be started as far down the tail, toward the tip, as possible. This allows for a “miss” yet gives another chance for injection more proximal to the base of the tail. If you start too high and miss, moving toward the tip will cause any dose to exit the tail in the previously made puncture.
5. PB harvest: You will need to consult your local Laboratory Animal Resource Center (LARC) for training. As mentioned in the “Methods” Subheading, this can be accomplished by one person, but it is more efficient and quicker with a helper. As one person handles the mouse, the other handles the capillary and collection tube. There are several products on the market for small-volume blood collection. But they require transferring of the sample to a flow-compatible tube for analysis. Therefore, we prefer to collect directly into the tube used for staining and analysis. While the collection person prepares the

next tube, the animal person can ready the next animal. Even though we use pre-heparinized capillaries, we like to add a little extra heparin to prevent clotting. Once the blood is collected, we attach to an expulsion bulb (Fisher, 22-170-406) and blow into the tube. Sometimes you may get a lot of bleeding from the puncture wound. This bleeding always stops when you release your grip of the mouse. If it does not, a small amount of “QuickStop” can be dabbed on the site.

6. Staining and flow cytometry analysis: Prior to RBC lysis, be careful when removing supernatant from flow tubes as blood does not form a tight cell pellet. For more accurate comparison between mice, staining equal volumes of blood is key (e.g., 20 μ l of blood for each flow tube). This will ensure equal concentration of antibodies for each tube. In addition, making a cocktail of the antibodies used for staining will minimize human error in distributing small volumes of antibody per tube. Finally, as one is comparing samples from month to month, following a standardized protocol step by step to ensure the procedure remains unchanged will allow for more accurate comparison between time points. For example, if for month 1 the PB was stained with antibodies for 15 min at room temperature, then do the same for month 2. Finally, pick fluorochromes that will not need much, if any, compensation and include the proper flow cytometry controls. Proper controls for flow include single-color controls, isotype controls, and unstained controls. This will allow one to compensate any overlap that may be occurring, to recognize any background staining, and to properly gate on single- and double-positive populations.

3 Competitive Transplant

3.1 Introduction

Competitive transplants are useful in determining if one population of cells has an advantage to home, engraft, proliferate, and self-renew over a competing population of cells and can be assessed by limiting dilution analysis of donor cells to calculate the competitive repopulating units (CRUs), a measure of the numbers of HSC [37]. The best way to determine this advantage is to put them in a head-to-head competition with competitor cells. Typically, we use C57BL/6 (CD45.1⁻ CD45.2⁺) as the donor population and BoyJ (CD45.1⁺ CD45.2⁻) as the competitor population. These are both co-transplanted into C57BL/6 \times BoyJ F1 recipients (CD45.1⁺ CD45.2⁺). However, in this model we transplant three diminishing doses of donor cells (e.g., 1×10^5 , 5×10^4 , and 2.5×10^4 cells/mouse) while maintaining competitor cells at the highest dose (1×10^5). If using more purified populations of donor cells (e.g.,

lineage-depleted or lineage-purified HSC/HPC cells), then one would start with much fewer cells and do dilution from this. The competitor cells can still be unseparated, and these numbers can remain the same as stated above. The resulting outcome will be a chimerism of the donor and competitor cells with the addition of any lingering host cell recovery. If the donor cells do have an advantage due to genetic modification or ex vivo/in vivo treatment, you hope to see the chimerism skew toward the donor phenotype (CD45.1⁻ CD45.2⁺):

- Scenario 1: Determine whether there is a selective advantage of a single-gene deletion “X” over WT cells in transplantation. The knockout (KO) and control mice must be on a C57BL/6 background. One would harvest donor BM (WT and KO, both on C57BL/6) and competitor (BoyJ) BM and infuse simultaneously per protocol. Control for this experiment would be WT C57BL/6 BM donor cells.
- Scenario 2: Determine whether ex vivo treatment of donor BM cells with compound “A” (at 1 µg/ml and 10 µg/ml) produces a selective advantage over non-treated donor cells in transplantation. Harvest donor (C57BL/6) BM and competitor (BoyJ) BM. Treat donor cells with and without compound A. Infuse simultaneously with competitor cells per protocol. Control (s) for this experiment would be WT C57BL/6 treated with control diluent and/or untreated WT C57BL/6 cells. See “Notes” for scenario 2 under “General Transplant” for information on input versus output groups for ex vivo expansion assays.
- Scenario 3: Evaluate the in vivo effects of compound “X” on donor cells to determine their selective advantage or disadvantage in transplantation. Inject three to five C57BL/6 mice per group with control diluent or test material as desired. Harvest donor (C57BL/6) BM and competitor (BoyJ) BM. Infuse simultaneously with competitor cells per protocol. Control (s) for this experiment would be BM from WT C57BL/6 injected with control diluent and/or BM from untreated C57BL/6 mice.

3.2 Materials

3.2.1 General

1. Donor mice: usually three to five mice per test group, as many groups as you wish:
 - C57BL/6 (CD45.1⁻ CD45.2⁺)
2. Competitor mice: $n = 2$ mice (BM will be pooled):
 - BoyJ (CD45.1⁺ CD45.2⁻)
3. Recipient mice: minimum $n = 5$ mice per test group:

- C57BL/6 × BoyJ F1 (CD45.1⁺ CD45.2⁺):
 - (a) F1 hybrids are used as recipients for consistency. The number needed depends on the number of test groups or desired number of recipients per group. Unlike in the general transplant, each test group will be transplanted at three different donor concentrations (1×10^5 , 5×10^4 , and 2.5×10^4 unseparated cells/mouse; when using more purified donor cell population, use fewer cells per mouse). Therefore, an “n” of at least five mice per group will be required for each dose.
 - (b) For example, in scenario 1 we have two groups, WT and KO, each recipient group infused at a donor cell dose of 1×10^5 , 5×10^4 , and 2.5×10^4 along with 1×10^5 donor cells/mouse. Therefore scenario 1 would require 30 recipients. In scenario 2, there are three groups: C57BL/6 BM treated with control diluent and compound “A” at 1 μg and 10 μg. Therefore, three groups at three cell concentrations would require 45 recipient mice.

4. Cesium 137 research irradiator.
5. Plexiglass pie, 12 place (Braintree, #MPC1).
6. 70% ethanol (spray bottle).
7. Sterile surgical instruments (scissors and forceps).
8. Sterile saline or DPBS (“buffer”).
9. Sterile tubes: polyethylene (12–15 ml), snap, or screw.
10. Sterile syringes: 5 ml and 10 ml.
11. Needles: 26 gauge.
12. Centrifuge.
13. Hemacytometer/cell counter.

3.2.2 *Infusion*

1. Syringes: 1-ml tuberculin
2. Needles: 26 gauge
3. Mouse restraint device for tail vein injections
4. Heating device: heat lamp or heating pad
5. Alcohol wipes

3.2.3 *PB Collection and Analysis*

1. 16-gauge needle or lancet
2. 70-μl heparinized capillary tubes (Fisher, 02-678)
3. Expulsion bulb (Fisher, 22-170-406)
4. Heparin (1000 U/ml)—optional
5. 12 × 75-mm polystyrene flow-compatible centrifuge tubes

3.2.4 Phenotype Staining Reagents

1. Red blood cell (RBC) lysis buffer: H₂O (800 ml), NH₄Cl (0.1544 M; 8.26 g), KHCO₃ (10.0 mM, 1 g), EDTA (0.1 mM, 32.7 mg), adjust pH to 7.2–7.4 with 1 N HCl. Add H₂O to 1 L. Filter-sterilize through a 0.2- μ m filter, and store at room temperature.
2. Staining buffer (1 \times DPBS + 1% BSA).
3. Anti-mouse CD16/CD32 Fc blocking antibody:
 - When staining samples that contain cells that express Fc receptors (which can non-specifically bind the Fc component of antibodies), using Fc blocking agents will guard against false-positive staining.
4. Fluorochrome-conjugated monoclonal antibodies (anti-mouse CD45.1 and anti-mouse CD45.2):
 - Optional additional antibodies can be used to determine myeloid and lymphoid cell numbers (e.g., anti-mouse CD3 [T cells], anti-mouse B220 [B cells], and anti-mouse CD11b and anti-mouse Gr-1 [myeloid cells]).
5. 1.5% paraformaldehyde—optional.
6. 12 \times 75-mm tubes (polystyrene).

3.3 Methods

- Note: All animal works should be conducted in accordance with the Institutional IACUC guidelines.

3.3.1 Obtain Recipient Mice

F1 hybrid (C57BL/6 \times BoyJ) animals should be on site no later than 14 days prior to transplant and allow them to acclimate to Laboratory Animal Resource Center (LARC) environment.

3.3.2 Start Recipient Prophylaxis

Seven days prior to transplant, place recipients on antibiotic feed (e.g., Uniprim, doxy) and treated water (e.g., acidified, Neosporin). Note: Consult with your LARC veterinarian as to what is available at your site.

3.3.3 Irradiate/Precondition Recipient Mice F1 Hybrid (C57BL/6 \times BoyJ)

Eighteen to 24 h prior to infusion, mice are placed in a 12-place Plexiglass irradiation pie, and a single dose of 950-cGy irradiation is administered via a cesium 137 research irradiator. (Alternatively, mice can receive a split dose of irradiation of 700/400 cGy.) Mice are then placed back in the original cages and rested until the following day.

3.3.4 Donor BM Cell Harvest

Steps are identical to general harvest.

3.3.5 Prepare Infusion Dilutions

We recommend infusing between 100–200 μ l per IV injection. Based on the number of recipient mice used per group at 0.2-ml fluid injected per mouse, calculate the volume desired,

remembering to always make extra (e.g., five recipients at 0.2 ml/mouse require 1 ml; therefore calculate for 1.5 ml):

1. Donor cells: Make three dilutions/tubes per test point:
 - Tube 1: 1.5 ml at 10×10^4 cells/0.2 ml/mouse = 7.5×10^5 cells
 - Tube 2: 1.5 ml at 5×10^4 cells/0.2 ml/mouse = 3.75×10^5 cells
 - Tube 3: 1.5 ml at 2.5×10^4 cells/0.2 ml/mouse = 1.875×10^5 cells
2. Competitor cells: Add to every tube of donor cells competitor cells to give the final cell concentration of 10×10^4 cells/0.2 ml/mouse:
 - Tube 1: 1.5 ml at 10×10^4 cells/0.2 ml/mouse = 7.5×10^5 cells
 - Tube 2: 1.5 ml at 10×10^4 cells/0.2 ml/mouse = 7.5×10^5 cells
 - Tube 3: 1.5 ml at 10×10^4 cells/0.2 ml/mouse = 7.5×10^5 cells
3. QS each tube to 1.5 ml with DPBS. Bringing the final concentrations and volumes to:
 - Tube 1: donor (10×10^4 cells) + competitor (10×10^4 cells) per 0.2 ml
 - Tube 2: donor (5×10^4 cells) + competitor (10×10^4 cells) per 0.2 ml
 - Tube 3: donor (2.5×10^4 cells) + competitor (10×10^4 cells) per 0.2 ml
4. Infuse within 1 h of preparing.

3.3.6 Infusion

Follow procedures outlined in “General Transplant.”

3.3.7 Post-transplant PB Collection

Follow procedures outlined in “General Transplant.”

3.3.8 Staining and Flow Cytometry Analysis

Follow procedures outlined in “General Transplant.”

3.4 Notes

1. Mouse strain selection: As in the previous Subheading (“General Transplant”), these congenic mouse strains provide invaluable tools to evaluate each player’s contribution to hematopoietic reconstitution. It must be noted again that since these experiments require two to four iterations, it is best to keep the iterations the same. For example, do not evaluate a C57BL/6 KO mouse with BoyJ competitors into

F1 recipients, and then repeat using BoyJ mice as recipients and F1s as competitors; keep it consistent.

2. Cell harvest/dilutions: Same as in the previous Subheading, “General Transplants.” The ability to pool your donor and competitor cells and then adjust to the final volume (QS) with the understanding that your stock pools are at least five to ten times more concentrated than your final desired infusion concentrations. It is suggested that you make your dilutions/mixes as close to infusion time as possible. This will also help ensure less clumping of cells.

As mentioned in the previous section’s notes, pooling before making infusion dilutions is important. The reason is that it helps minimize errors associated with devices and users. For example, one might ask since donor cells are used at three different concentrations in this assay, why not save a step and “pool” the appropriate number of cells from each mouse into each dilution (s), add your competitors (**step 2**), and QS as described (**step 3**). Every time one measures and dispenses a volume, there are errors associated with it. At least if one uses a pool of cells, those errors will represent each mouse equally rather than individually. This may not be of any real relevance, but transplants can yield “gray” results occasionally, and it is important to eliminate as many variables as possible.

In addition, for this transplant, one will have a pool of competitor cells as well. Therefore, if using scenario 1 from above, one wants to evaluate the influence of gene “X” KO BM in a competitive transplant compared to C57BL/6 WT. The infusion dilutions would be as noted in Table 2. Please note that these cell concentrations are for unseparated cells. When using more purified cell populations (e.g., lineage negative, LSK, or purified HSC), you need to lower donor cell numbers per injection.

3. Collection and processing of donor cells under hypoxia to enhance the number of detectable HSCs: In addition to cell enrichment or ex vivo treatment having an effect on the number of cells used for infusion, environmental effects can play a role as well. We have shown that harvesting BM under hypoxic conditions (3% O₂) versus atmospheric O₂ concentrations (~21%) with any and all subsequent enrichment steps being carried out in hypoxia as well significantly preserves the number of HSCs present at the time of harvest [11, 38]. Therefore, fewer hypoxia-harvested BM cells may be needed for engraftment.

Occasionally, one may not be able to combine donors with competitors if exposure to competitor cells may alter the donor cells (i.e. hypoxia collected donor cells). In these cases, these experiments will require an additional round of injections. For

Table 2
Example infusion dilutions

Recipient group	Point	Volume needed	Donor at 5×10^6 cells/ml	Comp pool at 5×10^6 cells/ml	QS volume (ml)
1	WT: control at 100,000 cells/mouse/0.2 ml	1.5 ml	150 μ l	150 μ l	1.200 ml
2	WT: control at 50,000 cells/mouse/0.2 ml	“	75 μ l	150 μ l	1.275 ml
3	WT: control at 25,000 cells/mouse/0.2 ml	“	37.5 μ l	150 μ l	1.3125 ml
4	KO at 100,000 cells/mouse/0.2 ml	“	150 μ l	150 μ l	1.200 ml
5	KO at 50,000 cells/mouse/0.2 ml	“	75 μ l	150 μ l	1.275 ml
6	KO at 25,000 cells/mouse/0.2 ml	“	37.5 μ l	150 μ l	1.3125 ml

example, our lab has previously studied the effects of hypoxia on HSC-repopulating capacity. As mentioned above, we know that exposure of mouse BM or human cord blood to ambient air O_2 concentrations for as little as 15 min can alter HSC numbers collected (*see* Fig. 5). Therefore, for these experiments, hypoxia test group(s) donor BM cells were harvested, processed, and injected into recipient mice in a hypoxia chamber [11]. Combining these donor cells with competitor cells harvested in air (normoxia) would change them. So the hypoxia test groups require donor cell injections and competitor cell injections to be separated. To eliminate those unnecessary variables mentioned early, the air control groups (air) should be injected in two rounds as well. So in these cases, separate infusion dilutions are required.

4. Injections: The injection notes for competitive transplants are the same as the general transplant. However, if you design an experiment requiring separate donor/competitor injection, it is highly recommended to space the heating process 30–60 min apart. Let the mice recover a bit before reheating for the second round. Doing these two injections at the same time has been met with little success.
5. PB harvest: Notes are the same as for the general transplant.

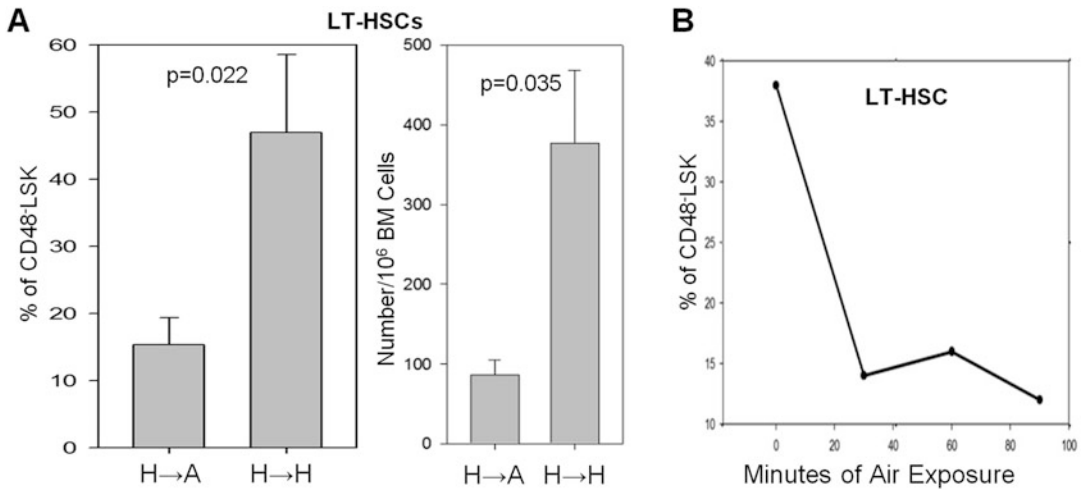


Fig. 5 (a) Data shows that LT-HSCs are drastically reduced/changed when BM is harvested under hypoxic (3% O₂) conditions and then moved to normoxia (21% O₂). **(b)** Shows that the LT-HSC phenotype is lost rapidly when exposed to air (Cell. 161:1553–1565)

6. Staining and flow cytometry analysis: Notes are the same as for the general transplant.
7. Additional analysis from using multiple-donor doses: By performing competitive transplants using multiple doses of donor cells, one may be able to analyze their data by performing a limiting dilution analysis (LDA). LDA allows one to quantify the number of human and mouse HSCs with the capacity to produce mature cells of all hematopoietic lineages in vivo, by estimating the number of competitive repopulating unit (CRU, mouse) and SCID repopulating cell (SRC, human) assays [30–34, 39–41]. There are multiple different software applications available that will assist one in analyzing the results of the LDA. For each experiment, values corresponding to dose of cells injected, total number of positive engraftments obtained per dose (determined by a set percent engraftment in the PB or BM at the indicated time point), and total number of mice per group are entered. From these data, the frequency of HSC within a given donor cell population capable of functionally engrafting is estimated [30–34, 39–41].

4 Xenograft Transplant

4.1 Introduction

Xenograft transplants are used to assess human cell engraftment into immune-deficient recipient mice. This is essentially the only way at present of evaluating the number, activity, and self-renewal capabilities of functional HSC populations from human-mobilized

PB, CB, or BM. Due to deficiencies in B cell, T cell, and natural killer cell numbers and defective dendritic cells and macrophages, the NSG (NOD.Cg-Prkdc^{scid}Il2rg^{tm1Wjl}/SzJ) mouse strain is ideal for serving as a living incubator for these evaluations, although there are also other more advanced immune-deficient mice available commercially that may be appropriate for other human cell engraftment studies. While whole-enriched populations of human cells can be used (e.g., low-density [LD] mobilized PB, LD, CB, or BM), more refined populations are best suited for human studies (e.g., CD34⁺ cells, lineage-depleted LD cells). Due to the fragile nature of these mice, only 300 cGy is used to open space in the BM for potential engraftment. Great care must be taken during conditioning and infusion and all other husbandry practices due to their compromised immune state. Importantly, as with the other transplants, prophylactic antibiotic food and treated water are recommended:

- Scenario 1: To evaluate the effects on engraftment and self-renewal capacity of human (H) CB CD34⁺ cells after 1-h ex vivo treatment with 2 µg, 5 µg, and 10 µg of compound “W.” For this experiment control donor cells would be untreated or “mock”-treated CB CD34⁺ cells.
- Note: When unenriched human cells are used, it can cause graft-versus-host disease (GvHD). Therefore we usually use CD34⁺ cells for these engraftment procedures, thus allowing recipient NSG mice to live longer for analysis of long-term engrafting potential of human HSC.

4.2 Materials

4.2.1 General

1. Donor cells: $n = 1$ since it is not necessarily advisable to combine human samples due to histocompatibility issues, only one human sample can be used per experiment. However, you can have as many groups as you wish:
 - For scenario 1 this would be human CB CD34⁺ treated with control medium or, for example, 2-µg, 5-µg, and 10-µg compound “W” and/or untreated cells.
2. Recipient mice: Minimum $n = 5$ mice per test group, usually 6–10-week-old male or female NSG mice:
 - As before, the number of recipient mice needed is determined by the number of test groups evaluated. For example, in scenario 1, we are evaluating four to five groups. Therefore, 20–25 recipient mice are required.
3. Cesium 137 research irradiator.
4. Plexiglass pie, 12 place (Braintree, #MPC1).
5. 70% Ethanol (spray bottle).
6. Sterile saline or DPBS (“buffer”).
7. Sterile tubes: polyethylene (12–15 ml), snap, or screw.

8. Sterile syringes: 5 ml and 10 ml.
9. Needles: 26 gauge.
10. Centrifuge.
11. Hemacytometer/cell counter.

4.2.2 Infusion

1. Syringes: 1-ml tuberculin
2. Needles: 26 gauge
3. Mouse restraint device for tail vein injections
4. Heating device: Heat lamp or heating pad
5. Alcohol wipes

4.2.3 PB Collection and Analysis

1. 16-gauge needle or lancet
2. 70- μ l heparinized capillary tubes (Fisher, 02-678)
3. Expulsion bulb (Fisher, 22-170-406)
4. Heparin (1000 U/ml)—optional
5. 12 \times 75-mm polystyrene flow-compatible centrifuge tubes

4.2.4 Phenotype Staining Reagents/Materials

1. Red blood cell (RBC) lysis buffer: H₂O (800 ml), NH₄Cl (0.1544 M; 8.26 g), KHCO₃ (10.0 mM, 1 g), EDTA (0.1 mM, 32.7 mg), adjust pH to 7.2–7.4 with 1 N HCl. Add H₂O to 1 L. Filter sterilize through a 0.2- μ m filter, and store at room temperature.
2. Staining buffer (1 \times DPBS + 1% BSA).
3. Anti-mouse CD16/CD32 Fc blocking antibody and anti-human Fc blocking antibody:
 - When staining samples that contain cells that express Fc receptors (which can non-specifically bind the Fc component of antibodies), using Fc blocking agents will guard against false-positive staining.
4. Fluorochrome-conjugated monoclonal antibodies (anti-human CD45 with the addition of the optional antibody anti-mouse CD45):
 - Optional additional antibodies can be used to determine myeloid (anti-human CD33) and lymphoid cell (anti-human CD3 for T cells and anti-human CD19 for B cell) numbers.
5. 1.5% paraformaldehyde—optional.
6. 12 \times 75-mm tubes (polystyrene) flow compatible.

4.3 Methods

- Note: All animal works should be conducted in accordance with the Institutional IACUC guidelines. Since primary human cells are being used, the Institutional Biosafety guidelines must be followed as well.

- 4.3.1 Obtain Recipient Mice** NSG animals should be on site no later than 14 days prior to transplant and allow them to acclimate to Laboratory Animal Resource Center (LARC) environment.
- 4.3.2 Start Recipient Prophylaxis** Seven days prior to transplant, place recipients on antibiotic feed (e.g., Uniprim, doxy) and treated water (e.g., acidified, Neosporin). Note: consult with your LARC veterinarian as to what is available at your site.
- 4.3.3 Irradiate/Precondition Recipient Mice NSG** Eighteen to 24 h prior to infusion, mice are placed in a 12-place Plexiglass irradiation pie, and a single dose of 300-cGy irradiation is administered via a cesium 137 research irradiator. Mice are then placed back in the original cages and rested until the following day.
- 4.3.4 Donor Cell Preparation**
1. Obtain human BM, CB, or other materials serving as source for human HSC.
 2. Perform isolations and enrichments as desired.
 3. Do final cell count.
- 4.3.5 Prepare Infusion Dilutions** We recommend infusing 100–200 μ l per IV injection.
- In general, xenograft transplants are not used to evaluate the competitiveness of donor cells. The question is simpler than that; do the human donor cells engraft. So usually, one high concentration is used to ensure that some cells engraft. However, multiple dilutions can be done if one desires to perform LDA to determine SCID repopulating cell (SRC) numbers, a way to estimate a number of functional human HSCs, as described in the notes for the “Competitive Transplant” Subheading.
1. If using lineage-depleted LD cells (CB, BM, PB), 1×10^3 – 100×10^3 cells/mouse/0.2 ml should be sufficient for engraftment.
 2. If using CD34⁺ cells, theoretically, you could get engraftment with 10–100 cells. Depending on how many you end up with after enrichment (<1% starting population), you may need to evenly divide your final product and use them all. Usually, 5×10^3 – 50×10^3 cells are possible and sufficient.
- 4.3.6 Infusion** Notes are the same as for the general transplant. In addition, disinfect or change gloves between cages, and follow procedures described in the previous sections. Careful handling of mice reduces the risk of infection in these severely immunocompromised mice.
- 4.3.7 Post-transplant PB Collection** Because the mice are hyper-sensitive to stress, extra care should be taken to eliminate any environmental or biological cross-contamination between cages by changing gloves or disinfecting gloves between recipient cages. Otherwise, sampling of recipient blood is performed as describe in the previous sections.

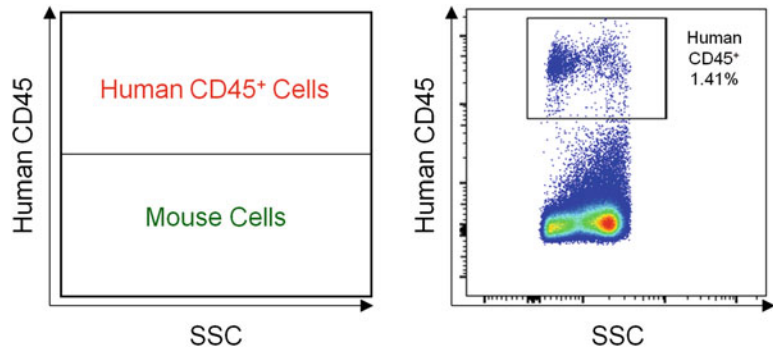


Fig. 6 Representative flow analysis for examining human CD34⁺ cell engraftment into sublethally irradiated NSG mice. Percent engraftment in the peripheral blood and/or bone marrow is determined by the percentage of human CD45⁺ cells

4.3.8 Staining for Flow Cytometry Analysis

Staining for flow cytometry analysis is similar to that of the other transplants described. However, instead of using antibodies against mouse CD45.1 and CD45.2, one should use fluorochrome-conjugated anti-human CD45. In addition, it is recommended that if an Fc blocking step is performed, those human and mouse Fc blocking agents are utilized.

4.3.9 Analysis by Flow Cytometry

Figure 6 shows illustrated analysis results for donor human cell engraftment by flow cytometry. We recommend collecting 500,000 events at slow to medium speed collection speed as human cell engraftment occurs in small percentages. Percent engraftment is determined by gating on the population of donor human cells in the PB at the indicated time points as determined by the human CD45 marker.

4.4 Notes

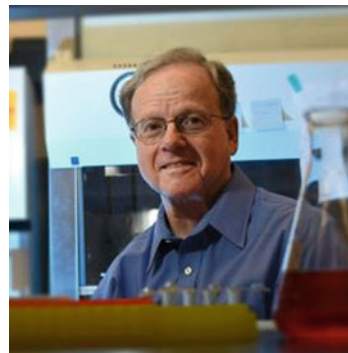
1. Controls: Remember that controls are crucial. If the experimental design allows for infusion on the same day as harvest, then the control group will be pretty straightforward (just use unmanipulated or “mock”-manipulated cells). However, if the experiment looks at, for example, a 4–7-day expansion incubation, two controls or more will be needed. It is critical to know whether the incubation time, itself, had an effect on the HSC population. Therefore, the first control must be time 0 input (pre-incubation) samples. The second control would be the mock-treated or untreated, but incubated, cell group. Remember that it’s always better to err on the side of too many controls than not enough.
2. Donor cells/dilutions: If your donor cells go through any treatment (e.g., expansion) for a period of time which changes the number of cells at time of infusion, you will need to decide to infuse a set volume or a recounted, post-expansion number.

For example, you found a new cytokine “S” that you think expands CD34⁺ cells while maintaining their self-renewing capacity. At the end of your culture period of 2 days, your mock-/control-treated population gives you 105% of your input number, while your S group returns 150% of your input number. So your test groups are as follows:

- Group 1: Day 0 input cells at 10,000 cells/mouse
- Group 2: Day 2 mock-treated cells at progeny of the equivalent number of input cells versus equal number of cells
- Group 3: Cytokine “S”-treated cells at progeny of the equivalent number of input cells versus equal number of cells

So the question is, do you infuse the post-treated cells based on the new cell numbers (not equal number but resultant progeny number from treatment and/or expansion) or a set number of cells? That is up to what question the experiment is trying to ask and must be determined at the time of transplant.

3. Injections: As mentioned a couple of times before, cleanliness and minimizing stress are extremely important when handling these mice. Clean your gloves or change them frequently, and alcohol the restraint device as well.
4. Staining and flow analysis: Please refer to the notes above.



Before this chapter went to production, Dr. Hal E. Broxmeyer died on December 8, 2021, from complications of thyroid cancer. Dr. Broxmeyer was a Distinguished Professor, Mary Margaret Walther Professor Emeritus, Professor of Microbiology and Immunology, and Senior Advisor to the Director of the NCI-designated Indiana University Simon Comprehensive Cancer Center at Indiana University School of Medicine. Dr. Broxmeyer was a consummate scientist and pioneer in the field of hematopoiesis. His innovations have impacted the world of medicine, and the most notable was his pioneering research efforts resulting in the first

umbilical cord blood transplant in 1988. Scott Cooper, a coauthor for this chapter, personally escorted the cell graft processed, evaluated and cryopreserved in Dr. Broxmeyer's laboratory at Indiana University to Paris. Dr. Broxmeyer personally made the trip to Paris to be present at the time of the transplant. To date more than 40,000 patients worldwide have benefited from his discovery of the potential and transplantability of this source of blood stem cells. His many awards, distinctions, and accomplishments can be found at <https://www.arnmortuary.com/obituary/DrHal-Broxmeyer>. Science, in general, and our field of blood stem cell research have lost a true icon who brought a passion for research, love of discovery, and unbounded commitment to creativity and collaboration to advance the understanding and utility of blood stem cells. Hal will be missed by his friends, colleagues, and collaborators worldwide but leaves behind a legacy of achievement in 838 peer-reviewed published and highly cited scientific papers. He willingly agreed to author this chapter to describe definitive assays for detection of functional HSC, despite his failing health; he was a firm believer of functional assays. This chapter may well be his final contribution to the field of hematopoiesis.

Louis M. Pelus, PhD

References

- Morrison SJ, Scadden DT (2014) The bone marrow niche for haematopoietic stem cells. *Nature* 505:327–334
- Nombela-Arrieta C, Pivarnik G, Winkel B, Canty KJ, Harley B, Mahoney JE, Park SY, Lu J, Protopopov A, Silberstein LE (2013) Quantitative imaging of haematopoietic stem and progenitor cell localization and hypoxic status in the bone marrow microenvironment. *Nat Cell Biol* 15:533–543
- Cooper S, Broxmeyer HE (1991) Clonogenic methods in vitro for the enumeration of granulocyte-macrophage progenitor cells (CFU-GM) in human bone marrow and mouse bone marrow and spleen. *J Tissue Cult Methods* 13:77–82
- Hoggatt J, Tate TA, Pelus LM (2014) Hematopoietic stem and progenitor mobilization in mice. In: *Hematopoietic stem cell protocols, methods in molecular biology*, vol 1185. Springer, New York
- Broxmeyer HE (1983) Colony assays of hematopoietic progenitor cells and correlations to clinical situations. *CRC Crit Rev Oncol* 1: 227–257
- Broxmeyer HE, Srour E, Orschell C, Ingram DA, Cooper S, Plett PA, Mead LE, Yoder MC (2006) Cord blood-derived stem and progenitor cells. *Methods Enzymol* 419:439–473
- Broxmeyer HE, Cooper S, Lasky LA, De Sauvage F (2005) Identification of a massive reserve of hematopoietic progenitors in mice. *Stem Cells Dev* 14:105–110
- Broxmeyer HE, Hangoc G, Cooper S, Anderson D, Cosman D, Lyman SD, Williams DE (1991) Influence of murine mast cell growth factor (c-kit ligand) on colony formation by mouse marrow hematopoietic progenitor cells. *Exp Hematol* 19:143–146
- Broxmeyer HE, Cooper S, Lu L, Hangoc G, Anderson D, Cosman D, Lyman SD, Williams DE (1991) Effect of murine mast cell growth factor (c-kit proto-oncogene ligand) on colony formation by human marrow hematopoietic progenitor cells. *Blood* 77:2142–2149
- Broxmeyer HE, Lu L, Cooper S, Ruggieri L, Li ZH, Lyman SD (1995) Flt3 ligand stimulates/costimulates the growth of myeloid stem/progenitor cells. *Exp Hematol* 23:1121–1129
- Mantel CR, O'Leary HA, Chitteti BR, Huang X, Cooper S, Hangoc G, Brustovetsky N, Srour EF, Lee MR, Messina-Graham S, Haas DM, Falah N, Kapur R, Pelus LM, Bardeesy N, Fitamant J, Ivan M, Kim KS, Broxmeyer HE (2015) Enhancing

- hematopoietic stem cell transplantation efficacy by mitigating oxygen shock. *Cell* 161:1553–1565
12. Zhang J, Ghosh J, Mohamad SF, Zhang C, Huang X, Capitano ML, Gunawan AM, Cooper S, Guo B, Cai Q, Broxmeyer HE, Srour EF (2019) CD166 engagement augments mouse and human hematopoietic progenitor function via activation of stemness and cell cycle pathways. *Stem Cells* 37:1319–1330
 13. Carow CE, Hangoc G, Cooper SH, Williams DE, Broxmeyer HE (1991) Mast cell growth factor (c-kit ligand) supports the growth of human multipotential progenitor cells with a high replating potential. *Blood* 78:2216–2221
 14. Carow CE, Hangoc G, Broxmeyer HE (1993) Human multipotential progenitor cells (CFU-GEMM) have extensive replating capacity for secondary CFU-GEMM: an effect enhanced by cord blood plasma. *Blood* 81:942–949
 15. Xiao M, Broxmeyer HE, Horie M, Grigsby S, Lu L (1994) Extensive proliferative capacity of single isolated CD34 human cord blood cells in suspension culture. *Blood Cells* 20:455–466
 16. Woehrer S, Miller CL, Eaves CJ (2013) Long-term culture-initiating cell assay for mouse cells. *Methods Mol Biol* 946:257–266
 17. Liu M, Miller CL, Eaves CJ (2013) Human long-term culture initiating cell assay. *Methods Mol Biol* 946:241–256
 18. Doulatov S, Notta F, Laurenti E, Dick JE (2012) Hematopoiesis: a human perspective. *Cell Stem Cell* 10:120–136
 19. van Galen P, Kreso A, Mbong N, Kent DG, Fitzmaurice T, Chambers JE, Xie S, Laurenti E, Hermans K, Eppert K, Marciniak SJ, Goodall JC, Green AR, Wouters BG, Dick JE (2014) The unfolded protein response governs integrity of the haematopoietic stem-cell pool during stress. *Nature* 510:268–272
 20. Chen Y, Yao C, Teng Y, Jiang R, Huang X, Liu S, Wan J, Broxmeyer HE, Guo B (2019) Phorbol ester induced ex vivo expansion of rigorously-defined phenotypic but not functional human cord blood hematopoietic stem cells: a cautionary tale demonstrating that phenotype does not always recapitulate stem cell function. *Leukemia* 33:2962–2966
 21. Capitano ML, Griesenauer B, Guo B, Cooper S, Paczesny S, Broxmeyer HE (2020) The IL-33 receptor/ST2 acts as a positive regulator of functional mouse bone marrow hematopoietic stem and progenitor cells. *Blood Cells Mol Dis*. (in press)
 22. Hoggatt J, Singh P, Sampath J, Pelus LM (2009) Prostaglandin E2 enhances hematopoietic stem cell homing, survival, and proliferation. *Blood* 113:5444–5455
 23. Broxmeyer HE, Christopherson K, Hangoc G, Cooper S, Mantel C, Renukaradhya GJ, Brutkiewicz RR (2012) CD1d expression on and regulation of murine hematopoietic stem and progenitor cells. *Blood* 119:5731–5741
 24. Broxmeyer HE, Orschell CM, Clapp DW, Hangoc G, Cooper S, Plett PA, Liles WC, Li X, Graham-Evans B, Campbell TB, Calandra G, Bridger G, Dale DC, Srour EF (2005) Rapid mobilization of murine and human hematopoietic stem and progenitor cells with AMD3100, a CXCR4 antagonist. *J Exp Med* 201:1307–1318
 25. Christopherson KW II, Hangoc G, Mantel CR, Broxmeyer HE (2004) Modulation of hematopoietic stem cell homing and engraftment by CD26. *Science* 305:1000–1003
 26. Broxmeyer HE, Hoggatt J, O’Leary HA, Mantel C, Chitteti BR, Cooper S, Messina-Graham S, Hangoc G, Farag S, Rohrabough SL, Ou X, Speth J, Pelus LM, Srour EF, Campbell TB (2012) Dipeptidylpeptidase 4 negatively regulates colony-stimulating factor activity and stress hematopoiesis. *Nat Med* 18:1786–1796
 27. Broxmeyer HE, Pelus LM (2014) Inhibition of DPP4/CD26 and dmPGE₂ treatment enhances engraftment of mouse bone marrow hematopoietic stem cells. *Blood Cells Mol Dis* 53:34–38
 28. Vormoor J, Lapidot T, Pflumio F, Risdon G, Patterson B, Broxmeyer HE, Dick JE (1994) Immature human cord blood progenitors engraft and proliferate to high levels in severe combined immunodeficient mice. *Blood* 83:2489–2497
 29. Broxmeyer HE, Lee MR, Hangoc G, Cooper S, Prasain N, Kim YJ, Mallett C, Ye Z, Witting S, Cornetta K, Cheng L, Yoder MC (2011) Hematopoietic stem/progenitor cells, generation of induced pluripotent stem cells, and isolation of endothelial progenitors from 21- to 23.5-year cryopreserved cord blood. *Blood* 117:4773–4777
 30. Guo B, Huang X, Cooper S, Broxmeyer HE (2017) Glucocorticoid hormone-induced chromatin remodeling enhances human hematopoietic stem cell homing and engraftment. *Nat Med* 23:424–428
 31. Guo B, Huang X, Lee MR, Lee SA, Broxmeyer HE (2018) Antagonism of PPAR- γ signaling expands human hematopoietic stem and progenitor cells by enhancing glycolysis. *Nat Med* 24:360–367

32. Capitano ML, Mor-Vaknin N, Saha AK, Cooper S, Legendre M, Guo H, Contreras-Galindo R, Kappes F, Sartor MA, Lee CT, Huang X, Markovitz DM, Broxmeyer HE (2019) Secreted nuclear protein DEK regulates hematopoiesis through CXCR2 signaling. *J Clin Invest* 129:2555–2570
33. Huang X, Guo B, Liu S, Wan J, Broxmeyer HE (2018) Neutralizing negative epigenetic regulation by HDAC5 enhances human haematopoietic stem cell homing and engraftment. *Nat Commun* 16:274
34. Xu D, Tang M, Capitano ML, Guo B, Liu S, Wan J, Broxmeyer HE, Huang XX (2020) Pharmacological activation of nitric oxide signaling promotes human hematopoietic stem cell homing and engraftment. *Leukemia* 35: 229
35. Capitano ML, Broxmeyer HE (2016) “CXCL12/SDF-1 and hematopoiesis” reference module in biomedical sciences. In: Bradshaw RA, Stahl PD (eds) *Encyclopedia of cell biology*, vol 3. Elsevier Publishing, Waltham/Oxford, pp 624–631
36. de Parseval A, Ngo S, Sun P, Elder JH (2004) Factors that increase the effective concentration of CXCR4 dictate feline immunodeficiency virus tropism and kinetics of replication. *J Virol* 78:9132–9143
37. Bonnefoix T, Callanan M (2010) Accurate hematopoietic stem cell frequency estimates by fitting multicell Poisson models substituting to the single-hit Poisson model in limiting dilution transplantation assays. *Blood* 116: 2472–2475
38. Huang X, Trinh T, Aljoufi A, Broxmeyer HE (2018) Hypoxia signaling pathway in stem cell regulation: good and evil. *Curr Stem Cell Rep* 4:149–157
39. Ploemacher RE, van der Sluijs JP, van Beurden CA, Baert MR, Chan PL (1991) Use of limiting-dilution type long-term marrow cultures in frequency analysis of marrow-repopulating and spleen colony-forming hematopoietic stem cells in the mouse. *Blood* 78: 2527–2533
40. Szilvassy SJ, Humphries RK, Lansdorp PM, Eaves AC, Eaves CJ (1990) Quantitative assay for totipotent reconstituting hematopoietic stem cells by a competitive repopulation strategy. *Proc Natl Acad Sci U S A* 87:8736–8740
41. Wang JC, Doedens M, Dick JE (1997) Primitive human hematopoietic cells are enriched in cord blood compared with adult bone marrow or mobilized peripheral blood as measured by the quantitative in vivo SCID-repopulating cell assay. *Blood* 89:3919–3924



Hematopoietic Stem and Progenitor Cell Identification and Transplantation in Zebrafish

Ellen Fraint, Peng Lv, Feng Liu, Teresa V. Bowman, and Owen J. Tamplin

Abstract

The zebrafish as a model organism is well known for its versatile genetics, rapid development, and straightforward live imaging. It is an excellent model to study hematopoiesis because of its highly conserved ontogeny and gene regulatory networks. Recently developed highly specific transgenic reporter lines have allowed direct imaging and tracking of hematopoietic stem and progenitor cells (HSPCs) in live zebrafish. These reporter lines can also be used for fluorescence-activated cell sorting (FACS) of HSPCs. Similar to mammalian models, HSPCs can be transplanted to reconstitute the entire hematopoietic system of zebrafish recipients. However, the zebrafish provides unique advantages to study HSPC biology, such as transplants into embryos and high-throughput chemical screening. This chapter will outline the methods needed to identify, isolate, and transplant HSPCs in zebrafish.

Key words Hematopoietic stem and progenitor cells (HSPCs), HSPC transplantation, Zebrafish, Transgenic reporter lines, Live imaging

1 Introduction

Transplantation remains the gold standard to test the fitness and function of hematopoietic stem and progenitor cells (HSPCs). However, studying HSPC transplantation in mammalian model systems has a number of limitations, including the cost to scale the number of animals and the difficulty of visualizing engrafted cells. Zebrafish are now well established as a highly conserved and efficient model for HSPC studies. Zebrafish have a hematopoietic system that is similar to mammals in both its gene regulatory programs and cell types [1, 2]. A notable difference between mammals and zebrafish is the sites of hematopoiesis [2]. During development HSPCs expand in the caudal hematopoietic tissue (CHT) instead of the fetal liver [3, 4]. In the adult, HSPCs reside in the kidney marrow and not bone. HSPC transplantation in the adult zebrafish has generally been performed using the same approach as in mammals: (1) conditioning of recipients using irradiation,

(2) harvesting of donor marrow, (3) injection of donor cells into the recipient, and (4) quantifying engraftment via flow cytometry [5]. Recent developments in zebrafish transplantation have built upon this paradigm and expanded the tool kit to more fully exploit the advantages afforded by the zebrafish. These innovations have greatly increased the potential for this model in studying hematopoiesis, and these new methods will be outlined in this chapter.

A tremendous advantage of the zebrafish model is the ability to directly visualize transplanted donor cells. This is made possible not only because of transparent *casper* recipients [6] but also by the many available transgenic reporter lines that provide labeled HSPCs and whole kidney marrow (WKM) (see Tables 1 and 2). HSPC-specific reporter lines can be sorted to reach stem cell purity that is similar to the best combinations of cell surface markers in mouse models, for example, *cd41:GFP^{lo}* [7], *gata2a:GFP+*; *Runx1+23:mCherry+* [8], and *Runx1+23:mCherry* and *Runx1+23:GFP*

Table 1
Zebrafish lines used as transplantation donors

Name of line	Expression pattern (WKM)	Reference(s)
<i>ubi:mCherry</i>	Nearly ubiquitous	[12]
<i>ubi:EGFP</i>	Nearly ubiquitous	[12]
<i>bactin1:EGFP</i>	Widely expressed, little to no expression in erythrocytes	[1, 9, 12, 29]
<i>bactin2:loxP-BFP-loxP-DsRed</i>	Widely expressed, little to no expression in erythrocytes	[8, 13]
<i>RedGlo</i> (DsRed2)	Ubiquitous	[9]
<i>cd41:GFP^{lo}</i>	Low, HSPCs; high, thrombocytes	[7]
<i>Runx1+23:mCherry</i>	HSPCs	[4]
<i>Runx1+23:GFP</i>	HSPCs	[4]
<i>gata2a:GFP+</i> ; <i>Runx1+23:mCherry+</i>	Double-positive population highly enriched for long-term repopulating HSPCs	[8]

Table 2
Zebrafish lines used as transplantation recipients

Name of line	Feature	Reference(s)
<i>casper</i>	Transparent pigmentation mutants	[6, 9]
<i>runx1^{W84X}</i>	Homozygous mutants are viable and lack definitive hematopoiesis	[16, 21, 22]
<i>foxn1/casper</i>	Homozygous mutants are viable and transparent and have a T cell deficiency	[15]

[4]. Ubiquitously expressed fluorescent proteins in donor cells allow HSPCs and all of their progeny to be tracked long term in recipients [4, 5, 8–13]. Multicolored labeling of the HSPC compartment using zebrafish and inducible *Cre^{ERT2}* provides a tool for studying clonal hematopoietic fate in the zebrafish [14]. Transparent *casper* recipients have been used for direct visualization of competitive red and green fluorescent donor marrow cells [9]. Flow cytometry analysis of fluorescent donor cells in the peripheral blood (PB) and WKM in recipient zebrafish allows easy analysis of donor chimerism and lineage contributions [1, 11, 15, 16].

Zebrafish, like humans, are non-isogenic so the donor and recipient must be immune matched for a successful HSPC transplant [11]. However, the recent development of multiple immunodeficient zebrafish models has allowed transplantation into unconditioned recipients, circumventing the need for highly damaging myeloablation [15–18]. This is also increasing the number of possibilities for xenotransplants that are already possible in zebrafish, such as transplant of human and mouse HPSCs [19, 20].

This chapter will highlight methods used to transplant sorted HSPCs and WKM into immunodeficient adults and larvae [15, 16]. The external development of zebrafish allows easy transplantation of donor cells into larvae and embryos [1, 4, 16]. Cells can be injected into the circulation of larvae that can then be raised to adulthood for analysis of marrow chimerism. Homozygous *runx1^{W84X}* mutants are viable and lack definitive hematopoiesis, meaning no adaptive immune cells develop and the niche is ready to receive donor cells without rejection [16, 21, 22]. Homozygous *foxn1/casper* mutants are viable and transparent and have a T cell deficiency [15]. Both the *runx1^{W84X}* and *foxn1/casper* mutants allow transplantation into unconditioned recipients, circumventing the need for damaging myeloablation [15, 16]. Together, these new approaches represent robust methods to transplant fluorescent donor cells into a large number of recipients that can be housed at high density and easily visualized.

2 Materials

2.1 Zebrafish

All adult zebrafish are raised at 28.5 °C in system water (conductivity at 500–550 µs/cm and pH at 7.0–7.5).

2.1.1 Larval Transplantation Recipients

Homozygous *runx1* mutant zebrafish are utilized for larval transplantation. Multiple different *runx1* null mutant lines have been made, but we use the *runx1^{W84X}* mutant, created by the Liu lab [21, 22] on an AB background. The W84X point mutation leads to a premature stop codon resulting in loss-of-function and a *runx1* null phenotype in homozygous mutants. Most of these mutants are unable to perform definitive hematopoiesis as they have defects in

hematopoietic stem cell initiation in the dorsal aorta. With a functionally empty stem cell niche, these mutant larvae are able to engraft donor hematopoietic cells without radiation or any other preconditioning [16] (see **Note 1**).

2.1.2 Larval Transplantation Donors

Donor zebrafish with fluorescent hematopoietic cells are used to facilitate visualization of transplanted cells and engraftment read-out. Adult Tg(*ubi:GFP*) fish (hereafter referred to as *ubi:GFP*), which ubiquitously express green fluorescent protein under the control of the *ubiquitin* promoter, are commonly used [23]. Although the GFP should be completely ubiquitous, some variability in expression is noted in erythroid and lymphoid lineages [16] (see **Note 2**).

2.1.3 Adult Transplantation Recipients

Transparent *casper* [24] zebrafish are used as controls, and *foxn1/casper* immunodeficient zebrafish line, which was obtained through outcrossing *foxn1* mutant with the *casper* line [15], are utilized for non-conditioned HSPC transplantation. The immunodeficient *foxn1/casper* line should be kept in sterilized fish water supplemented by penicillin (100 units/mL) and streptomycin (100 µg/mL) before and after transplantation (for up to 90 days if needed to assess long-term engraftment).

2.1.4 Adult Transplantation Donors

Previous studies have shown that *cd41:GFP^o* cells fulfill generally accepted criteria for HSPCs in zebrafish [7]. Thereby, several transplant studies using *cd41:GFP^o* HSPCs have shown an efficient engraftment and reconstitution ability in zebrafish recipients [15, 16]. As such, the Tg(*ubi:dsRed/cd41:GFP*) double transgenic line was used for adult transplantation studies into *foxn1/Casper* mutants.

2.2 Reagents and Supplies

1. FACS buffer I (for donor kidney marrow collection): 0.9× Dulbecco's phosphate-buffered saline (DPBS), 5% fetal bovine serum, and 1% Pen/Strep antibiotics. Store at 4 °C. Good for up to 6 months.
2. Transplant injection buffer: FACS buffer I supplemented with 500-µM EDTA and 1 µL/2 units TURBO DNase (Life Technologies) per 20 µL of buffer. This solution is made fresh the day of transplant.
3. Flow cytometry buffer: FACS buffer I supplemented with diamidino-2-phenylindole (DAPI) or propidium iodide (PI), depending on emission spectra of the FACS experiment (follow the manufacturer's guidelines for dilution). This solution is made fresh on the day of assessment.
4. FACS buffer II: 1× phosphate-buffered saline, 2% fetal bovine serum.

5. Red cell lysis buffer: Two stock solutions prepared in sterile water are needed: Stock 1 (0.16-M NH₄Cl) and Stock 2 (0.17-M Tris-HCl pH 7.65). Stock solutions can be stored at room temperature for up to 1 year. A working solution of 9-mL Stock 1 + 1-mL Stock 2 should be made fresh on the day of assessment.
6. Tricaine stock: 4-mg/mL stock of pharmaceutical grade buffered tricaine methane sulfonate (MS-222) is made in water and stored in an opaque glass bottle at 4 °C for up to 1 month. A working solution of anesthetic was made by adding 2.5 mL of 4-mg/mL tricaine stock to 100 mL of tank or system water (final concentration 100 mg/L; buffer to pH 7–7.5).
7. Embryo dissociation mix: add 40-μL 100-mg/ml collagenase (from *Clostridium histolyticum* in PBS; 40-μL aliquots stored at –20 °C for single use) to 460-μL 0.25% trypsin-EDTA.
8. Phosphate-buffered saline (PBS): 1× without calcium and magnesium.
9. DMEM: 1× with 4.5-g/L glucose, L-glutamine, and sodium pyruvate.
10. 1× E3 fish water: 5-mM NaCl, 0.17-mM KCl, 0.33-mM CaCl₂, 0.33-mM MgSO₄.
11. 70% ethanol.

2.3 Tools and Instruments

1. Dissecting scissors.
2. Two pairs of micro-dissecting forceps (Dumont Tweezers #5, 11-cm, Straight, 0.1 × 0.06-mm Tips).
3. Hemocytometer or other device to count cells.
4. Petri dishes for zebrafish embryos.
5. Injection plate: 1% agarose in E3 fish water poured into petri dish. Larvae 48 hpf are laid flat on the agarose for injection. Alternatively, to make an injection plate with grooves, float a plastic zebrafish larval injection mold (World Precision Instruments) in 2% agarose until it sets, then remove gently.
6. Needles: A borosilicate capillary tube without a filament (World Precision Instruments, 4 in, OD 1.0 mm, No Filament (TW100-4) is used to decrease shearing of the cells during injection. We use the following program to pull needles on a heat-filament instrument (Sutter Instrument Model P97): Pressure 200, Heat 515, Pull 150, Velocity 150, Delay 90. Prior to loading the needle, forceps are used to pinch off the needle tip to create a small-bore opening. Beveled tips work best, but any shape can be utilized depending on bore size. Bore size should be tailored to create droplets of approximately 5 nL.

7. Slide micrometer.
8. 1.5-mL microcentrifuge tubes.
9. P1000 and P200 pipet tips.
10. 5-mL FACS tubes.
11. 40- μ m and 70- μ m mesh cell strainers.
12. 50-mL conical tubes.
13. Heat block (set at 30 °C for dissociation of larvae).
14. Centrifuge.
15. 26s-gauge Hamilton 80366 syringe.
16. Flow cytometer: LSR II (BD) analyzer or MoFlo XDP (Beckman).
17. Imaging flow cytometer: FlowSight (Merck Millipore).
18. Irradiator: Cesium-137 based, Quasar, RS2000.

3 Methods

3.1 Donor Cell Harvest from Adult Zebrafish WKM

The procedure was followed and modified based on those previously reported [25, 26]. Donor HSPCs for transplantation into adult recipients are obtained from a 3-month-old adult WKM or 3-day post fertilization (dpf) caudal hematopoietic tissue (CHT) of *Tg(ubi:dsRed/cd41:GFP)* lines (see Fig. 1).

Previously, we have also used *Tg(Runx1+23:mCherry/ubi:GFP)* and *Tg(Runx1+23:GFP/ubi:mCherry)* lines as HSPC donors [4]. HSPC-specific reporters (e.g., *cd41:GFP*, *Runx1+23:GFP*, *Runx1+23:mCherry*) together with a ubiquitous reporter (e.g., *ubi:GFP*, *ubi:mCherry*) allow measurement of donor HSPC contribution and differentiated lineage output, respectively. Donor

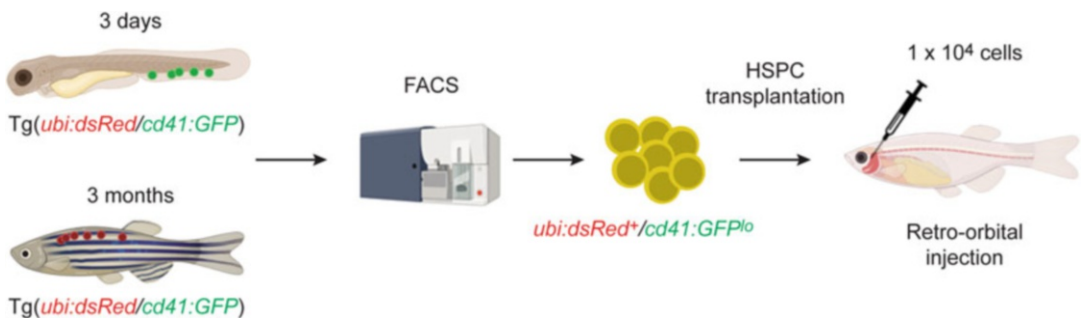


Fig. 1 Diagram showing workflow of donor cell harvest by FACS and transplantation of HSPCs into adult recipients. Donor cells are harvested from 3 days post fertilization (dpf) caudal hematopoietic tissue (CHT, upper left) or 3-month-old adult whole kidney marrow (WKM, lower left) of *Tg(ubi:dsRed/cd41:GFP)* lines. Sorted *ubi:dsRed⁺/cd41:GFP^{lo}* donor HSPCs (1×10^4) are transplanted into adult transparent *casper* recipients by retro-orbital injection

HSPCs for transplantation into larval recipients are obtained from the WKM of Tg(*ubi:GFP*) line [23]:

1. Euthanize adult zebrafish donors using an IACUC-approved method, such as submersion in ice water or tricaine overdose.
2. Once euthanized, lay the zebrafish on paper towel, then use a dissecting microscope to visualize the dissection. Using forceps, prop the fish on its back with ventral side facing up.
3. Using small scissors, make a small incision into the peritoneal cavity near the anal fin. Lift the tip of the scissors to lift the skin away from visceral organs to minimize damage, then cut the skin ventrally from the anus to the gills.
4. Spread the peritoneal cavity open with one forceps, and use other forceps to carefully remove visceral organs, swim bladder, and eggs for females.
5. Using closed forceps, scrape the pigmented kidney off the dorsal side of the inner peritoneal cavity, then pick up the kidney and place it into a microcentrifuge tube containing 1-mL donor collection media (*see* Fig. 2 and **Note 3**). If using a single donor, proceed to step 6. If pooling donors, then repeat steps 1–5 until all donors are dissected.
6. Gently pipet up and down the 1 mL of cells in collection media with a P1000 tip (≥ 15 times) to flush the marrow cells out of

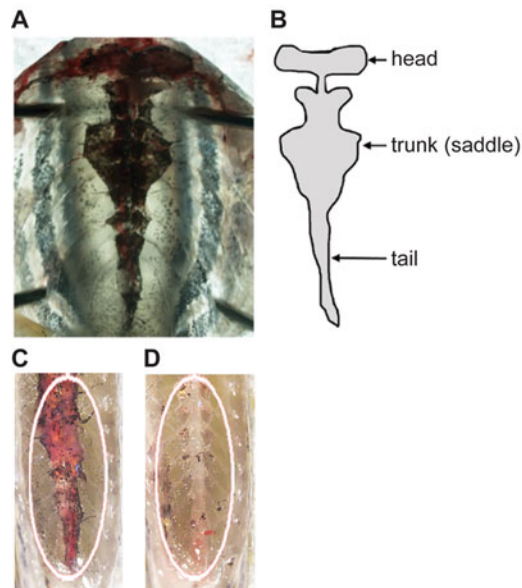


Fig. 2 Image (a) and schematic (b) of the kidney on the dorsal surface of the peritoneal cavity in adult zebrafish. This was adapted with permission from Gerlach et al. [28]. The donor WKM before (c) and after (d) dissection. (Credit: PL and FL)

the kidney. Strain through a 40- μm cell strainer into a new microcentrifuge tube.

7. For counting, dilute 10 μL of the cell suspension into 90- μL FACS buffer I to make a 1:10 dilution. Use 10 μL of this dilution to load a hemocytometer.
8. Count the white blood cells (*see* **Note 4**) in one of the four corner boxes, or take the average count from all four corners. This number is equal to N . To calculate the total number in your solution: $N \times 10$ dilution factor $\times 10^4$ cells/mL.
9. Pellet the filtered cell suspension by spinning for 5 min at 2500 rpm.
10. If transplanting WKM directly into larval recipients, resuspend the cells in the necessary volume of transplant injection buffer to achieve a final concentration of 500 cells/nL (i.e., 2500 cells per injection droplet).
11. If transplanting WKM directly into adult recipients, resuspend in FACS buffer I to inject 1.5–2 million cells per recipient in less than 5- μL volume. We have also successfully used 1X PBS to resuspend cells for transplantation, if FBS is not compatible with your experiment.
12. If sorting cells prior to transplantation, please see Subheading **3.3** below.

3.2 Donor Cell Harvest from Zebrafish Embryos and Larvae

These methods were adapted directly from Bresciani et al. [27]. We present the method for 5 dpf larvae, but stages from 2–16 dpf are described in the original paper [27]. It is very important that all steps are performed at room temperature (RT), unless otherwise noted, and cells are not kept on ice at any point in the experiment, even during sorting:

1. Thaw a fresh aliquot of 100-mg/ml collagenase.
2. Prepare fresh DMEM-10% FBS and have it ready in a water bath at 30 °C.
3. Prepare 500- μL aliquot of embryo dissociation mix for each tube of larvae (maximum $n = 20$ 5 dpf larvae per tube). Keep ready in a water bath at 30 °C.
4. Collect zebrafish larvae. Tricaine is highly toxic to 5 dpf larvae so use briefly to stop movement and quickly proceed to the next step.
5. Transfer larvae into 1.5-mL microcentrifuge (maximum $n = 20$ 5 dpf larvae per tube).
6. Wash twice in 1-mL PBS.
7. For dissociation with trypsin and collagenase, add 500 μL of pre-warmed (30 °C) dissociation mix.

8. Vigorously pipet larvae up and down using a P1000 and then P200, alternating 30-s intervals of pipetting and heating in water bath at 30 °C until the tissue is completely dissociated (5–10 min).
9. Stop by adding 800 µL of embryo dissociation stop buffer.
10. Before centrifugation, pass dissociated larvae through a 70-µm nylon mesh into a clean 1.5-mL microcentrifuge tube to remove excess debris and prevent clumping during the next centrifugation step.
11. Centrifuge 5 min at 700 g at RT.
12. Wash the cells by resuspending the pellet in 1-mL PBS, and then centrifuge again for 5 min (700 g at RT).
13. Discard the supernatant and resuspend in 500-µL PBS-2% FBS for cell sorting (or 1 mL if two to three tubes are pooled, resuspending each tube in the same aliquot of PBS-2% FBS to further concentrate the cells).
14. Again, pass dissociated larvae through a 70-µm nylon mesh into a polypropylene FACS tube to prevent clogging during the sort.
15. If sorting cells prior to transplantation, please see Subheading 3.3 below.

3.3 FACS of Donor Cells for Transplantation

Cells from dissected WKM, or dissociated embryos or larvae, are stained with DAPI or PI, depending on emission spectra of the FACS experiment, to exclude dead cells (follow the manufacturer's guidelines for dilution). Wild-type non-fluorescent zebrafish cells (adult WKM, dissociated embryos, or larvae, depending on the experiment) are used as the negative control to gate fluorescent HSPCs (e.g., *ubi:dsRed⁺/cd41:GFP^{lo}*). Cells are sorted into 500–1000-µl FACS buffer II. The sorted cells are then centrifuged at 1000 g for 8 min and resuspended in proper volumes for transplantation. Alternatively, if very small numbers of cells are sorted, collection can be done directly into PCR tubes with 30–50 µl of FACS buffer II.

3.4 Larval Transplantation

3.4.1 Larval Transplantation: Prepare Recipient Embryos

1. Three nights prior to transplantation, set up breeding of homozygous *runx1* mutant fish. Collect the embryos the following morning, and allocate approximately 40 fertilized, viable embryos per dish. Embryos that are 48 h post fertilization (hpf) are used as transplant recipients.
2. Dechorionate embryos (*see Note 5*).
3. Anesthetize larvae in tricaine (final concentration 100 mg/L), just enough that they are temporarily paralyzed, typically about 10–20 drops of stock solution from a transfer pipet per petri dish.

3.4.2 Larval
Transplantation: Cell
Injection into Larval
Recipients

We utilize a microinjector to hold the injection needle and enable rapid precise larval injections. We inject with PSI 29 for 100 ms, although lower pressures can be utilized:

1. Load 2–3 μL of the donor cell suspension into the prepared needle, and eject into fish water to ensure that the needle is patent and that an adequate cell dose is achieved.
2. Place one to five anesthetized embryo(s) onto the injection plate, and remove as much excess water as possible (*see Note 6*). Avoid putting more than five embryos onto the injection plate at a time to avoid losing track of which larvae have already been injected. Alternatively, if you are using an agarose plate made with a larval injection mold, line up ~5 larvae in the groove, and inject them in order.
3. Advance the needle into the common cardinal vein by first puncturing the yolk ball laterally and advancing through the yolk ball into the cardinal vein posteriorly through the membrane that divides them (*see Fig. 3* and **Note 7**). An alternative injection method is to perform retro-orbital injection of the embryo or larva.
4. For issues with needle care and clogging, *see Note 8*.



Fig. 3 Injection into larval zebrafish recipient showing the location of the needle approaching laterally through yolk into the posterior wall of the common cardinal vein

3.4.3 Larval Transplantation: Post-transplant Care of Larval Recipients

1. After injecting cells, immediately place larvae into fresh embryo water without tricaine.
2. When larvae are visualized by fluorescence microscopy, transplanted cells can be seen circulating through the vasculature within minutes following transplant.
3. Graduate transplanted and control zebrafish larvae into the aquatic system nursery on day 5 post fertilization (*see Note 9*). Housing of ten recipients per 3-L tank results in robust survival of transplanted animals.

3.5 Adult Transplantation

1. Irradiation: Conditioned *casper* zebrafish recipients are irradiated with 10–15 Gy X-irradiation 2 days before transplantation. Non-conditioned *casper* recipients are the negative controls. The *foxn1/casper* recipients do not need the preconditioning.
2. Anesthetize recipients: Zebrafish recipients are first anesthetized via submersion in 100-mg/L tricaine.
3. Syringe washing: Prior to injection, the 26s-gauge Hamilton 80366 syringe should be washed three times by using 70% ethanol. Then, rinse five times with 1× DPBS.
4. Fish placement: Remove the anesthetized zebrafish gently with forceps or small spoon, and lay the fish on its one side on the damp sponge and head toward the left.
5. Injection: Hold the syringe with the right hand and with your index finger on the plunger, and stabilize the fish with the left hand. Position the needle with the bevel facing up at a 45-degree angle to the retro-orbital sinus (*see Fig. 4*). Gently insert the needle 1–2 mm into the retro-orbital sinus and slowly depress the plunger.
6. Transplanted fish recovery: Place the transplanted fish into fresh fish water. Keep fish off flow for 1 week with daily water changes, supplemented with penicillin (100 units/mL) and streptomycin (100 µg/mL) to avoid infection.

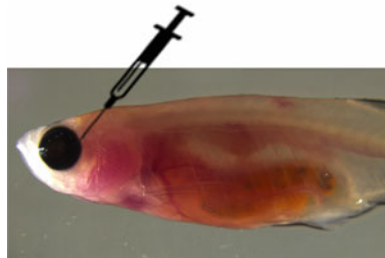


Fig. 4 Retro-orbital injection into adult zebrafish recipient

3.6 Measuring Engraftment in Transplant Recipients

To quantitatively measure donor-derived engraftment, flow cytometry can be performed on the whole kidney marrow of transplanted zebrafish. Fish are usually large enough to perform dissection by 6–8 weeks old. Short-term engraftment is assessed at 6–8 weeks post transplantation, and long-term engraftment is assessed beyond 3 months post transplantation.

3.6.1 Imaging-Based Engraftment Assessment

1. For visual assessment of engraftment within living adult zebrafish, photographs of whole adult fish are first taken by Nikon SMZ1500, and the images of blood cells are taken using Nikon A1 confocal microscopy. At 2 h post transplantation, *cd41:GFP^{lo}* cells are readily observed in the blood flow at the head and tail region. After 60 days post transplantation, the engrafted dsRed⁺ or GFP⁺ cells are directly observed in the recipient KM.
2. An imaging flow cytometer is used for single-cell image analysis of different hematopoietic lineages.

3.6.2 Flow Cytometry-Based Engraftment Assessment

These methods are adapted from Traver et al. [5]. Examination of hematopoietic lineages in the whole kidney marrow is performed using a flow cytometer. When these are not available, other instruments can be used, but the distribution of hematopoietic lineages might appear different and less distinct. Zebrafish red blood cells are elliptical which can cause irregular forward and side scatter of the cells. When this happens, these cells obfuscate the other populations and appear as a large spread of red blood cell events across the plot. In these instances, red blood cell lysis is desirable to visualize the white blood cell plots (*see Note 10*). Analysis can be performed using FlowJo (10.5.0) or Summit (5.1.0) software:

1. Harvest kidneys as described in Subheading 3.1, placing individual dissected kidneys into wells of a 24-well plate containing 400- μ L flow cytometry buffer.
2. Gently pipet up and down to flush the marrow cells out of the kidneys and strain each through a 40- μ m strainer into a FACS tube.
3. To exclude dead cells, use a live cell impermeable dye, such as DAPI or PI. Gate on live cells by excluding dye-positive events.
4. Gate for single cells by excluding doublets and small debris based on forward (FSC) and side (SSC) scatter parameters (FSC-H vs FSC-W and SSC-H vs SSC-W).
5. If male fish are dissected and sperm has contaminated the cell suspension, exclude the sperm from the analysis, as seen in Fig. 5a.
6. Gate for the hematopoietic lineages using FSC-A (linear) vs SSC-A (log) plot. Sample plots of whole kidney marrow on

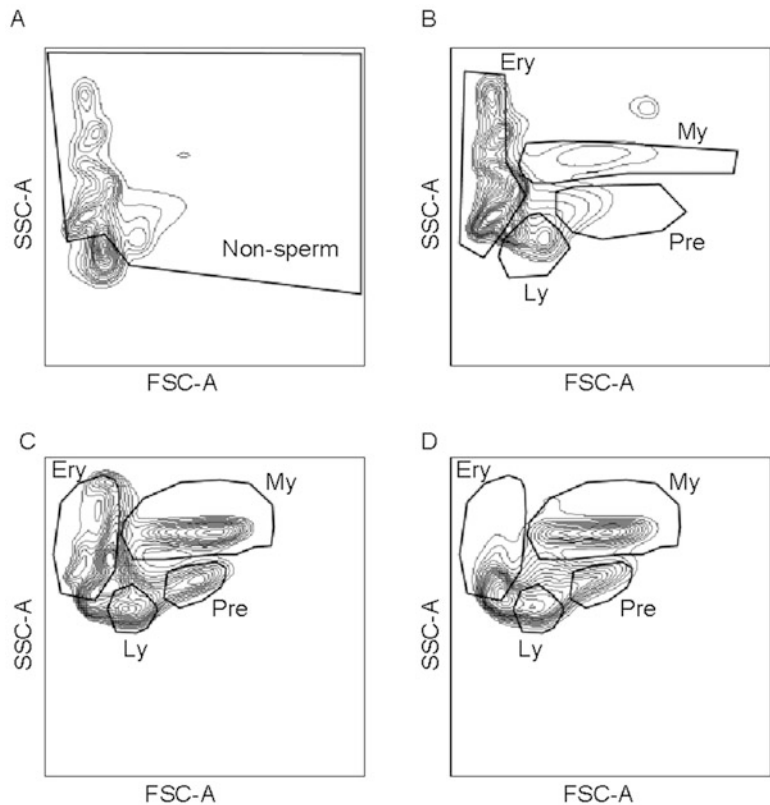


Fig. 5 Sample flow cytometry plots. **(a)** Whole kidney marrow from a male fish to demonstrate gating used to exclude the sperm from further analysis. After excluding sperm, gating is performed for the hematopoietic lineages based on forward and side scatter characteristics. **(b)** Representative plot using a LSR II analyzer. **(c and d)** Representative plots using a Fortessa analyzer before **(c)** and after **(d)** red blood cell lysis. Gating is shown for myeloid (My), erythroid (Ery), lymphoid (Ly), and precursor (Pre) cells

flow cytometers (LSR II and Fortessa) are seen in Fig. 5b and Fig. 5c and d, respectively. The analysis on the Fortessa was performed before and after red blood cell lysis.

7. Set up proper gates for fluorescent proteins used in your study based on negative and positive controls. For example, WKM cells from untransplanted siblings of recipient fish are an appropriate negative control, and WKM cells from donors are a good positive control.
8. Assess the contribution of donor-derived cells by determining the percentage of cells in the myeloid gate that are positive for ubiquitous donor marker, such as *ubi:GFP* or *ubi:dsRed*. The percent of myeloid cells that express the donor fluorescent protein is the recipient's chimerism.

4 Notes

1. The lethal phenotype of the *runx1* mutant is variable. The vast majority of *runx1* mutant larvae will die within 2–3 weeks post fertilization, as they outgrow their primitive blood supply and oxygen supply by diffusion. However, approximately 10–20% survive to adulthood. Thus, not all of the fish that survive transplantation will demonstrate robust donor chimerism. Nevertheless, more *runx1* homozygous mutants engraft and display markedly higher donor chimerism than *runx1* heterozygotes.
2. As described in Fraint et al. [16], the *ubi:GFP* fish has nearly but not completely ubiquitous GFP expression. The erythroid and lymphoid cells in particular have highly variable GFP positivity. However, the myeloid cells are nearly universally GFP+ and therefore are an excellent marker of donor cell origin. As well, myeloid cells are the lineage with the fastest cell turnover and thus are a better marker of donor-derived hematopoietic stem cell contribution.
3. Also demonstrated in Gerlach et al. [28], the kidney is a thin black membrane attached via connective tissue to the dorsal surface of the peritoneal cavity. It is important to be very careful to remove the visceral organs en bloc without puncturing and spilling the contents of the viscera or spilling sperm all over the peritoneal cavity. Also take care when removing the visceral organs to not accidentally remove the kidney. Once uncovered, the kidney can then be carefully peeled or scraped off the fish with a pair of forceps.
4. The white blood cells are very bright and round cells, whereas the red blood cells are elliptical-shaped and nucleated and appear duller. Note that if your sample is contaminated with sperm, these will also appear as very small, very bright round cells. They can be distinguished from white blood cells as the flagella are often visible and motile.
5. We manually dechorionate embryos to prevent any potential damage from pronase over digestion. However, pronase may be used to dechorionate larger quantities of recipient embryos.
6. We remove the water with an extra-fine plastic pipet. The goal is to have minimal water around the larvae to make sure it stays in place when a needle is inserted. If your larvae roll to the side when you try to insert the needle, you need to remove more water. Alternatively, if you use an agarose plate made with a larval injection mold, tilt the plate as you release larvae into the groove from a transfer pipet with minimal volume. This allows the larvae to fall into the groove, and the excess water will run down to the inner edge of the petri dish where it can be easily removed.

7. Injecting through the yolk is easier and causes less damage to the larvae than trying to puncture the cardinal vein directly through the skin. This approach also causes less damage to the larvae than trying to inject into the dorsal vein along the tail. Alternatively, if performing retro-orbital injections in the embryo or larva, correct injection into the sinus is confirmed by a brief expansion of the vessel around the eye.
8. Over time, while injecting 50–100 larvae with one needle, the cells in suspension will settle due to gravity. This can clog the needle and also lead to some variability in the cell dose of each droplet over time. Ejecting a few droplets into the fish water after several larval injections can help prolong needle patency. When the needle becomes clogged, focus the microscope up to visualize the needle tip. Without removing the needle from the microinjector, use the forceps to clip off a very small piece of the needle tip, and eject to see if the clog has been relieved. Repeat clipping off tiny bits of the needle tip and pumping the foot pedal as needed until the clog is relieved. If you need to clip off so much of the tip that the droplet size and cell dose are now too large, prepare a new needle loaded with fresh donor cell suspension. If it appears that the cell dose being injected into the larvae is starting to look too dilute, it is time to load a new needle as your cell suspension has been exhausted. The best results are achieved when larval injections are efficient, so that as many transplants can be performed as possible before cell settling occurs.
9. Due to the more fragile nature of transplanted *runx1* mutant larvae, they fare best when moved from petri dishes in the incubator to fish tanks at 5 days post fertilization (dpf), although waiting until 6 or 7 dpf can also be okay. It is best to have sham-injected or sham-uninjected controls to compare survival, as there can be significant procedure-related mortality, especially when first learning. This is often seen as a large drop-off in survival after entering the aquatic system.
10. Perform red blood cell lysis when using flow cytometers other than LSR II. After harvesting transplant recipient whole kidney marrow into FACS buffer I, gently pipet up and down to create a cell suspension, and filter each through a 40- μ m cell strainer into a FACS tube. Pellet the cells by centrifuging at 2500 rpm for 5 min. Remove FACS buffer I, then resuspend the pellets in 500- μ L red cell lysis buffer working solution (made fresh from stock solutions). Mix and let it sit at room temperature for 15 min. Add 500- μ L FACS buffer I to stop the lysis process, and pellet again by centrifuging at 2500 rpm for 5 min. Resuspend cell pellets in 400- μ L flow cytometry buffer and analyze as above.

Acknowledgments

OJT was supported by the National Institutes of Health: National Heart, Lung, and Blood Institute (R01HL142998) and National Institute of Diabetes and Digestive and Kidney Diseases (K01DK103908). OJT was also supported by an American Society of Hematology (ASH) Junior Faculty Scholar Award. Additional funding was provided by the University of Wisconsin-Madison. TVB was supported by the American Cancer Society RSG-129527-DDC, DOD BM180109, and NIH 1R01DK121738-01A1 and the Edward P. Evans Foundation. FL was supported by grants from the National Key Research and Development Programmes of China (2018YFA0800200); the Strategic Priority Research Program of the Chinese Academy of Sciences, China (XDA16010207); the National Natural Science Foundation of China (31830061, 31425016, and 81530004); and the State Key Laboratory of Membrane Biology, China. EF was supported by the American Society of Hematology Research Training Award for Fellows.

References

1. Traver D, Paw BH, Poss KD, Penberthy WT, Lin S, Zon LI (2003) Transplantation and in vivo imaging of multilineage engraftment in zebrafish bloodless mutants. *Nat Immunol* 4:1238–1246
2. Orkin SH, Zon LI (2008) Hematopoiesis: an evolving paradigm for stem cell biology. *Cell* 132:631–644
3. Murayama E, Kissa K, Zapata A, Mordélet E, Briolat V, Lin H-F, Handin RI, Herbomel P (2006) Tracing hematopoietic precursor migration to successive hematopoietic organs during zebrafish development. *Immunity* 25:963–975
4. Tamplin OJ, Durand EM, Carr LA, Childs SJ, Hagedorn EJ, Li P, Yzaguirre AD, Speck NA, Zon LI (2015) Hematopoietic stem cell arrival triggers dynamic remodeling of the perivascular niche. *Cell* 160:241–252
5. Traver D, Winzler A, Stern HM, Mayhall EA, Langenau DM, Kutok JL, Look AT, Zon LI (2004) Effects of lethal irradiation in zebrafish and rescue by hematopoietic cell transplantation. *Blood* 104:1298–1305
6. White RM, Sessa A, Burke C, Bowman T, Leblanc J, Ceol C, Bourque C, Dovey M, Goessling W, Burns CE, Zon LI (2008) Transparent adult zebrafish as a tool for in vivo transplantation analysis. *Cell Stem Cell* 2:183–189
7. Ma D, Zhang J, Lin H-F, Italiano J, Handin RI (2011) The identification and characterization of zebrafish hematopoietic stem cells. *Blood* 118:289–297
8. Kobayashi I, Kondo M, Yamamori S, Kobayashi-Sun J, Taniguchi M, Kanemaru K, Katakura F, Traver D (2019) Enrichment of hematopoietic stem/progenitor cells in the zebrafish kidney. *Sci Rep* 9:14205
9. Li P, Lahvic JL, Binder V, Pugach EK, Riley EB, Tamplin OJ, Panigrahy D, Bowman TV, Barrett FG, Heffner GC, McKinney-Freeman S, Schlaeger TM, Daley GQ, Zeldin DC, Zon LI (2015) Epoxyeicosatrienoic acids enhance embryonic haematopoiesis and adult marrow engraftment. *Nature* 523:468–471
10. Pugach EK, Li P, White R, Zon L (2009) Retro-orbital injection in adult zebrafish. *J Vis Exp JoVE* 34
11. de Jong JLO, Burns CE, Chen AT, Pugach E, Mayhall EA, Smith ACH, Feldman HA, Zhou Y, Zon LI (2011) Characterization of immune-matched hematopoietic transplantation in zebrafish. *Blood* 117:4234–4242
12. Mosimann C, Kaufman CK, Li P, Pugach EK, Tamplin OJ, Zon LI (2011) Ubiquitous transgene expression and Cre-based recombination driven by the ubiquitin promoter in zebrafish. *Development (Cambridge, England)* 138:169–177

13. Kobayashi I, Kobayashi-Sun J, Kim AD, Pouget C, Fujita N, Suda T, Traver D (2014) Jam1a-Jam2a interactions regulate haematopoietic stem cell fate through Notch signalling. *Nature* 512:319–323
14. Henninger J, Santoso B, Hans S, Durand E, Moore J, Mosimann C, Brand M, Traver D, Zon L (2017) Clonal fate mapping quantifies the number of haematopoietic stem cells that arise during development. *Nat Cell Biol* 19: 17–27
15. Lv P, Ma D, Gao S, Zhang Y, Bae YK, Liang G, Gao S, Choi JH, Kim CH, Wang L, Liu F (2020) Generation of foxn1/Casper mutant zebrafish for allograft and xenograft of normal and malignant cells. *Stem Cell Rep* 15: 749–760
16. Fraint E, Feliz Norberto M, Bowman TV (2020) A novel conditioning-free hematopoietic stem cell transplantation model in zebrafish. *Blood Adv* 4:6189–6198
17. Moore JC, Tang Q, Yordán NT, Moore FE, Garcia EG, Lobbardi R, Ramakrishnan A, Marvin DL, Anselmo A, Sadreyev RI, Langenau DM (2016) Single-cell imaging of normal and malignant cell engraftment into optically clear prkdc-null SCID zebrafish. *J Exp Med* 213: 2575–2589
18. Tang Q, Abdelfattah NS, Blackburn JS, Moore JC, Martinez SA, Moore FE, Lobbardi R, Tenente IM, Ignatius MS, Berman JN, Liwski RS, Houvras Y, Langenau DM (2014) Optimized cell transplantation using adult rag2 mutant zebrafish. *Nat Methods* 11:821–828
19. Hamilton N, Sabroe I, Renshaw SA (2018) A method for transplantation of human HSCs into zebrafish, to replace humanised murine transplantation models. *F1000Research* 7: 594–512
20. Parada-Kusz MM, Clatworthy A, Hagedorn EJ, Penaranda C, Nair AV, Henninger JE, Ernst C, Li B, Riquelme R, Jijon H, Villablanca EJ, Zon LI, Hung D, Allende M (2017) Generation of mouse-zebrafish hematopoietic tissue chimeric embryos for hematopoiesis and host-pathogen. *Interact Stud* bioRxiv:216895
21. Sood R, English MA, Belele CL, Jin H, Bishop K, Haskins R, McKinney MC, Chahal J, Weinstein BM, Wen Z, Liu PP (2010) Development of multilineage adult hematopoiesis in the zebrafish with a runx1 truncation mutation. *Blood* 115:2806–2809
22. Jin H, Sood R, Xu J, Zhen F, English MA, Liu PP, Wen Z (2009) Definitive hematopoietic stem/progenitor cells manifest distinct differentiation output in the zebrafish VDA and PBI. *Development (Cambridge, England)* 136: 647–654
23. Mosimann C, Kaufman CK, Li P, Pugach EK, Tamplin OJ, Zon LI (2011) Ubiquitous transgene expression and Cre-based recombination driven by the ubiquitin promoter in zebrafish. *Development* 138:169–177
24. White RM, Sessa A, Burke C, Bowman T, LeBlanc J, Ceol C, Bourque C, Dovey M, Goessling W, Burns CE, Zon LI (2008) Transparent adult zebrafish as a tool for in vivo transplantation analysis. *Cell Stem Cell* 2:183–189
25. Tang Q, Abdelfattah NS, Blackburn JS, Moore JC, Martinez SA, Moore FE, Lobbardi R, Tenente IM, Ignatius MS, Berman JN, Liwski RS, Houvras Y, Langenau DM (2014) Optimized cell transplantation using adult rag2 mutant zebrafish. *Nat Methods* 11:821–824
26. Pugach EK, Li P, White R, Zon L (2009) Retro-orbital injection in adult zebrafish. *J Vis Exp* 34:1645
27. Bresciani E, Broadbridge E, Liu PP (2018) An efficient dissociation protocol for generation of single cell suspension from zebrafish embryos and larvae. *MethodsX* 5:1287–1290
28. Gerlach GF, Schrader LN, Wingert RA (2011) Dissection of the adult zebrafish kidney. *J Vis Exp* 54
29. Burket CT, Montgomery JE, Thummel R, Kassen SC, LaFave MC, Langenau DM, Zon LI, Hyde DR (2008) Generation and characterization of transgenic zebrafish lines using different ubiquitous promoters. *Transgen Res* 17:265–279



Establishing a Murine Model of the Hematopoietic Acute Radiation Syndrome

P. Artur Plett, Louis M. Pelus, and Christie M. Orschell

Abstract

The hematopoietic system is one of the most sensitive tissues to ionizing radiation, and radiation doses from 2 to 10 gray can result in death from bleeding and infection if left untreated. Reviewing the range of radiation doses reported in the literature that result in similar lethality highlights the need for a more consistent model that would allow a better comparison of the hematopoietic acute radiation syndrome (H-ARS) studies carried out in different laboratories. Developing a murine model of H-ARS to provide a platform suited for efficacy testing of medical countermeasures (MCM) against radiation should include a review of the Food and Drug Administration requirements outlined in the Animal Rule. The various aspects of a murine H-ARS model found to affect consistent performance will be described in this chapter including strain, sex, radiation type and dose, mouse restraint, and husbandry.

Key words Mice, Lethal irradiation model, Husbandry

1 Introduction

Applications in medicine, energy, or the military for radioactive material increase the likelihood of accidental or intentional radiation exposure which will require effective medical countermeasures (MCM) and importantly a model with which to test these MCM. Our laboratory has focused on developing an appropriate mouse model for the hematopoietic acute radiation syndrome (H-ARS) satisfying the requirements of the Food and Drug Administration's (FDA) Animal Rule in studies when "adequate and well-controlled clinical studies in humans cannot be ethically conducted and field efficacy studies are not feasible" [1].

While lower doses of total-body irradiation (TBI) of 1–2 gray (Gy) are generally not life-threatening, higher radiation exposures of 2–10 Gy result in life-threatening neutropenia and thrombocytopenia, which accompanied by infection and/or bleeding can result in death. In humans, lethal radiation dose for 50% of individuals at 60 days post-irradiation (LD50/60) ranges between 3.5

and 4.5 Gy [2, 3], and survival can be significantly increased with administration of antibiotics and fluids as supportive care [4, 5], emphasizing the importance of supportive care in an H-ARS model.

Mice are selected as a model system for a variety of reasons: (1) previously published information and available reagents from studies in the mouse hematopoietic system in general and after radiation, (2) well-characterized housing and husbandry parameters, and (3) well-defined mouse strains enabling characterization of not only the hematopoietic but also lung and gastrointestinal ARS, as well as delayed radiation effects in aged irradiated survivors.

The murine model setup that will be described below was utilized in C57BL/6 mice to characterize the radiation dose–response relationship (DRR), effect of supportive care including antibiotics, peripheral hematopoietic blood parameters, chronoradiosensitivity, and other variables that influence radiosensitivity [6–9].

2 Materials

2.1 Mice

Several criteria will be outlined below that should be considered in choosing the mice to establish an H-ARS model:

1. Strain: Variation in radiosensitivity was reported early on for different inbred mouse strains [10, 11] with the LD50/30 dose varying by as much as 2.5 Gy in the most commonly used strains BALB/c, C3H/HeN, B6D2F1, and C57BL/6 [12]. Outbred mice, such as CD-1 (Charles Rivers) and J:DO (Jackson), are more radioresistant than inbred mice [13, 14]. Genetic causes for the variation in radiosensitivity in different mouse strains have been extensively addressed elsewhere and should be considered when choosing a mouse strain. This is especially important if the genetic pathways affecting radiosensitivity overlap with those affected by the MCM. In addition, if a more radioresistant strain is chosen, higher radiation doses required to obtain useful lethality could result in an overlap between H-ARS and gastrointestinal ARS possibly affecting the efficacy of an MCM.
2. Age: Younger mice are more radiosensitive than young adult mice, with aged mice showing varying radioresistance relative to young adult mice ([15–18] and results from our lab, manuscript in preparation). A model (including the DRR, discussed below) for each age wishing to be studied must be established first and strictly adhered to, particularly in very young mice (2–8 weeks old), where radiosensitivity can vary significantly with each additional week of age [19].

3. Sex: While an effect of sex was noted in biomarker response to radiation [20], radiation-induced lethality in adult male and female C57Bl/6mice do not vary greatly [6], but this may differ in other strains and may not be the case in pediatric and geriatric mice. Therefore, both males and females should be included in the H-ARS model to better represent the human population and allow for detection of sex-based differences in radiation and MCM efficacy that will inform further development and application of these MCM.
4. Weight: Even though controlling age and sex as described above will result in a more constrained weight range, particularly in inbred mice, care must be taken to examine and possibly exclude mice with drastically higher or lower weights [16] (e.g., >2 standard deviations from the mean) [6]. Significantly under- or overweight mice may have health-related conditions that could affect lethality independent of irradiation. Weights in outbred mice vary much more than inbred mice [14], and more inclusive weight ranges will need to be established. Weights in pediatric mice will change much more rapidly than adult or aged mice and should be measured as close to the desired age as possible.
5. Vendor: Mice should be sourced from one reliable vendor exclusively and obtained from the same specific pathogen-free barrier if possible. Mice from less stringent barriers and/or different vendors can present with an infectious syndrome termed “swollen muzzle” which results in acute morbidity and death that obscures the effect of MCM treatment [21]. Genetic drift, handling and care procedures, and microbiome differences between vendors [22] for the same strain can also add variability to the radiation-induced lethality.

2.2 Mouse Housing and Husbandry

1. Cages and racks: Due to the immunocompromised status of lethally irradiated mice, barrier cages with filter-tops are recommended to restrict environmental contamination of the cages after irradiation. These filter-top cages should be placed onto specialized racks with HEPA-filtered air that is pumped into the cages. Alternatively, the filter-top cages can be placed on open racks but will require more frequent cage changes.
2. Feed: Mouse chow should be chosen by nutritional content, ability to be autoclaved, texture, and consistent vendor quality control (a requirement of conducting FDA-approved Good Laboratory Practice (GLP) pre-clinical studies), since all these properties or changes in these properties can affect lethality. Some diet supplements such as vitamins, hormones, or soy products can be radioprotective [23–25], while the inability of mice to chew hard pellets or changes in diet formulation [26, 27] can affect lethality and reproducibility.

3. Water: The water source should be tested, or testing records should be obtained to ensure that no contaminants or toxic compounds are present (required for GLP studies). In addition, sterile or sterilized water is preferred since lethally irradiated mice are immunocompromised. Water is commercially available in sterile disposable containers or can be autoclaved prior to placing in mouse cages. Automatic watering racks can be set up to dispense reverse osmosis water that should limit contaminants. Another option that controls contamination of the water is acidification, which lowers the drinking water pH to 2.5.
4. Bedding: As with the feed, mouse bedding and nesting material should be chosen based on the ability to absorb moisture of excreted urine, non-abrasive texture, aid in thermoregulation [28, 29], and consistent vendor quality control to detect environmental contaminants that could result in toxicity to the irradiated mice [30] (required for GLP studies).
5. Identification: An appropriate method of identification needs to be chosen if mice within a cage are assigned to different groups. Metal ear tags or electronic chips may not be compatible with irradiation, while tattoos may result in tail injury and may fade over time. Ear notches are compatible with irradiation; however, any identification that involves injury or tissue damage should be done with enough time to allow the wound to heal prior to irradiation.

2.3 Irradiation Materials

1. Source: The choice of radiation (most commonly gamma or X-rays) will be based on availability and access at each institution, practicability, and efficiency of irradiating animals. It is essential to account for the differences in quality, penetrance, relative biological effectiveness, and dose rate of the source being used as each one of these factors will influence the lethality. Dose and dose rates should be in the relevant range for the radiation scenario to be modeled. Low-dose rates will result in longer irradiation times increasing the stress of restraint and also have varying effects on irradiation outcome [31, 32]. For reference, 0.7–1.03 Gy/min was used in the C57BL/6 model established in our laboratory [6]. A detailed discussion of the radiation types is outside the scope of this chapter, and it is recommended to work with a radiation physicist to establish all the parameters mentioned above in addition to the scatter or attenuation that may result from interaction of the radiation and the irradiation device (discussed below).
2. Dosimetry: Again, close collaboration with a radiation physicist is important to determine the accuracy, uniformity, and reproducibility of the radiation dose delivered and absorbed. The use of phantoms and dosimeters adapted to the chosen irradiation

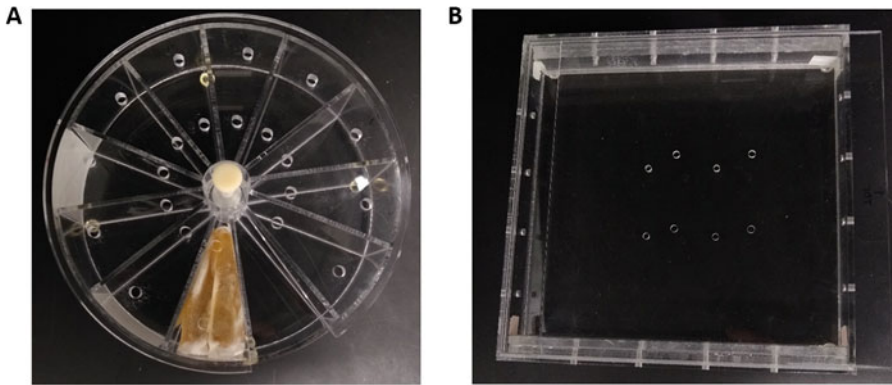


Fig. 1 Irradiation devices with individual compartments (**a**) were used for both gamma and X-ray irradiation in our studies and without compartments (**b**) used in partial-body X-ray irradiation and required anesthesia to immobilize mice during irradiation. Note the breathing holes in both devices, a sample phantom shown in (**a**), and the extra layers in two of the sidewalls (**b**) that were recommended and tested by the radiation physicist to minimize X-ray scatter

device is encouraged to confirm that radiation doses delivered remain accurate over time, which is essential for a stable model.

3. Device: The design of the irradiation device (examples shown in Fig. 1) can influence lethality due to:
 - (a) Stress the mouse experiences during irradiation if the device is too constricting and/or not ventilated properly, which requires adjusting the spacing of the individual sections according to the size of the mice being irradiated. Breathing holes are also required to avoid overheating and suffocation of the mice. The use of a small air pump to provide fresh air in the irradiation chamber may also aid in reducing overheating of the mice.
 - (b) Non-uniform exposure or partial shielding if the device is not constricting enough allowing mice to move in front of or on top of each other and thereby interfering with or blocking the radiation to other mice.
 - (c) Shielding or scatter of the radiation depending on the type of material, thickness, and angles.
4. Dose–response relationship: The lethal radiation dose response should be established in the local laboratory and animal facility by irradiating sufficient mice with a range of doses predicted by the literature to result in 0–100% survival in the particular strain chosen. A probit analysis of these results will allow the prediction of a radiation dose that should result in a specific LDXX/30. In our studies the DRR for C57BL/6 mice was established with radiation doses ranging from 7.25 to 9.0 Gy in increments of 0.25 Gy [6, 33, 34] (*see* Fig. 2). Larger radiation dose ranges may be required for the more radioresistant outbred strains [14].

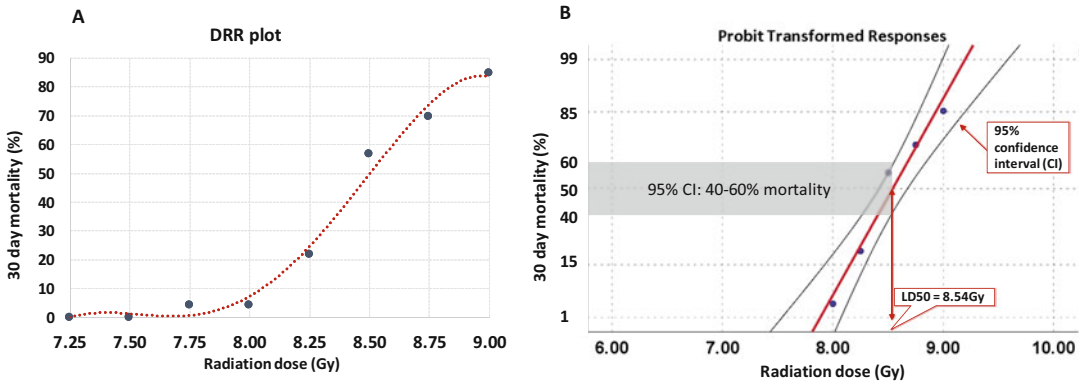


Fig. 2 DRR curve results of mice mortality after acute gamma irradiation with 7.25Gy–9.0 Gy in 0.25 Gy increments are plotted in (a) with a polynomial regression line to estimate the LD50/30. A probit plot which is used to predict the LDXX/30 from a DRR (b) was derived from the linear portion of the survival curve in (a), showing a linear regression line and the 95% confidence intervals (CI). 8.54 Gy was predicted to result in an LD50/30. Note that due to the steepness of the curve (a characteristic of inbred mice) the 95% CI indicates that 8.54 Gy could result in mortality anywhere from 40% to 60% (shown in the gray box), highlighting the difficulty of obtaining a consistent LDXX/30 in inbred mice

5. Anesthesia: If the irradiation device does not have individual sections, shielding for partial-body irradiation will be utilized, or any other parameters requiring immobilization, mice will need to undergo anesthesia. The anesthesia administered should be tested to ensure that mice will remain anesthetized throughout the time of irradiation. The DRR should also be carried out initially in anesthetized mice to account for the potential effect of the anesthesia on lethality.
6. Supportive care: The presence of antibiotics and fluids are the standard of care for humans after irradiation and should be considered in designing the model, unless the supportive care interferes with the MCM. The presence of supportive care such as wetted feed in mice can enhance survival of lethally irradiated mice in the absence of any other MCM [6, 35, 36] and may allow more time for the MCM to be effective.

3 Methods

3.1 Mice and Husbandry

1. Determine the caging, mouse chow, and bedding to be utilized for the studies and sterilization techniques thereof. Obtain quality control documentation on the feed and bedding to verify the lack of contaminants and consistency over time.
2. Establish husbandry parameters including temperature, humidity, air changes in the room, and light/dark cycle (*see* **Notes 1** and **2**).

3. Establish a water, feed, and cage change-out schedule. Parameters established for the husbandry might be modified after irradiation (*see* Subheading 3.2).
4. Obtain enough male and female mice (*see* **Note 3** and comments above) of the chosen strain and appropriate age for the radiation model to be established.
5. Acclimate the mice from 10 to 14 days prior to irradiation during which the mice may be identified by the method selected (*see* comments above) approximately 2 weeks before irradiation if possible (*see* **Note 4**).
6. Weigh the mice approximately 1 week before irradiation, and ensure that the weight is uniformly distributed among all the groups, unless a different weighing schedule is necessary as in the case of pediatric mice.

3.2 Irradiation

1. Select the time of day that irradiation will be carried out (*see* **Note 5**).
2. Calculate the time required to deliver the desired irradiation dose according to the DRR utilizing the radioactive decay-adjusted dose rate obtained from the radiation physicist (or vendor; *see* **Note 6**).
3. Clean and sanitize the irradiation device selected (*see* comments above).
4. Place mice in the irradiation device so that both males and females from all groups are represented and therefore evenly distributed over the entire time range of irradiation.
5. Cover the device with hairnets or similar material to minimize environmental contamination while allowing airflow into the breathing holes of the device. Transport the mice to the irradiator as soon as possible (*see* **Note 7**).
6. Place mice in the irradiator (*see* **Note 6**), and enter the required time to deliver the appropriate radiation dose. Document the start and stop time.
7. Promptly transfer mice back into their cages.
8. Depending on the H-ARS model design and application, ensure mice are to receive any supportive care that is being planned for the model (e.g., autoclaved/sterile water, wet feed, antibiotics).
9. Dose mice according to the study protocol, and obtain any samples planned such as blood or tissues (*see* **Notes 8** and **9** for potential confounders).
10. Designate a monitoring schedule for the mice, and in collaboration with veterinary and animal husbandry staff, establish a euthanasia criteria based on health status scoring of factors including posture, activity, and eyes (*see* **Note 10**).

4 Notes

1. The temperature range for mouse rooms for animal housing is kept between 19 and 21 °C as dictated by the Association for Assessment and Accreditation of Laboratory Animal Care International (AAALAC). This temperature range should be verified and documented to ensure it is being kept constant. Humidity can vary during the year, especially in places with distinct and/or extreme seasons. High humidity in the summer (>80%) can affect the environment inside the cage and coupled with higher temperatures can result in mold/bacterial growth in the feed, water, or bedding. Mold is undesirable in any study but more so in irradiated, immunocompromised mice. Low humidity (<20%) in the winter can affect the mucous membranes of mice already compromised by lethal radiation. To control the humidity will require monitoring and use of a dehumidifier or a humidifier to counteract high or low humidity, respectively. Air changes in the room or within the cages is important to evacuate any contaminants brought in by caretakers or laboratory staff, and air changes within the cage help control humidity in the cage.
2. A 12-h light/dark cycle is commonly used and should be monitored at regular intervals and verified as it is tied to the circadian rhythm of mice affecting their activity, feeding, and importantly the cell cycle of HSC [37]. The proliferative status of HSC and other cells at the time of irradiation in turn will greatly influence their radiosensitivity and therefore mouse lethality [7, 8].
3. The number of mice should be determined with a power analysis, which will dictate how many mice are needed to obtain statistical differences for the anticipated effect of the MCM. In our studies, 20 mice/group (10M/10F) are generally used and powered to detect an effect of at least 30–40% of treatment over control.
4. Identification is necessary to randomize the groups within each cage which is strongly recommended as in our experience whole cages can succumb to radiation lethality. Distributing groups evenly among the cages decreases the overall impact of the loss of an entire cage.
5. Since HSPC cycling is linked to the circadian rhythm and peak HSPC cycling occurs in the hours after lights turn on, irradiating mice in the morning (if lights are turned on at 7 AM) will result in greater lethality than irradiating later in the day [6]. For greater stability and reproducibility of the model, the time of irradiation should be kept consistent.

6. When calculating, irradiation dose of gamma radiation (^{137}Cs or ^{60}Co sources) account for radioactive decay based on the sources' half-life. A decay factor will be provided by the vendor or the radiation physicist. If X-rays are being used, the dose rate will be determined by the output of the X-ray tube, the filter being utilized, and the position in the irradiator (i.e., distance from the X-ray source). X-ray output should be confirmed routinely due to variations that can occur in the X-ray tube efficiency over time.
7. Transportation should be as prompt as possible to limit the time spent in the irradiation device as this will cause stress due to constraints, increased body temperature, and lack of access to drinking water, all factors that might affect lethality.
8. MCM dosing parameters can affect lethality and require careful consideration to balance the risk/benefit ratio of multiple doses. Control groups should also be matched to treatment groups as relates to dosing frequency. Depending on the site of treatment administration, subcutaneous, intradermal, intraperitoneal, intramuscular, intravenous, or oral gavage, volumes should not exceed the recommendations given in the National Research Council's Guide for the Care and Use of Laboratory Animals as this may cause stress, pain, and tissue damage which may affect lethality. The volume administered may also help hydrate the mice given the reduced water intake for hours to days post-TBI [6]. Therefore, the injection volume should be kept consistent among both treatment and vehicle-control groups. Finally, increased frequency of dosing can affect survival [33] likely due to increased stress caused by the handling and dosing procedures [20, 38, 39]. Given the effect of these factors, it is not advisable to compare lethality within treatment groups or to a control group with very different administration schedules (e.g., if the treatment groups receive one, five, or ten doses of drug, but only one vehicle-control group is used that receives the maximal ten doses of vehicle, increased lethality caused by increased handling stress may result in a misleading survival benefit if compared to the one-dose treatment group).
9. Sampling frequency and types of tissue (e.g., blood for CBC) that may result in wounding or tissue damage need to be considered carefully as they will affect lethality [6] in an irradiated mouse potentially becoming a confounder when interpreting the benefit of a treatment. To avoid these situations, pilot experiments should determine the maximum number of sampling time points that do not affect survival, or alternatively, additional mice may be added to the study that are designated for sampling only and shall not be included in the survival calculations.

10. The euthanasia criteria should be based on a scoring system developed in-house with the help of veterinary staff that will help determine when the mouse health has deteriorated enough to require euthanasia. A maximal score for factors such as posture (hunching), reduced to no activity, and closed eyes or eye exudate, among others, can then be used to determine when euthanasia is necessary. Scoring of the mice should be done in a blinded fashion to avoid biases toward the treatment group. Personnel executing the monitoring should be trained so that the scoring and euthanasia are consistent among all laboratory personnel. Although body weight is frequently used as a euthanasia criterion, we feel that the stress of weighing a mouse, unless a specific endpoint in the study, can also become a confounding variable masking the effect of treatment in the irradiated mouse. The method of humane euthanasia will depend on internal regulations and veterinary staff recommendations and should take into consideration the severe depletion of red blood cells that may affect CO₂ euthanasia times.

Acknowledgments

This project has been funded in whole or in part with federal funds from the National Institute of Allergy and Infectious Diseases (NIAID) under contracts HHSN266200500043C and HSN272201000046C, 1U01AI107340-01, 2R44 AI088288-03A1, and National Institute of Aging R01AG046246-01, National Institutes of Health, Department of Health and Human Services.

References

1. Crawford L (2002) New drug and biological drug products; Evidence needed to demonstrate effectiveness of new drugs when human efficacy studies are not ethical or feasible., vol 21 CFR parts 314 and 601, FDA, HHS; ACTION: Final Rule, 105 edn. Federal Register
2. Lushbaugh C (1969) Reflections on some recent progress in human radiobiology. In: Augenstein L, Mason R, Zelle M (eds) *Advances in radiation biology*. Academic, New York, p 277
3. Vriesendorp H, Van Bekkum D (1984) Susceptibility to total-body irradiation. In: Broerse J, MacVittie T (eds) *Response of different species to total body irradiation*. Martinus Nijhoff, Amsterdam
4. Dainiak N (2002) Hematologic consequences of exposure to ionizing radiation. *Exp Hematol* 30:513–528
5. Anno GH, Young RW, Bloom RM, Mercier JR (2003) Dose response relationships for acute ionizing-radiation lethality. *Health Phys* 84: 565–575
6. Plett PA, Sampson CH, Chua HL, Joshi M, Booth C, Gough A, Johnson CS, Katz BP, Farese AM, Parker J, MacVittie TJ, Orschell CM (2012) Establishing a murine model of the hematopoietic syndrome of the acute radiation syndrome. *Health Phys* 103:343–355
7. Palombo P, Moreno-Villanueva M, Mangerich A (2015) Day and night variations in the repair of ionizing-radiation-induced DNA damage in mouse splenocytes. *DNA Repair (Amst)* 28: 37–47

8. Haus E (2002) Chronobiology of the mammalian response to ionizing radiation. Potential applications in oncology. *Chronobiol Int* 19: 77–100
9. DiCarlo AL, Perez Horta Z, Rios CI, Satyamitra MM, Taliaferro LP, Cassatt DR (2020) Study logistics that can impact medical countermeasure efficacy testing in mouse models of radiation injury. *Int J Radiat Biol*:1–17
10. Kohn H, Kallman K (1956) The influence of strain on acute x-ray lethality in the mouse. I. LD₅₀ and death rate studies. *Radiat Res* 5:309–317
11. Storer J (1966) Acute responses to ionizing radiation. In: Gree E (ed) *Biology of the laboratory mouse*, Second edn. Dover Publications Inc., New York
12. Williams JP, Brown SL, Georges GE, Hauer-Jensen M, Hill RP, Huser AK, Kirsch DG, MacVittie TJ, Mason KA, Medhora MM, Moulder JE, Okunieff P, Otterson MF, Robbins ME, Smathers JB, McBride WH (2010) Animal models for medical countermeasures to radiation exposure. *Radiat Res* 173:557–578
13. Tajima G, Delisle AJ, Hoang K, O’Leary FM, Ikeda K, Hanschen M, Stoecklein VM, Lederer JA (2013) Immune system phenotyping of radiation and radiation combined injury in outbred mice. *Radiat Res* 179:101–112
14. Patterson AM, Plett PA, Chua HL, Sampson CH, Fisher A, Feng H, Unthank JL, Miller SJ, Katz BP, MacVittie TJ, Orschell CM (2020) Development of a model of the acute and delayed effects of high dose radiation exposure in Jackson diversity outbred mice; comparison to inbred C57BL/6 mice. *Health Phys* 119: 633–646
15. Crosfill ML, Lindop PJ, Rotblat J (1959) Variation of sensitivity to ionizing radiation with age. *Nature* 183:1729–1730
16. Abrams HL (1951) Influence of age, body weight, and sex on susceptibility of mice to the lethal effects of X-radiation. *Proc Soc Exp Biol Med* 76:729–732
17. Trujillo TT, Spalding JF (1962) Radiation-induced aging as a function of dose rate, measured by the survival of irradiated mice to cold stress. *LA Rep LAMS-2780:98–102*
18. Sacher GA (1957) Dependence of acute radiosensitivity on age in adult female mouse. *Science* 125:1039–1040
19. Patterson AM, Sellamuthu R, Plett PA, Sampson CH, Chua HL, Fisher A, Vemula S, Feng H, Katz BP, Tudor G, Miller SJ, MacVittie TJ, Booth C, Orschell CM (2021) Establishing pediatric mouse models of the hematopoietic acute radiation syndrome and the delayed effects of acute radiation exposure. *Radiat Res* 195:307–323
20. Jones JW, Alloush J, Sellamuthu R, Chua HL, MacVittie TJ, Orschell CM, Kane MA (2019) Effect of sex on biomarker response in a mouse model of the hematopoietic acute radiation syndrome. *Health Phys* 116:484–502
21. Garrett J, Sampson CH, Plett PA, Crisler R, Parker J, Venezia R, Chua HL, Hickman DL, Booth C, MacVittie T, Orschell CM, Dynlacht JR (2019) Characterization and etiology of swollen muzzles in irradiated mice. *Radiat Res* 191:31–42
22. Rasmussen TS, de Vries L, Kot W, Hansen LH, Castro-Mejia JL, Vogensen FK, Hansen AK, Nielsen DS (2019) Mouse vendor influence on the bacterial and viral gut composition exceeds the effect of diet. *Viruses* 11:435
23. Landauer MR, Harvey AJ, Kaytor MD, Day RM (2019) Mechanism and therapeutic window of a genistein nanosuspension to protect against hematopoietic-acute radiation syndrome. *J Radiat Res* 60:308–317
24. Changizi V, Haeri SA, Abbasi S, Rajabi Z, Mirdoraghi M (2019) Radioprotective effects of vitamin A against gamma radiation in mouse bone marrow cells. *MethodsX* 6:714–717
25. Jafari E, Alavi M, Zal F (2018) The evaluation of protective and mitigating effects of vitamin C against side effects induced by radioiodine therapy. *Radiat Environ Biophys* 57:233–240
26. Pellizzon M (2016) Choice of laboratory animal diet influences intestinal health. *Lab Anim (NY)* 45:238–239
27. Pearson AE, Phelps TA (1981) Radiation effects on mouse incisor teeth following whole-body doses of up to 16 gray. *Int J Radiat Biol Relat Stud Phys Chem Med* 39:409–417
28. Maher RL, Barbash SM, Lynch DV, Swoap SJ (2015) Group housing and nest building only slightly ameliorate the cold stress of typical housing in female C57BL/6J mice. *Am J Phys Regul Integr Comp Phys* 308:R1070–R1079
29. Gaskill BN, Gordon CJ, Pajor EA, Lucas JR, Davis JK, Garner JP (2012) Heat or insulation: behavioral titration of mouse preference for warmth or access to a nest. *PLoS One* 7(3): e32799
30. Smith E, Stockwell JD, Schweitzer I, Langley SH, Smith AL (2004) Evaluation of cage micro-environment of mice housed on various types of bedding materials. *Contemp Top Lab Anim Sci* 43(4):12–17
31. MacVittie TJ, Faresse AM, Jackson W 3rd (2015) The hematopoietic syndrome of the acute radiation syndrome in rhesus macaques:

- a systematic review of the lethal dose response relationship. *Health Phys* 109:342–366
32. Travis EL, Peters LJ, McNeill J, Thames HD Jr, Karolis C (1985) Effect of dose-rate on total body irradiation: lethality and pathologic findings. *Radiother Oncol* 4:341–351
 33. Plett PA, Sampson CH, Chua HL, Jackson W, Vemula S, Sellamuthu R, Fisher A, Feng H, Wu T, MacVittie TJ, Orschell CM (2015) The H-ARS dose response relationship (DRR): validation and variables. *Health Phys* 109:391–398
 34. Finney DJ (1971) Statistical logic in the monitoring of reactions to therapeutic drugs. *Methods Inf Med* 10:237–245
 35. Dainiak N (2018) Medical management of acute radiation syndrome and associated infections in a high-casualty incident. *J Radiat Res* 59(suppl_2):ii54–ii64
 36. Waselenko JK, MacVittie TJ, Blakely WF, Pesik N, Wiley AL, Dickerson WE, Tsu H, Confer DL, Coleman CN, Seed T, Lowry P, Armitage JO, Dainiak N, Strategic National Stockpile Radiation Working G (2004) Medical management of the acute radiation syndrome: recommendations of the Strategic National Stockpile Radiation Working Group. *Ann Intern Med* 140:1037–1051
 37. Garrett RW, Gasiewicz TA (2006) The aryl hydrocarbon receptor agonist 2,3,7,8-tetrachlorodibenzo-p-dioxin alters the circadian rhythms, quiescence, and expression of clock genes in murine hematopoietic stem and progenitor cells. *Mol Pharmacol* 69:2076–2083
 38. Gouveia K, Hurst JL (2013) Reducing mouse anxiety during handling: effect of experience with handling tunnels. *PLoS One* 8:e66401
 39. Balcombe JP, Barnard ND, Sandusky C (2004) Laboratory routines cause animal stress. *Contemp Top Lab Anim Sci* 43(6):42–51



Chapter 17

Purinergic Signaling and Its Role in Mobilization of Bone Marrow Stem Cells

Malwina Suszynska, Mateusz Adamiak, Arjun Thapa, Monika Cymer, Janina Ratajczak, Magdalena Kucia, and Mariusz Z. Ratajczak

Abstract

Mobilization or egress of stem cells from bone marrow (BM) into peripheral blood (PB) is an evolutionary preserved and important mechanism in an organism for self-defense and regeneration. BM-derived stem cells circulate always at steady-state conditions in PB, and their number increases during stress situations related to (a) infections, (b) tissue organ injury, (c) stress, and (d) strenuous exercise. Stem cells also show a circadian pattern of their PB circulating level with peak in early morning hours and nadir late at night. The number of circulating in PB stem cells could be pharmacologically increased after administration of some drugs such as cytokine granulocyte colony-stimulating factor (G-CSF) or small molecular antagonist of CXCR4 receptor AMD3100 (Plerixafor) that promote their egress from BM into PB and lymphatic vessels. Circulating can be isolated from PB for transplantation purposes by leukapheresis. This important homeostatic mechanism is governed by several intrinsic complementary pathways. In this chapter, we will discuss the role of purinergic signaling and extracellular nucleotides in regulating this process and review experimental strategies to study their involvement in mobilization of various types of stem cells that reside in murine BM.

Key words Purinergic signaling, Mobilization, Stem cells, Mouse models

1 Introduction

The roles of peptide-based factors (members of the growth factor, cytokine, and chemokine families) and certain bioactive phospholipids in hematopoiesis are well studied [1–9]. However, novel evidence has emerged that extracellular nucleotides (EXNs), including extracellular adenosine triphosphate (eATP) and its metabolite extracellular adenosine (eAdo), a product of eATP metabolism/degradation by the cell-surface-expressed ectonucleotidases CD39 and CD73 (*see* Fig. 1), play an important role in regulating the trafficking of HSPCs and maintaining hematopoiesis in steady-state conditions as well as in stress situations [10]. Both eATP and eAdo are crucial mediators of purinergic signaling that is

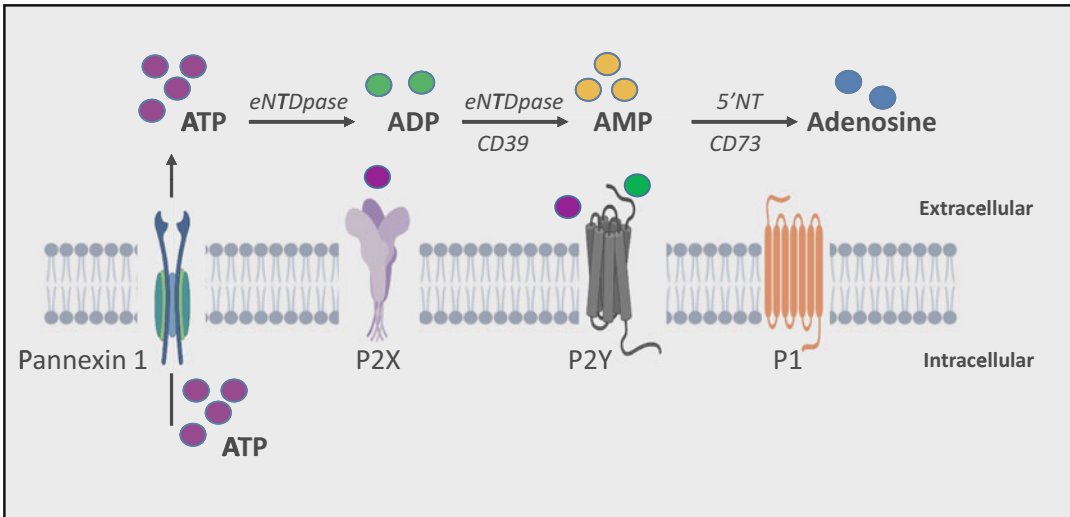


Fig. 1 Overview on purinergic signaling. Extracellular ATP (eATP) secreted from cells by pannexin-1 channels is processed to eADP, eAMP, and adenosine (eAdo), mainly by ecto-nucleoside triphosphate diphosphohydrolase (eNTPDase, also known as CD39) and 5-nucleotidase (5'-NT, also known as CD73). Overall, the purinergic signaling involves inotropic P2X and G protein-coupled P2Y and P1 receptors

a primordial form of extracellular cell–cell communication [11]. Purinergic signaling in addition to eATP and eAdo involves also certain rare extracellular pyrimidines, such as extracellular UTP (eUTP) and UDP (eUDP). Purinergic receptors are evolutionary conserved represented by several members of this family, including P1, P2X, and P2Y receptors (*see* Fig. 1), which are among the most abundant receptors in living organisms. The P1 receptor family consists of four G protein-coupled receptor subtypes (A1, A2a, A2b, and A3), which are activated by eAdo. The P2X ionotropic channel receptor family consists of seven members (P2X1, P2X2, P2X3, P2X4, P2X5, P2X6, and P2X7), which are activated by eATP. The P2 family includes a total of eight receptors (P2Y1, P2Y2, P2Y4, P2Y6, P2Y11, P2Y12, P2Y13, and P2Y14) identified so far, which are also G protein-coupled receptors and respond to stimulation by eATP, eADP, eUTP, and eUDP [12–14].

EXNs have emerged as important players in regulating hematopoiesis [10, 14–17]. eATP, the major positive member in this process, is secreted as a signaling molecule from activated/stressed innate immunity cells (granulocytes, macrophages, and dendritic cells) [18–20] as part of the “sterile inflammation” induced in bone marrow (BM) during infection, tissue organ damage, strenuous exercise, or what is relevant to this chapter after administration of pro-mobilizing agents [21–24].

In humans, a successful transplantation requires a sufficient number of harvested HSPCs per kg body weight of the patient, and a fast, consistent, and long-term multilineage HSPC engraftment requires the intravenous infusion of a minimum of 2×10^6

CD34⁺ stem cells/kg recipient body weight; however, a higher dose of 5×10^6 CD34⁺ cells/kg is considered preferable. Therefore, to assure satisfaction of this requirement, when obtaining cells from mPB for grafting, it is important to apply efficient pharmacological mobilization protocols. Unfortunately, some patients are resistant to standard pro-mobilizing agents, such as granulocyte colony-stimulating factor (G-CSF) and the CXCR4-blocking small molecule AMD3100 (Plerixafor), and thus there is a need to further optimize/improve existing strategies by enhancing this procedure [25–28]. It is important to mention that, in addition to G-CSF and AMD3100, also some chemokines, in particular the growth-related oncogene protein beta (Gro- β) [29], and certain cytostatics (e.g., cyclophosphamide) facilitate this process [30–33].

Mice are an established experimental model that is employed widely to study mobilization process with an aim to design more optimal and efficient mobilization strategies [3, 5, 34–37]. Our recently published results indicate that eATP and its metabolite eAdo regulate the mobilization and homing efficiency of HSPCs in opposite ways (*see Fig. 2*).

In other chapters in this book, the strategies employed to study mobilization of HSPCs in murine experimental models are described in detail. Herein, we will focus mainly on selected important tools to study the role of purinergic signaling in this phenomenon. We will also briefly highlight strategies to study the role of purinergic signaling in egress not only of HSPCs but in addition also of other BM-residing cells, including mesenchymal stroma cells (MSCs), endothelial progenitors (EPCs), and very small embryonic-like stem cells (VSELs) from BM into PB.

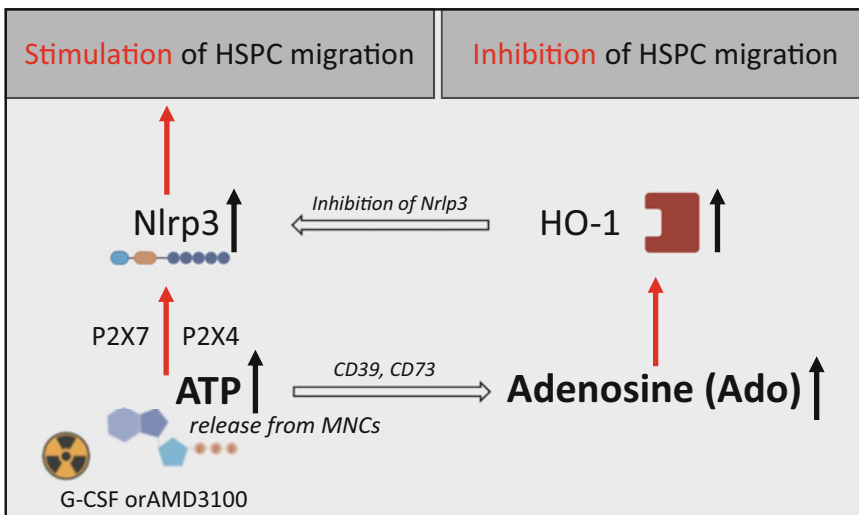


Fig. 2 Opposing positive/negative (“Yin-Yang”) effects of eATP and eAdo on stem cell trafficking. As proposed, Ado-induced intracellular heme oxygenase-1 (HO-1) inhibits stem cell trafficking via inhibiting Nlrp3 inflammasome

2 Materials

2.1 Purinergic Receptor Activators and Inhibitors

Our data indicate that murine BMMNC and HSPCs highly express P2X4, P2X7, P2Y1, P2Y2, P2Y13, A2A, and A2B purinergic receptors. Modulation of these receptors by small molecular agonists and antagonists allows to understand better besides available models of knock-out mice, their role in trafficking of HSPCs. The most relevant agonists and antagonists to study the activities of various purinergic signaling receptors are listed in Table 1. Receptors that are of particular interest due to their relative high expression on hematopoietic cells are indicated in red bold font. Our already generated data indicate that inhibition or stimulation of some of these receptors has a profound effect in modulation G-CSF- and AMD3100-induced mobilization. In particular, mice exposed to P2X7 and P2X4 receptor inhibitors are poor G-CSF-induced mobilizers, which indicates that activation of these receptors is required for optimal egress of cells from BM. This has been later on confirmed employing P2X7-KO and P2X4-KO mice [38]. These crucial identified so far receptors are highlighted in bold and red. The involvement of other receptors expressed on hematopoietic cells still requires further studies.

2.2 Inhibitors of Ectonucleotidases

As demonstrated in Fig. 1, extracellular adenosine triphosphate (eATP) is metabolized to extracellular adenosine (eAdo) by the cell-surface-expressed ectonucleotidases CD39 and CD73. Table 2 shows small molecular inhibitors of these enzymes. We demonstrated that exposure of mice to these inhibitors enhances mobilization of stem cells and even their engraftment of HSPCs after transplantation. Similarly, engraftment of HSPCs is enhanced after inhibition of CD39 and CD73 by small molecular inhibitors on cells in the hematopoietic graft. This is explained by the decreasing level of eAdo endogenously generated from autocrine-secreted eATP from HSPCs as well as eAdo generated in host microenvironment conditioned for transplantation by myeloablative therapy (*see* Fig. 2). Accordingly, mice exposed to these small inhibitors mobilize better HSPCs in response to G-CSF and AMD3100 [10]. This has been subsequently confirmed employing CD73-KO animals [38].

2.3 Other Crucial Proteins Involved in Purinergic Signaling and Its Biological Downstream Effects

eATP is released from activated or exposed to stressor cells in pannexin-1 channel-dependent manner [39–41]. Inhibition of this channel by small inhibitory peptide ¹⁰Panx decreases as we demonstrated egress of stem cells from BM into PB in response to G-CSF and AMD3100 [23]. To explain this, we have reported that eATP activates P2X7 and P2X4 receptors on HSPCs, and this

Table 1
Purine receptor ligands to study purinergic signaling

Receptor	Agonist	Antagonist
<i>P2X receptors (ligand-gated ion channel receptors)</i>		
P2X1	ATP	–
P2X2	ATP	PSB-1011
P2X3	ATP	RO-3
P2X4	ATP; ivermectin (positive allosteric modulator)	5-BDBD/PSB-12054
P2X5	Homomeric receptor is non-functional in humans	–
P2X6	ATP	–
P2X7	ATP	Brilliant Blue G, A 438079
<i>P2Y receptors (G protein-coupled receptors)</i>		
P2Y1	ADP, MRS2365	MRS2279
P2Y2	ATP, UTP, PSB-1114	AR-C118925 (<i>not ideal due to moderate potency; better antagonists are to be developed</i>)
P2Y4	UTP, MRS-4062	–
P2Y6	UDP, PSB-0474	MRS2578 (<i>irreversible mechanism of inhibition; has many drawbacks</i>)
P2Y11	ATP, NF546	NF340
P2Y12	ADP, (2-methylthio-ADP)	PSB-0739
P2Y13	ADP	–
P2Y14	UDP-glucose, MRS2690	–
<i>P1 receptors (G protein-coupled receptors)</i>		
Adenosine A1	eAdo, CCPA	PSB-36
Adenosine A2A	eAdo, CGS21680; PSB-0777	ANR 94, MSX-2/MSX-3
Adenosine A2B	eAdo, BAY60-6583 (partial agonist)	PSB-603
Adenosine A3	eAdo, Cl-IB-MECA	PSB-10

activation leads to stimulation of Nlrp3 inflammasome [42]. Mice that are exposed to small molecular inhibitor of Nlrp3 inflammasome that is MCC950 respond poorly to G-CSF- and AMD3100-induced mobilization. This observation has been subsequently confirmed by employing Nlrp3 inflammasome KO mice. In contrast activation of Nlrp3 inflammasome by eATP or an antibiotic drug nigericin enhances mobilization efficiency. In contrast, as

Table 2
Ectonucleotidase inhibitors: Most important to study hematopoietic cells

Enzyme	Inhibitor
NTPDase1 (CD39)	ARL67156
Ecto-5'-nucleotidase (CD73)	AMPCP

Table 3
Other proteins important for purinergic signaling

Proteins	Stimulator	Inhibitor
Pannexin-1 channel	–	Pannexin-1 blocking peptide
Nlrp3 inflammasome	Nigericin, ATP	MCC950
Heme oxygenase-1 (HO-1)	Protoporphyrin IX (SnPP-IX)	SnPP

described [43] and depicted in Fig. 2, biological effects of Nlrp3 inflammasome activation are mitigated by intracellular heme oxygenase-1 (HO-1), which is upregulated in response to eAdo. To support this notion, we already reported that mice that lack HO-1 mobilized better than control wild-type mice [44]. A similar effect is observed during exposure of mobilized animals to small molecular inhibitor of HO-1 that is SnPP. The summary of other proteins important for purinergic signaling with their stimulators and inhibitors is presented in Table 3.

2.4 Mobilization of Murine Stem Cells

2.4.1 Animals

Six- to eight-week-old C57Bl/6 mice.

2.4.2 Reagents

1. G-CSF (Amgen, Neupogen®).
2. AMD3100 (Sigma-Aldrich, Cat. No. A5602).
3. ¹⁰Panx (Tocris, Cat. No. 3348).
4. Probenecid (Sigma-Aldrich, Cat. No. P8761).
5. eATP (Sigma-Aldrich, Cat. No. A2383).
6. Brilliant Blue G (Sigma-Aldrich, Cat. No. B0770).
7. 5-BDBD (Aobious, Cat. No. AOB3817).
8. MCC950 (Cayman Chemical, Cat. No. 17510).
9. Nigericin (Tocris, Cat. No. 4312).

2.5 FACS Analysis of Stem Cells Mobilized into PB

2.5.1 Reagents

1. 70% ethanol
2. EDTA solution: UltraPure™ 0.5-M EDTA, pH 8.0 (Invitrogen™, Cat. No. 15575020)
3. 1X Lysis Buffer: Lysis Buffer 10× (BD Pharm Lyse™, Cat. No. 555899), diluted to a 1X concentration with water (e.g., HyClone™ Water, Molecular Biology Grade; GE Healthcare, Cat. No. SH30538.02) and warmed to room temperature
4. RPMI-1640 Medium supplemented with 1% Penicillin-Streptomycin Mixture (P-S; Lonza, Cat. No. 17-602E; the dilution ratio 1:100) and with 2% Fetal Bovine Serum (FBS; Avantor Seradigm, Cat. No. 1300-500; Heat Inactivated: 56 °C, 30 min; the dilution ratio 1:50)
5. Monoclonal antibodies (mAb) against murine epitopes (*see* Table 4)

2.5.2 Equipment

1. Sterile fine tweezers and surgical scissors
2. Styrofoam tray and pins
3. 21-G to 25-G needle with 3-ml syringe, flushed through and filled with a small volume of EDTA solution
4. 50-ml Polypropylene Conical Tubes (Falcon, Cat. No. 352098) filled with a small volume of EDTA solution
5. 5-ml Round-Bottom Polystyrene Tubes compatible with the available flow cytometer (Falcon, Cat. No. 352054)
6. Cell Strainer with 40- μ M pores (Falcon, Cat. No. 352340)
7. Centrifuge
8. Flow cytometer equipped with three lasers (405, 488, and 633 nm) and the appropriate bandpass filters for FITC (530/30), PE (575/26), PE-Cy5 (670/30), APC (670/14), V450 (450/50), and BV510 (525/50)

2.6 Confocal Analysis of Membrane Lipid Rafts

2.6.1 Reagents

1. DMEM (no phenol red) supplemented with 5% FBS.
2. DMEM supplemented with 2.5% bovine serum albumin (BSA; Sigma Aldrich, Cat. No. A2153).
3. PBS (phosphate-buffered saline) without calcium and magnesium (VWR, Cat. No. VWRVE504).
4. Nunc™ Glass Base Dish, 12 mm (Thermo Scientific, Cat. No. 12-567-400).
5. Fibronectin, human plasma (Sigma Aldrich, Cat. No. 341635), 10 μ g/ml.
6. Fluorochrome-labeled primary antibodies for immunostaining. These antibodies may vary in number and specificities depending on the phenotypic definition of the cells that will be identified and analyzed by confocal microscopy.

Table 4**List of monoclonal antibodies (mAb) used in flow cytometry analysis to enumerate stem/progenitor cells in mobilized PB**

mAb	Fluorochrome	Clone	Producer	Cat. No.
<i>Lineage mix</i>				
Rat Anti-Mouse TER-119/Erythroid Cells	PE	TER-119	BD Pharmingen™	553673
Rat Anti-CD11b	PE	M1/70	BD Pharmingen™	557397
Rat Anti-Mouse Ly-6G and Ly-6C	PE	RB6-8C5	BD Pharmingen™	553128
Hamster Anti-Mouse TCR β Chain	PE	H57-597	BD Pharmingen™	553172
Hamster Anti-Mouse γδ T-Cell Receptor	PE	GL3	BD Pharmingen™	553178
Rat Anti-Mouse CD45R/B220	PE	RA3-6B2	BD Pharmingen™	553089
<i>Sca-1 mix</i>				
Rat Anti-Mouse Ly-6A/E (Sca-1)	Biotin	E13-161.7	BD Pharmingen™	553334
Streptavidin	PE-Cy™5		BD Pharmingen™	554062
<i>Other mAb</i>				
Rat Anti-Mouse CD117 (c-Kit)	FITC	2B8	BD Pharmingen™	553354
Rat Anti-Mouse CD31	APC	MEC 13.3	BD Pharmingen™	551262
Rat Anti-Mouse CD45	V450	30-F11	BD Horizon™	560501
Rat Anti-Mouse CD90.2	BV510	30-H12	BD OptiBuild™	740103
<i>Isotype controls</i>				
Rat IgG2b, κ Isotype Control	PE	A95-1	BD Pharmingen™	553989
Hamster IgG2, λ1 Isotype Control	PE	Ha4/8	BD Pharmingen™	553965
Hamster IgG2, κ Isotype Control	PE	B81-3	BD Pharmingen™	550085
Rat IgG2a, κ Isotype Control	PE	R35-95	BD Pharmingen™	553930
Rat IgG2a κ Isotype Control	Biotin	R35-95	BD Pharmingen™	553928
Rat IgG2b, κ Isotype Control	FITC	A95-1	BD Pharmingen™	553988
Rat IgG2a κ Isotype Control	APC	R35-95	BD Pharmingen™	553932
Rat IgG2b, κ Isotype Control	V450	A95-1	BD Horizon™	560457
Rat IgG2b, κ Isotype Control	BV510	R35-38	BD Horizon™	562951

7. Cholera Toxin B Subunit from *Vibrio cholerae* FITC conjugate (Sigma, Cat. No. C1655).
8. Mouse CXCR4 Antibody, Monoclonal Rat IgG_{2B} Clone # 247506 (R&D Systems, Cat. No. MAB21651).
9. Goat anti-Rat IgG (H+L) Cross-Adsorbed Secondary Antibody, Alexa Fluor 594 (Life Technologies, Cat. No. A-11007).

10. DAPI (4',6-diamidino-2-phenylindole, dihydrochloride) (Life Technologies, Cat. No. D1306).
11. Cell fixative reagent such as 3.7% paraformaldehyde.
12. 0.1% Triton X-100: Triton X-100 (1%) (Invitrogen™, Cat. No. HFH10) diluted in PBS containing 0.1% BSA and sodium azide.

2.6.2 Equipment

1. Refrigerated benchtop centrifuge with plate adaptors
2. Incubator
3. Laser scanning microscope—e.g., FluoView FV1000 MPE (Olympus)

2.6.3 Software

1. For example, FV10-ASW 4.1 (Olympus)

3 Methods

3.1 Application of Small Molecular Modulators of Purinergic Signaling in Stem Cell Mobilization Experiments

We employed in our experiments some of the small molecular modulators of purinergic signaling in performed stem cell mobilization studies [10, 38, 45]. These data gave us important information, and further experiments performed employing available KO mice confirmed these observations [38]. Below we will briefly describe the procedures and non-toxic doses of small molecular compounds employed in our experiments.

3.1.1 Modulators of Pannexin-1 Signaling

1. ¹⁰Panx—Panx-1 mimetic inhibitory peptide that blocks pannexin-1 gap junctions. Dose: 10 mg/kg for 10 days, intravenous injection (soluble in PBS buffer).
2. Alternative inhibitor of Panx-1 channel is also a drug, probenecid. Dose, 200 mg/kg for 4 days, intraperitoneal injection (soluble in 1 M NaOH) (*see Note 1*).
3. eATP—purinergic signaling receptor activator. Dose: 15 mg/kg for 3 days, intraperitoneal injection (soluble in water).

3.1.2 P2X7 and P2X4 Inhibitors

1. Brilliant Blue G—P2X7R (purinergic receptor) antagonist. Dose: 50 mg/kg for 3 days, intraperitoneal injection (soluble in PBS buffer)
2. 5-BDBD—potent P2X4 antagonist. Dose: 3 mg/kg for 8 days, subcutaneous injection (soluble in DMSO) (*see Note 1*)

3.1.3 Modulators of Nlrp3 Activity

1. MCC950—selective inhibitor of Nlrp3. Dose: 50 µg/kg for 3 days, subcutaneous injection (soluble in DMSO) (*see Note 1*).
2. Nigericin—acts as a potassium ionophore, inducing a net decrease in intracellular levels of potassium which is critical

for the oligomerization of the Nlrp3 inflammasome and activation of caspase-1 in pyroptosis. Dose: 1 mg/kg for 3 days, intraperitoneal injection (soluble in ethanol) (*see Note 1*).

3.2 Analysis of Different Population of BM Mobilized Cells in Murine PB

BM is a major source of HSPCs that reside in stem cell niches and are responsible for the supply of cells circulating in PB. However, it is also well known that BM in addition to HSPCs contains also other types of stem/progenitor cells including mesenchymal stroma cells (MSCs), endothelial progenitors (EPCs), and very small embryonic-like stem cells (VSELs) [46–49]. These cells along with HSPCs are also released into circulation in stress situations as well as after administration of pro-mobilizing drugs [50]. These different stem/progenitor cell types can be enumerated in mobilized PB by employing FACS analysis as described below.

3.2.1 Mobilization of Mice

Mice are mobilized with G-CSF for 3 (short mobilization) or 6 days (full mobilization) at 100 µg/kg/day by subcutaneous injection (SC) or with AMD3100 for 1 h at 5 mg/kg by intraperitoneal injection (IP). At 6 h after the last G-CSF injection or 1 h after AMD3100 injection, PB is obtained from the vena cava. MNCs are obtained by hypotonic lysis of RBCs in 1× Lysis Buffer as described below (*see Note 2*).

3.2.2 Peripheral Blood Collection of Murine Cells and Red Blood Cell Lysis for FACS Analysis

1. Euthanize mice in accordance with established guidelines using CO₂ chamber or other protocols approved by the institutional animal care committee (*see Note 3*).
2. Disinfect the skin with 70% ethanol, place the animal on a dissection styrofoam tray, and affix the extended limbs with pins.
3. Perform a V-incision through the skin and then abdominal wall using the surgical scissors and tweezers. Carefully shift the intestines and liver over to make the inferior vena cava visible.
4. Insert the needle into the widest part of the inferior vena cava, draw blood slowly until it stops flowing, and you feel resistance (*see Note 4*). Wait for the vein to fill again without removing the needle. Repeat procedure several times to collect more blood.
5. Distribute the peripheral blood into a sterile 50-ml tube with EDTA solution, and mix gently.
6. To remove red blood cells, add 10 ml of 1× Lysis Buffer per 1 ml of blood. Gently shake the tube and incubate at room temperature for 5 min.
7. Fill the tube with RPMI-1640 Medium supplemented with P-S, and centrifuge at 500 × *g* at 4 °C for 10 min.

8. Carefully aspirate supernatant, and resuspend the pellet in 5 ml of $1 \times$ Lysis Buffer; repeat the procedure (*see Note 5*).
9. Carefully aspirate supernatant, and resuspend the pellet in 0.5-ml RPMI-1640 Medium supplemented with P-S and 2% FBS for further staining with mAb.

3.2.3 Staining with Monoclonal Antibodies (mAb)

1. Transfer and separate the cells into the following 5-ml Round-Bottom Tubes: (a) unstained sample, (b) FITC sample, (c) PE sample, (d) PE-Cy5 sample, (e) APC sample, (f) V450 sample, (g) BV510 sample, (h) isotype control sample, and (i) tested sample (*see Notes 6 and 7*).
2. Prepare the following mixes of mAb (*see Note 8*): (a) lineage mix (the mix of mAb against different epitopes, which are present on various adult blood cells, conjugated to the same fluorochrome to allow for the negative selection of these cells): TER-119/Erythroid Cells (PE) + CD11b (PE) + Ly-6G and Ly-6C (PE) + TCR β Chain (PE) + $\gamma\delta$ T-Cell Receptor (PE) + CD45R/B220 (PE). (b) Sca-1 mix: Sca-1/Ly-6A/E (Biotin) + Streptavidin (PE-Cy5). (c) Isotype controls mix: all isotype controls listed in Table 4. Then (d) all-antibodies mix: c-Kit (FITC) + lineage mix (PE) + Sca-1 mix (PE-Cy5) + CD31 (APC) + CD45 (V450) + CD90.2 (BV510). The full names of mAb, their clones, and catalog numbers are listed in Table 4.
3. Add mAb to the appropriate tubes with cells and vortex gently: (a) unstained sample (no mAb added). (b) FITC sample (c-Kit (FITC) mAb added). (c) PE sample (lineage mix (PE) added). (d) PE-Cy5 sample (Sca-1 mix (PE-Cy5) added). (e) APC sample (CD31 (APC) mAb added). (f) V450 sample (CD45 (V450) mAb added). (g) BV510 sample (CD90.2 (BV510) added). (h) isotype control sample (isotype controls mix added). (i) tested sample (all-antibodies mix added).
4. Incubate cells on ice for 30 min, protecting from light.
5. Wash all samples by filling tubes with RPMI-1640 medium supplemented with P-S and 2% FBS and centrifuging at $500 \times g$ at 4 °C for 10 min. Decant the supernatant, and resuspend cells in 0.5-ml RPMI-1640 medium supplemented with P-S and 2% FBS. Keep the tubes on ice until flow cytometer analysis protecting from light. Filter cell suspension through a 40- μ M strainer into a new 50-ml tube (*see Note 9*).

3.2.4 Flow Cytometry Analysis

1. Run the unstained sample, and adjust FSC and SSC voltages in a linear scale to visualize cells from PB on the FSC vs. SSC dot plot. Next, set the voltages for fluorescence channels (FITC, PE, PE-Cy5, APC, V450, and BV510) in a logarithmic scale to visualize unstained cells in the first decade on the histograms.

2. Perform fluorescence compensation procedure (automatically or manually) to correct spectral overlap. Briefly, run single-color sample (tubes (b) to (g)) one by one, and adjust the compensation settings until no positive signal is seen in the remaining fluorescence channels.
3. Run the isotype control sample to estimate the level of background staining with specific isotypes of antibodies.
4. Create gating strategy to identify VSELs as $FSC^{low}/SSC^{low}/Lin^{-}/CD45^{-}/Sca-1^{+}$ cells, HSCs as $Lin^{-}/CD45^{+}/Sca-1^{+}$ cells, SKL as $Lin^{-}/Sca-1^{+}/c-Kit^{+}$ cells, EPCs as $CD45^{-}/Sca-1^{+}/CD31^{+}$ cells, and MSCs as $CD45^{-}/CD31^{-}/CD90^{+}$ cells, as shown in Fig. 3, taking into account signals from control samples (unstained, single-color, and isotype control samples) (*see Note 10*).
5. Run tested sample, and acquire at least 1,000,000 events in G1 (the more the better, as very rare cells are analyzed).

3.3 Confocal Analysis of Membrane Lipid Raft Formation

The cell cytoplasmic membrane consists of a phospholipid bilayer with embedded proteins that is held together via non-covalent interactions between the hydrophobic tails. Under physiological conditions, phospholipid molecules in the cell membrane are in a liquid crystalline state; however, the cytoplasmic membranes of cells also contain combinations of glycosphingolipids and protein receptors organized into glycoprotein microdomains, called lipid rafts [51]. Evidence has accumulated that lipid rafts play an important role in the proper assembling and functioning of cell surface receptors involved in cell migration. We proposed that an autocrine or paracrine release of extracellular eATP from HSPCs enhances membrane lipid raft formation on the leading edge of cells and increases their responsiveness to chemotactic gradients present in PB that promote egress of HSPCs into circulation. Membrane lipid rafts can be visualized by employing confocal microscopy as described below (*see Note 11*). To study the distribution of lipid rafts in B cells before and during activation, we made use of CTB, which binds to the GM1 ganglioside, a component of lipid raft membrane microdomains in the outer leaflet of the plasma membrane:

1. Prepare plates by covering the glass part of the plate with fibronectin (10 $\mu\text{g}/\text{ml}$), and incubate for 1 h in 37 °C incubator.
2. Remove fibronectin and air-dry the plate.
3. Centrifuge sorted cells at $500 \times g$ for 15 min.
4. Decant supernatant and resuspend the cells in DMEM with 5% FBS in 150 μl .

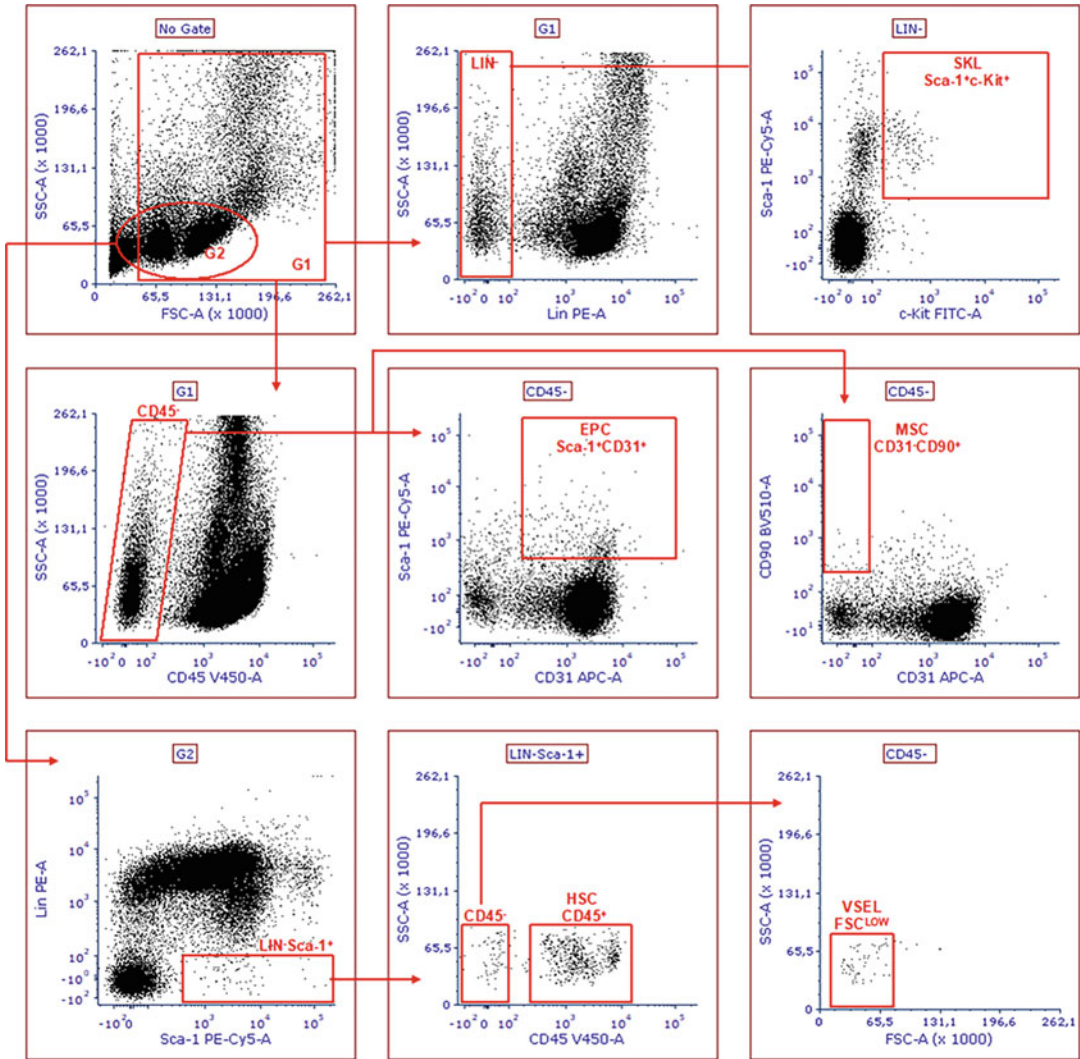


Fig. 3 Gating strategy for analysis of mobilized HSCs and populations enriched in EPCs, MSCs, and VSELS. Gating strategy for SKL HSC and populations enriched in EPC, MSC, and VSELS. Total nucleated cells (TNC) derived from murine PB are visualized on the FSC vs. SSC dot plot (reflecting the size and granularity/complexity of the cell, respectively) in gate G1 (upper panel). TNC are further analyzed for hematopoietic lineage marker expression on the Lin vs. SSC dot plot, and only cells negative for lineage markers are gated in region LIN-. Lineage negative cells are further analyzed for c-Kit and Sca-1 expression on the c-Kit vs. Sca-1 dot plot, and double-positive cells are gated as SKL population; TNC gated on the FSC vs. SSC dot plot are also analyzed for CD45 expression on the CD45 vs. SSC dot plot (middle panel), and only CD45-negative cells are gated in region CD45-. CD45-negative cells are further analyzed for CD31 and Sca-1 expression on the CD31 vs. Sca-1 dot plot, and double-positive cells are gated as population enriched in EPC; in parallel, CD45-negative cells are analyzed for CD31 and CD90 expression on the CD31 vs. CD90 dot plot, and cells negative for CD31 and positive for CD90 are gated as population enriched in MSC. Agranular cells (SSC^{low}), including also very small events (FSC^{low}), are gated in region G2 on the FSC vs. SSC dot plot. Cells from G2 are further analyzed for Sca-1 and lineage marker expression on the Sca-1 vs. Lin dot plot (lower panel). Cells negative for lineage markers and positive for Sca-1 are gated in region Lin Sca-1⁺ and next visualized on CD45 vs. SSC dot plot. Cells positive for CD45 marker are gated as population enriched in HSC, while cells negative for CD45 are visualized by back-gating on the FSC vs. SSC dot plot, and only FSC^{LOW} cells are gated as VSEL population

5. Single-pass sort 30,000 SKL cells directly into glass-bottom fibronectin-covered plate containing 150 μ L of media alone.
6. Incubate the plate at 37 °C, 5% CO₂ for 12 h.
7. Decant medium and wash cells three times with PBS and fixed with 3.7% of buffered methanol-free formaldehyde during 20 min of incubation at room temperature.
8. Wash cells with PBS, treat samples with 0.1% Triton X-100 at RT for 1 min to permeabilize cell membranes, and then wash again.
9. Decant PBS, and block unspecific binding in DMEM with 2.5% BSA for 1 h in a 37 °C incubator.
10. Label with a primary antibody: mouse CXCR4 antibody, followed by a secondary goat anti-Rat IgG (H+L) Cross-Adsorbed Secondary Antibody conjugated with Alexa Fluor 594 and subsequently Cholera Toxin B Subunit from *Vibrio cholerae* FITC—1.5 h each at room temperature.
11. After each antibody wash cells at least three times with PBS.
12. Stain nuclei with DAPI.
13. Perform imaging of cells with confocal laser scanning microscope equipped with proper lasers. Using FFV1000 MPE laser scanning microscope, turn LD559 nm, multi-AR 458 nm 488 nm 515 nm, and HeNe (G) (643 nm) on; select the objective lens Plan Apo N 60x/1.42 Oil, ∞ /0.17/FN26.5; and perform image acquisition.
14. Using FV10-ASW 4.1 software, perform 2D image co-localization analysis. Enclose region of interest by ROI. Select threshold from annotation mode. Information of co-localization is listed under the scatter plot (*see* Fig. 4).

4 Notes

1. All reagents for analysis of purinergic signaling that are soluble in DMSO, ethanol, or NaOH need to be first dissolved at the highest possible concentration and then diluted to proper concentration in PBS buffer.
2. Make sure that all required reagents and equipment, including appropriately labeled collection tubes and syringes/tubes, are filled with a small volume of EDTA solution before starting blood collection.
3. If there are many mice employed in the experiment, euthanize them one by one to avoid blood clotting.
4. To collect peripheral blood, we recommend to use the collection from the inferior vena cava (~0.8–1.2 ml blood volume);

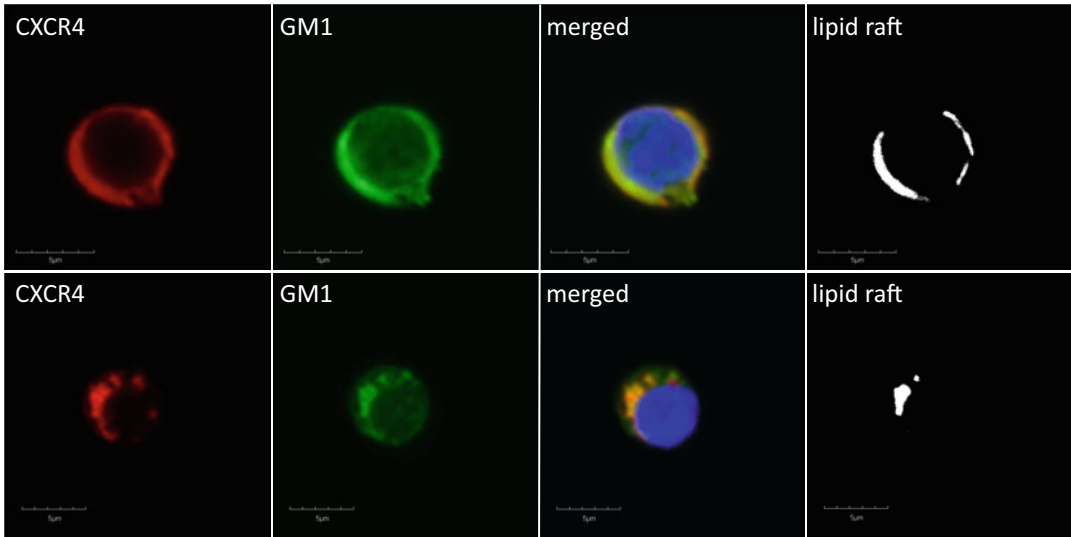


Fig. 4 Imaging of lipid raft formation. Representative images of SKL cells sorted from the bone marrow of C57Bl/6 mice, stimulated with SDF-1 (50 ng/ml) and LL-37 (2.5 μ g/ml), stained with Cholera Toxin B Subunit (GM1—a lipid raft marker) conjugated with FITC and rat anti-mouse CXCR4 followed by goat anti-rat Alexa Fluor 594, and evaluated by confocal microscopy for the formation of membrane lipid rafts. Using FV10-ASW 4.1 software and 2D image co-localization analysis using FV10-ASW 4.1 software. Our data indicate that exposure to eATP increases membrane lipid raft formation (submitted manuscript)

however, depending on the requirements of the experiment, other blood collection methods can be selected.

5. For FACS analysis of VSELs, we recommend during the preparation of mononuclear cells a second round of lysis to remove residual red blood cells, as they could be gated on FSC/SSC plot during flow cytometric analysis. If a population of VSEL is not to be analyzed, you can skip the second lysis and gate out residual red blood cells on FSC/SSC plot, or you can perform other separation procedures such as centrifugation on Ficoll-Paque.
6. Fewer cells can be transferred to tubes (a) to (h), which serve as control samples.
7. We recommend an isotype control sample at least in the first experiment to be aware of unspecific staining.
8. Since this step work with the lights in the laminar flow hood turned off.
9. If the cells clump, filter the cell suspension again before flow cytometry analysis.
10. To characterize better EPC and MSC in murine PB, alternative panels of antibodies are described in the literature. For example, antibodies against CD34 and VEGFR-2 are employed to analyze murine EPC, and antibodies against CD29, CD44,

and CD105 to analyze murine MSC. If only one stem/progenitor cell population is to be analyzed, or if more lasers and fluorescence channels are available, the use of additional markers is recommended to better characterize these populations.

11. Membrane lipid rafts can be also analyzed by fluorescence correlation and cross-correlation spectroscopy (FCS/FCCS) or fluorescence resonance energy transfer (FRET), which detects either the mobility of the fluorochrome in the membrane or its distribution. When more cells are available, lipid rafts can also be studied by employing Western blotting after separation of cell membrane fractions enriched in lipid rafts and co-localizing these fractions with proteins that are components of lipid rafts (e.g., CXCR4, VLA-4, c-kit, and Lyn). Another experimental strategy to study lipid raft function is to deplete cholesterol from lipid rafts by employing (a) methyl- β -cyclodextrin (M β CD), (b) inhibitors of cholesterol synthesis (statins), or (c) drugs that sequester cholesterol, such as nystatin and amphotericin. These membrane cholesterol-targeted experimental manipulations destroy lipid raft structure and negatively affect its biological effects.

Acknowledgments

This work was supported by NIH grants 2R01 DK074720, Stella and Henry Hoenig Endowment, OPUS grant UMO-2018/29/B/NZ4/01470 to MZR, and OPUS grant 2016/21/B/NZ4/00201 to MK. AT was supported by NIH T32 HL134644 to MZR.

References

1. Hoggatt J, Pelus LM (2011) Many mechanisms mediating mobilization: an alliterative review. *Curr Opin Hematol* 18:231–238
2. Ratajczak MZ (2015) A novel view of the adult bone marrow stem cell hierarchy and stem cell trafficking. *Leukemia* 29:776–782
3. Golan K, Vagima Y, Ludin A et al (2012) S1P promotes murine progenitor cell egress and mobilization via S1P1-mediated ROS signaling and SDF-1 release. *Blood* 119:2478–2488
4. Massberg S, Schaerli P, Knezevic-Maramica I et al (2007) Immunosurveillance by hematopoietic progenitor cells trafficking through blood, lymph, and peripheral tissues. *Cell* 131:994–1008
5. Ratajczak MZ, Lee H, Wysoczynski M et al (2010) Novel insight into stem cell mobilization-plasma sphingosine-1-phosphate is a major chemoattractant that directs the egress of hematopoietic stem progenitor cells from the bone marrow and its level in peripheral blood increases during mobilization due to activation of complement cascade/membrane attack complex. *Leukemia* 24:976–985
6. Broxmeyer HE, Orschell CM, Clapp DW et al (2005) Rapid mobilization of murine and human hematopoietic stem and progenitor cells with AMD3100, a CXCR4 antagonist. *J Exp Med* 201:1307–1318
7. Hoggatt J, Pelus LM (2010) Eicosanoid regulation of hematopoiesis and hematopoietic stem and progenitor trafficking. *Leukemia* 24:1993–2002
8. Lapidot T, Kollet O (2002) The essential roles of the chemokine SDF-1 and its receptor CXCR4 in human stem cell homing and

- repopulation of transplanted immune-deficient NOD/SCID and NOD/SCID/B2m(null) mice. *Leukemia* 16:1992–2003
9. Adamiak M, Borkowska S, Wysoczynski M et al (2015) Evidence for the involvement of sphingosine-1-phosphate in the homing and engraftment of hematopoietic stem cells to bone marrow. *Oncotarget* 6:18819–18828
 10. Adamiak M, Bujko K, Brzezniakiewicz-Janus K et al (2019) The inhibition of CD39 and CD73 cell surface ectonucleotidases by small molecular inhibitors enhances the mobilization of bone marrow residing stem cells by decreasing the extracellular level of adenosine. *Stem Cell Rev Rep* 15:892–899
 11. Verkhratsky A, Burnstock G (2014) Biology of purinergic signalling: its ancient evolutionary roots, its omnipresence and its multiple functional significance. *Bioessays* 36:697–705
 12. Burnstock G (2018) Purine and purinergic receptors. *Brain Neurosci Adv* 2:2398212818817494
 13. Di Virgilio F, Dal Ben D, Sarti AC et al (2017) The P2X7 receptor in infection and inflammation. *Immunity* 47:15–31
 14. Rossi L, Salvestrini V, Ferrari D et al (2012) The sixth sense: hematopoietic stem cells detect danger through purinergic signaling. *Blood* 120:2365–2375
 15. Ratajczak MZ, Adamiak M, Kucia M et al (2018) The emerging link between the complement cascade and purinergic signaling in stress hematopoiesis. *Front Immunol* 9:1295
 16. Jing L, Tamplin OJ, Chen MJ et al (2015) Adenosine signaling promotes hematopoietic stem and progenitor cell emergence. *J Exp Med* 212:649–663
 17. Zeiser R, Robson SC, Vaikunthanathan T et al (2016) Unlocking the potential of purinergic signaling in transplantation. *Am J Transplant* 16:2781–2794
 18. Scanzano A, Cosentino M (2015) Adrenergic regulation of innate immunity: a review. *Front Pharmacol* 6:171
 19. Praetorius HA, Leipziger J (2009) ATP release from non-excitable cells. *Purinergic Signal* 5:433–446
 20. Kronlage M, Song J, Sorokin L et al (2010) Autocrine purinergic receptor signaling is essential for macrophage chemotaxis. *Sci Signal* 3:ra55
 21. Mendez-Ferrer S, Chow A, Merad M et al (2009) Circadian rhythms influence hematopoietic stem cells. *Curr Opin Hematol* 16:235–242
 22. Mobius-Winkler S, Hilberg T, Menzel K et al (1985) (2009) Time-dependent mobilization of circulating progenitor cells during strenuous exercise in healthy individuals. *J Appl Physiol* 107:1943–1950
 23. Adamiak M, Ciechanowicz A, Skoda M et al (2020) Novel evidence that purinergic signaling – Nlrp3 inflammasome axis regulates circadian rhythm of hematopoietic stem/progenitor cells circulation in peripheral blood. *Stem Cell Rev Rep* 16:335–343
 24. Ratajczak MZ, Adamiak M, Thapa A et al (2019) NLRP3 inflammasome couples purinergic signaling with activation of the complement cascade for the optimal release of cells from bone marrow. *Leukemia* 33:815–825
 25. Karpova D, Rettig MP, DiPersio JF (2019) Mobilized peripheral blood: an updated perspective. *F1000Res* 8:2125
 26. Miyazaki K, Suzuki K (2018) Poor mobilizer and its countermeasures. *Transfus Apher Sci* 57:623–627
 27. Huang X, Guo B, Capitano M et al (2019) Past, present, and future efforts to enhance the efficacy of cord blood hematopoietic cell transplantation. *F1000Res* 8:1833
 28. Ballen K (2017) Umbilical cord blood transplantation: challenges and future directions. *Stem Cells Transl Med* 6:1312–1315
 29. Hoggatt J, Singh P, Tate TA et al (2018) Rapid mobilization reveals a highly engraftable hematopoietic stem cell. *Cell* 172:191–204.e10
 30. Levesque JP, Hendy J, Takamatsu Y et al (2003) Disruption of the CXCR4/CXCL12 chemotactic interaction during hematopoietic stem cell mobilization induced by G-CSF or cyclophosphamide. *J Clin Invest* 111:187–196
 31. Bonig H, Papayannopoulou T (2013) Hematopoietic stem cell mobilization: updated conceptual renditions. *Leukemia* 27:24–31
 32. Karpova D, Rettig MP, Ritchey J et al (2019) Targeting VLA4 integrin and CXCR2 mobilizes serially repopulating hematopoietic stem cells. *J Clin Invest* 129:2745–2759
 33. Winkler IG, Pettit AR, Raggatt LJ et al (2012) Hematopoietic stem cell mobilizing agents G-CSF, cyclophosphamide or AMD3100 have distinct mechanisms of action on bone marrow HSC niches and bone formation. *Leukemia* 26:1594–1601
 34. Juarez JG, Harun N, Thien M et al (2012) Sphingosine-1-phosphate facilitates trafficking of hematopoietic stem cells and their mobilization by CXCR4 antagonists in mice. *Blood* 119:707–716
 35. Borkowska S, Suszynska M, Mierzejewska K et al (2014) Novel evidence that crosstalk between the complement, coagulation and fibrinolysis proteolytic cascades is involved in

- mobilization of hematopoietic stem/progenitor cells (HSPCs). *Leukemia* 28:2148–2154
36. Hoggatt J, Mohammad KS, Singh P et al (2013) Prostaglandin E2 enhances long-term repopulation but does not permanently alter inherent stem cell competitiveness. *Blood* 122:2997–3000
 37. Pruijt JF, Verzaal P, van Os R et al (2002) Neutrophils are indispensable for hematopoietic stem cell mobilization induced by interleukin-8 in mice. *Proc Natl Acad Sci U S A* 99:6228–6233
 38. Adamiak M, Bujko K, Cymer M et al (2018) Novel evidence that extracellular nucleotides and purinergic signaling induce innate immunity-mediated mobilization of hematopoietic stem/progenitor cells. *Leukemia* 32:1920–1931
 39. Woehrle T, Yip L, Elkhali A et al (2010) Pannexin-1 hemichannel-mediated ATP release together with P2X1 and P2X4 receptors regulate T-cell activation at the immune synapse. *Blood* 116:3475–3484
 40. Burnstock G (2016) P2X ion channel receptors and inflammation. *Purinergic Signal* 12:59–67
 41. Volonte C, Apolloni S, Skaper SD et al (2012) P2X7 receptors: channels, pores and more. *CNS Neurol Disord Drug Targets* 11:705–721
 42. Ratajczak MZ, Bujko K, Cymer M et al (2020) The Nlrp3 inflammasome as a "rising star" in studies of normal and malignant hematopoiesis. *Leukemia* 34:1512–1523
 43. Cao YA, Wagers AJ, Karsunky H et al (2008) Heme oxygenase-1 deficiency leads to disrupted response to acute stress in stem cells and progenitors. *Blood* 112:4494–4502
 44. Wysoczynski M, Ratajczak J, Pedziwiatr D et al (2015) Identification of heme oxygenase 1 (HO-1) as a novel negative regulator of mobilization of hematopoietic stem/progenitor cells. *Stem Cell Rev Rep* 11:110–118
 45. Lenkiewicz AM, Adamiak M, Thapa A et al (2019) The Nlrp3 inflammasome orchestrates mobilization of bone marrow-residing stem cells into peripheral blood. *Stem Cell Rev Rep* 15:391–403
 46. Asahara T, Murohara T, Sullivan A et al (1997) Isolation of putative progenitor endothelial cells for angiogenesis. *Science* 275:964–967
 47. Yoder MC (2009) Defining human endothelial progenitor cells. *J Thromb Haemost* 7(Suppl 1):49–52
 48. Phinney DG, Prockop DJ (2007) Concise review: mesenchymal stem/multipotent stromal cells: the state of transdifferentiation and modes of tissue repair – current views. *Stem Cells* 25:2896–2902
 49. Kucia M, Reza R, Campbell FR et al (2006) A population of very small embryonic-like (VSEL) CXCR4(+)SSEA-1(+)Oct-4+ stem cells identified in adult bone marrow. *Leukemia* 20:857–869
 50. Kucia MJ, Wysoczynski M, Wu W et al (2008) Evidence that very small embryonic-like stem cells are mobilized into peripheral blood. *Stem Cells* 26:2083–2092
 51. Lingwood D, Simons K (2010) Lipid rafts as a membrane-organizing principle. *Science* 327:46–50

INDEX

A

Autofluorescence 128, 130, 144, 149, 150, 156

B

Bone marrow 3–6, 15, 18, 30, 31, 36, 40, 49, 63, 65, 73, 75, 95, 96, 99, 100, 106, 109, 114, 115, 119–122, 127, 128, 130, 136, 138, 163–179, 181–188, 191, 206, 211, 215, 228, 263–278
Bone marrow microenvironment 5, 6, 99, 147–148, 183, 264

C

CD34 25, 49, 56, 67, 69, 70, 73, 75–80, 87–97, 106, 107, 128, 186–188, 225, 227, 229, 264, 265, 277
CD34⁺ cell 49, 70, 76, 78, 87, 187, 228
CD90 56, 88–90, 92–97, 186, 188, 270, 273–275
CFU-F 186
Characterization 4–6, 99–111, 183, 252
Chips 29, 30, 35, 36, 148, 254
C-Kit 30, 106, 127–130, 132, 135, 157, 270, 273–275, 278
Clustered, regularly interspaced short palindromic repeats (CRISPR) 40–43, 45, 46, 48–51, 53, 97
Comet assays 12–14, 17, 21, 25
Confocal and multi-photon microscopy 144, 147, 157, 244, 269–270, 274, 276, 277
CyTOF 5, 113–126

D

Dissection 103, 105, 130, 132, 146, 239, 244, 272
DNA damages 4, 11–27

E

Electrophoresis 11–13, 17, 21, 54, 55
Engraftments 64, 66, 87, 88, 109, 144, 157, 163, 206–208, 211, 214–216, 222, 224, 225, 227, 228, 234, 236, 244, 264, 266
Epigenetics 29

Ex vivo 6, 40, 64, 69, 75, 88, 181–188, 207, 208, 215, 218, 222, 225

F

Fast Halo assay (FHA) 11, 12
Fetal liver 5, 18, 99–111, 233
FGD5 128–130, 135
Flow cytometry 4–6, 53, 56, 74, 77, 80, 88–90, 106–108, 113, 114, 127–129, 135, 136, 138, 139, 183, 186, 188, 193, 197, 198, 209, 211, 214, 216, 217, 224, 228, 234–236, 244, 245, 247, 270, 273, 277

G

Gene editing 39–59
Gene therapies 3, 4, 63, 64, 66, 87, 88

H

Hematopoiesis 5, 63, 65, 99, 100, 107, 109, 113, 114, 127, 130, 132, 143, 144, 163, 229, 233–235, 263, 264
Hematopoietic methods 3–6
Hematopoietic progenitor cell (HPC) 30, 31, 139, 205, 214, 218
Hematopoietic protocols 4–6, 57, 65, 148, 182
Hematopoietic stem and progenitor cell (HSPC) 4, 5, 29–59, 63–82, 87, 88, 92, 94, 96, 106, 107, 145, 181–188, 233–236, 238, 241, 258, 263–266, 272, 274
Hematopoietic stem cell transplantation (HSCT) 63, 78, 205–229
Hematopoietic stems (HSCs) 3–7, 11, 12, 15, 16, 18–20, 25, 30, 63, 81, 87, 88, 99–101, 104–111, 113–130, 132, 134, 135, 137–139, 143–148, 150, 153, 154, 156–159, 163, 205, 206, 214, 215, 218, 222–225, 227, 228, 230, 236, 246, 258, 274, 275
Histone acetylation 4, 29–38
Histones 29, 30, 36
Homing 144, 163, 215, 265
HSPC transplantation 64, 236
Human thymus stroma 191–200
Husbandry 225, 252, 255, 257

I

Intravital imaging 174
 Intravital microscopy (IVM) 5, 144,
 145, 147, 148, 155–157, 163, 169
 In vivo imaging 6, 148, 149,
 154, 172, 174, 177
 In vivo models 6
 Irradiations 5, 19, 36, 65,
 75, 109–111, 128–130, 132, 135, 136, 138, 139,
 148, 157, 206, 210, 220, 227, 233, 243, 251,
 253–259

L

Lentiviral vector (LV) 64–66, 69,
 70, 73, 81
 Lethal irradiation model 109, 139,
 148, 206
 Leukemia 163
 Live imaging 96, 128, 134, 244

M

Mass cytometry 113, 114, 117, 122
 Mesenchymal stromal cells (MSC) 181–188,
 196, 199, 275, 277, 278
 Mice 4, 6, 15, 18, 25,
 29–38, 57, 66, 67, 77, 100, 101, 103, 109–111,
 114, 115, 117, 120, 121, 124, 127–130, 133,
 135, 136, 139, 145–159, 163, 167, 172–174,
 177–179, 192, 194, 195, 199, 200, 205–229,
 235, 252–260, 265–268, 270, 272, 276, 277
 Mobilization 65, 154, 263–278
 Mouse models 6, 97, 144,
 157, 206, 207, 234, 251
 MSC trilineage differentiation 183
 Murine thymus stroma 196, 199

N

Niches 4–6, 99, 109, 114,
 136, 143–145, 154, 157, 181–188, 235, 236, 272

Nonhuman primate (NHP) 4, 5, 56,
 63–82, 87–97

P

Pelvic bones 129, 130, 132, 133
 Plasma mediated laser ablation 164, 169
 Purinergic signaling 6, 263–278

R

Radiation 3, 5, 6, 12,
 19, 127, 130, 236, 251–260

S

Signaling Lymphocytic Activation Molecule
 (SLAM) 108, 118, 128, 130, 135–137
 Single cell proteomics 113, 184, 192
 Spine 130, 132, 133, 136, 148
 Stem cells 3–7, 11–27, 30,
 49, 55, 63, 65, 69, 88, 96, 99–111, 114, 118,
 127–139, 143, 163, 181, 186, 205, 206, 215,
 230, 234, 236, 246, 263–278

T

3-dimensional image analysis 147
 Thymic stromal cells 191, 192, 195, 200
 Thymus 4, 6, 191–200
 Thymus cell harvesting 192
 Tissue dissociation 192–194, 197
 Transduction 4, 52, 53, 58, 63–82
 Transgenic reporter lines 234
 Transplantation 6, 53, 57, 63,
 64, 66, 70, 75, 80, 82, 87, 88, 97, 100, 106,
 109–111, 143, 145, 155–157, 163, 182, 191,
 208, 218, 233–236, 238–241, 243, 244, 246,
 264, 266

Z

Zebrafish 6, 233–237, 239, 241–244